Ph.D Thesis:

The Excimer Laser Ablation of Picture Varnishes.

An evaluation with reference to light-induced deterioration

Charalampos Theodorakopoulos

Royal College of Art,
RCA/V&A Conservation,

In collaboration with:

Foundation of Research & Technology – Hellas (FORTH)
FORTH – Institute of Electronic Structure and Lasers (IESL)

Foundation for Fundamental Research on Matter (FOM),
FOM Institute for Atomic and Molecular Physics, (AMOLF)

Supervisors:

Professor Dr. V. Zafiropulos, IESL/FORTH

Professor Dr. J. J. Boon, FOM-AMOLF

Examination held on May 27, 2005 at the RCA, London

to my parents and Irini

Table of Contents

Preface

This thesis provides a study on the laser cleaning of aged coatings (dammar, mastic and copal oil varnishes) with KrF excimer laser (248 nm) nanosecond pulses. Most of the attention is paid on the contribution of the chemistry of the aged varnishes to the process. Since consecutive laser pulses interact with subsequent depths across the thickness of the same film, it was essential to study the organic chemistry of these coatings as a function of depth. In laser cleaning applications of historical and cultural objects, the remaining material is more important than the material ablated. Therefore the present study determines the impact of the laser-varnish interaction to the varnish. The coatings tested were clearly separated into two groups: (i) natural resin 'spirit' varnishes and (ii) pre-polymerised resin-oil varnishes. Findings of the first group are expected to correspond to the majority of aged organic coatings with low or moderate molecular weights, which are the most frequently used varnishes. The second group is an exceptional case, which highlights the efficiency of UV short-pulsed laser induced removal of insoluble coatings.

Taking advantage of the etching resolution of 248 nm laser pulses (sub-micron scale), this work is the first systematic study on the depth-depended oxidation and crosslinking profiles of aged natural resin varnishes. It is established herein that after ageing, natural resin varnishes undergo depth-depended, decreasing gradients in the degrees of oxidation and condensation (crosslinking and polymerisation). In addition, it is determined that their oxidation profiles change qualitative with depth. A first indication of the existence of gradients across the films was provided by the change of the ablation rate against fluence with depth. Using constantly 'optimal' fluences, which maximised the ablation yield per incident laser photon on the surface, it was observed that the ablation step was minimised particularly after the removal of the uppermost surface layers of dammar and mastic films. Analysis of the ablation plume

across depth with Laser-induced Breakdown Spectroscopy (LIBS) showed that the carbon dimer emission, the intensity of which has been previously associated with the degree of crosslinking and polymerisation, decreases abruptly after the removal of the 15 μm surface layers. The intensity and the rate of the laser light transmission as a function of the reducing thickness were different upon ablation of surface and bulk layers. Under these conditions, a range of consecutive depth-steps was etched in the films to study the chemical profiles across depth. Analysis was separated into two groups: (i) directly on the ablated surfaces with Attenuated Total Reflection - Fourier Transformed Infrared Spectroscopy (ATR-FTIR) and Matrix-Assisted Laser Desorption/Ionisation - Time-Of-Flight - MS (MALDI-TOF-MS) and (ii) on the remaining films with UV/VIS spectrophotometry, Direct Temperature-resolved MS (DTMS) and the Multivariant Factor Discriminant Analysis (DA) thereof, as well as High Performance - Size Exclusion Chromatography (HP-SEC).

The determined oxidation and condensation gradients explain preliminary observations such as increasing solubility, decreasing yellowing and decreasing ablation steps with depth. The decreasing oxidation with depth highlights that there is no laser-induced deterioration of the ablated varnishes. The formation of the gradients was found to be the effect of the reducing ambient light transmission into the films, according to UV/VIS data. A detailed study indicated that UV-induced oxidation is limited at the 15 μm surface layers of the natural resin films, which completely absorbed radiation with $\lambda < 350$ nm. In addition, the abrupt change of the ablation step below 15 μm was also attributed to the decrease of MW with depth, shown by DTMS-TIC's and HP-SEC. Both dammar and mastic were almost unaffected from ageing at depths longer than 25 μm from surface, albeit the extreme accelerated ageing process that preceded laser ablation tests. This finding showed that the depth-wise reducing yellowing was not a matter of laser induced bleaching of known chromophores formed during autoxidation. Instead, it is proven herein that these chromophores are not even produced at long depths from surface in such coatings.

In a sharp contrast, the depth profile of the aged copal oil varnish was virtually homogenous. Evaluation of the ageing of the film was carried out with Pyrolysis-Gas Chromatography / MS with online derivatisation with tetramethylammomium

hydroxide (TMAH) (Py-TMAH-GC/MS). The results supported earlier studies on the reduction of the concentration of the resin component upon ageing. Oxidation was monitored by the increased concentration of saturated fatty diacids over unsaturated fatty acids of the oil component. Several oxygenated fatty acids were generated from polyunsaturated fatty acids, such as cyclic octadecanoic fatty acids formed via Diels-Alder cyclisation and/or intermolecular cyclisation of heat-induced conjugation. In contrast to the aged natural resin films, the aged oil varnish had a stable interaction with the KrF excimer laser at all depths, determined by (i) the identical laser ablation rate versus fluence, (ii) the constant ablation step, (iii) the steady laser induced transmission through surface and bulk layers and (iv) the constant intensity of carbon dimer emission across depth monitored by LIBS. ATR-FTIR showed that absorption due to carbonyl groups remained constant at all depths, while UV/VIS data showed that the film was a low absorber and optically saturated. A fingerprint DTMS study on the leaser etched depth-steps showed that the film was a homogeneous, polar and crosslinked polymer in which there was a negligible volatile fraction.

The findings of this PhD thesis indicate that a certain methodology should be followed for the safe laser cleaning of varnished works of art. In the case of highly polymerised oil varnishes with homogenous depth profiles, most of the varnish can be removed down to a depth at which the optical density of the film prevents laser light transmission to the substrate. Laser cleaning in this case is the only known method to improve the appearance of a painted object without affecting the painted layers. The application bears more risks in the presence of aged natural resin varnishes. Safety is provided as long as the laser-varnish interaction is limited at the highly degraded surface layers of the aged varnishes. Below these layers the transmission of the laser photons increases more than the optical absorption lengths at the surface of the varnishes indicate. The removal of surface layers of a maximum thickness of 15 μm improves the appearance of the underlying paint, because no significant degrees of yellowing, oxidation and condensation were identified at these depths.

Acknowledgements

The present doctoral thesis would not have been possible without the generous support from several European research and academic institutes, universities, museums, conservation departments, long-term scholarships and sort-term grants. It would be an omission not to mention my gratitude to all individuals involved regardless of their status, position and the magnitude of their contribution. It has been a pleasure and a great adventure to work with incredible technological tools such as lasers for the preservation of works of art. Moreover, it was a remarkable experience working in the background of three wonderful European cities: Heraklion-Crete, London, and Amsterdam.

The introduction to places, institutions and individuals, during the course of my research had a major impact to my work. Thus, I consider these as key stages which I owe to refer to. I must pay my respect and thankfulness to Prof. Dr Costas Fotakis, director of IESL/FORTH, who, back in 1999, accepted me as a postgraduate student at FORTH, even before I had suspected that there was so much work I would do. The day we met I was introduced to Prof. Dr Vassilis Zafiropulos, who later became my supervisor. I am most grateful to Vassilis because he gave me the confidence to extend my studies to the doctoral level and he was always the first to discuss findings, achievements and difficulties. I thank all the research and technical personnel at IESL/FORTH and in particular Aleka Manousaki, Krystalia Melissanki and Dr Paraskevi Pouli, who were always keen to provide their valuable scientific assistance.

I wish to acknowledge Prof Alan Cummings at the Royal College of Art, London, who, being the head of the joint course between the RCA and the V&A Museum in London in 2000, accepted me to conduct my PhD research. Alan became my supervisor but was appointed as the Pro-Rector of the RCA soon after I started my research. William Lindsay, head of RCA/V&A conservation to date, was a key figure

in my studies and was always there for valuable advice. I thank Alan Phenix, who became my supervisor when he was Research Fellow at the RCA. Alan was the first person at the RCA to discuss with me analytical and scientific issues for varnishes, which had a major impact to my studies. I am grateful to him because in the short term he was involved in my research he introduced me to Prof. Dr Jaap Boon in the FOM institute AMOLF. Unfortunately, Alan left the RCA in 2001/02 having accepted a post elsewhere, which apparently he could not turn down.

I wish to express my gratitude to Prof. Dr Jaap Boon, head the Molecular Painting Research at AMOLF, whom I visited in 2002 at AMOLF, Amsterdam, to discuss the potential of a short collaboration. It turned out to be the most influential moment after my introduction to the laser world. Apparently, I wrote three and a half chapters out of six in this PhD thesis based on my work at AMOLF. Jaap's work, widely known via numerous publications and a series of PhD projects, which reflect the quality of the MOLART project at AMOLF, speaks by itself. My presence at AMOLF and the fact that I was discussing my research directly with Jaap was simply an inspiration. There was no other thought from that moment on but to deliver the best possible work. Eventually, Jaap became my second supervisor and I am grateful because he spent time with my work, albeit his very busy programme. I also thank the research and technical personnel at AMOLF for their assistance; in particular, Jerre van der Horst, Marc Duursma, Annelies van Loon and Dr Ester Ferreira.

Although my research was mainly carried out at the RCA, FORTH and AMOLF, I was based at the V&A Museum. There, I had the chance to talk with conservators on a daily basis about regular difficulties of their profession. I am thankful to Charlotte Hubbard, head of V&A Sculpture Conservation, who hosted me in the conservation studio at the V&A during my studies. The 'little room' at the V&A Sculpture studio helped to put my thoughts together. Victor Borges and Sofia Marques, the two sculpture conservators at the V&A, were always the first people to meet when I used to open the door of 'the little room'. It would have been an omission if I wouldn't acknowledge my two good friends, Victor and Sofia, for the lunches and coffees we had together, which kept me going until late hours. I also thank the V&A Science group, Graham Martin, Boris Pretzel, Dr Brenda Keneghan and Dr Lucia Burgio, for

letting me using their equipments. I also acknowledge Nicola Costaras, senior painting conservator, for her interest in my work, which was materialised with samples provided for my preliminary studies.

I thank Stephen Hackney, Dr Joyce Townsend and Tim Green of the conservation department of the Tate Gallery, London for their interest in my research and for their valuable sample supply. I acknowledge Dr Christina Young at the Courtauld Institute of Art, London for our short collaboration and for giving me access to the accelerating ageing facilities at the Courtauld Department of Conservation and Technology. I must express my gratitude to Dr Stamatis Boyatzis, whose help was essential for my sample fabrication, which was one of the most puzzling tasks I dealt with. I am also thankful to Dr Panagiotis Argitis, director of research at the Institute of Microelectronics at the National Centre of Scientific Research "Demokritos" in Athens, who enabled my access to the IMEL laboratories. I wish to thank Dr Vincent Daniels, research fellow at the RCA/V&A conservation, who did the final language editing of my thesis.

I acknowledge the essential financial contribution of the Foundation of State Scholarships – Hellas, which fully supported my PhD studies. RCA Conservation also contributed to my studies by a two-year bursary. Access to IESL/FORTH was enabled by the Ultraviolet Laser Facility of the Cluster of Large Scale Laser Installations (LIMANS) and the TMR Programme of the EC Project DGXII, ERBFMGECT 950021. Access to AMOLF was made possible by the FOM Program 49 funded by FOM and NWO.

I am most grateful to my parents, who were always there to encourage me and my choices financially and psychologically. Last but not least, I wish to express my great appreciation to Irini for her encouragement at the beginning of this journey and for her emotional and psychological support throughout this project.

1. An Introduction on the Laser Cleaning of Paintings

Abstract

This chapter explores briefly the up-to-date cleaning techniques for paintings and introduces the potential of recently proposed laser cleaning applications. A chronological review of all the investigations on the laser-cleaning studies in conservation from the early 1970s up to the latest LACONA V international conference (2003) brings to light the background studies, collaborations and contradictions on diverse aspects of laser cleaning of paintings. The fundamental mechanisms of the interactions of UV laser photons with polymers are described to support the later studies. A model of 'photophysical' ablation is described based on the current understanding of the sequence of actions following the incidence of an excimer laser pulse. Finally a rationalisation of the following project is attempted based on preliminary findings on recently discovered properties of aged natural resins, the application requirements for a 'safe' utilisation of UV pulsed lasers on paintings and the understanding of excimer laser ablation of resins.

The aims of the thesis within the framework of conservation

Using the advances of laser cleaning for paintings, the content of the following PhD thesis aims at a better understanding of the properties of aged varnishes used as painting coatings compared to knowledge so far. A good understanding of the ageing of varnishes has long been pointed out to enhance the cleaning methodology of paintings, regardless of the cleaning technique and the cleaning tools employed. In particular, such an understanding aims at addressing the actions to be taken in order to remove a deteriorated varnish from a work of art while keeping the risks of cleaning-induced damage (Section 1.1) at a minimum. The combination of several disciplines spanning from conservation aspects (ethical and practical), the chemistry of painting varnishes and their ageing mechanisms as well as laser physics may seem too complex for the practical conservator. However complicated this might seem the integration of such multidisciplinary backgrounds provide the essential understanding that enables simple and confident answers that everybody seeks in the conservation profession. In particular the present work as explained in Sections 1.1 and 1.5 is an attempt to answer to the following:

– Is there a simple way to employ laser cleaning to remove an aged varnish from a painted surface without running the risk of laser-induced damage to the paint?

– A common way to assess a conservation cleaning method is to address the extent of possible damage due to this technique. Therefore a reasonable question to be addressed is whether the high-powered laser action on a varnish damages the remaining varnish. The rationale behind this is that by limiting the possible damage

in the varnish during its removal, it may be possible to eliminate or even avoid damage to the underlying valuable painted surface of the object.

– According to preliminary findings and early theories on the degradation of organic films and varnishes, all the deterioration mechanisms reduce exponentially from the exposed surface towards the bulk (chapters 3, 4 and 5). This has a direct impact in conservation. For example, a very solvent-resistant aged varnish may become increasingly more soluble with depth, as explained in chapter 2. Other issues arising from such a gradual reduction of ageing with depth, which in this work is termed gradient, concern the reduction of yellowing and micro-cracking that are the most obvious visually perceived effects of varnish ageing. So far these gradients have never been experimentally proved or systematically studied. Taking advantage of the selective removal capacities of lasers the existence of gradients is the main research question to be addressed in this project.

By addressing the latter question, answers may be provided for the appropriate use of all the cleaning methods known to date for paintings and not only for laser cleaning. In particular for the lasers, the knowledge for the existence of gradients could be crucial for generating a methodology to be followed by the practical conservator. Thus, we may develop an optimum cleaning of paintings using lasers, because the possibility of the induced damage to the paint would be under control by controlling the amount of varnish to be removed. Therefore the most important question to be answered is:

– Using the deterioration properties of aged varnishes and the selectivity of excimer lasers, can we obtain a methodical and simple methodology for an

acceptable cleaning of paintings, both in terms of aesthetics and of cleaning-induced damage elimination?

1.1 Introduction

Broadly speaking, varnishes are applied to paintings because of both their protective and aesthetic role. Varnishes protect the underlying paint layers from ambient radiation, atmospheric pollution, dust deposition and friction or other mechanical damage. Varnishes are also considered as part of the artworks, since they contribute to the appearance of a painting (Thomson 1957, De la Rie 1987, Berns and De la Rie 2002, 2003a). A well-chosen varnish can regulate the perception of a painted surface by controlling the levels of saturation and glossiness (Bruxelles and Mahlman 1954, Clulow 1972, Hunter 1975, Brill 1980). A significant role in the appearance of paintings is played by the refractive indices of the varnish and the paint, and especially that of their interface (Thomson 1957, De la Rie 1987, Berns and De la Rie 2002). The refractive index of the interface was indicated to be greater than 0.06 for a sufficient perception of the underlying paint layers by the human eye (Thomson 1957). Varnishes of low molecular weight, i.e. low viscosity, improve the saturation of the underlying colours, since they produce smooth surfaces over rough paint surfaces (De la Rie 1987, Berns and De la Rie 2002, 2003b). Recently it was shown that of the two main factors, i.e molecular weight and refractive index, the molecular weight is the principal one influencing the appearance of oil paintings (Berns and De la Rie 2003b). Both refractive indices and molecular weights however change eventually with age.

Regardless of their original properties when freshly applied to painted surfaces, natural varnishes undergo degradation mainly because of their chemical instability. The most significant factor, which causes degradation, is the absorption of the UV wavelengths of the ambient light and, in particular, those in the daylight wavelengths (~ 290-750 nm) that induce a free radical chain reactivity (Al-Malaika 1993, Scott 1993) leading to autoxidation and crosslinking (De la Rie 1988b, Van der Doelen 1999, Dietemann 2003). The chemical changes of natural resins have nowadays been studied extensively and the deteriorative action of UV wavelengths has been established on the molecular level (De la Rie 1988a, Van der Doelen, *et al.* 1998, Zumbühl, *et al.* 1998, Van der Doelen, *et al.* 2000, Dietemann 2003, Scalarone, *et al.* 2003). Even if kept indoors and 'protected' by glass in ordinary windows, which cuts wavelengths shorter than ~ 310 – 315 nm (Feller 1994a), varnishes deteriorate via photochemical initiation reactions with UV photons absorbed by the various easily broken covalent bonds of hydroperoxides and carbonyl groups (Scott 1993). Unsaturated carboxylic acids, esters and lactones have similar end absorption up to 240 nm and are unlikely to break under ambient radiation (Silverstein, *et al.* 1991). Photochemical initiation reactions, however, are commenced with α,β-unsaturated aldehydes and ketones containing conjugated carbonyl groups, which absorb (weakly) at wavelengths longer than 310 nm (Silverstein, *et al.* 1991). Once UV light has been absorbed, radical chain reactions are responsible for a gliding oxidative deterioration (De la Rie 1988b, Van der Doelen 1999, Dietemann 2003). The devastating effects of varnish degradation include discolouration and brittleness or crazing, as consequences of crosslinking and oxidation.

This development suggests the need for a 'cleaning' action, which in effect requires the removal of dirt deposits and aged varnish to reveal the original colour combinations of the painting. The most common cleaning methods are associated with varnish dissolution using organic solvents (Stolow 1985). The basic methods involve mechanical, integrated chemical and mechanical treatments and application of aqueous gels. Mechanical cleaning, that is abrasion, fragmentation and unpeeling of the aged varnish, is a non-selective process and thereby never employed alone (Ruhemann 1968). Integrated chemical and mechanical cleaning, involving the implementation of the less possible polar solvents to swell the aged varnish, which is then removed by a scalpel (Hedley 1980), is the most popular treatment, which nowadays is applied with acceptable control (Phenix 1998, 2002a, b). However, there are several risks for damaging the paint, since a variety of factors, such as the quantity, the polarity, the evaporation time of the solvent, as well as the time of contact with the varnish (Stolow 1985) are empirically assessed, and hence the overall control is up to the practical experience of the conservator. Aqueous solutions in the form of gels (Wolbers 2000) provide a better degree of selectivity in removing aged varnishes, although removal may be time consuming and results uncertain when gels come into contact with the paint.

There are two major aspects that influence the control of established chemical treatments on paintings; the composition of the removable varnish and the concentration of the paint. An 'ideal' case comprises of non-polymerised 'spirit varnishes' (De la Rie 1987, Carlyle 2001), which never become completely insoluble (De la Rie 1988b), especially if the resin polymer has been removed prior to varnish

formation (Koller, *et al.* 1997, Dietemann 2003), over drying oil paint media, whose component triglycerides polymerise forming an insoluble film in non-acidic and non-basic organic solvents (Mills and White 1994). In practice, solvent diffusion into the paint may result in leaching of unreacted triglycerides from the paint, rendering the medium brittle and dense, especially if it is relatively young (Stolow 1985). The nature of pigments and their density in the medium are significant factors that influence the degree of paint vulnerability in dissolution. For example, organic pigments, such as carbon blacks, have antioxidant properties and inhibit the oxidative polymerisation of drying oils (Mills and White 1994), while others, such as mercuric sulphide (vermilion), catalyse the oxidation of the oil (Rasti and Scott 1980). Dense paint films, in terms of the pigment component, are generally more soluble than sparse films (Sutherland 2001), while clusters of pigments straddling the varnish/ paint interface are susceptible to be removed with the solvent. Notwithstanding the paint composition, the degree of solubility of the varnish is the principal factor influencing the success of chemical cleaning. There are certain indications suggesting that spirit varnishes generate an insoluble high MW fraction, which is not removable with common low polarity cleaning solvents, thus remaining on the paint (Boon and van der Doelen 1999), and presumably may introduce partial insolubility of previously used varnishes via their integration. Cleaning problems are also encountered when robust, insoluble polymers are applied on paintings[1]. Some coatings, such as oil-varnishes, which are mixtures of 'hard' resins, such as copal and amber, and oils (Brommelle 1956, Carlyle 2001), polymerise in such a degree to

[1] Sutherland (2001) referred to an unpublished report in the National Gallery of Art, Washington DC, by Lomax, S, reporting that polyurethane and other chemically resistant polymers have been used as varnishes on paintings.

become insoluble with age (Feller, *et al.* 1985). In any case, amber and copal resins are difficult to dissolve in organic solvents even in their pure form (Gettens and Stout 1966). Similar compositions to oil varnishes were used as paint media (megilps) during the eighteenth and nineteenth century, although the resin component was commonly mastic (Carlyle 2001). Unlike the insoluble fraction of oil varnishes, megilps are prone to dissolution, owing to the hindering action of the vulnerable resin component on the drying oil polymerisation. There are several examples of this period, such as paintings by Stubbs (Shepherd 1984), Reynolds (Jones, *et al.* 1999), Constable (Cove 1998), Delacroix and Turner (Swicklik 1993), in which varnish removal is practically impossible without potential loss of paint (Sutherland 2001).

Another major problem encountered in chemical cleaning applications involves the presence of overpaints. Dissolution of overpaints with a similar medium to that of the original paint may induce partial dissolution of the original binding medium, even if the overpaint medium is readily soluble. On the other hand, there are examples, such as in the case of Delacroix and Turner (Swicklik 1993), who 'retouched' their original paintings after completion and varnishing. These 'retouchings' are rightfully considered as part of the original work and should never be altered. A solvent-based removal of the varnish above these 'retouchings' would weaken the primary varnish applied below these overpaints (Sutherland 2001). Thus, several risks encountered with the application of traditional cleaning methods may result either in a serious damage to a painting or leaving a painting with an aged discoloured coating.

The desire to sustain old masterpieces has promoted investigations of advanced cleaning techniques, such as a fast solvent-based varnish removal on a nineteenth

century solvent-sensitive wax oil painting (Boon and van Och 1996). Lasers are considered as a new tool in conservation, promising very selective 'cleaning' applications. Already, Nd:YAG lasers are established for controlled cleaning treatments of inorganic materials, such as stones, sandstones, marble etc. (Larson, *et al.* 2000, Pini, *et al.* 2000a, Esbert, *et al.* 2003, Pouli, *et al.* 2005). UV pulsed laser ablation, which has been proposed for the cleaning of paintings (Zafiropulos 2002), seems to be a suitable method for cases, in which the implementation of organic solvent agents carries greater risks than benefits, such as those described above. However, new methods bring new risks, justifying a range of research projects on laser cleaning methods for several conservation tasks, which are described below.

From industrial (Boyd 1992, Tam, *et al.* 1992, Chrisey and Hubler 1994, Miller and Haglund Jr 1998) and medical (Azema and Laude 1994, Bäuerle 2000) applications, it is known that UV photons react directly with chemical bonds of organic materials, causing direct photo-dissociation (Srinivasan and Braren 1989). Thus, ablation that is carried out directly on the surface layers of the aged varnish, provides a dry, step-wise removal of aged coatings in a micron scale, while the process can be monitored online (Zafiropulos and Fotakis 1998). With each UV laser pulse removing material not deeper than ~1-1.5 microns, it is readily appreciated that varnish removal from paintings can be a very selective process. Underlying paint layers are not affected unless directly irradiated (Castillejo, *et al.* 2002) or in case of uncontrollable transmission of the laser beam below the varnish/paint interface (Zafiropulos 2002). The application is governed by the interaction of aged varnishes with the UV laser photons at successive depth-steps etched into the ablated varnish. Therefore, to study

this interaction using a UV pulsed laser, with a certain pulse duration and fluence, the characteristic properties of a varnish that influence the ablation of the material should be studied as a function of depth.

1.2 Literature Review

1.2.1 A Chronological Review of Laser-Cleaning Studies for Conservation

In principal, the concept of using lasers to implement a controlled cleaning of works of art is attributed to preliminary spin-off studies carried out by Professor John Asmus, University of California, UC San Diego. In 1973 Asmus and co-workers, while examining the possibilities of holographic interferometry of a Venetian sculpture using a ruby laser (λ = 690 nm) (Asmus, *et al.* 1973a), noticed that by changing the laser parameters it was possible to enable removal of the black encrustation from the aged marble surface without any perceivable change of the substrate (Asmus, *et al.* 1973b, Lazzarini and Asmus 1973). Two years later, in 1976, Asmus reported results regarding the threshold fluence values of both the vaporisation of black encrustation and the marble for the 690 nm laser, with the former being lower than the latter (Asmus, *et al.* 1976). This meant that while encrustation was being removed with the laser, the marble substrate could be left visually 'intact'.

In 1975 Asmus investigated the possibility of laser cleaning of stained glass (Asmus 1975), again with a ruby laser, which had promising results for future applications. In the same year Asmus and co-workers investigated the possibility of laser-induced-removal of superimposed lime layers to uncover a Leonardo da Vinci mural fresco in Florence, Italy (Asmus, *et al.* 1975). Using relatively high fluences they removed the

lime layers, but also partly the underlying paint layers of the fresco. The research group decided then to apply a saturated solution of copper sulphate on the lime surface in pursuit of absorptivity enhancement of the latter. Thus, the lime layers required lower fluences for efficient removal and, at the same time, removal of the mural's paint was prevented. In 1976 Vitkus and Asmus used a ruby laser to remove fungi from parchment and mildew from leather (Vitkus and Asmus 1976). They concluded that in the first case the laser radiation disturbed the fibres of the vellum, thus requiring more investigation towards the optimisation of the laser cleaning process. In the second case, the application was promising, but they noted that using these optical thermal settings, mildew was somewhat destructed within the reach of the laser beam.

In 1976 Asmus developed a prototype 'statue cleaner' that was operated with a pulsed ruby laser with a pulse duration ranging between 0.6 and 1 ms (Asmus 1976). One year later, in 1977, the first Nd:YAG laser (λ = 1060 nm) promising enhanced applications was presented also by Asmus and co-workers (Asmus, *et al.* 1977). He made it clear though, that since the suitability of a certain type of laser for a certain object is case specific, with regards to the appropriate wavelength and pulse duration, the laser is by no means a 'completely universal system' (Asmus 1978). This is true since a laser covering the entire parameter range that is required for removal treatments of diverse materials did not exist. Moreover, in 1986, Asmus stressed that although laser cleaning facilitated difficult jobs, it was hard to obtain uniform results (Asmus 1986).

In the meantime, in 1981, preliminary tests on the potential of dirt and varnish removal from easel paintings, using two different devices emitting 308 nm nanosecond pulses (XeCl excimer laser and TE-290 laser) with rather high fluences (~3 J/cm^2), were reported at the Canadian Conservation Institute (Carlyle 1981). This report is the first cited work on laser cleaning of paintings in the international bibliography. Problems, such as marks of the laser beam on the paintings after cleaning, paint discolouration, canvas singeing were encountered, but according to the authors the results were encouraging. It was suggested that advanced research was required to find the suitable wavelength or wavelengths for particular applications on paintings. Moreover, the authors suggested that a detailed investigation on interaction properties of common coatings and paint films with lasers, using mathematical models and studying absorption coefficients at several wavelengths, thermal conductivities, boiling points, was essential. Despite the lack of technical know-how, this report was an optimistic message for future investigations.

Investigations on the use of lasers for conservation were carried out in the late eighties in Europe, mainly in United Kingdom, France and Italy, while the laser industry was continuously evolving. In 1989, an Nd:YAG laser for the cleaning of a selection of objects such as marble, limestone, silver and stained glass was employed in the framework of a project in the Laboratoire de Recherche de Monuments Historiques in France (Orial and Gaufillet 1989). SEM investigations revealed that, while using a 12 ns pulse duration (Q-switched mode), the remaining surfaces were better preserved, in contrast to the millisecond pulse durations (normal mode), which resulted in diverse effects on the different objects. Marble and limestone surfaces were cleaned

successfully, but on the silver object there were dulling effects rather than cleaning and the stained glass exhibited vaporisation effects on the laser-cleaned surface owing to thermal mechanisms applied. Despite the side-effects, the authors obtained better cleaning rates than those reported by Asmus in 1976 (Asmus 1976) and given the success of the application on marble and limestone they suggested that the development of a commercial portable laser cleaning system should be investigated.

During the late 1980s, dedicated research on the cleaning of painted works of art became one of the top subjects of the fairly new established laboratories, the Institute of Electronic Structure and Lasers (IESL), of the Foundation of Research and Technology – Hellas (FORTH), in Heraklion of Crete in Greece. The researchers at FORTH collaborated closely with conservators of the National Gallery in Athens to understand the various tasks encountered on painting conservation. Judging from the progress made since then on the laser cleaning of painted works of art, the input of this technical know-how on both conservation and optical aspects in the potential of this method was successful. The first article describing this potential was published in 1993 (Hontzopoulos, *et al.* 1993). A detailed review on the progress of laser cleaning of painted artworks is illustrated in the next section (1.2.2).

In 1992, Cooper and co-workers carried out a comparative study on different types of lasers, including a short-pulsed krypton fluoride (KrF) excimer laser (λ = 248 nm), a dye (λ = 590 nm), a Q-switched Nd:YAG (λ = 1,060 nm) and a carbon dioxide laser (λ = 10,600 nm) for the removal of black encrustations from a limestone sculpture (Cooper, *et al.* 1992). The authors revealed that the best results were obtained with the Q-switched Nd:YAG laser, although either mode resulted in slight discolouration of

the substrate. Later in 1993 and 1995 the same group published the existence of a certain laser fluence range at which the removal of the unwanted layers from the limestone substrate is a 'self-limiting' process (Cooper, *et al.* 1993, 1995). In other words, the excessive absorbed laser photons after the total removal of the crust did not cause removal of the limestone substrate. In reality, the term 'self-limiting' is misleading, since other effects were taking place in the substrate demonstrated by discolouration, although there was no removal of the substrate. However, the authors regarded these results as being really encouraging and proposed to built a commercial system (Cooper 1994). At the time, affordable Nd:YAG laser systems became commercially available in Europe, which raised the interest of conservators and restorers (Teppo and Galcagno 1995).

In October of 1995 Fotakis and his co-workers organised an international workshop, called Lasers in the Conservation of Artworks (LACONA) in Crete, Greece (Kautek and König 1997), to discuss the development of the laser technology for conservation. This workshop had a significant impact bringing the conservation community closer to the new developments that enabled the implementation of the laser technology into practical work on the care of various objects. As a consequence, a second LACONA conference in 1997, held in Liverpool, United Kingdom, brought together a greater number of scientists and conservators. Subsequently, investigation towards the utilisation of laser technology in conservation was extended to the treatment of masterpieces, with some other conservation fields remaining under investigation. The success of these meetings, in terms of debates over particular problems, expertise exchange and establishment of collaborations, established LACONA as a biennial

international conference, with the third held in Florence, Italy in 1999 (Salimbeni and Bonsanti), the fourth in Paris, France in 2001 (Vergés-Belmin) and the fifth in Osnabrück, Germany in 2003 (Dickmann, *et al.* 2005).

Even from the first LACONA workshop in 1995, when the prediction on the impact of such a meeting was not possible, it was demonstrated that working with lasers had already started to integrate into the conservation profession in Europe. The submission of papers regarding laser cleaning investigations on architectural monuments (Calcano, *et al.* 1997, Vergés-Belmin 1997, Zehetner 1997), wall paintings (Shekede 1997), easel paintings and icons (Zergioti, *et al.* 1997), parchment (Kautek, *et al.* 1997), paper (Friberg, *et al.* 1997), stained glass (Olaineck, *et al.* 1997, Salimbeni, *et al.* 1997), metals (Cottam and Emmony 1997), archaeological human bones and skulls (Karoutis and Hellidonis 1997) outlined in the best possible way that investigation of laser-cleaning methods was spread in several research groups in Europe, each of which was focused in a certain category of materials comprising objects of enormous cultural significance. These papers had a historical importance, because they reflected the interest and the hope of the cultural heritage community, even though there was not any common international organisation for administration and funding for laser based research in conservation at the time. Later on, the growth in interest was such that more researchers participated in the LACONA international conferences from all around the world, with USA and Korea being the first countries breaking the evident European dominance.

Today, it is evident that Nd:YAG laser, operated in its fundamental (ω, λ = 1064 nm), second (2ω, λ = 532 nm), third (3ω, λ = 355 nm) and fourth (4ω, λ = 266 nm)

harmonics, is established as the most frequently laser tool employed for conservation applications. There are numerous examples in Nd:YAG laser cleaning on architectural and archaeological sites, metallic artefacts, paper, parchment, wood, textiles, fossils and wall paintings. For instance, today Nd:YAG laser is established as an essential tool for controlled cleaning treatments in architectural monuments (stones, sandstones, marbles etc.) in Italy (Appolonia, *et al.* 2000, Armani, *et al.* 2000, Lanterna and Matteini 2000, Pini, *et al.* 2000a, Sabatini, *et al.* 2000), France (Labourè, *et al.* 2000, Bromblet, *et al.* 2003), United Kingdom (Chapman 2000, Fowles 2000, Larson, *et al.* 2000), Austria (Calcano, *et al.* 2000), Germany (Siedel, *et al.* 2003) and Spain (Esbert, *et al.* 2003). Research on improving the laser cleaning applications with Nd:YAG laser is performed in France (Eichert, *et al.* 2000, Wazen 2000), Italy (Aldrovandi, *et al.* 2000, Margheri, *et al.* 2000, Siano, *et al.* 2000), United Kingdom (Feely, *et al.* 2000), the Czech Republic (Svobodova, *et al.* 2003) and Greece (Marakis, *et al.* 2003, Zafiropulos, *et al.* 2005). Research at IESL in Greece resulted in the resolution of the discolouration problem (Skoulikidis, *et al.* 1995, Alessandrini, *et al.* 1997, Vergés-Belmin 1997, Klein, *et al.* 2001) on laser cleaned marble and stone substrates. It was determined that yellowing is not effected when cleaning is performed under a regime of combined wavelengths of the fundamental and third harmonics (Marakis, *et al.* 2003). This technique is now being used for the cleaning of the Parthenon in Athens (Pouli, *et al.* 2005). Nd:YAG lasers are also employed for cleaning of metal artefacts with research in progress in Greece and the USA on the cleaning of daguerreotypes (silver coated copper photographic plates) (Golovlev, *et al.* 2000, Golovlev, *et al.* 2003), in the UK on lead sculpture (Naylor 2000), in Italy on gilded bronze (Matteini, *et al.* 2003, Siano, *et al.* 2003a), in France

and Greece on silver and copper threads (Degrigny, *et al.* 2003), in Korea and Sweden on silver threads (Lee, *et al.* 2003). Laser cleaning of paper is being studied using Nd:YAG lasers in Slovenia, Austria and Germany (Kolar, *et al.* 2000, Kolar, *et al.* 2003), Poland (Ochocinska, *et al.* 2003) and Spain (Perez, *et al.* 2003). Other Nd:YAG laser cleaning applications are on parchment, UK and Denmark (Sportun, *et al.* 2000) on wood, Germany (Wiedemann, *et al.* 2000) and UK (Cooper, *et al.* 2003) on cotton textiles, UK (Sutcliffe, *et al.* 2000) on fossils (Landucci, *et al.* 2000) and wall paintings (Gaetani and Santamaria 2000) in Italy.

Despite the wide use of the Nd:YAG laser there are cases in which other laser wavelengths were studied. For instance, XeCl and KrF excimer lasers (emitting at 308 nm and 248 nm respectively) were tested for the removal of black crust from sandstones in Greece and Germany (Marakis, *et al.* 2000) and a direct xenon flashlamp (UV and visible wavelengths) divestment technique was studied to remove lichen from marble (Leavengood, *et al.* 2000) in USA. For the cleaning of metals, other types of lasers have been also used, such as XeCl excimer laser (Pini, *et al.* 2000b) and Nd:YAP laser (λ = 1,340 nm) in Italy (Siano, *et al.* 2003b) and TEA CO_2 laser (λ = 10,600 nm) in Sweden (Koh and Sarady 2003). The XeCl excimer laser has been also used for detailed studies on the cleaning of parchment in Germany and Austria (Kautek, *et al.* 2000, Kautek, *et al.* 2003). Research on cleaning of stained glass has been studied extensively on the basis of KrF excimer laser in Germany (Drewello, *et al.* 2000, Fekrsanati, *et al.* 2000, Roemich and Weinmann 2000, Hildenhagen and Dickmann 2003a, Römich, *et al.* 2003). As discussed below, Nd:YAG lasers have been proven unsuitable for varnish removal from paintings. The

most suitable lasers have been proven to be excimer lasers emitting UV pulses, although other laser types and wavelengths have been proposed. The following section presents a review of the laser cleaning of paintings.

1.2.2 History of Research on the Laser Cleaning of Paintings

Twelve years after the first report (Carlyle 1981) a paper came to light describing the first thorough investigation on the use of excimer lasers to clean paintings (Hontzopoulos, *et al.* 1993). The authors reported preliminary work on the use of ultraviolet laser light as a tool for a range of art restoration applications, which was apparently motivated from similar treatments on polymers. The work was focused on whether short ultraviolet photons could induce an effective ablation of aged discoloured varnishes and/or inorganic and biological deposits from the surface of painted works of art. At the same time the authors were concerned with the potential for removing overpaintings from the original painting's surface. In addition, they discussed the possibility of online control during the laser ablation of art objects. The analytical techniques proposed then were digital image processing and reflectography. Later in the same year, Morgan (1993) published a paper reporting that excimer lasers were utilised for the restoration of fourteenth century icons with satisfactory results. In 1995, Fotakis published a paper describing the potential for laser cleaning of artworks based on preliminary experimental results of the research group at FORTH (Fotakis 1995). In the same year, 1995, in the framework of the first LACONA workshop, the research group of FORTH, teamed with conservators from the National Gallery in Athens, presented results on some case studies restored with excimer lasers (Zergioti, *et al.* 1997). It was reported that nanosecond excimer lasers could be

employed for three painting conservation tasks that should be approached separately depending on the interactions and the mechanisms evolved. The tasks included (i) the removal of aged varnishes and/or contaminated regions of the painting's surface, (ii) cleaning of the support material and (iii) the removal of overpaintings. Laser Induced Breakdown Spectroscopy (LIBS) along with reflectography was proposed to provide online monitoring, which would certify the safety of the artwork during the laser cleaning procedure. The researchers at FORTH set up an experimental workstation comprised of a computer controlled x-y-z mechanical translator on which the painting was mounted (see Chapter 3). The laser beam was delivered onto the surface by a series of optics, and image processing techniques along with broadband reflectography and LIBS were incorporated in the system with the intention of continuous and online monitoring.

In 1997 the FORTH team presented their progress on laser applications for painted works of art (Fotakis, *et al.* 1997, Zafiropulos, *et al.* 1997). It was made clear then that they did not only consider lasers as a means for implementation of cleaning but also as a complete tool for analysis prior, during and after the laser cleaning process. Their concept was to develop a system that would provide cleaning applications, analysis of pigments and media, imaging techniques of surface and underlying layers, authentication applications and diagnostics of defects of surface and/or infrastructure, which may be induced during and after the laser cleaning process. Alongside the optimistic message delivered in these papers the authors implied that everything was still under investigation. As far as the cleaning process was concerned, they addressed some major issues under investigation, which were: (i) the required laser parameters,

such as the appropriate ultraviolet wavelength, the suitable fluence and pulse duration, (ii) the ambient conditions in which the cleaning should occur and (iii) the material's optical and thermodynamic parameters, such as absorptivity, heat capacity, thermal diffusivity and conductivity. They insisted on the employment of excimer lasers and therefore attempted an abstract rationalisation of the photochemical, thermal and mechanical effects on the resinous materials, when interacting with such lasers. Information on laser ablation rates for dammar resin and gum lac when interacting with a nanosecond KrF excimer laser were also provided. Unfortunately the preprints of the second LACONA conference in Liverpool were never published but the results described in these papers appeared elsewhere (Zafiropulos and Fotakis 1998). The authors proposed image processing and LIBS as the main techniques to be applied for online monitoring. With respect to the effectiveness of the procedure and the safety of the artwork it was stressed that the user should consider keeping a thin layer of the aged varnish on the painted surface to prevent the excess of UV photons penetrating the paint layers. Penetration of UV photons could result in devastating effects, like medium ablation, pigment desorption and paint discolouration.

As a consequence of the progress of these studies, a major European project (1998) was shared between several research institutes, industrial and conservation companies from Germany, Greece, Ireland, the Netherlands, Portugal and Spain. The project aimed at developing a laser cleaning workstation, operated with excimer lasers based on advances at IESL-FORTH (Zergioti, *et al.* 1997). Preliminary results of this European collaboration were presented in 1999, in the framework of LACONA III (Scholten, *et al.* 2000). The excimer laser beam, delivered at the output of the laser

unit, was directed within an optical arm that allowed both the laser and the work of art to remain still during the operation. The optical arm contained a set of UV mirrors, appropriate for the particular UV laser wavelength, in a 'periscopic' configuration. Upon the user's commands via specialised software, the mechanism allowed the arm to move and rotate across the surface of the painting, maintaining the same laser beam profile and the orientation of the etching spot. At the same time the distance between the convex lens, into the scanning head of the optical arm, and the surface of the painting remained constant, keeping the selected operating fluences as well as the obtained spot sizes unchanged. In addition, several optical fibres connected to a spectrograph were attached to the scanning head providing online LIBS, while laser cleaning was in progress. In case of total removal of the varnish layer/s, which can be monitored online using LIBS providing spectroscopic identification of pigments into the ablation plume, the laser irradiation at the particular area would automatically cease and the process would continue at a neighbouring area with the coating that required removal.

In parallel with this collaboration, another project was conducted in the UK on researching the potential of excimer laser cleaning of easel paintings. On the basis of this project, Hill and co-workers (2000) tested the ablation characteristics of several varnishes using a XeCl excimer laser (308 nm) and noted that there is a threshold fluence at 100 mJ/cm^2, under which neither varnish ablation nor pigment discolouration occurs. With regards to discolouration the authors referred to an unpublished paper submitted in LACONA II, in which they described discolouration effects detected on pigments on laser irradiation on the basis of XRD analysis. In

agreement with previous work at FORTH, as well as with the partners of the aforementioned EU project, Hill and co-workers reported that a residual varnish layer should be left on the painted surface to prevent damage to the underlying layers. In line with the up to then knowledge they also stressed the requirement of online control and monitoring of the cleaning process. They proposed Laser Induced Fluorescence (LIF) and Thermal Wave Detection (TM). The former technique would address the fluorescence of the gradually removed varnish and TM would determine the remaining thickness of the varnish layer/s based on the thermal wave phase shift. Given that the thickness of the varnish layer to be left on the paint should be larger than the absorption depth (optical length) of the cleaning laser, the authors suggested that the cleaning application should terminate at the point, which yields the highest fluorescence on the basis of LIF.

In 1999 Scholten and co-workers (2000), reported tests on the effects of UV laser cleaning on egg tempera dosimeter systems of which the molecular structures and the ageing processes are well-understood (Odlyha, *et al.* 1997). They recognised some chemical processes in egg tempera (Van den Brink, *et al.* 1997) that could be used to monitor the effects of the UV laser. At the same time Athanassiou *et al.* reported a study on the KrF excimer laser-induced discolouration of iron oxide yellow pigments into linseed oil, based on XRD, LIF and Raman spectroscopy (Athanassiou, *et al.* 2000). In some cases, raw sienna and yellow ochre, discolouration was quite intense and it was attributed to thermally generated, release of water molecules from the crystal lattice of the pigments. Although the examined pigments are principally composed of the mineral goethite, FeO(OH), after the 248 nm laser intervention

haematite, Fe_2O_3, and – possibly – magnetite, Fe_3O_4, were formed. However, discolouration was also traced after laser cleaning on substrates of lead chromate, $PbCrO_4$, which does not contain water. The authors concluded that discolouration of pigments embedded in linseed oil, could be also due to discolouration of the linseed oil or the impurities therein. It should be mentioned though that for this particular study a critically low laser fluence of the order of 100mJ/cm^2 was employed. As described in the next section, working with such low fluences, approaching the ablation threshold of the ablated film, thermal mechanisms apply on the surface caused upon vaporisation. Thus, these observations may be attributed to these effects.

In 2001 in Paris (LACONA IV), the partners of the EU project (1998) presented two papers on their progress (Castillejo, *et al.* 2003, Teule, *et al.* 2003). An effect study on KrF excimer laser treated egg tempera dosimeter systems was carried out with reflectance spectrophotometry, CIE - $L^*a^*b^*$ colorimetry, LIF, LIBS, FT-Raman, FTIR, DTMS, LDI-MS, MALDI-MS, while surface morphology changes were studied with stylus profilometry. The UV radiation doses absorbed by the underlying layers were determined by *in situ* transmission studies, during the laser pulse irradiation on samples applied on quartz plates. Upon direct laser irradiation, most of the pigments of the paint systems tested showed diverse degrees of discolouration, as reported by Castillejo and co-workers (Castillejo, *et al.* 2002, Castillejo, *et al.* 2003). Discolouration was observed only at a few micrometers from the surface of these samples. The same paint systems were not discoloured when a residual varnish layer was left on the surface. Pigment discolouration effects were attributed to either a change in the oxidation state of the pigment (Zafiropulos, *et al.* 2001) or to formation

of a thin layer of charred particles formed by laser intervention in the organic material (Teule, *et al.* 2003). MALDI-MS analysis indicated that deterioration of the post-aged, laser ablated, egg tempera binding medium might have developed as a long term effect and the authors suggested that further investigations should be carried out on this particular issue. UV transmission studies showed that it is possible to adjust the laser parameters so as to maximise and/or localise the absorption of the UV photons in the varnish layer/s and prevent, or minimise, their transmission into the underlying paint layers. According to the authors, a few trials of excimer laser cleaning on old paintings had encouraging results. A discoloured varnish was partly removed, since it was observed that after thinning the varnish, the painted surface appears more saturated and 'cleaned'. Successful removal of an unwanted retouching layer and of a black carbonised layer on top of a varnished painted surface were also reported (Teule, *et al.* 2003).

Along with the abovementioned studies on pigment discolouration, the interaction of pigments with infrared lasers has also been studied. Papers from the United Kingdom (Pouli and Emmony 2000) and Italy (Sansonetti and Realini 2000) determined that pigment discolouration effects are also obtained with Nd:YAG laser pulses. Based on both experimental and theoretical analytical data, it was recently determined that the discoloured layer on cinnabar particles is concentrated on the irradiated outer surface of the pigments in a depth of a few tens of nanometers (Luk'yanchuk and Zafiropulos 2002). This effect was attributed to the sharp temperature dependence of the nucleation rate on the irradiated part of the pigment particle and therefore the

thickness of the discoloured layer, i.e. formation of metacinnabar, is significantly smaller than the heat penetration depth or the optical absorption depth of the pigment.

Additional work on cleaning processes has been carried out on the removal of black candle stain, comprised of soot and dirt, from the surface of a Russian icon using the third harmonic of Nd:YAG lasers, with the authors reporting satisfactory results (Hildenhagen and Dickmann 2003b). A radical alternative on the laser cleaning of painted surfaces was discussed by De Cruz, Wolbarcht and co-workers (1999, 2000). This group proposed a mixed method based on thermal vaporization of a solvent wetted painted surface with means of Er:YAG (λ = 2940 nm). A critical condition for this method was that the solvent should be very polar, and therefore it could be just water, to reduce the vast thermal diffusion of the surface due to the long wavelength employed. The authors suggested that following an incident Er:YAG pulse, the phase change of water into steam, prevents the thermal damage of the underlying painting's layers. In this method, the hydroxy bond of water is the main absorber at the 2940 nm laser wavelength, although it was acknowledged (de Cruz, *et al.* 2000) that the exact wavelength for the highest absorption of hydroxyl groups in the near and mid infrared electromagnetic region is quite ambiguous (Centeno 1941, Bayly, *et al.* 1963, Bramson 1968, Robertson and Williams 1971, Vodop'yanov 1988, Zafiropulos, *et al.* 1999). According to the authors, the application on a few case studies had encouraging results (de Cruz, *et al.* 2000), although no analytical results were demonstrated. In 2001, a paper from the same group collaborating with researchers from Italy was submitted for the preprints of LACONA IV (Bracco, *et al.* 2003). The team tested the laser cleaning efficiency in artificially aged samples and old paintings.

The auxiliary hydroxylated wetting liquids prior to laser operation comprised mixtures of water with alcohols and aliphatic hydrocarbons with glycols. After treatment, the surfaces of the samples demonstrated increased scattering as well as a melted texture resulted from the vast heat exposure due to the 2940 nm photons. However, the authors were more satisfied with the results obtained on paintings, but no analytical results were presented regarding the morphology or the chemistry of these paintings after application (Bracco, *et al.* 2003). In the above work no reference was made to the swelling and leaching of the binding medium and the potential of some defects on the paint upon the diffusion of polar solvents (Stolow 1971, 1985, Phenix 2002a, b). It should be reminded that paintings with eighteenth and nineteenth solvent-sensitive media (Shepherd 1984, Swicklik 1993, Cove 1998, Jones, *et al.* 1999) or other works with original retouchings by the artist, such as in the case of Delacroix or Turner (Swicklik 1993), are extremely susceptible to chemical treatment. Hence, such a method should be not appropriate for these cases. The concept of using a laser to treat painted surfaces is to avoid the use and the disadvantages of solvents, especially if the degree of polarity thereof is as high as that of water.

In contrast to the alternative laser wavelengths and techniques tested, most of the studies up to date have revealed that ultraviolet laser pulses with duration of about 25 nanoseconds or less obtain the finest results with respect to varnish removal. In a good agreement with the studies described above, this argument was once more verified in a recent study on the contribution of 1064 nm, 532 nm, 355nm, 351 nm (XeF excimer) and 248 nm (KrF excimer) pulsed lasers to the removal of a wide range of adhesives, consolidants and varnishes used by artists (Madden, *et al.* 2005). The

authors concluded that, as far as the varnish removal is concerned, no better results could be obtained with any laser beam other than that provided by the excimer laser radiation.

1.3 Fundamentals of UV-pulsed laser interaction with organic coatings

UV laser processing of polymerised materials is nowadays accepted as a delicate tool offering advantages, which cannot be met with any other technique. Some of the advantages are micrometer precision in the removed material, with minor thermal degradation to the remaining film depending on the UV pulsed laser wavelength; a high degree of reproducibility, given that the application parameters and the material are kept identical; a large decrease in the time needed for such a fine etching facility, in contrast to long times required for similar applications with 'conventional' methods; a remarkable resolution and control of the etching; and the potential to interact with a variety of laser induced analytical techniques for online control or analysis along the process. The same advantages apply to the laser cleaning of paintings based on excimer lasers, as far as the removal of discoloured and deteriorated varnishes is concerned. Therefore this section provides a description of the fundamental mechanisms of UV pulsed laser ablation as has been studied mainly on polymers and is expected to apply to aged varnishes (Georgiou, *et al.* 1998).

1.3.1 UV- pulsed lasers

In short, UV pulsed lasers are emitted by appropriate excitations of various media. The only solid-state laser that can produce UV pulsed radiation is the Nd:YAG laser, which genuinely emits at 1064 nm. However, by the appropriate multiplication of its

emission frequency, i.e. third, fourth or fifth harmonic, it emits monochromatic radiation at characteristic wavelengths of 355, 266 or 213 nm respectively. Emission of all other UV pulsed lasers is based on discharge generation in gas mixture media. These lasers are generally termed as excimer lasers because they generate 'molecules' based on the association of an excited atom with another atom in its ground state (Srinivasan and Braren 1989, Azema and Laude 1994, Srinivasan 1994, Bäuerle 2000). The commercially available UV-pulsed lasers, shown in Table 1.3.1, up to

Laser	Wavelength (nm)	Photon Energy (eV)	Pulse duration	Absolute Maximum Pulse Energy (Joule)
Excimer Laser Types/Active Medium				
F_2	157	7.9	10-30 ns	0.060
ArF	193	6.42		0.8
KrCl	222	5.58		0.2
KrF	248	5		2
XeCl	308	4.03		3
XeF	351	3.53		0.65
N_2	337	3.68		0.01
Pulsed Solid-State Laser				
Nd:YAG	1064 (ω)	1.17	normal mode: ms Q-switched: ns	100
	532 (2ω)	2.33	ns	1
	355 (3ω)	3.50		0.75
	266 (4ω)	4.66		0.2
	213 (5ω)	5.82		0.01

Table 1.3.1 Commercially available UV pulsed lasers. Excimer lasers are the most common although Nd:YAG laser can also emit UV radiation.

248 nm cause direct photo-dissociation leading to bond-breakage with minor or no thermal effects on the surface of the treated organic coating, depending mainly on the laser wavelength but also on the application parameters (Srinivasan and Braren 1989, Srinivasan 1994, Bäuerle 2000).

In general, excimer lasers are considered as the ideal sources for demanding and highly controlled applications in diverse fields, such as analytical chemistry (Karas and Hillenkamp 1988, Tanaka, *et al.* 1988, Bäuerle 2000, Hillenkamp and Karas 2000), microelectronics (Boyd 1992, Tam, *et al.* 1992, Azema and Laude 1994, Chrisey and Hubler 1994, Miller and Haglund Jr 1998) and medicine (Azema and Laude 1994, Bäuerle 2000). The reason of their successful input in scientific communities is mainly ascribed to the following factors: (i) their highly multimode output containing about 10^5 transverse modes, (ii) the high photon energies provided by the short UV laser wavelengths, (iii) the high energy per pulse of some excimer laser beams, namely that of KrF and XeCl excimer lasers, (iv) the short pulse durations, which are typically in the nanosecond scale (1ns = 10^{-9}sec), and (v) the high relative homogeneity in the beam profile: top-hat and Gaussian profiles in direct directions.

The multimode output permits optimal applications with no or negligible interference drawbacks, which could be problematic when using imaging applications (Bäuerle 2000). The high UV photon energy provides a direct photodissociation of the irradiated molecules. In addition there is a strong optical absorption, which prevents an optical penetration deeper than a few microns into the treated surface. In pursuit of controlled removal or cleaning applications of organic resin and/or polymer films, the films should have a critical thickness, greater than the inverse absorption coefficient for the particular laser wavelength employed (Srinivasan 1994, Bäuerle 2000). This feature should be taken into account when determining the thickness of a remaining

processed film, especially if that film must completely absorb the incident laser radiation to prevent transmission into radiation sensitive underlying layers.

The high energy per pulse provides a considerable advantage in laser cleaning processes that require scanning processes, such as the proposed application for removal of aged varnishes (Zafiropulos 2002). Experimentally, it has been observed that the pulse energy of 2 Joule per pulse of the KrF excimer laser suffices for the predominance of the photochemical action upon ablation of aged varnishes. Looking at the equivalent wavelength of Nd:YAG laser, i.e. 266 nm, 4ω (Table 1.3.1), it is seen that the pulse energy (0.2 Joules/pulse) is ten times less than that of the KrF excimer laser (2 Joules/pulse). At 213 nm, 5ω of Nd:YAG laser the pulse energy becomes 200 times less than that of KrF excimer laser. Thus, the laser beam of KrF excimer laser can be better manipulated in terms of applications, such as the laser cleaning of paintings, where large spots are utilised for sufficient scanning of an aged varnish (Zafiropulos and Fotakis 1998). This is not readily obtainable with Nd:YAG lasers. The short pulse duration allows for spatially and chemically stoichiometric ablation with virtually no damage to the surrounding material, in particular for heat sensitive coatings and multi-component substrates (Bäuerle 2000). Finally, the relatively high homogeneity permits a fine manipulation of the incident laser beam on the surface and therefore uniform patterns can be obtained by employing the appropriate overlapping parameters.

Especially for the application on painting's varnishes the most commonly employed laser wavelengths are 248 nm and 193 nm of KrF and ArF active media respectively

(Zafiropulos 2002). These particular lasers permit the choice between the high pulse energy with negligible thermal effects of the former and the neat photochemical interaction of the latter. Since the pulse energy of KrF excimer laser is more than double than that of the ArF laser, the former is the most common choice for treatments on paintings, although it has been pointed out that for delicate applications ArF excimer laser ablation is recommended (Zafiropulos 2002).

Using excimer lasers, the rate of a laser based cleaning process, e.g. aged varnish removal, can be really fast, since the repetition rate of excimer lasers ranges between a few Hz and 1 KHz. However, mechanical stresses and heat accumulation on the treated films upon high repetition rates should be taken into consideration. These effects have not been reported under low repetition rates of a few Hz. It should be also considered that excimer lasers have low power efficiency, since the laser power output is only up to 3% of the electrical input power required (Bäuerle 2000). Finally, the potential users must take into account the high operation cost, which increases considerably with decreasing wavelengths and with shortening of the pulse durations, especially in picosecond and femtosecond (10^{-15} sec) scales.

1.3.2 Laser Ablation; a Definition

At this point a definition of the term ‘laser ablation’ is attempted since it characterises a certain interaction. Although Asmus used the term ‘ablation’ to describe material ejection from the surface of the object to be cleaned as a result of the action of very short IR laser pulses (Asmus 1978, 1986), the term ‘ablation’ is being normally used to describe a direct bond-breakage process upon UV laser pulses resulting into selective dissociation of polymer surfaces. This remark has been previously made by

Watkins (1997) in the opening paper of LACONA I and is very useful especially nowadays that a wide range of laser wavelengths are utilised for various conservation tasks. According to Watkins, 'spallation' describes the former IR laser induced action more precisely. The term spallation might also imply other actions in the implementation of IR laser pulses determined by Asmus, such as selective evaporation of encrustation; surface scouring by rapidly expanding vapours requiring water application prior to IR laser irradiation; and, delamination of superficial deposits based upon thermal expansion mismatch with the substrate (Asmus, *et al.* 1973a, Asmus 1978, 1986). Asmus has also established that IR laser irradiation can be also employed for thermal and photodecomposition of superficial layers that are subsequently easily removed by washing, and removal of small adherent particles as a result of selective excitation of the particles or the substrate. It is clear that none of these mechanisms are involved in the selective removal of aged varnishes or paint layers with UV laser pulses (Zafiropulos and Fotakis 1998, Zafiropulos 2002). This mechanism is better defined in UV laser induced polymer processing.

Upon the incidence of an ultraviolet laser pulse onto a polymerised surface a clear acoustic signal demonstrates the nature of the interaction between the group of the UV laser photons in the pulse and the surface of the material involved (Gorodetsky, *et al.* 1985, Dyer and Srinivasan 1986, Azema and Laude 1994, Srinivasan 1994, Bäuerle 2000). As a consequence of this interaction, the material, having absorbed the UV laser photons, escapes the surface with immense velocities of the order of $10^3 – 10^4$ m/sec (Danielzik, *et al.* 1986, Srinivasan, *et al.* 1987, Srinivasan and Braren 1989, Srinivasan 1994, Bäuerle 2000). Fragments from the surface are forced to ejection and

entrained into the gas phase forming a rapidly dispersing plasma, which is commonly noticeable with naked eye owing to a simultaneous light emission (Srinivasan and Braren 1989, Srinivasan 1994, Bäuerle 2000). The generated laser plume may extend up to a few millimetres from the surface, depending on the compounds involved and the energy of the pulse responsible for this action (Srinivasan and Braren 1989). Provided that parameters, such as the laser wavelength, the pulse duration, the repetition rate, the fluence and the chemistry of the organic substance employed are under a certain control, this rather violent feature of the UV laser-matter interaction results in a well-defined etched spot on the surface of the processed organic substance (Srinivasan and Braren 1989, Azema and Laude 1994, Srinivasan 1994, Bäuerle 2000). This interaction is described by the term 'ablation', which comes from the Latin word 'ablatio' and contains the meaning of removal.

1.3.3 Mechanisms of Excimer Laser Ablation

In this section a short description is given of the mechanisms that occur upon the incidence of a UV laser pulse, while the short and long terms effects on selected laser ablated coatings are investigated in Chapters 3, 4, 5 and 6. Upon infrared laser pulses the molecular bonds of an irradiated substance are significantly thermalised, so that if this substance is an organic film, i.e. resin or polymer, the immense temperature increase results in its melting with some material loss that is described with the term 'vaporization' (Bäuerle 2000). If the temperature increase is vast it can cause very intense stresses in the material that may result in explosive vaporization, significant melting and interfacial detachments when two films are attached. IR laser pulses are evidently unsuitable for the dry ablation of aged varnishes. Laser pulses with

wavelengths shorter than 200 nm, such as the 193 nm ArF excimer laser, providing electronic excitation energies as high as 6.2 eV result in neat photochemical interactions and pure desorption of ablated photofragments with no thermal effects (Küper, *et al.* 1993). Investigation of short wavelength laser pulses with polymers has shown that the photochemically dissociated bonds undergo such stresses that the ablated material is finally desorbed via localised photomechanical forces. ArF excimer laser is recommended only for selective, very delicate cases since the application can be extremely lengthy and therefore expensive (Zafiropulos 2002), because of the moderate pulse energy (0.8 Joules maximum) that requires considerable consumption of the gas medium. This is probably the only disadvantage of this laser for applications such as conservation.

The question of what mechanisms dominate UV pulsed laser ablation at wavelengths longer than 200 nm, has brought many contradictions to light among research groups, especially with respect to the ablation of polymers. This is because KrCl, KrF, XeCl and XeF excimer lasers emitting at 222 nm, 248 nm, 308 nm and 351 nm in that order generate both photochemical and thermal effects (Luk'yanchuk, *et al.* 1993a). Factors, such as the large number of species formed with high translational energies, and the absence of equilibrium between translational, vibrational and rotational temperatures within the ablated products, are used in favour of the domination of the photochemical mechanisms. In contrast, the Arrhenius-type behaviour of the ablation rate (see Chapter 3) near and under the ablation threshold (Küper, *et al.* 1993), is the strongest argument in favour of additional participation of thermal mechanisms. Thus, in UV laser ablation of organic films, both thermal and photochemical mechanisms apply

(Dyer and Srinivasan 1986, Srinivasan, *et al.* 1986b, Sutcliffe and Srinivasan 1986, Yeh 1986a, Luk'yanchuk, *et al.* 1993a, b, Luk'yanchuk, *et al.* 1994, Luk'yanchuk, *et al.* 1996, Bäuerle 2000) and the application is called photophysical ablation. Investigations based on theoretical models have shown that the temperatures obtained in photophysical ablation are much lower than in pure thermal ablation (Luk'yanchuk, *et al.* 1996). It has been also pointed out that the thermal effects are profoundly less than the photochemical ones, in particular as the wavelength decreases. Despite the existence of a few thermal effects, photophysical ablation was finally viewed through the ability of the UV laser photons to result in direct bond-breakage (Srinivasan 1984, Yeh 1986a, Sauerbrey and Pettit 1989, Srinivasan and Braren 1989, Cain, *et al.* 1992a, Cain, *et al.* 1992b, Küper, *et al.* 1993, Pettit and Sauerbrey 1993). Most of these studies show that laser pulses up to 248 nm result mainly in bond-breakage, while the lack of thermal damage on the remaining heat-sensitive films ensures that the thermal effects are negligible. This fact along with the higher pulse energy of KrF excimer laser compared with lasers of shorter than 248 nm wavelengths make the KrF excimer laser the most efficient laser for the ablation of paintings' coatings (Zafiropulos and Fotakis 1998).

Figure 1.3.3.1 delineates the different temporal stages of photophysical ablation upon the incidence of a laser pulse with UV photons of moderate energy ($E < 6.2$ eV) on organic materials. As mentioned above, the incidence of a laser pulse is signified by a typical acoustic signal shown in Figure 1.3.3.1(a) (Gorodetsky, *et al.* 1985, Dyer and Srinivasan 1986, Azema and Laude 1994, Srinivasan 1994, Bäuerle 2000). Surface excitations due to single- and/or multiphoton action (Srinivasan, *et al.* 1987,

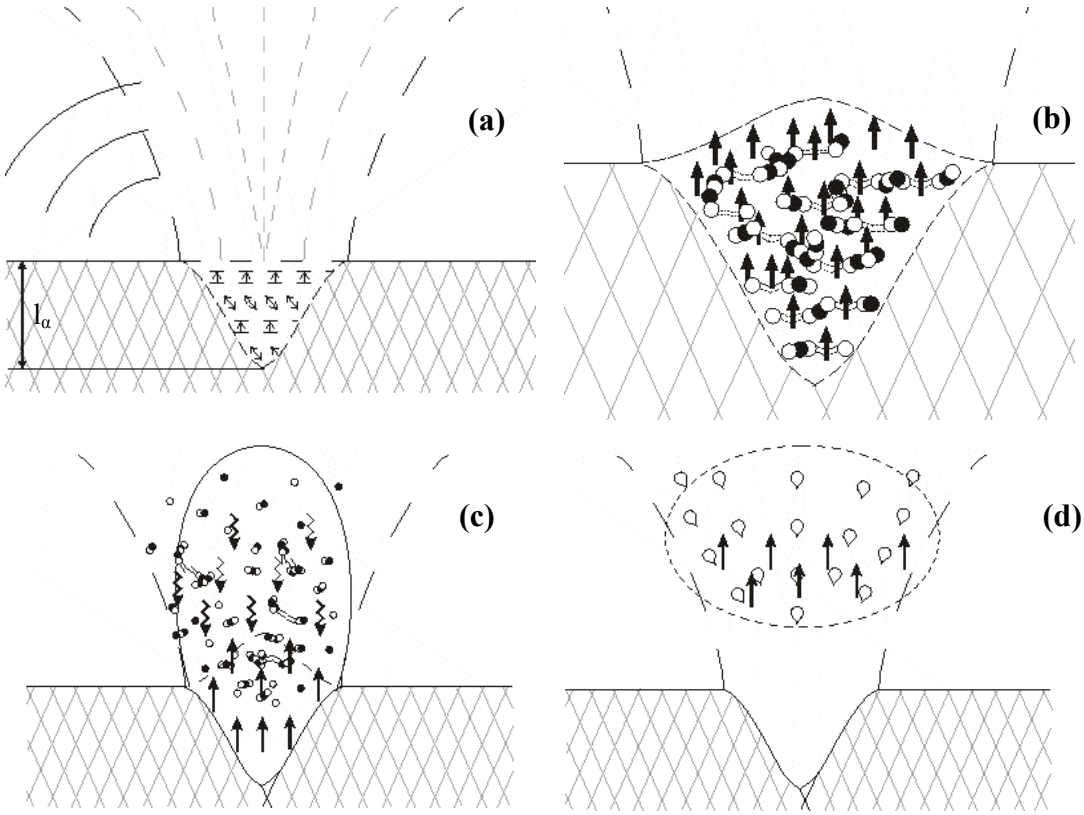

Figure 1.3.3.1 Different temporal stages of photophysical laser ablation upon the incidence of a single UV pulse: **(a)** Incidence of pulse followed by acoustic signal ( ) and surface excitations into the irradiated substance along the optical absorption length, l_α. The electronic excitations involve elevation to higher electronic states ( ) and vibration upon return to the ground states ( ). **(b)** Initiation of bond-breakage, minor temperature increase, mechanical stresses, instant surface swelling and pressure among the excited compounds. **(c)** Final bond-breakage, desorption of species into the gas phase, accompanied by light emission ( ), corresponding to a first stage of energy dissipation, and then thermal dissipation ( ) into the plume. **(d)** Liquid phase succeeding the gas phase a few μs after the incidence of the pulse. The melted compounds into the plume transformed into droplets are blown away with high velocity.

Srinivasan and Braren 1989, Pettit and Sauerbrey 1993, Bäuerle 2000) are considered as the initial act of the process (Bäuerle 2000). Owing to photochemical mechanisms single- and multiphoton excitations to higher electronic states result in ionisation and decomposition of the irradiated molecular systems with minimal heat formation. The latter is generated as soon as the electronic excitations of the involved bonds return from elevated to ground states, where vibrational manifold activity result in thermal

energy dissipation (Srinivasan and Braren 1989, Luk'yanchuk, *et al.* 1993a, Bäuerle 2000).

The distribution of chromophores in the irradiated surface and the property of transport of the electronic excitations between those chromophores, determine the distribution of excitations upon the absorption of the laser photons (Birks 1970, Berlman 1973, Frank, *et al.* 1985). The photon excitations of the surface generate electron-hole pairs, which alter the optical properties of the ablated material and thereby its interaction with the incident laser light (Bäuerle 2000).

Free radicals, formed in the irradiated surface upon direct laser photodissociation, become the main carriers of the laser photons (Bäuerle 2000). Some of these radicals may recombine inside the bulk, while others diffuse or finally desorb with rates dependent on their relative concentration in the irradiated surface area. The recombination reactions are indicated to be direct, that is the case when two laser-generated free radicals react with each other to form a new or the parent molecule. Moreover, multi-carrier (Auger) recombinations have been also observed. For sufficient ablation the laser photons must generate a greater rate of electron excitation compared to the rate of energy dissipation occurring via various reactions. Thus, the electrons participating in molecular bonds become highly excited and obtain the essential energy to produce electron-hole pairs, resulting in ionisation of the surrounding molecules (Bäuerle 2000). This effect involves high electron densities and is known as avalanche ionisation.

At intermediate wavelengths, such as 248 nm, and when the optical penetration length is longer than the heat penetration depth (Futzikov 1990, Cain, *et al.* 1992a, Bäuerle 2000), the photochemical mechanisms are more important than the thermal ones and the interaction proceeds with direct bond-breakage of the irradiated compounds within the surface. This is represented in Figure 1.3.3.1 (b). The initiation of the bond-breakage procedure causes mechanical stresses and pressure among the compounds, which force them away from the surface. Stresses of this nature are termed shock waves (Koren 1988, Kelly, *et al.* 1992), which along with a moderate temperature rise cause an instant and localised surface swelling followed by volume explosion of the masses from the area that received the pulsed laser radiation dose. The ejecting mass compresses the material that is ahead of it and eventually forms a blast wave (Dyer and Sidhu 1988). However, if the energy density of the pulse is low, as occurs when low fluences near the ablation threshold are employed, surface excitations are so low that they result in incubation effects (Sutcliffe and Srinivasan 1986, Küper and Stuke 1988, Meyer, *et al.* 1988, Chuang and Tam 1989). In that case the rate of electron excitation is lower than the energy dissipation from the irradiated species, thereby requiring a few UV pulses to modify the optical properties of the substance before some (minimal) ablation yield is obtained. When this happens, the rate of compound desorption becomes relatively stable. As will be demonstrated in Chapter 3, it is not recommended to work in this low fluence regime for the ablation of aged varnishes applied on paintings, because the thermal effects near the ablation threshold maximise owing to an Arrhenious-type behaviour (Luk'yanchuk, *et al.* 1994).

Figure 1.3.3.1 (c) delineates the desorption of the species from the surface while their bonds are being broken under simultaneous light emission, corresponding to a first stage of energy dissipation. The chromophores that had absorbed the UV photons, which, with 248 nm laser pulses, are mainly carboxylic acid groups (Srinivasan and Braren 1989), break down to various photofragments including gaseous products, such as CO and CO_2, that finally drive the resulting plume away from the surface (Dyer and Srinivasan 1989). In that instance the desorbed compounds are like an expanding gas and therefore this stage of the plume is described as the gas phase. After sufficient bond-breakage and while the photo-fragments are already into the gas phase, the species relax from their photochemical photon excitation and return to their electronic ground states. Due to the minor thermal photon excitations, the vibrational manifolds of their ground states are still excited. After a second relaxation time their excitation energy dissipates into heat, while the ablated products are still in the gas phase (Bäuerle 2000).

The increase of the temperature within the gas phase results in melting of the species and for a short time window, of the order of a few μs after the pulse incidence, liquid droplets might form as represented in Figure 1.3.3.1 (d). This step was determined by ultrafast, zoomed photos taken during the ablation of polymethyl methacrylate (PMMA) using a KrF excimer laser (Srinivasan 1993). At this stage the plume is described to be like a spray rather than a gas, suggesting that there is a liquid phase succeeding the gas phase. The high velocities (Danielzik, *et al.* 1986, Srinivasan, *et al.* 1987) that the compounds obtain prevents them sticking on the ablated surface and the plume expands far away. If this final step of thermal energy dissipation is active

before all excited compounds are far enough from the surface, the last photofragments still within the surface would be vaporised and stick around the walls of the ablated spot (Srinivasan and Braren 1989). Therefore, a critical condition for controlled laser ablation of polymerised substances is the requirement of longer chemical than thermal relaxation times (Bäuerle 2000).

In addition, time also plays a crucial role in terms of the duration of the UV-laser pulse. Before the laser pulse comes to an end and with increasing time, the ablation products desorb from a decreasingly smaller, central portion of the irradiated spot. This characteristic of the excimer laser ablation on polymers was suggested to be disastrous (Dyer and Srinivasan 1989). According to Srinivasan this phenomenon is caused by the asymmetric shape of the laser beam, which is stronger in its centre and weakens with radial distance (Srinivasan 1993). If the laser pulse is long enough to irradiate the substrate, while the ablation plume is in progress, which is often the case for nanosecond pulses, the ablation products absorb and scatter the incident radiation. This causes a well-defined effect termed screening (Brannon, *et al.* 1985, Keyes, *et al.* 1985, Srinivasan, *et al.* 1986a, Sutcliffe and Srinivasan 1986, Küper and Stuke 1988, Mahan, *et al.* 1988, Sauerbrey and Pettit 1989, Futzikov 1990, Cain, *et al.* 1992a, Soberhart 1993) that results in critical elimination of the excessive laser energy before reaching the substrate. The extensive irradiation that is scattered and absorbed by the species in the plume causes rapid collisions between photons, electrons and photofragments resulting into various degrees of ionisation (Bäuerle 2000).

1.3.3.1 The Influence of Relaxation and Reaction Times

The degree of selectivity of the laser ablation process is determined by the ratio of the rates of excitation and relaxation, and the reactions of the irradiated species as a function of their lifetime during the different temporal stages of their excitation (Bäuerle 2000). The ablation becomes more selective, when the excitation rate is higher than the relaxation rate. It should be acknowledged that relaxation is not a simple process, because it is highly depended on various reactions that occur between the irradiated compounds. Therefore, it is practical to separate the temporal stages of excited species in the following time windows: t_{E^*}, the time required for the desorbed compounds to react (between each other) in their electronically excited states; $t_{E,}$ the time in which the compounds may react after returning into their vibrationally excited ground states; and t_{Th}, the time required for a final thermal relaxation (Bäuerle 2000). If t_{Ex}, is set as the time frame for both excitation and desorption of a compound from the irradiated surface, the following points have been determined: (i) If the time required for thermal relaxation of the excited compound, t_{Th}, is much shorter than the excitation and desorption time, i.e. $t_{Th} << t_{Ex}$, as commonly happens with IR laser irradiation, the process proceeds with surface thermalisation, melting and/or explosive vaporization; (ii) If $t_{Th} \geq t_{Ex}$, the process is mainly photochemical or photophysical. Hence, using UV pulsed lasers the latter condition is fulfilled.

In the $t_{Th} \geq t_{Ex}$ regime, the excited compound obtains the energy to react with another excited compound, or with the substrate. The second case might occur if the stresses in the ablated surface are not strong enough to compress the compound far into the gas phase (Bäuerle 2000). The time frame of this reaction influences the thermal or

photochemical mechanisms obtained on and/or outside the remaining ablated surface. In particular, the required reaction time can be separated into two different values. These are, t_{E*}, corresponding to the reaction time when the compound is still in its electronically excited state and t_E, corresponding to the reaction time after the compound has returned to its vibrational manifolds in the ground state.

If $t_{Th} > t_{E*}$, while $t_{E*} << t_E$, the reaction occurs when the compound is still in its electronically excited state and therefore the process is photochemically activated. In this regime any energy dissipation will be in the form of light emission, readily observable within the ablation plume (Bäuerle 2000). To the contrary, if $t_{Th} << t_{E*}$, while $t_E << t_{E*}$, the reaction occurs after the compound returns to its ground state, where, as mentioned above, it is vibrationally excited. In this case the reaction is thermally activated and the energy dissipation is actually heat emission. In fact, these two cases are the extreme time dependences that do not take place in KrF excimer laser ablation. Usually in excimer laser ablation both reaction times of the compound in its ground and electronically excited state, t_E and t_{E*}, are longer than the thermal relaxation time, i.e. $t_{Th} < t_E$, t_{E*} (Bäuerle 2000). In addition, excimer lasers provide shorter reaction times of the ablated compounds, when they are still electronically excited rather than after arrival at their vibrational ground states, i.e. $t_{E*} < t_E$. The degree of this time reaction variation depends on the UV photon energy. Despite the UV photon energy, faster photochemically activated reactions are guaranteed within this regime (Bäuerle 2000). In case of $t_{E*} \leq t_E$, the ablated compounds react when they are still in their electronically excited state, although for some compounds limited thermally activated reactions may occur (liquid phase) (Srinivasan 1993, 1994).

Therefore, according to the model described in Section 1.3.3, excimer ablation produces less vaporisation (melting effects), when these thermal activated reactions occur far enough from the surface.

1.3.3.2 Ablation Products

The most frequently used and probably the best reference regarding the nature of the ablated products of polymerised films upon UV laser ablation was written by Srinivasan and Braren (1989). This study referred to excimer laser ablation of PMMA, but the results should apply for aged resins used as paint varnishes. A significant difference lies in composition of the films. In the case of polymers, such as PMMA, the starting material is MMA that polymerises readily to form PMMA consisting of long covalently bonded PMMA molecules of high molecular weight. In contrast, the most commonly used varnishes for paintings, such as triterpenoid resins, have a complex composition consisting of several types of triterpenoid parent molecules, which do not polymerise like polymers but rather form three-dimensional condensation oligomers by photochemical degradation (De la Rie 1988a, Papageorgiou, *et al.* 1997, Van der Doelen, *et al.* 1998, Dietemann 2003, Scalarone, *et al.* 2003). Thus, in order to develop into covalently bonded three-dimensional network, such resins have to be deteriorated and 'aged'. Since oxidation, isomerisation, crosslinking and degradation occur during ageing, their composition becomes a mixture of crosslinked parent and oxidised molecules, depending upon the degree and the type of ageing, as will be shown in Chapter 2. This crosslinked mixture is therefore expected to have some impact in the ablation process. To appreciate what

type of products should be expected a short review is provided for the corresponding studies on polymers.

The nature and abundance of the ablation products, i.e. the photofragments desorbed from the surface into the plume, depend basically on the UV laser wavelength, the chemistry of the material and the energy density, or fluence (Srinivasan, *et al.* 1986a, Srinivasan and Braren 1989, Srinivasan 1994). Srinivasan, observed that using an ArF excimer laser (193 nm) to determine the ablation products of PMMA the abundance of the MMA monomer was much higher than that when a KrF excimer laser (248 nm) was employed on the same film (Srinivasan, *et al.* 1986a). At 248 nm the majority of products in the plume were higher molecular weight molecules and radicals, the abundance of which at 193 nm was sensationally less.

Srinivasan and Braren discriminated four classes of ablated material derived from polymers upon exposure to excimer laser pulses. The first category contains volatile compounds, whose molecular weight does not surpass a critical value of 200 Daltons. In principle, this class consists of atoms, sole or clustered, small molecules, molecular fragments and ions, the most common of which being C_2, CO, CO_2 and monomers. The second category consists of much higher molecular weight compounds, such as large crosslinked molecules and a few monomeric units joint together. Products of this class are species found as solid material precipitated commonly on the sides of the laser ablated spot (Srinivasan and Braren 1989). The third category consists of excited diatomic species in the ablation plume, which are formed by secondary photolysis (Yeh 1986b) of some of the products that belong to the first two classes. The uppermost layer of an ablated surface, down to a depth which depends upon the

absorption coefficient of the material – for the laser wavelength employed – is rated as the fourth category of products (Srinivasan and Braren 1989).

In spite of the species deposited on the sides, most of which belong to the second class, the processed surface acquires material which has already been modified by the last UV laser pulse/s and its chemistry is a precursor to the process that will occur in the plume on arrival of the next pulse (Srinivasan and Braren 1989). However, localised or non-localised electronic or vibrational states of impurities deposited on the surface may impair the predicted interaction of the first few pulses (Bäuerle 2000), which might have an impact in the ablation products generated upon the first few pulses. This may well be the case in laser ablation of aged resin films applied on works of art, which may be covered by a thin layer of dust particles. After desorption of the latter, the process is fully controlled and predictable (Zafiropulos and Fotakis 1998, Zafiropulos 2002).

1.4 Preliminary results on the laser ablation of aged varnishes

Preliminary studies on the excimer laser ablation of aged varnishes of painted works of art demonstrate that the process dictates its termination after the removal of a very thin varnish layer from the surface, regardless of the thickness of the original aged varnish. A recent study shows that upon laser cleaning of naturally aged varnishes at 248 nm using 'optimal' fluences (see Chapter 3), the appearance of the remaining varnishes is gradually improved, i.e. discolouration and crack density decrease, as deteriorated varnish layers were selectively removed from the surface at rates of ~ 0.2 to ~ 0.7 μm per pulse (Theodorakopoulos and Zafiropulos 2003). The investigated

case studies were three nineteenth century Byzantine-style icons, whose varnishes had never been removed or over-coated in a later treatment. Thus, the condition of the objects was such that a cleaning application was essential to remove their discoloured, crazed and obscuring organic coatings.

Table 1.4.1 Visual observations across depth profiles of naturally aged varnishes coating paints using a KrF excimer laser.

Ablated Material (μm)	**Visual observations:**
Case A: Fluence ≈ 0.5 J/cm^2. Ablation rate 0.66 μm/pulse	Total thickness: 102 ± 15 μm
Surface	Discoloured, crazed and cracked, with dirt layer on top
- 3.00 μm	Reduction of the dirt density; slight crazing reduction– Same discolouration, cracks intensity
- 7.00 μm	Dirt layer removed; further crazing reduction – Same discolouration and cracks intensity
- 10.0 μm	Further crazing reduction; Slight discolouration reduction – Same cracks intensity
- 13.0 μm	Further discolouration reduction, crazing reduction & slight reduction of cracks intensity
- 16.5 μm	Further reduction of discolouration, crazing & cracks intensity
- 23.0 μm	Further reduction of discolouration; Crazing vanished; critical elimination of cracks
- 33.0 μm	Further reduction of discolouration & further elimination of cracks
- 49.5 μm	Significant reduction of discolouration & further elimination of cracks
- 66.0 μm	No more discolouration: More saturated appearance compared with previous zone – further cracks elimination
- 82.5 μm	Slightly melted on surface – Further cracks reduction.
Case B: Fluence ≈ 0.2 J/cm^2. Ablation rate 0.25 μm/pulse	Total thickness: 15 ± 2 μm
Surface	Discoloured, with dirt layer on top
- 1.25 μm	Partial removal of dirt – Same discolouration
- 2.50 μm	Removal of dirt – Same discolouration
- 3.75 μm	Slight discolouration reduction
- 5.00 μm	Further discolouration reduction – Higher saturation
- 6.25 μm	Critical discolouration reduction.
- 7.50 μm	Discolouration almost vanished
- 8.75 μm	No change
- 10.0 μm	No change
Case C: Fluence ≈ 0.3 J/cm^2. Ablation rate 0.21 μm/pulse	Total thickness: 35 ± 6 μm
Surface	Dark brown discolouration; Cracks; Thick dirt layer on top
- 1.00 μm	No change
- 2.00 μm	No change
- 3.00 μm	Slight change
- 4.00 μm	No change
- 5.00 μm	Reduction of dirt intensity – Discolouration & cracks remain
- 6.00 μm	Further reduction of dirt – Discoloration reduction – Same cracks intensity
- 7.00 μm	Dirt layer vanished – Further discolouration reduction – Same cracks intensity
- 8.00 μm	Further discolouration reduction; higher saturation of paint – Same cracks intensity
- 9.00 μm	Further discolouration reduction; higher saturation of paint – Same cracks intensity
- 10.0 μm	Further discolouration reduction; higher saturation of paint – Decrease of cracks intensity
- 15.5 μm	No change
- 21.0 μm	No change in saturation – Further reduction of cracks intensity
- 26.0 μm	Cracks vanished – Further increase in saturation

A KrF excimer laser was employed to remove varnish in a number of successive zones, each of which was scanned a few microns deeper than the adjacent one, based on a methodology that is described in Chapter 3. The depth of the deepest depth-steps was a few microns less than the total varnish thicknesses to avoid penetration of the 248 nm laser photons into the painted surfaces. In addition, the laser parameters, defined for each case separately, were kept constant during the process. Using an optical microscope, some gradient effects across the depth profiles of all three cases were observed (Table 1.4.1). These corresponded to steady reductions of the extent of discolouration, crazing and crack density (visually assessed), resulting in a gradual increase in saturation and brightness of the underlying paint with depth, while the residual varnish became glossier.

These changes could be associated with determined factors of varnish ageing that influence the appearance of paintings (De la Rie 1987, Berns and De la Rie 2002, 2003b), other than the decreasing thickness of the varnishes. For instance, the slope in the reduction of crazing in case A down to a depth of 10 μm from surface is accompanied by a slight gradual increase in saturation of the paint, even before the discolouration of the varnish started a spectacular gradient. In the absence of cracks that scatter the incident ambient radiation, the increasing colour saturation upon the successive laser pulses may be attributed either to a decreasing roughness of the uncovered surfaces and/or to a decreasing trend in discolouration across the depth profile of the examined varnishes. Gloss of a surface is a function of its roughness, with the smoother coatings' surfaces obtaining a glossier appearance of the underlying

paint, owing to increased specular light reflection (Bruxelles and Mahlman 1954, Clulow 1972, Hunter 1975, Brill 1980).

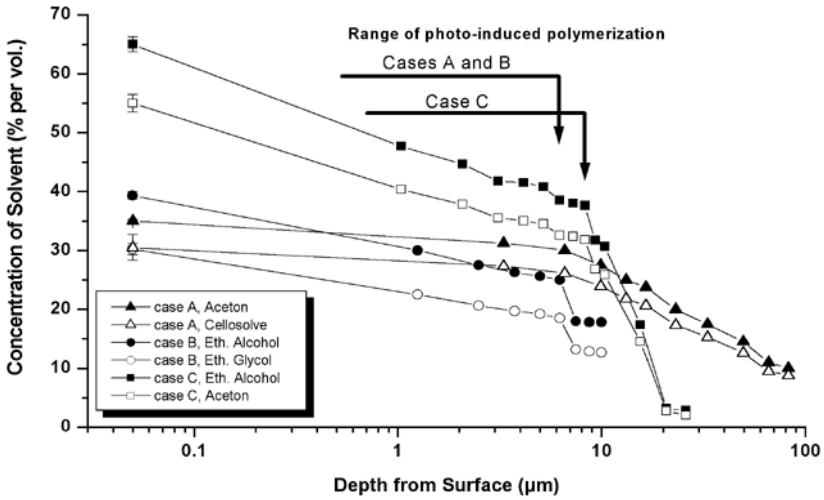

Figure 1.4.1 Polarity gradient across the depth profiles of three different laser-ablated aged varnishes ablated with a KrF excimer laser. The solvent systems employed slightly affected the remaining laser-ablated surfaces and did not dissolve the remaining films. The process was carried out under continuous observation with a stereomicroscope. With depth the proportion of the most polar solvent was eliminated in favor of the less polar one (Theodorakopoulos and Zafiropulos 2003)

The visually (only) indicated gradient in yellowing may be attributed either to a depth-wise elimination of conjugated diketones and/or quinones, to which yellowing of natural resins is ascribed (Formo 1979, De la Rie 1988b), or to bleaching of these compounds by interaction with the 248 nm laser photons. As discussed below (Chapter 2), formation of yellow compounds is mainly caused via autoxidation (De la Rie 1988b) and condensation (Formo 1979) reactions (Dietemann 2003). Thus, based on the visually-determined gradient in yellowing, it may be suggested that the degree of oxidation, which is responsible for the degree of polarity (Feller, *et al.* 1985), decreases as a function of depth. This suggests that the aged varnishes tested were preserved in a relatively non-oxidative and apolar state in their bulk layers, since no yellowing was observed after ablation of the surface layers. Indeed, rough solubility

tests based on application of solvent systems, which marginally affected the surfaces of the laser ablated steps, indicated that polarity, and therefore oxidation, follows a decreasing gradient across the uncovered depth, as shown in Figure 1.4.1 (Theodorakopoulos and Zafiropulos 2003). These results are in agreement with findings regarding the gradient in absorptivity of light across the depth profile of aged dammar films (Zafiropulos 2000).

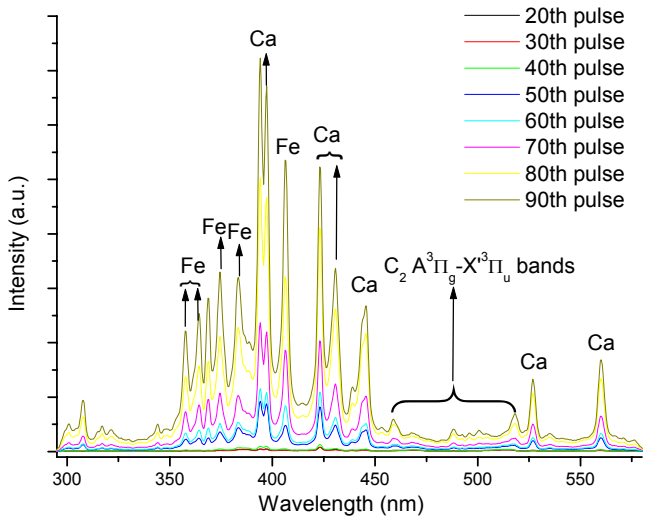

Figure 1.4.2 Successive LIBS spectra across depth profile of pigmented resin film upon KrF excimer laser pulses at ~ 1 J/cm^2.

Furthermore, it has been established that yellowing compounds are abundant in the crosslinked fraction of aged natural resins (Van der Doelen and Boon 2000, Dietemann 2003), and hence the visually observed reduction of yellowing indicates also that crosslinking is decreasing with depth. This may affect laser ablation. While absorption of the UV laser photons is the principal mechanism at the start of the interaction (Section 1.3.3), polymerisation has been determined as a significant factor influencing the interaction of organic films with the UV laser photons (Srinivasan and Braren 1989, Zafiropulos 2002). A preliminary suggestion on whether or not there is a gradient in polymerisation as a function of depth was obtained by monitoring the

ablation plume of a 150 μm aged resin film, mixed with haematite, Fe_2O_3 (red), using a KrF excimer laser and Laser-Induced Breakdown Spectroscopy. Figure 1.4.2 shows a range of LIBS spectra every ten pulses from the twentieth to the ninetieth pulse.

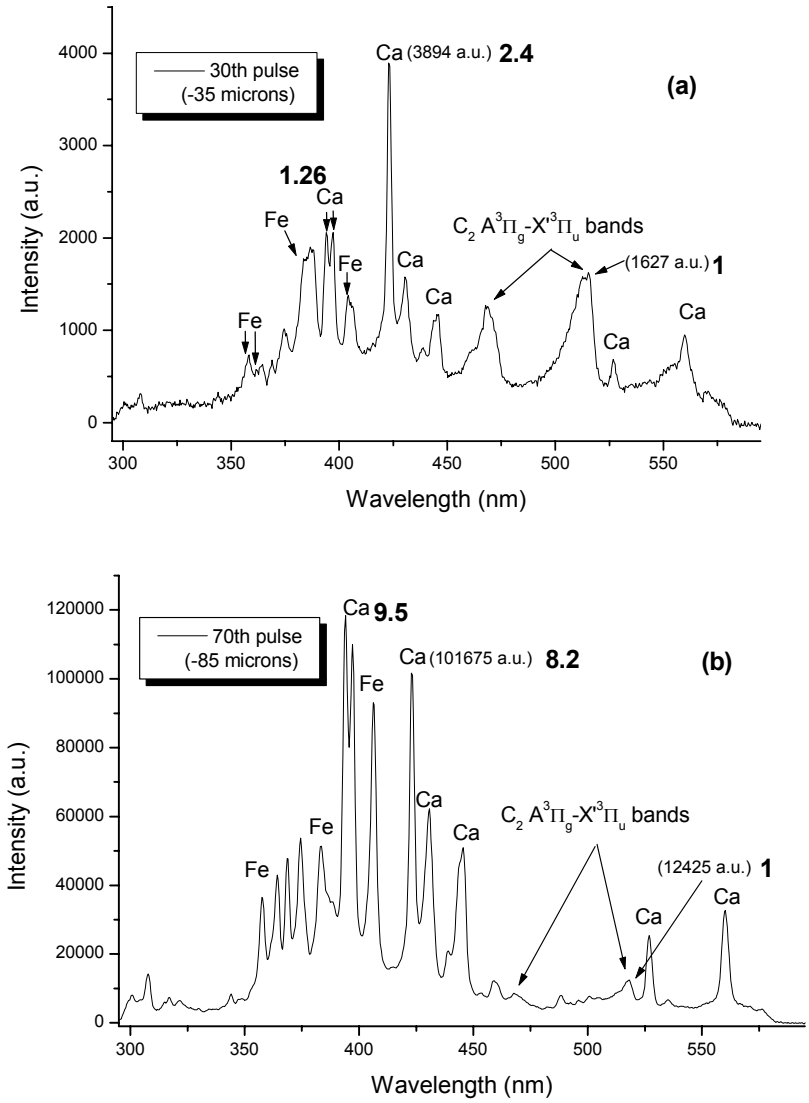

Figure 1.4.3 Ratios of C_2 to Ca and Fe emission bands detected with LIBS. The spectra belong to depths at 35 μm (a) and 85 μm (b) from surface ablated with a KrF excimer laser.

All LIBS spectra detected emissions of Fe, Ca and C_2. The intensity of the carbon dimer emission ($A^3\Pi_g$-$X'^3\Pi_u$ bands or C_2 Swan bands), emerging within the 460 to 520 nm wavelength region, is associated with the length of the molecular chains

forced in the gas phase per laser pulse (Srinivasan and Braren 1989), and thus with the degree of polymerisation of the material (Zafiropulos 2002). Figure 1.4.3 shows that upon successive pulses the laser-induced photofragments consisted of proportionally less carbon dimers, while ablation was propagating from the surface downwards. This can be visualised for example in the spectrum obtained from a depth of 85 μm below the surface, showing that there was almost a negligible amount of C_2 in the ablation plume. We may attribute this observation to a precipitation of pigments in the bulk, but because of the presence of resin in the bulk, even in low quantities, such a low intensity of C_2 emission cannot be effectively explained (Zafiropulos 2002). Therefore, there is still a possibility that the low carbon dimer emission in the bulk is due to a gradual reduction of the degree of polymerisation.

Ablation for this particular study was carried out with a 1 J/cm^2 fluence yielding an ablation rate of 1.2 μm/pulse. Despite the fact that pigments were denser with depth, which would influence the ablation step because of changes of the absorption of the irradiated film, the ablation step was determined to be constant at each pulse. This phenomenon delineates that by approaching deeper layers except for the ablation of resin ablation there was additional pigment removal, which should have caused explosive vaporisation to the irradiated surface of the sample (Asmus, *et al.* 1976, Watkins 1997). Thus, the constant ablation step may have been a pure coincidence, since in case of a gradient in the polymerisation of the resin, the ablation step should be eliminated with depth and thermal effects should somewhat increase (Luk'yanchuk, *et al.* 1994, Srinivasan 1994, Bäuerle 2000). In situ microscopic observations of the ablation spot on the sample suggested that apart from the charring of the irradiated

pigments (Zafiropulos, *et al.* 2001, Castillejo, *et al.* 2003) the bottom of the spot appeared increasingly melted as we were etching deeper in the bulk. This observation indicates that indeed polymerisation decreases with depth (Zafiropulos 2002), since in the absence of sufficient covalent bonds to be broken by the laser photons, the excited species in the ablated film do not desorb, but remain in the surface undergoing eventually thermal energy dissipation (Srinivasan 1994). Thus, the gradient of carbon dimer emission as a function depth, shown in Figure 1.4.4, suggests that the film constantly releases shorter molecular chains, which implies that the degree of polymerisation is reducing as a function of depth.

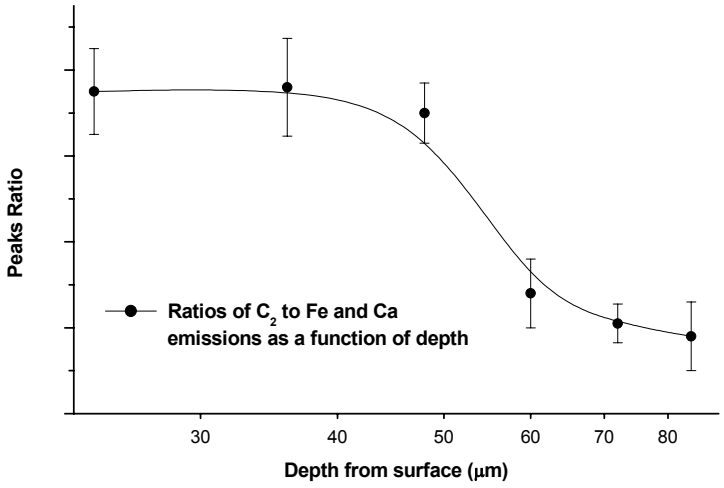

Figure 1.4.4 Ratios of C_2 to Fe and Ca emissions detected with LIBS as a function of ablated depth.

Despite the fact that all the varnishes tested in these preliminary studies were unrelated in terms of composition, origin, ageing and deterioration, the close resemblance of the trends shown in Figures 1.4.1 and 1.4.4 indicates that gradients in photodegradation and photoxidation should be a common phenomenon in varnishes applied on paintings. Similar characteristics have been also detected in polymers (Furneaux, *et al.* 1980 - '81, Fukushima 1983, Schoolenberg and Vink 1991) with the

most related example in conservation being the gradients determined in soluble polyamides (Fromageot and Lemaire 1991). A review of some similar cases is provided by Feller (Feller 1994b), attributing these effects to Beer's Law and to oxygen starvation in the bulk, since the lack of oxygen leads to recondensation of radicals (Fukushima 1983).

1.5 Rationalisation

In principal, excimer laser ablation at 248 nm is affected first by the absorption properties and subsequently by the degree of polymerisation of the irradiated substance (Srinivasan and Braren 1989). While the former is responsible for the amount of photons absorbed upon the release of a laser pulse the latter regulates the extent of photochemical versus the minor thermal effects generated in the surface (Zafiropulos 2002). A principal difference in the excimer laser ablation of polymers with that of natural varnishes is that polymers generate a 'hard' covalently bonded lattice as soon as they solidify, while varnishes generate some crosslinking after sufficient ageing especially in the presence of light (De la Rie 1988b, Van der Doelen 1999, Dietemann 2003). The property of polymers to form long macromolecules upon solidification seems to have been taken for granted[2] in the ablation experiments leading to the theoretical models discussed in Section 1.3. Zafiropulos (2002) determined that UV laser pulses onto non-polymerised films cause melting owing to vaporisation, thereby waiving the control of the process. Therefore, a critical condition for the removal of natural varnish with means of excimer laser ablation is that the varnish should be aged (Zafiropulos 2002).

[2] This is true for all the papers referred in Section 1.3 on the fundamental studies on UV pulsed laser ablation of polymers.

There are specific indications that ageing of natural varnishes under light does not lead to a homogeneous oxidised and crosslinked film, but it obtains gradients in the degradation phenomena as a function of depth (Feller 1994b, Boon and Van der Doelen 1999, Zafiropulos, *et al.* 2000, Theodorakopoulos and Zafiropulos 2003). For example, using a KrF excimer laser and measuring the absorption of aged dammar films with a wide range of thicknesses, it was determined that the mean optical density of dammar decreases with depth (Zafiropulos, *et al.* 2000). The preliminary results shown above imply that both oxidation and crosslinking of aged painting's varnishes perform gradients. Upon laser cleaning of paintings, where the successive laser pulses interact continuously with deeper parts of the same varnish, the existence of these gradient phenomena are expected to influence the process. The decreasing optical densities would result in increasing optical absorption lengths (Bäuerle 2000) in the remaining film, which in the case of paintings would endanger the protection of the paint layers form the UV laser photons (Castillejo, *et al.* 2003). At the same time, the decreasing degree of crosslinking would result in less laser induced bond-breaking, causing less desorption of excited species in the gas phase (Srinivasan and Braren 1989). In combination with the longer optical absorption length and the non-desorbed excited species in the film, which eventually will undergo thermal dissipation in the material, the surface of the varnish will be vaporised and melted along the thermally affected zone (Srinivasan 1994, Zafiropulos 2002). Despite the fact that optical absorption lengths and the length of the thermally affected zone in the material reduce exponentially with distance from the irradiated surface (Bäuerle 2000), this problem may eventually impair the underlying layers if not enough coating

is left on the painting to act as a filter (Zafiropulos and Fotakis 1998). This seems to be the greatest risk of excimer laser ablation of painting varnishes.

Because of specific risks of causing discolouration to irradiated paints containing inorganic pigments (Castillejo, *et al.* 2003) if the delineated gradients are not taken into consideration, excimer laser ablation of painting varnishes is bound to be studied along with the gradients that are generated upon ageing. Therefore, the present study aims at the determination of depth-dependent gradients of aged painting varnishes using a KrF excimer laser. In order to shed some light on the laser-varnish interaction, three different painting varnishes are investigated. These are two triterpenoid varnishes, the so-called non-polymerisable dammar and mastic, which upon ageing deteriorate mainly because of increasing oxidation that influences their absorptivity (De la Rie 1988a, Zumbühl, *et al.* 1998, Van der Doelen 1999, Dietemann 2003, Scalarone, *et al.* 2003), and a copal oil varnish (Brommelle 1956, Carlyle 2001), which in contrast to the former is characterised by extensive polymerisation, mainly of the oil components, causing insolubility upon ageing (Mills and White 1994). A critical decision for the investigations presented below was associated with the degree of ageing. It was decided to replicate extreme ageing conditions to create a situation where lasers operating with optimal parameters, such as those proposed for real application for conservation of paintings, would be favoured for a selective cleaning application, without running the risks of the chemical cleaning listed in the introduction of this chapter. A major task in this approach is also to address the role of the interaction on the remaining films. Thus, questions arise such as: whether the UV pulses induces autoxidation in deeper layers, while removing surface layers; whether

crosslinking is increasing upon recombination of laser-induced, non-desorbed radicals in the material (Georgiou, *et al.* 1998); and whether the laser bleaches the irradiated varnish.

1.6 Thesis outline

The following thesis is divided in another five chapters. Chapter 2 is an introduction on the examined varnishes and the preparation of ageing that was decided to be used for the present investigations. An introduction to the materials and a short review of the present knowledge of their deterioration processes is also presented.

Chapter 3 introduces the ablation properties of dammar, mastic and copal oil varnish films using a KrF excimer laser (248 nm, 25 ns). In particular, a study on the optimisation of the photon-varnish interaction based on mean laser ablation rate studies, which were carried out both at surface and bulk layers of each varnish. Comparison of ablation rate data obtained at deep and shallow etchings in thick and thin films, all aged under the same conditions (Chapter 2). These studies determine the 'optimal' fluences that were employed to scan the coatings step by step, using a methodology that has been proposed for the laser cleaning of paintings (Zafiropulos and Fotakis 1998), which is described in detail. Differences in the ablation of the triterpenoid varnishes and the copal oil varnish were reflected both in the resultant ablation rates and the final depth steps. Finally, plume emission was monitored using LIBS.

Chapter 4 presents a spectroscopic investigation at successive etched depths of the aged dammar, mastic and copal oil varnish films. An online transmission study upon

the KrF excimer ablation of the films is introduced. This particular investigation monitors the transmission of laser light online with ablation of the surface layers and its aim is the detection of the energy fluence that minimises it (Zafiropulos 2002). Besides this task some indications about the optical properties of the ablated films at the laser wavelength are given. UV/VIS spectrophotometry was employed to determine the absorbencies at the different depth steps of the ablated film. UV/VIS data were also utilised to determine the mean optical densities across the depth profiles of the ablated films. Finally, ATR-FTIR analysis straight on the laser treated surfaces provided some preliminary structural information.

A molecular characterisation of the laser ablated light aged dammar and mastic films across their depth profiles is given in Chapter 5. The gradient in oxidation is studied with direct temperature-resolved / mass spectrometry (DTMS) at the 16 eV electron ionisation (EI) and the 250 eV ammonia chemical ionisation (NH_3/CI) modes. Since sampling for each DTMS run included the remaining ablated film at each laser ablated depth step, the corresponding mass spectra and total ion currents (TIC's) obtained average information about the incorporated compounds across the remaining thicknesses. The trends monitored with DTMS, were also demonstrated with multivariant factor discriminant analysis (DA) of the EI-DTMS. Selective examination of compounds on the ablated surfaces was obtained with matrix assisted laser/desorption ionisation – time-of-flight MS (MALDI-TOF MS). Finally, the gradient in crosslinking was investigated with high performance size exclusion chromatography (HP-SEC). Based on the present and earlier findings a model of

ageing of triterpenoid varnishes is proposed and the contribution of excimer laser ablation is discussed.

EI-DTMS was employed for a fingerprint molecular characterisation of the depth profile of the copal oil varnish film, which is described in Chapter 6. Analysis was based on monitoring of specific m/z marker peaks and the results were supported with a Pyrolysis-TMAH-GC/MS pilot study of the unaged and aged copal-oil varnish (control) samples. Various compounds generated and/or reduced via autoxidation are monitored in the EI-DTMS summation mass spectra, while the crosslinked polymer network at different depth-steps of the film is delineated with the EI-DTMS total ion currents.

1.7 References

'European research project 'Advanced workstation for controlled laser cleaning of artworks' ENV4-CT98-0787', (1998).

Aldrovandi, A., Lalli, C., Lanterna, G., and Matteini, M., 'Laser cleaning: a study on greyish alteration induced on non-patinated marbles', *Journal of Cultural Heritage (Suppl. 1)* **1** (2000) s55-s60.

Alessandrini, G., Sansonetti, A., and Pasetti, A. 'The cleaning of stone surfaces: comparison between laser and traditional methods. Evaluation of the harmfulness'. In *Proceedings of the 4th International Symposium on the Conservation of Monument in the Mediterranean Basin*, Eds. A. Moropoulou, F. Zezza, E. Kollias, and I. Papachristodoulou, Vol. 3, Technical Chamber of Greece, Athens, May 6-11, Rhodes, (1997), 19-30.

Al-Malaika, S. 'Autoxidation'. In *Atmospheric oxidation and antioxidants*, Ed. G. Scott, Vol. I, Elsevier Science Publishers B.V., Amsterdam, (1993), 45 - 82.

Appolonia, L., Bertone, A., Brunneto, A., and Vaudan, D., 'The St. Orso Priori: the comparison and testing of clenaing methods', *Journal of Cultural Heritage (Suppl. 1)* **1** (2000) s105-s110.

Armani, E., Calcano, G., Menichelli, C., and Rosseti, M., 'The church of the Maddalena in Venice: the use of laser in the cleaning of the facade', *Journal of Cultural Heritage (Suppl. 1)* **1** (2000) s99-s104.

Asmus, J. F., Guattari, G., Lazzarini, L., Musumeci, G., and Wuerker, R. F., 'Holography in the Conservation of Statuary', *Studies in Conservation* **18** (1973a) 49-63.

Asmus, J. F., Murpgy, C. G., and Munk, W. H., 'Studies on the interaction of laser radiation with art artifacts', *Proceedings of SPIE* **41** (1973b) 19-27.

Asmus, J. F., 'Use of lasers in the conservation of stained glass', *Conservation in Archaeology and in the Applied Arts* (1975) 139-142.

Asmus, J. F., Westlake, D. L., and Newton, H. T., 'Laser technique for the divestment of a lost Leonardo da Vinci mural', *Journal of Vacuum Science and Technology* **12** (1975) 1352-1355.

Asmus, J. F., 'The development of a laser statue cleaner', *Proceedings of the 2nd International Symposium on the Deterioration of Building Stones, Athens* (1976) 137-141.

Asmus, J. F., Seracini, M., and Zetler, M. J., 'Surface morphology of laser-cleaned stone', *Lithoclastia* **1** (1976) 23-46.

Asmus, J. F., Lazzarini, L., Martini, A., and Fasina, V., 'Performance of the Venice statue cleaner', *Preprints of the Fifth Annual Meeting of the American Institute for*

Conservation of Historic and Artistic Works, Boston, Massachusetts, 30 May - 2 June, 5-11 (1977).

Asmus, J. F., 'Light cleaning: laser technology for surface preparation in th arts', *Technology and Conservation* **3** (1978) 14-18.

Asmus, J. F., 'More light in art conservation.' *IEEE Circuits and Devices Magazine* **2** (1986) 6-15.

Athanassiou, A., Hill, A. E., Fourrier, T., Burgio, L., and Clark, R. J. H., 'The effects of UV laser light radiation on artist's pigments', *Journal of Cultural Heritage (Suppl. 1)* **1** (2000) s209-s213.

Azema, A. G. and Laude, L. D. Excimer Lasers, Kluwer Academic Publishers, Dordrecht, The Netherlands (1994) 447.

Bäuerle, D. *Laser Processing and Chemistry, Third, revised and enlarged edition*, Springer-Verlag, Berlin, Heidelberg, New York, 2000.

Bayly, J. G., Kartha, V. B., and Stevens, W. H., 'The absorption spectra of liquid phase H_2O, HDO and D_2O from 0.7 μm to 10 μm', *Infrared Phys.* **3** (1963) 211-223.

Berlman, I. B. *Energy transfer Parameters of Aromatic Compounds*, Academic, New York, 1973.

Berns, R. S. and De la Rie, E. R. 'The relative importance of surface roughness and refractive index in the effects of varnishes on the appearance of painitngs'. In *Preprints of the 13th triennial meeting of the ICOM Committee for Conservation*, Ed. V. R., Vol. I, James & James (Science Publishers) Ltd, Rio de Janeiro, (2002), 211-216.

Berns, R. S. and De la Rie, E. R., 'Exploring the optical properties of picture varnishes using imaging techniques', *Studies in Conservation* **48** (2003a) 73-82.

Berns, R. S. and De la Rie, E. R., 'The effect of the refractive index of a varnish on the appearance of oil paintings', *Studies in Conservation* **48** (2003b) 251-262.

Birks, J. B. *Photophysics of Aromatic Molecules*, Wiley Interscience, New York, 1970.

Boon, J. J. and van Och, J., 'A Mass Spectrometric Study of the Effect of Varnish Removal from a 19th Century Solvent-sensitive Wax Oil Painting'. In *ICOM Committee for Conservation 11th Triennial Meeting Edinburgh, Scotland*, Ed. J. Bridgland, Vol. I, James & James, London, (1996), 197-205.

Boon, J. J. and van der Doelen, G. A. 'Advances in the current understanding of aged dammar and mastic triterpenoid varnishes on the molecular level'. In *Firnis: Material - Aesthetik - Geschichte, International Kolloquium, Braunschweig, 15-17 Juni 1998*, Ed. A. Harmssen, Hertog-Anton-Ulrich-Museum, Braunschweig, (1999), 92-104.

Boyd, I. A. *Photochemical Processing of Electronic Materials*, Academic Press, London, 1992.

Bracco, P., Lanterna, G., Matteini, M., Nakahara, K., Sartiani, O., de Cruz, A., Wolbarsht, M. L., Adamkiewicz, E., and Colomboni, M. P., 'Er:YAG laser: an

innovative tool for controlled cleaning of old paintings: testing and evaluation', *Journal of Cultural Heritage (Suppl. 1)* **4** (2003) 202s-208s.

Bramson, M. A. *Infrared Radiation-A Handbook for Applications (Translation: R.B. Rodman)*, Plenum Press, New York, 1968.

Brannon, J. H., Lankard, J. R., Baise, A. I., Burns, F., and Kaufman, J., 'Excimer laser etching of polyimide', *Journal of Applied Physics* **58** (1985) 2036-2043.

Brill, T. B. *Light; Its interaction with art and antiquities*, Plenum Press, New York, 1980.

Bromblet, P., Labourè, M., and Orial, G., 'Diversity of the cleaning procedures including laser for the restoration of carved portals in France over the last 10 years', *Journal of Cultural Heritage (Suppl. 1)* **4** (2003) 17s-26s.

Brommelle, N., 'Material for a history of conservation', *Studies in Conservation* **2** (1956) 176-186.

Bruxelles, G. N. and Mahlman, B. H., 'Glossiness of nitrocellulose lacquer coating', *Official Digest of the Federation of Paint and Varnish Production* **351** (1954) 299-314.

Cain, S. R., Burns, F. C., and Otis, C. E., 'On single-photon ultraviolet ablation of polymeric materials', *Journal of Applied Physics* **71** (1992a) 4107-4117.

Cain, S. R., Burns, F. C., Otis, C. E., and Braren, B., 'Photothermal description of polymer ablation: Absorption behavior and degradation time scales', *Journal of Applied Physics* **72** (1992b) 5172-5178.

Calcano, G., Koller, M., and Nimmrichter, H., 'Laserbased cleaning on stonework at St. Stephen's Cathedral, Vienna', *LACONA I, Restauratotenblätter Sonderband, Wien, Austria* (1997) 39-43.

Calcano, G., Pummer, E., and Koller, M., 'St. Stephen's church in Vienna: critieria for Nd:YAG laser cleaning on an architectural scale', *Journal of Cultural Heritage (Suppl. 1)* **1** (2000) s111-s117.

Carlyle, L., 'Laser interactions with paintings: results and proposals for further study. Unpublished report at the Canadian Conservation Insitute, Ottawa, 16 November 1981', (1981).

Carlyle, L. A. *The artist's assistant: Oil painting Instruction manuals and handbooks in Britain 1800-1900: with reference to selected eighteenth century sources*, Archetype Publications, London, 2001.

Castillejo, M., Martin, M., Oujja, M., Silva, D., Torres, R., Manousaki, A., Zafiropulos, V., Van den Brink, O. F., Heeren, R. M. A., Teule, R., Silva, A., and Gouveia, H., 'Analytical study of the chemcial and physical changes induced by KrF laser cleaning of tempera paints', *Analytical Chemistry* **74** (2002) 4662-4671.

Castillejo, M., Martin, M., Oujja, M., Santamaria, J., Silva, D., Torres, R., Manousaki, A., Zafiropulos, V., Van den Brink, O. F., Heeren, R. M. A., Teule, R., and Silva, A.,

'Evaluation of the chemical and physical changes induced by KrF laser irradiation of tempera paints', *Journal of Cultural Heritage (Suppl. 1)* **4** (2003) 257s-263s.

Centeno, M., 'The retractive index of liquid water in the near infrared spectrum', *Journal of the Optical Society of America* **31** (1941) 244-247.

Chapman, S., 'Laser technology for graffiti removal', *Journal of Cultural Heritage (Suppl. 1)* **1** (2000) s75-s78.

Chrisey, D. B. and Hubler, G. K. *Pulsed Laser Desorption of thin films*, Wiley-Intrscience, New York, 1994.

Chuang, M. C. and Tam, A. C., 'On the saturation effect in the picosecond near ultraviolet laser ablation of polyimide', *Journal of Applied Physics* **65** (1989) 2591-2595.

Clulow, F. W. *Color; Its principles and their applications*, Morgan and Morgan, New York, 1972.

Cooper, M., Solajic, M., Usher, G., and Ostapkowicz, J., 'The application of laser technology to the conservation of Haida totem pole', *Journal of Cultural Heritage (Suppl. 1)* (2003) 165s-173s.

Cooper, M. I., Emmony, D. C., and Larson, J. H., 'A comparative study of the laser cleaning of limestone'. In *Proceedings of the 7th International Congress on Deterioration and Conservation of Stone*, Eds. J. Delgado-Rodirigues, F. Henriques, and F. Telmo-Jeremias, Lisbon, June 1992, (1992), 1307-1315.

Cooper, M. I., Emmony, D. C., and Larson, J. H. 'The evaluation of laser cleaning of stone sculpture'. In *Structural Repair and Maintenance of Histrorical Buildings III*, Eds. C. Brebbia and R. Frewer, Computational Mechanics Publications, (1993), 259-266.

Cooper, M. I., 'Laser cleaning of stone sculpture', Loughborough University, (1994), 188-208.

Cooper, M. I., Emmony, D. C., and Larson, J. H., 'Characterisation of laser cleaning of limestone', *Optics and Laser Technology* **27** (1995) 69-73.

Cottam, C. A. and Emmony, D. C., 'Laser cleaning of metals at infra-red wavelengths', *LACONA I, Restauratotenblätter Sonderband, Wien, Austria* (1997) 95-98.

Cove, S., 'Mixing and mingling: John Constable's oil paint mediums c.1802-37, including the analysis of the 'Manton' paint box'. In *IIC Congress, Painting Techniques, History, Materials and Studio Practice*, Eds. R. Ashok and P. Smith, Dublin, 7-11 September, (1998), London, 211-216.

Danielzik, B., Fabricius, N., Rowekamp, M., and von der Linde, D., 'Velocity distribution of molecular fragments from polymethylmethacrylate irradiated with UV lasers pulses', *Applied Physics Letters* **48** (1986) 212-214.

de Cruz, A., Hauger, S. A., and Wolbarsht, M. L., 'The role of lasers in fine arts conservation and restoration', *Optics and Photonics News* **10** (1999) 36-40.

de Cruz, A., Wolbarsht, L., and Hauger, S. A., 'Laser removal of contaminants from painted surfaces', *Journal of Cultural Heritage (Suppl. 1)* **1** (2000) s173-s180.

De la Rie, E. R., 'The influence of varnish on the appearance of paintings', *Studies in Conservation* **32** (1987) 1-13.

De la Rie, E. R., 'Stable Varnishes for Old Master Paintings', PhD Thesis University of Amsterdam, (1988a).

De la Rie, E. R., 'Photochemical and thermal degradation of films of dammar resin', *Studies in Conservation* **33** (1988b) 53-70.

Degrigny, C., Tanguy, E., Le Gall, R., Zafiropulos, V., and Marakis, G., 'Laser cleaning of tarnished silver and copper threads in museum textiles', *Journal of Cultural Heritage (Suppl. 1)* (2003) 152s-156s.

Dickmann, K., Fotakis, C., and Asmus, J. F.(Eds.), Proceedings of the International Conference LACONA V - Lasers in the Conservation of Artworks, September 15-18 2003, Osnabrueck, Germany. In *Springer Proceedings in Physics*. Vol. 100, Springer, Berlin, Heidelberg (2005).

Dietemann, P., 'Towards more stable natural resin varnihses for painintgs', PhD Thesis Swiss Federal Institute of Technology, Zurich, (2003).

Drewello, U., Weißmann, R., Rölleke, S., Müller, E., Würtz, S., Fekrsanati, F., Troll, C., and Drewello, R., 'Biogenic surface layers on historical window glass and the effect of excimer laser cleaning', *Journal of Cultural Heritage (Suppl. 1)* **1** (2000) s161-s171.

Dyer, P. E. and Srinivasan, R., 'Nanosecond photoacoustic studies on ultraviolet laser ablation of organic polymers', *Applied Physics Letters* **48** (1986) 445-447.

Dyer, P. E. and Sidhu, J., 'Spectroscopic and fast photographic studies of excimer laser polymer ablation', *Journal of Applied Physics* **64** (1988) 4657-4663.

Dyer, P. E. and Srinivasan, R., 'Pyroelectric detection of ultraviolet laser ablation products from polymers', *Journal of Applied Physics* **66** (1989) 2608-2612.

Eichert, D., Vergés-Belmin, V., and Kahn, O., 'Electronic paramagnetic resonance as a tool for studying the blackening of Carrara marble due to irradiation by a Q-switched YAG laser', *Journal of Cultural Heritage (Suppl. 1)* **1** (2000) s27-s45.

Esbert, R. M., Grossi, C. M., Rojo, A., Alonso, F. J., Montoto, M., Ordaz, J., Pérez de Andrés, M. C., Escudero, C., Barrera, M., Sebastian, E., Rodriguez-Navarro, C., and Elert, K., 'Application limits of Q-switched Nd:YAG laser irradiation for stone cleaning based on colour measurements', *Journal of Cultural Heritage (Suppl. 1)* **4** (2003) 50s-55s.

Feely, J., Williams, S., and Fowles, S. P., 'An initial study into the particulates emitted during the laser ablation of sulphation crusts', *Journal of Cultural Heritage (Suppl. 1)* **1** (2000) s65-s70.

Fekrsanati, F., Hildenhagen, J., Dickmann, K., Troll, C., Drewello, U., and Olaineck, C., 'UV-laser radiation: basic research of the potential for cleaning stained glass', *Journal of Cultural Heritage (Suppl. 1)* **1** (2000) s155-s160.

Feller, R. L., Stolow, N., and Jones, E. H. 'On picture varnishes and their solvents.' Revised and enlarged edition 1985. Washington DC: National Gallery of Art., (1985).

Feller, R. L. 'Accelerated Aging: Photochemical and Thermal Aspects', Ed. D. Berland, The Getty Conservation Institute, Los Angeles, USA, (1994a).

Feller, R. L. 'Depth of Penetration of Light into Coatings (in Chapter 5); and Influence of Sample Thickness and Oxygen Diffusion (in Chapter 9)'. In *Accelerated Aging: Photochemical and Thermal Aspects*, Ed. D. Berland, The Getty Conservation Institute, USA, (1994b), 56-61 and 135-137.

Formo, M. W. 'Paints, varnishes and related products: Discolouration'. In *Baile's Industrial Oil and Fat Products*, Ed. D. Swern, Vol. 1, John Wiley & Sons, New York, (1979), 722-724.

Fotakis, C., 'Lasers for art's sake', *Optics and Photonics News* **6** (1995) 30-35.

Fotakis, C., Zafiropulos, V., Anglos, D., Balas, C., Fandidou, D., Georgiou, S., Tornari, V., Zergioti, I., and Doulgeridis, M., 'Lasers in the Conservation of Painted Artworks,' *submitted in Restauratorenblätter, Sonderband, for the proceedings of Lacona II (this extra volume of the journal was never published)* (1997).

Fowles, P. S., 'The garden at Ince Blendel: a case study in the recording and non-contact replication of decayed sculpture', *Journal of Cultural Heritage (Suppl. 1)* **1** (2000) s89-s91.

Frank, C. W., Fredrickson, G. H., and Andersen, H. G. In *Photophysical and Photo-chemical Tools in Polymer Science, NATO, A SI Series C,*, Ed. M. A. Winnik, Vol. 182, (1985), 495.

Friberg, T., Zafiropulos, V., Petrakis, Y., and Fotakis, C., 'Removal of fungi and stains from paper substrates using laser cleaning strategies', *LACONA I, Restauratotenblätter Sonderband, Wien, Austria* (1997) 79-82.

Fromageot, D. and Lemaire, J., 'The prediction of the long-term photo-aging of soluble polyamides used in conservation', *Studies in Conservation* **Vol. 36** (1991) 1-8.

Fukushima, T., 'Deterioration Processes of Polymeric Materials and their Dependence on Depth from Surfaces', *Durability of Building Materials* **Vol. 1** (1983) 327 - 343.

Furneaux, G. C., Ledbury, J., and Davis, A., 'Photo-oxidation of thick polymer samples. Part I: The variation of photo-oxidation with depth in naturally and artificially weathered low density polyethylene', *Polymer Degradation and Stability* **Vol. 3** (1980 - '81) 431 - 442.

Futzikov, N. P., 'Approximate theory of highly absorbing polymer ablation by nanosecond laser pulses', *Applied Physics Letters* **56** (1990) 1638-1640.

Gaetani, M. C. and Santamaria, U., 'The laser cleaning of wall paintings', *Journal of Cultural Heritage (Suppl. 1)* **1** (2000) s199-s207.

Georgiou, S., Zafiropulos, V., Tornari, V., and Fotakis, C., 'Mechnistic Aspects of Excimer Laser Restoration of Painted Artworks', *Laser Physics* **8** (1998) 307-312.

Gettens, R. and Stout, G. *Painting materials: a short encyclopaedia*, Dover Publications, New York, 1966.

Golovlev, V. V., Gresalfi, M. J., Miller, J. C., Romer, G., and Messier, P., 'Laser characterization and cleaning on nineteenth century daguerreotypes', *Journal of Cultural Heritage (Suppl. 1)* **1** (2000) s139-s144.

Golovlev, V. V., Gresalfi, M. J., Miller, J. C., Agglos, D., Melesanaki, K., Zafiropulos, V., Romer, G., and Messier, P., 'Laser characterization and cleaning of 19th century daguerreotypes II', *Journal of Cultural Heritage (Suppl. 1)* (2003) 134s-139s.

Gorodetsky, G., Kazyaka, T. G., Melcher, R. L., and Srinivasan, R., 'Calorimetric and acoustic study of ultraviolet laser ablation of polymers', *Applied Physics Letters* **46** (1985) 828-830.

Hedley, G., 'Solubility parameters and varnish removal: a survey.' *The Conservator* **4** (1980) 12-18. (Re-printed, with corrections, in Measured Opinions (1993), ed. C. Villers. London: United Kingdom Institute for Conservation: 128-134).

Hildenhagen, J. and Dickmann, K., 'Excimer laser for fundamental studies in cleaning hewn stone and medieval glass', *Journal of Cultural Heritage (Suppl. 1)* **4** (2003a) 118s-122s.

Hildenhagen, J. and Dickmann, K., 'Nd:YAG laser with wavelengths from IR to UV (w,2w,3w,4w) and corresponding applications in conservation of various materials', *Journal of Cultural Heritage (Suppl. 1)* **4** (2003b) 174s-178s.

Hill, A. E., Athanassiou, A., Fourrier, T., Anderson, J., and Whitehead, C., 'Progress in the use of excimer lasers to clean easel paintings'. In *Proceedings of the 5th International Conference on Optics Within Life Sciences (OWLS V)*, Eds. C. Fotakis, T. G. Papazoglou, and C. Kalpouzos, Springer Verlag, Aghia Pelagia, Crete, Greece, 1998, (2000), 203-207.

Hillenkamp, F. and Karas, M., 'MALDI - an Experience', *International Journal of Mass Spectrometry* **200** (2000) 71-77.

Hontzopoulos, E. I., Fotakis, C., and Doulgeridis, M., 'Excimer laser in art restoration'. In *SPIE; 9th International Symposium on Gas Flow and Chemical Lasers*, Eds. C. Fotakis, C. Kalpouzos, and T. G. Papazoglou, Vol. 1810, Bellingham, Washington, (1993), 748-751.

Hunter, R. S. *The measurement of appearance*, John Wiley & Sons, New York, 1975.

Jones, R., Townsend, J., and Boon, J. J., 'A technical assessment of eight portraits by Reynolds being considering for conservation'. In *ICOM Committee for Conservation 12th Triennial Meeting Lyon, France*, (1999), 375-380.

Karas, M. and Hillenkamp, F., 'Laser Desorption Ionization Of Proteins With Molecular Masses Exceeding 10000 Daltons', *Analytical Chemistry* **60** (1988) 2299-2301.

Karoutis, A. D. and Hellidonis, E., 'A new method of cleaning ancient skulls by means of ArF excimer laser', *LACONA I, Restauratotenblätter Sonderband, Wien, Austria* (1997) 99-102.

Kautek, W. and König, E. Lasers in the Conservation of Artworks, Workshop, 4-6 October 1995, Heraklion, Crete, Greece, *LACONA I)*, Verlag Mayer & Comp., Restauratotenblätter Sonderband, Wien, Austria (1997).

Kautek, W., S, P., König, E., and Krüge, J., 'Laser cleaning of antique parchements', *LACONA I, Restauratotenblätter Sonderband, Wien, Austria* (1997) 69-78.

Kautek, W., Pentzien, S., Röllig, M., Rudolph, P., Krüger, J., Maywald-Pitellos, C., Bansa, H., Grösswang, H., and König, E., 'Near-UV laser interaction with contaminants and pigments on parchment: laser cleaning diagnostics by SE-microscopy, VIS-, and IR-spectroscopy', *Journal of Cultural Heritage (Suppl. 1)* **1** (2000) s233-s240.

Kautek, W., Pentzien, S., Conradi, A., Leichtfried, D., and Puchinger, L., 'Diagnostics of parchment in the near-ultraviole and near-infrared scanning electron microscopy study', *Journal of Cultural Heritage (Suppl. 1)* **4** (2003) 179s-184s.

Kelly, R., Miottello, A., Braren, B., and Otis, C. E., 'On the debris phenomenon with laser sputtered polymers', *Applied Physics Letters* **60** (1992) 2980-2982.

Keyes, T., Clarke, R. H., and Isner, J. M., 'Theory of photoablation and its implications for laser phototherapy', *Journal of Physical Chemistry* **89** (1985) 4194-4196.

Klein, S., Fekrsanati, F., Hildenhagen, J., Dickmann, K., Uphoff, H., Marakis, Y., and Zafiropulos, V., 'Discoloration of marble during laser cleaning of by Nd:YAG laser wavelengths', *Applied Surface Science* **171** (2001) 242-251.

Koh, Y. and Sarady, I., 'Cleaning of corroded iron artfacts using pulsed TEA CO_2- and Nd:YAG-lasers', *Journal of Cultural Heritage (Suppl. 1)* **4** (2003) 129s-133s.

Kolar, J., Strlic, M., Mueller-Hess, D., Gruber, A., Troschke, K., Pentzien, S., and Kautek, W., 'Near-UV and visible pulsed laser interaction with paper', *Journal of Cultural Heritage (Suppl. 1)* **1** (2000) s221-s224.

Kolar, J., Strlic, M., Müller-Hess, D., Gruber, A., Troschke, K., Pentzien, S., and Kautek, W., 'Laser cleaning of paper using Nd:YAG laser running at 532 nm', *Journal of Cultural Heritage (Suppl. 1)* **4** (2003) 185s-187s.

Koller, J., Baumer, U., Grosser, D., and Schmid, E. 'Mastic'. In *Baroque and Rococo Lascquers*, Eds. K. Walch and J. Koller, Vol. 81, Arbeitshefte des Bayerischen Landesamtes fuer Denkmalpflege, Karl M. Lipp Verlag, Muenchen, (1997), 347-358.

Koren, G., *Appl. Phys B* **46** (1988) 147.

Küper, S. and Stuke, M., 'Femtosecond UV excimer laser ablation', *Applied Physics B* **44** (1988) 199-201.

Küper, S., Brannon, J., and Brannon, K., 'Threshold Behavior in Polyimide Photoablation: Single-Shot Rate Measurements and Surface-Temperature Modeling', *Applied Physics A 56* **56** (1993) 43-50.

Labourè, M., Bromblet, P., Orial, G., Weiderman, G., and Simon-Boisson, C., 'Assessment of laser cleaning rate on limestones and sandstones', *Journal of Cultural Heritage (Suppl. 1)* **1** (2000) s21-s27.

Landucci, F., Pini, R., Siano, S., Salimbeni, R., and Pecchioni, E., 'Laser cleaning of fossil vertebrates: a priliminary report', *Journal of Cultural Heritage (Suppl. 1)* **1** (2000) s263-s267.

Lanterna, G. and Matteini, M., 'Laser cleaning of stone artefacts: a substitute or alternative cleaning?' *Journal of Cultural Heritage (Suppl. 1)* **1** (2000) s29-s35.

Larson, J. H., Madden, C., and Sutherland, I., 'Ince Blundell: the preservation of an important collection of classical sculpture', *Journal of Cultural Heritage (Suppl. 1)* **1** (2000) s79-s87.

Lazzarini, L. and Asmus, J. F., 'The application of laser radiation to the cleaning of statuary', *Bulletin of the AIC* **13** (1973) 39-49.

Leavengood, P., Twilley, J., and Asmus, J. F., 'Lichen removal from Chines Spirit Path figures of marble', *Journal of Cultural Heritage (Suppl. 1)* **1** (2000) s71-s74.

Lee, J. M., Yu, J. E., and Koh, Y. S., 'Experimental study on the effect of wavelength in the laser cleaning of silver threads', *Journal of Cultural Heritage (Suppl. 1)* (2003) 157s-161s.

Luk'yanchuk, B., Bityurin, N., Anisimov, S., and Bäuelre, D., 'The role of excited species in UV-Laser Material Ablation, Part I: Photophysical Ablation of Organic Polymers', *Applied Physics A* **57** (1993a) 367-374.

Luk'yanchuk, B., Bityurin, N., Anisimov, S., and Bäuelre, D., 'The role of excited species in UV-Laser Material Ablation, Part II: The stability of the ablation front', *Applied Physics A* **58** (1993b) 449-455.

Luk'yanchuk, B., Bityurin, N., Anisimov, S., and Bäuerle, D. 'Photophysical Ablation of Organic Polymers'. In *Excimer Lasers*, Ed. L. D. Laude, Kluwer Academic Publishers, The Netherlands, (1994), 59-77.

Luk'yanchuk, B., Bityurin, N., Anisimov, S., Arnold, N., and Bäuelre, D., 'The role of excited species in UV-Laser Material Ablation, Part III: Non-stationary regimes in ablation', *Applied Physics A* **62** (1996) 397-401.

Luk'yanchuk, B. and Zafiropulos, V. 'On the theory of discolouration effect in pigments at laser cleaning'. In *Optical Physics, Applied Physics and Material Science: Laser Cleaning*, Ed. B. S. Luk'yanchuk, World Scientific, Singapure, New Jersey, London, Hong Kong, (2002), 393-414.

Madden, O., Abraham, M., Scheerer, S., and Werden, L., 'The effects of laser radiation on adhesives, consolidants and varnishes', In *Lacona V Proceedings, Osnabrück, Germany, September 15-18, 2003*, Eds. K. Dickmann, C. Fotakis, and J.

F. Asmus, Springer Proceedings in Physics, Vol. 100, Springer-Verlang, Berlin Heidelberg, (2005), 247-254.

Mahan, G. D., Cole, H. S., Liu, Y. S., and Philipp, H. R., 'Theory of polymer ablation', *Applied Physics Letters* **53** (1988) 2377-2379.

Marakis, G., Maravelaki, P., Zafiropulos, V., Klein, S., Hildenhagen, J., and Dickmann, K., 'Investigations on cleaning of black sandstone using different UV-pulsed lasers', *Journal of Cultural Heritage (Suppl. 1)* **1** (2000) s61-s64.

Marakis, G., Pouli, P., Zafiropulos, V., and Maravelaki-Kalaitzaki, P., 'Comparative study on the application of the 1st and 3rd harmonic of a Q-switched Nd:YAG laser system to clean black encrustation on marble, in: Proceedings of LACONA IV, September 11-14 2001, Paris, France, (ed. V. Vergés-Belmin)', *Journal of Cultural Heritage (Suppl. 1)* **4** (2003) 83s-91s.

Margheri, F., Modi, S., Mascotti, L., Mazzinghi, P., Pini, R., Siano, S., and Salimbeni, R., 'SMART CLEAN: a new laser system with improved emission characteristics and transmission through long optical fibres', *Journal of Cultural Heritage (Suppl. 1)* **1** (2000) s119-s123.

Matteini, M., Lalli, C., Tosini, I., Giusti, A., and Siano, S., 'Laser cleaning tests for the conservation of the Porta del Paradiso by Lorenzo Ghiberti', *Journal of Cultural Heritage (Suppl. 1)* (2003) 147s-151s.

Meyer, J., Feldeman, D., Kutzner, J., and Welge, K., *Appl Phys B* **45** (1988) 7.

Miller, J. C. and Haglund Jr, R. F. Laser Ablation and Desorption; Experimental Methods in the Physical Sciences 30, Academic Press, San Diego, CA (1998).

Mills, J. S. and White, R. *The Organic Chemistry of Museum Objects*, 2nd edition, Butterworth-Heinemann, Oxford, 1994.

Morgan, N., 'Excimer lasers restore 14th century icons', *Opto and Laser Europe* **7** (1993) 36-37.

Naylor, A., 'Conservation of the eighteenth century lead statue of George II and the role of laser cleaning', *Journal of Cultural Heritage (Suppl. 1)* **1** (2000) s145-s149.

Ochocinska, K., Kaminska, A., and Sliwinski, G., 'Experimental investigations of stained paper documents cleaned by the Nd:YAG laser pulses', *Journal of Cultural Heritage (Suppl. 1)* **4** (2003) 188s-193s.

Odlyha, M., Boon, J. J., Van den Brink, O. F., and Bacci, M., 'ERA: Environmental Research for Art conservation', *European Cultural Heritage Newsletter on Research* **10** (1997) 67-77.

Olaineck, C., Dickmann, K., and Bachmann, F., 'Restoring of cultural values from glass with excimer laser', *LACONA I, Restauratotenblätter Sonderband, Wien, Austria* (1997) 89-94.

Orial, G. and Gaufillet, J. P., 'Nettoyage des monuments historiques par dısincrustation photonique des salissures', *Technologie Industrielle Conservation*

Restauration du Patrimoine Culturel, Colloque AFTPV/SFIIC, Nice 19-22 September (1989) 118-125.

Papageorgiou, V. P., Bakola-Christianopoulou, M. N., Apazidou, K. K., and Psarros, E. E., 'Gas chromatographic-mass spectrometric analysis of the acidic triterpenic fraction of mastic gum', *Journal of Chromatography A* **769** (1997) 263-273.

Perez, C., Barrera, M., and Diaz, L., 'Positive findings for laser use in cleaning cellulosing supports', *Journal of Cultural Heritage (Suppl. 1)* **4** (2003) 194s-200s.

Pettit, G. H. and Sauerbrey, R., 'Pulsed Ultraviolet Laser Ablation', *Applied Physics A* **56** (1993) 51-63.

Phenix, A., 'Solubility parameters and the cleaning of paintings: an update and review', *Zeitschrift fór Kunsttechnologie und Konservierung* **12** (1998) 387- 409.

Phenix, A., 'The swelling of artists' paints in organic solvents Part 1 - a simple method for measuring the in-plane swelling of unsupported paint films', *Journal of the American Institute for Conservation* **41** (2002a) 43-60.

Phenix, A., 'The swelling of artists' paints in organic solvents Part 2 - comparative swelling powers of selected organic solvents and solvent mixtures', *Journal of the American Institute for Conservation* **41** (2002b) 61-90.

Pini, R., Siano, S., Salimbeni, R., Piazza, V., Giamello, M., Sabatini, G., and Bevilacqua, F., 'Application of a new laser cleaning procedure to the mausoleum of Theodoricq', *Journal of Cultural Heritage (Suppl. 1)* **1** (2000a) s93-s97.

Pini, R., Siano, S., Salimbeni, R., Pasquinucci, M., and Miccio, M., 'Tests of laser cleaning on archeological metal artefacts', *Journal of Cultural Heritage (Suppl. 1)* **1** (2000b) s129-s137.

Pouli, P. and Emmony, D. C., 'The effect of Nd:YAG laser radiation on medieval pigments', *Journal of Cultural Heritage (Suppl. 1)* **1** (2000) s181-s188.

Pouli, P., Frantzikinaki, K., Papakonstantinou, E., Zafiropulos, V., and Fotakis, C., 'Pollution encrustation removal by means of combined ultraviolet and infrared laser radiation: The application of this innovative methodology o the surface of the Parthenon West Frieze', In *Lacona V Proceedings, Osnabrück, Germany, September 15-18, 2003*, Eds. K. Dickmann, C. Fotakis, and J. F. Asmus, Springer Proceedings in Physics, Vol. 100, Springer-Verlang, Berlin Heidelberg, (2005), 333-340.

Rasti, F. and Scott, G., 'The effects of some common pigments on the photo-oxidation of linseed oil based paint media', *Studies in Conservation* **25** (1980) 145-156.

Robertson, C. W. and Williams, D., 'Lambert absorption coefficients of water in the infrared', *Journal of the Optical Society of America* **61** (1971) 1316-1320.

Roemich, H. and Weinmann, A., 'Laser cleaning of stained glass windows. Overview on an interdisciplinary project', *Journal of Cultural Heritage (Suppl. 1)* **1** (2000) s151-s154.

Ruhemann, H. *The cleaning of paintings*, Faber and Faber, London, 1968.

Römich, H., Dickmann, K., Mottner, P., Hildenhagen, J., and Müller, E., 'Laser cleaning of stained glass windows - Final results of a research project', *Journal of Cultural Heritage (Suppl. 1)* **4** (2003) 112s-117s.

Sabatini, G., Giamello, M., Pini, R., Siano, S., and Salimbeni, R., 'Laser cleaning methodologies for stone facades and monuments: laboratory on lithotypes of Siena architecure', *Journal of Cultural Heritage (Suppl. 1)* **1** (2000) S9-S19.

Salimbeni, R. and Bonsanti, G. Lasers in the Conservation of Artworks III, Proceedings of the International Conference, April 26-29 1999, Florence, Italy, *LACONA III)*, Journal of Cultural Heritage, **1**, Suppl. 1, 2000.

Salimbeni, R., Pini, R., Siano, S., Vannin, M., and Corallini, A., 'Excimer laser cleaning of stained glass samples', *LACONA I, Restauratotenblätter Sonderband, Wien, Austria* (1997) 83-88.

Sansonetti, A. and Realini, M., 'Nd:YAG laser effects on inorganic pigments', *Journal of Cultural Heritage (Suppl. 1)* **1** (2000) s189-s198.

Sauerbrey, R. and Pettit, G. H., 'Theory of the etching of organic materials by ultraviolet laser pulses', *Applied Physics Letters* **55** (1989) 421-423.

Scalarone, D., van der Horst, J., Boon, J. J., and Chiantore, O., 'Direct-temperature mass spectrometric detection of volatile terpenoids and natural terpenoid polymers in fresh and artifficially aged resins', *Journal of Mass Spectrometry* **38** (2003) 607-617.

Scholten, J. H., Teule, J. M., Zafiropulos, V., and Heeren, R. M. A., 'Controlled laser cleaning of painted artworks using accurate beam manipulation and on-line LIBS-detection', *Journal of Cultural Heritage (Suppl. 1)* **1** (2000) s215-s220.

Schoolenberg, G. E. and Vink, P., 'Ultra-violet degradation of polypropylene: 1. Degradation Profile and thickness of the embrittled surface layer', *POLYMER* **Vol. 32 No 3** (1991) 432 - 437.

Scott, G. 'Autoxidation and antioxidants: historical perspective'. In *Atmospheric oxidation and antioxidants*, Ed. G. Scott, Vol. I, Elsevier Science Publishers B.V., Amsterdam, (1993), 1 - 44.

Shekede, L., 'Lasers: a preliminary study on the their potential for the cleaning and uncovering of wall paintings', *LACONA I, Restauratotenblätter Sonderband, Wien, Austria* (1997) 51-56.

Shepherd, R. "A conservator's note". In *George Stubbs 1724-1806*, Ed. J. Egerton, Tate Gallery, London, (1984), 20-21.

Siano, S., Fabiani, F., Pini, R., Salimbeni, R., Giamello, M., and Sabatini, G., 'Determination of damage thresholds to prevent side effects in laser cleaning of pliocene sandstone of Siena', *Journal of Cultural Heritage (Suppl. 1)* **1** (2000) s47-s53.

Siano, S., Salimbeni, R., Pini, R., Giusti, A., and Matteini, M., 'Laser cleaning methodology for the preservation of the Porta del Paradiso by Lorenzo Ghiberti', *Journal of Cultural Heritage (Suppl. 1)* (2003a) 140s-146s.

Siano, S., Casciani, A., Giusti, A., Matteini, M., Pini, R., Porcinai, S., and Salimbeni, R., 'The Santi Quattro Coronati by Nanni di Banco: cleaning of the gilded decorations', *Journal of Cultural Heritage (Suppl. 1)* **4** (2003b) 123s-128s.

Siedel, H., Neumeister, K., and Gordon Sobott, R. I., 'Laser cleaning as part of the restoration process: removal of aged oil paint from a Renaissance sandstone portal in Dresden, Germany', *Journal of Cultural Heritage (Suppl. 1)* **4** (2003) 11s-16s.

Silverstein, R. M., Bassler, G. C., and Morrill, T. C. 'Ultraviolet Spectrometry'. In *Spectrometric Identification of Organic Compounds, 5th edition*, John Wiley and Sons, Inc., USA, (1991), 289-315.

Skoulikidis, T., Vassiliou, P., Papakonstantinou, P., Moraitou, A., Zafiropulos, V., Kalaitzak, A., Spetsidou, I., Perdikatsis, V., and Maravelaki, P., 'Some remarks on Nd:YAG and excimer UV lasers for cleaning soiled sulphated monument surfaces', *Workshop on Lasers in the Conservations of Artworks, Heraklion Crete, 4-6 October 1995, Book of Abstracts* (1995).

Soberhart, J. R., 'Polyamide ablation using intense laser beams', *Journal of Applied Physics* **74** (1993) 2830-2833.

Sportun, S., Cooper, M., Stewart, A., Vest, M., Larsen, R., and Poulsen, D. V., 'An investigation into the effect of wavelength in the laser cleaning of parchment', *Journal of Cultural Heritage (Suppl. 1)* **1** (2000) s225-s232.

Srinivasan, R. In *Laser Processing and Diagnostics, Springer Series in Chemical Physics*, Ed. D. Bäuerle, Springer, New York, (1984), 343-354.

Srinivasan, R., Braren, B., Seeger, D. E., and Dreyfus, R. W., 'Photochemical cleavage of a polymeric solid: details of the ultraviolet laser ablation of poly(methyl methacrylate) at 193 nm and 248 nm', *Macromolecules* **19** (1986a) 916-921.

Srinivasan, R., Braren, B., and Dreyfus, R. W., 'Ultraviolet laser ablation of polyimide films', *Journal of Applied Physics* **61** (1987) 372-376.

Srinivasan, R. and Braren, B., 'Ultraviolet laser ablation of organic polymers', *Chemical Reviews* **89** (1989) 1303-1316.

Srinivasan, R., 'Ablation of polymethyl methacrylate films by pulsed (ns) ultraviolet and irradiated (9.17 μm) lasers: A comparative study by ultrafast imaging', *Journal of Applied Physics* **73** (1993) 2743-2750.

Srinivasan, R. 'Interaction of laser radiation with organic polymers'. In *Laser Ablation: Principles and Applications*, Ed. J. C. Miller, Vol. 28, Springer Series of Material Science, Springer, Berlin, Heidelberg, (1994), 107.

Srinivasan, V., Smrtic, M. A., and Babu, S. V., 'Excimer laser etching of polymers', *Journal of Applied Physics* **59** (1986b) 3861-3867.

Stolow, N. 'Part II: Solvent Action'. In *On picture varnishes and their solvents.*, Eds. R. L. Feller, N. Stolow, and E. H. Jones, Revised edition 1971. Cleveland, Ohio: Case Western Reserve University. Revised and enlarged edition 1985. Washington DC: National Gallery of Art., (1985).

Sutcliffe, E. and Srinivasan, R., 'Dynamics of UV laser ablation of organic polymer surfaces', *Journal of Applied Physics* **60** (1986) 3315-3322.

Sutcliffe, H., Cooper, M., and Farnsworth, J., 'An initial investigation into the cleaning of new and naturally aged cotton textiles using laser radiation', *Journal of Cultural Heritage (Suppl. 1)* **1** (2000) s241-s246.

Sutherland, K. R., 'Solvent extractable components of oil paint films', PhD Thesis University of Amsterdam, (2001).

Svobodova, J., Slovak, M., Prikryl, R., and Siegl, P., 'Effect of low and high fluence on exerimentally laser-cleaned sandstone and marlstone tablets in dry and wet conditions', *Journal of Cultural Heritage (Suppl. 1)* **4** (2003) 45s-49s.

Swicklik, M. 'French painting and the use of varnish, 1750-1900'. In *Conservation Research*, National Gallery of Art, Washington DC, (1993), 157-174.

Tam, A. C., Leung, W. P., Zapka, W., and Ziemlich, W., 'Laser-cleaning techniques for removal of surface particulates', *Journal of Applied Physics* **71** (1992) 3515-3523.

Tanaka, K., Waki, H., Ido, Y., Akita, S., Yoshida, Y., and Yoshida, T., 'Protein and polymer analysis up to m/z 100,000 by laser ionization time-of-flight mass spectrometry', *Rapid Communications in Mass Spectrom.* **2** (1988) 151-153.

Teppo, E. and Galcagno, G., 'Restoration with lasers halts decay of ancient artefacts', *Laser Focus World, June* (1995) 55-59.

Teule, R., Scholten, H., van den Brink, O. F., Heeren, R. M. A., Zafiropulos, V., Hesterman, R., Castillejo, M., Martin, M., Ullenius, U., Larsson, I., Guerra-Librero, F., Silva, A., Gouveia, H., and Albuquerque, M. B., 'Controlled UV laser cleaning of painted artworks: a systematic effect study on egg tempera paint samples', *Journal of Cultural Heritage (Suppl. 1)* **4** (2003) 209s-215s.

Theodorakopoulos, C. and Zafiropulos, V., 'Uncovering of scalar oxidation within naturally aged varnish layers.' *Journal of Cultural Heritage (Suppl. 1)* **4** (2003) 216s-222s.

Thomson, G., 'Some picture varnishes', *Studies in Conservation* **3** (1957) 64-79.

Van den Brink, O. F., Boon, J. J., and van den Hage, E. R. E., 'Dosimetry of paintings: molecular changes in paintings as a tool to determine the impact of environment on works of art', *European Cultural Heritage Newsletter on Research* **10** (1997) 142-144.

Van der Doelen, G. A., van der Berg, K. J., and Boon, J. J., 'Comparative chromatographic and mass spectrometric studies of triterpenoid varnishes: fresh material and aged samples from paintings', *Studies in Conservation* **43** (1998) 249-264.

Van der Doelen, G. A., 'Molecular studies of fresh and aged triterpenoid varnishes', PhD Thesis University of Amsterdam, (1999).

Van der Doelen, G. A., Van den Berg, K. J., and Boon, J. J., 'A comparison of weatherometer aged dammar varnish and aged varnishes from paintings'. In *Art &*

Chimie: La Couleur: Actes du Congres, Eds. J. Goupy and J.-P. Mohen, CNRS Editions, Paris, (2000), 146-149.

Van der Doelen, G. A. and Boon, J. J., 'Artificial ageing of varnish triterpenoids in solution', *Journal of Photochemistry and Photobiology A: Chemistry* **134** (2000) 45-57.

Vergés-Belmin, V. Lasers in the Conservation of Artworks IV, Proceedings of the International Conference, September 11-14 2001, Paris, France, *LACONA IV)*, Journal of Cultural Heritage, **4**, Suppl. 1, 2003.

Vergés-Belmin, V., 'Comparison of three cleaning methods - microsandblasting, chemical pads and Q-switched YAG laser - on the portal of the cathedral Notre-Dame in Paris, France', *LACONA I, Restauratotenblätter Sonderband, Wien, Austria* (1997) 17-24.

Vitkus, J. R. and Asmus, J. F., 'Treatment of leather and vellum with transiet heating', *Preprints of 4th Annual Meeting of American Institute for Conservation of Historic and Artistic Works* (1976) 111-117.

Vodop'yanov, M. E. e. a., 'Dynamics of the interaction of laser light with λ=2.94 micrometers with a thin layer of liquid water', *Soviet Technical Physics Letters* **14** (1988) 143-145.

Watkins, K. G., 'A review of materials interaction during laser cleaning in art restoration', *LACONA I, Restauratotenblätter Sonderband, Wien, Austria* (1997) 7-15.

Wazen, P., '80 W average power of Q-switched Nd:YAG laser with otpical fibre beam delivery for laser cleaning application', *Journal of Cultural Heritage (Suppl. 1)* **1** (2000) s125-s128.

Wiedemann, G., Schulz, M., Hauptmann, J., Kusch, H. G., Müller, S., Panzner, M., and Wust, H., 'Laser cleaning applied in restoration of a medieval wooden panel chamber at Pirna', *Journal of Cultural Heritage (Suppl. 1)* **1** (2000) s247-s258.

Wolbers, R. *Cleaning Painted Surfaces: Aqueous Methods*, Archetype Publications Ltd, London, 2000.

Yeh, J. C., 'Laser ablation of polymers', *Journal of Vacuum Science and Technology A* **4** (1986a) 653-658.

Yeh, J. T. C., 'Laser Ablation of Polymers', *Journal of Vacuum Science and Technology A* **4** (1986b) 653-658.

Zafiropulos, V., Maravelaki, P., and Fotakis, C., 'Ablation Rate studies and LIBS as an on-line control technique in the removal of unwanted selected layers', *submitted in Restauratorenblätter, Sonderband, for the proceedings of Lacona II (this extra volume of the journal was never published)* (1997).

Zafiropulos, V. and Fotakis, C. 'Lasers in the Conservation of painted Artworks'. In *Laser in Conservation: an Introduction*, Ed. M. Cooper, Butterworth Heineman, Oxford, (1998), 79.

Zafiropulos, V., Georgiou, S., and Agglos, D., 'Lasers in art restoration (letters to the editor)', *Optics and Photonics News* **10** (1999) 4-5.

Zafiropulos, V., Manousaki, A., Kaminari, A., and Boyatzis, S., 'Laser Ablation of aged resin layers: A means of uncovering the scalar degree of aging', *ROMOPTO: Sixth Conference on Optics, Vlad V. I. (Ed.), SPIE Vol. 4430 (SPIE The International Society for Optical Engineering, Washington, (2001) 181-185.* (2000).

Zafiropulos, V., Stratoudaki, T., Manousaki, A., Melesanaki, K., and Orial, G., 'Discoloration of pigments induced by laser irradiation', *Surface Engineering* **17** (2001) 249-253.

Zafiropulos, V. 'Laser ablation in cleaning of artworks'. In *Optical Physics, Applied Physics and Material Science: Laser Cleaning*, Ed. B. S. Luk'yanchuk, World Scientific, Singapure, New Jersey, London, Hong Kong, (2002), 343-392.

Zafiropulos, V., Pouli, P., Kylikoglou, V., Maravelaki-Kalaitzaki, P., Luk'yanchuk, B. S., and Dogariu, A., 'Synchronous use of IR and UV laser pulses in the removal of encrustation: Mechanistic aspects, discoloration phenomena and benefits', In *Lacona V Proceedings, Osnabrueck, Germany, September 15-18, 2003*, Eds. K. Dickmann, C. Fotakis, and J. F. Asmus, Springer Proceedings in Physics, Vol. 100, Springer-Verlang, Berlin Heidelberg, (2005), 311-318.

Zehetner, W., 'The restoration of the "Riesentor", the great western portal at Vienna's St. Stephen's Cathedral', *LACONA I, Restauratotenblätter Sonderband, Wien, Austria* (1997) 37-38.

Zergioti, I., Petrakis, A., Zafiropulos, V., and Fotakis, C., 'Laser applications in paintings conservation', *LACONA I, Restauratotenblätter Sonderband, Wien, Austria* (1997) 57-60.

Zumbühl, S., Knochenmuss, R., Wülfert, S., Dubois, F., Dale, M. J., and Zenobi, R., 'A graphite-assisted laser desorption/ionisation study of light-induced ageing in triterpene dammar and mastic varnishes.' *Analytical Chemistry* **70** (1998) 707-715.

2. *Preparation and evaluation of extremely light aged varnish films for excimer laser ablation experiments*

Abstract

Dammar, mastic 'spirit' varnishes and a copal oil varnish were spin-coated and aged under UV-including for 500 h with a stabilised 60°C temperature, then for 45 days under free oxygen exposure and subsequent storage in the dark for at least a month, with the aim of preparation of extremely deteriorated films for excimer laser ablation experiments. The aged natural resin 'spirit' varnishes were evaluated with Direct Temperature resolved Mass Spectrometry (DTMS) and the aged copal oil varnish with Pyrolysis-GC/MS with online derivatisation with tetramethylammomium hydroxide (TMAH) (Py-TMAH-GC/MS). The accelerated aged natural resins developed high degrees of polymerisation and polarity both qualitatively and quantitatively. In particular, extreme oxidative degradation was indicated by the intense presence of A-ring oxidised dammarane type molecules, whereas unaffected triterpenoids, oxidised oleanane type and other oxidised dammarane type molecules, identical to oxidised triterpenoids found in paintings and in moderate UV-excluding accelerated light ageing, were present. DTMS total ion currents detected a strong increase in polarity, as well as in the degree of

condensation corresponding to an increase in the molecular weight of the aged films. Upon ageing, the copal oil varnish reduced its concentration in the copal resin components and underwent extreme deterioration in addition to the expected polymerisation. High degrees of oxidation, cyclisation and saturation became evident.

2.1 Introduction

In painting conservation, traditional chemical cleaning is accepted as an efficient varnish removal method for many cases which have undergone moderate ageing in the UV free environment of museums and galleries (Hedley 1980, Stolow 1985, Phenix 1998, 2002a, b). Laser cleaning has been proposed to deal with extreme ageing problems (Chapter 1), such as those that might occur in very old paintings varnished centuries ago. In effect, laser cleaning can be a valuable method when it is difficult to predict the ambient conditions these objects were subjected to, when the aged varnish is not soluble (Gettens and Stout 1966, Feller 1985, Stolow 1985, Sutherland 2001), and/or when the paint is solvent-sensitive (Shepherd 1984, Stolow 1985, Swicklik 1993, Cove 1998, Jones, *et al.* 1999, Carlyle 2001). Therefore, for the present study it was suggested to investigate varnishes aged under extreme conditions, with high degrees of oxidation and polymerisation, which would not be essentially compatible with moderate ageing problems that are commonly encountered in conservation of paintings. Therefore, heavily deteriorated coatings were tested with parameters that have been proposed for conservation treatments of paintings, including a KrF excimer laser (248 nm, 25 ns), optimal fluences and plume emission control (Zafiropulos 2002).

Oxidation and polymerisation are very important factors in the interaction of excimer laser pulses with organic films. Oxidation increases the absorption in the UV because of the generation of carbonyl and carboxylic acid groups (Scott 1993, Feller 1994, Mills and White 1994), the presence of which define the amount of UV laser photons absorbed onto the irradiated surface (Luk'yanchuk, *et al.* 1994, Srinivasan 1994). Upon the release of an excimer laser pulse, polymerisation regulates the extent of photochemical versus (minor) thermal effects generated in the surface, although the latter are minor, since a higher degree of polymerisation provides many covalent bonds to be broken by the absorbed laser photons (Srinivasan and Braren 1989, Zafiropulos 2002).

The first choice therefore was associated with the type of varnishes to be subjected to laser cleaning tests. These were two natural resin varnishes: dammar and mastic, whose principal problem is oxidation (De la Rie 1988b, Van der Doelen 1999, Dietemann 2003). Polymerisation in these cases does not evolve to the extent it does in high molecular weight polymers, such as for example drying oils, polyvinyl acetate, polyesters and Paraloid[1] polymers, which have been occasionally used as varnishes. Another case study was a copal oil varnish, whose main problems are polymerisation and saturation (Van den Berg, *et al.* 1999), generated initially by the thermally induced manufacturing, involving strong temperatures in the range of 300-350 °C (Mantell, *et al.* 1949, Mills and White 1994, Carlyle 2001), and by the subsequent ageing. The second choice was related to the ageing conditions these varnishes would be subjected to. From a variety of accelerated ageing methods, which are listed below

[1] This polymer is called Paraloid in Europe and Acryloid in USA

in Section 2.2, UV including xenon-arc radiation, which has been proven to produce the most extreme degradation consequences in natural resin varnishes (Zumbühl, *et al.* 1998b, Van der Doelen, *et al.* 2000), was chosen. Subsequently, the irradiated varnishes were left for 45 days near an open window in the Victoria & Albert Museum in London to consume fresh oxygen from the atmosphere. A problem encountered is that accelerated light ageing of natural varnishes does not result in discolouration (De la Rie 1988b, Feller 1994). Essentially, this is problematic because discolouration (yellowing) is the most significant visually observed degradation effect (De la Rie 1987, Van der Doelen, *et al.* 1998a). This effect is attributed to bleaching of the chromophores that are responsible for discolouration during the intense irradiation (De la Rie 1988b, Feller 1994, Dietemann 2003). Therefore the degraded varnishes were kept for a month in the dark prior to the investigations. In the presence of free radicals, autoxidation proceeds even in dark, similarly but in a lower rate than in light (Dietemann 2003). This way some yellowing was obtained in the tested varnishes.

The final choice depended on the need to investigate the depth profile of the tested deteriorated varnishes. The fabricated varnishes were chosen to be thick enough to enable the generation of successive depth-step zones with the laser (Chapter 3). Therefore thin and thick varnish films were prepared with means of spin-coating, with the thickest ones being 56 μm for dammar, 53 μm for mastic and 30 μm for the copal oil varnish. Spin-off findings aside excimer laser ablation tests showed the existence of gradients in absorption and polymerisation as a function of depth in a variety of aged varnishes, which were unrelated in terms of composition, origin, ageing and

deterioration (e.g. Figures 1.4.1 and 1.4.4). Essentially, these gradients influence the UV pulsed laser ablation of the material since successive pulses interact with successive depths of the same varnish. Investigations of these gradients were chosen to be carried out on highly degraded material not only qualitatively but also quantitatively. Hence, the samples were exposed to radiation which included UV for 500h to induce extreme oxidation, polymerisation and probably depolymerisation at least for the natural resin varnishes (Zumbühl, *et al.* 1998b). This would allow testing the interaction with the laser at different depth levels, as well as to detect whether these gradients are a systematic trend even in the most extreme conditions.

The ageing of the natural resin varnishes was monitored using Direct Temperature-resolved MS (DTMS) (Boon 1992), which has been very effective in the molecular characterisation of volatile and high molecular weight fractions of dammar and mastic (Van der Doelen 1999, Scalarone, *et al.* 2003a). The deterioration of the copal oil varnish film was monitored using Pyrolysis-GC/MS with online derivatisation in a methanolic solution of tetramethylammonium hydroxide (TMAH), which has been successful in analysis of complicated mixtures of paints and oil varnishes (Van den Berg, *et al.* 1996).

2.2 Part I: Natural triterpenoid resins: Dammar and Mastic

Dammar and mastic are the most frequently used natural resins employed for ‘spirit varnishes’ originally introduced in the seventieth century replacing coatings made of oil or mixtures of oils and resins (Carlyle 2001). Natural resin varnishes were fabricated by dissolution of the resins in volatile solvents, usually oil of turpentine

(De la Rie 1989, Carlyle 2001), which eventually was replaced by more contemporary solvents (De la Rie 1989).

Dammar resin originates from the trees of the family *Dipterocarpaceae*, which grow in the Malay States and in the East Indies (Mills and White 1994, Wenders 2001). Dammar used in the West, probably originates from *Hopea*, *Shorea*, *Balanocarpus*, and *Vateria*, all belonging to the *Dipterocarpaceae* family. However, the genus *Canarium* of the *Burseraceae* family also obtains a resin considered to be dammar (Poehland, *et al.* 1987, Coppen 1995). Mastic resin originates from the *Pistacia lentiscus* L. tree of the *Anacardiaceae* family. The major source of commercial mastic resin are the mastic trees in the Greek island of Chios, although *Anacardiaceae* trees are distributed along large coastal regions of the Mediterranean (Perikos 1993, Koller, *et al.* 1997, Papageorgiou, *et al.* 1997). Other *Pistachia* resins are the Indian Bombay mastic from the species *Pistacia khinjuk* Stocks and *Pistacia cabulica* Stocks, although the Chios mastic is the most frequently used and studied (Koller, *et al.* 1997, Dietemann 2003).

Both dammar and mastic resins exude naturally onto the surface of the bark, but their collection involves a careful process mainly based on gentle incisions of the parent tree (Torquebiau 1984, Koller, *et al.* 1997). Mastic also contains a minor quantity (~ 2%) of essential oil (Papageorgiou, *et al.* 1981, Koller, *et al.* 1997). After harvesting, the resin particles are sorted out by their particle size and their degrees of transparency and purity (Torquebiau 1984, Koller, *et al.* 1997). Several considerations have been expressed on how 'fresh' is a freshly harvested, commercially available triterpenoid resin. Although meticulous investigations on these considerations have

been made for mastic, the same should apply for dammar because of the similar harvesting conditions (Torquebiau 1984, Koller, *et al.* 1997).

Prior to commercial distribution, mastic particles, in particular, undergo an additional purification process, involving washing with large amounts of water and 'green soap' to remove unwanted impurities and soil inclusions, which occasionally renders the resin teardrops yellow and cloudy (Koller, *et al.* 1997). During the harvesting period the mastic teardrops are exposed to sunlight (Koller, *et al.* 1997), which was proved to initiate autoxidative radical chain reactivity in the resin particles (Dietemann 2003). The latter author determined that mastic harvested in the dark develops a minor amount of free radicals, while the number of radicals increases with increasing the duration of the harvesting period under sunlight. Investigations on commercially available 'fresh' mastic harvested in the same period, showed that the amount of free radicals in the teardrops increases as the teardrops decrease in size. This in fact is a good indicator regarding the property of such resins to block the propagation of light in their bulk. Inevitably, this has an impact on the quality of the resin that is bought as 'fresh'. Dietemann (2003) showed that while the usual commercial available 'fresh' resin has a rather yellow hue, mastic exuded and harvested in the dark is completely transparent. Hence, the commercially available resins are to some extent deteriorated. Even if the resins are completely fresh, generation of free radicals starts within a few weeks as soon as a thin varnish film is created (Dietemann 2003).

To date, the molecular characterisation of dammar (Mills 1956, Arigoni, *et al.* 1960, Brewis and Halsall 1961, Cerny, *et al.* 1963, Brewis, *et al.* 1970, Harrison, *et al.* 1971,

Dammarane Skeleton Molecules

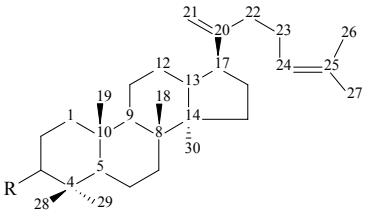

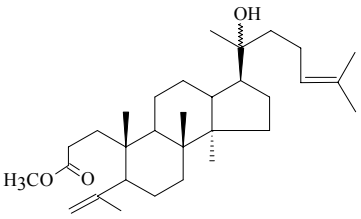

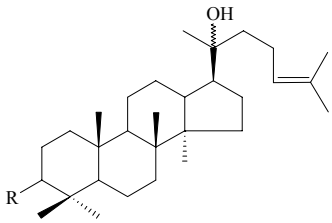

R = OH, H dammaradienol
R = O dammaradienone

Dammarenolic acid

R = O hydroxydammarenone
R = OH, H dammarenediol

Oleanane and Ursonic Molecules

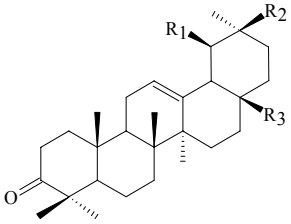

R_1 = H, R_2 = CH_3, R_3 = CHO oleanolic aldehyde
R_1 = CH_3, R_2 = H, R_3 = CHO ursonic aldehyde
R_1 = H, R_2 = CH_3, R_3 = COOH oleanolic acid
R_1 = CH_3, R_2 = H, R_3 = COOH ursonic acid
R_1 = H, R_2 = CH_3, R_3 = COOH monoric acid (double bond at C_{18})

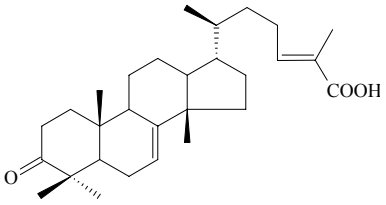

(iso)masticadienonic acid

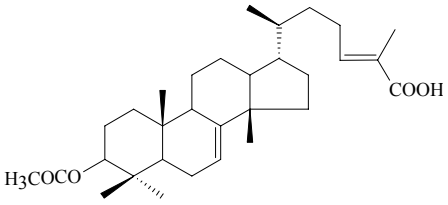

3-O-acetyl-3-epi(iso)masticdienolic acid

Figure 2.2.1 Common triterpenoid molecular structures present in dammar and mastic

Poehland, *et al.* 1987, De la Rie 1988a, Van der Doelen, *et al.* 1998a, Van der Doelen, *et al.* 1998b, Boon and van der Doelen 1999, Van der Doelen, *et al.* 2000) and mastic (Barton and Seoane 1956, Seoane 1956, Boar, *et al.* 1984, Marner, *et al.* 1991, Koller, *et al.* 1997, Papageorgiou, *et al.* 1997, Van der Doelen, *et al.* 1998a, Van der Doelen, *et al.* 1998b, Boon and van der Doelen 1999, Van der Doelen, *et al.* 2000, Dietemann 2003) has been exhaustive, and comprehensive reviews are already provided (De la Rie 1988b, Van der Doelen 1999, Dietemann 2003). Both resins consists of volatile triterpenoid (C30) molecules, the most characteristic of which are shown in Figure 2.2.1, and in a lesser extent of hydrocarbon polymers and sesquiterpenoids (C15) (De la Rie 1989, Mills and White 1994, Boon and van der Doelen 1999). While several

acids based on the characteristic masticadienonic and masticadienolic skeleton have been recognised only in mastic (Barton and Seoane 1956, Seoane 1956, Papageorgiou, *et al.* 1997), all the other triterpenoids shown in Figure 2.2.1 are contained in both resins in different proportions (Section 2.3). In addition, both resins have a polymeric fraction, caused by polycadinene (Van Aarssen, *et al.* 1990) and cis-1,4-poly-β-myrcene (Van den Berg, *et al.* 1998), which are the polymers of dammar and mastic respectively (see below, Figure 2.2.3).

2.2.1 The ageing of natural resin varnishes

Fundamental studies on the ageing mechanisms of triterpenoid resins have been reported by De la Rie (1988a, b) and Van der Doelen and co-workers (1998a and b, 1999 and 2000). Zumbühl and co-workers (1998a and b) emphasized the consequences of light-induced ageing for mechanical behavior, while Dietemann (2003) shed some light on the yellowing processes that occur under both natural light and in darkness. Ageing of triterpenoid resins results in oxidation, crosslinking polymerisation and decomposition of the incorporated compounds (De la Rie 1988b, Van der Doelen 1999). While these three processes contribute to the overall degradation, oxidation has been pinpointed as the most prominent problem of aged natural varnishes. Degradation in general has been ascribed to autoxidative radical chain reactions (Scott 1993, Feller 1994):

Initiation:	R-H	+	$X^{\cdot}$ (initiator)	→	$R^{\cdot}$	+	X-H	(i)
Propagation:	$R^{\cdot}$	+	O_2	→	$ROO^{\cdot}$			(ii)
	$ROO^{\cdot}$	+	RH	→	ROOH	+	$R^{\cdot}$	(iii)
Branching:			ROOH	→	$RO^{\cdot}$	+	$^{\cdot}OH$	(iv)

Termination:	$RO^{\cdot}$	+	$R'O^{\cdot}$	→	ROOR'	(v)
	$RO^{\cdot}$	+	$R'^{\cdot}$	→	ROR'	(vi)
	$R^{\cdot}$	+	$R'^{\cdot}$	→	RR'	(vii)

Once a radical is formed (i) it instantly reacts with an oxygen molecule available (ii). The resulting peroxyl radicals are relatively stable and therefore step (iii) is rate determining. Hydrogen abstraction from a molecule in step (iii) competes also with addition to double bonds (Scott 1993, Feller 1994), which as shown below (Figure 2.2.4) provides a first step in the process of discolouration. Homolytic cleavage of hydroperoxides is induced via heat or light depending on the energy (iv), producing alkoxy radicals $RO^{\cdot}$, which are very reactive with alcohols, ethers and ketones. Some of the known oxidation products of natural resins, although not expected to be directly formed via this procedure, have been indicated to be related to secondary reactions related to the principal autoxidation process (Van der Doelen, *et al.* 1998a, Van der Doelen, *et al.* 1998b).

2.2.1.1 Oxidation

Oxidation of natural resins takes place both in light and darkness, though the rate is faster in light (De la Rie 1989, Dietemann 2003). Consumption of oxygen via autoxidation leads to products containing hydroxy, ether, carbonyl and carboxylic acid groups (Scott 1993). Several studies have shown that upon oxidation the total amount of original triterpenoid compounds become less abundant in favour of oxidation products (Poehland, *et al.* 1987, De la Rie 1988a, Koller, *et al.* 1997, Papageorgiou, *et al.* 1997, Van der Doelen, *et al.* 1998a, Van der Doelen, *et al.* 1998b, Zumbühl, *et al.* 1998b, Boon and van der Doelen 1999, Van der Doelen, *et al.* 2000,

Dietemann 2003). Natural ageing leads to side chain oxidation of triterpenoids with the dammarane skeleton and oxidation in positions C-11, C-17 and C-28 of oleanane and ursane skeletons, as shown in Figure 2.2.2 (a) and (b) (Van der Doelen, *et al.* 1998a). Similar oxidation products have been observed after accelerated ageing under fluorescent tube light and xenon-arc light excluding the UV wavelengths (Carlyle, *et al.* 1998, Van der Doelen, *et al.* 1998b).

In the presence of UV in the xenon arc weatherometer, triterpenoid products with oxidised A-rings at position C-2, originating from molecules with the dammarane skeleton, are formed (Figure 2.2.2 (c)), which are not generated in natural ageing (Van der Doelen, *et al.* 2000). Most of these products are ketones that almost quantitatively degrade to acids via Norrish type reactions. Direct irradiation behind a window, which cuts wavelengths shorter than 310 - 315 nm, does not lead to A-ring oxidation (Van der Doelen, *et al.* 2000, Dietemann 2003). An innovative method of artificial ageing of triterpenoid varnishes in solution and subsequent irradiation under fluorescent light generated similar oxidation products to that of natural ageing (Van der Doelen and Boon 2000). If the polymer of the resins (Figure 2.2.3) is removed (Koller, *et al.* 1997), the oxidation procedure becomes faster and stronger, as shown by Dietemann (2003) for mastic. According to the latter author, commercially available natural resins, even if considered 'fresh', are already in an advanced stage of oxidation, and therefore control samples used to study the effects of ageing under various conditions abundantly contain free radicals. This has been also observed by Zumbühl and co-workers (1998b) using graphite-assisted laser desorption/ionisation MS.

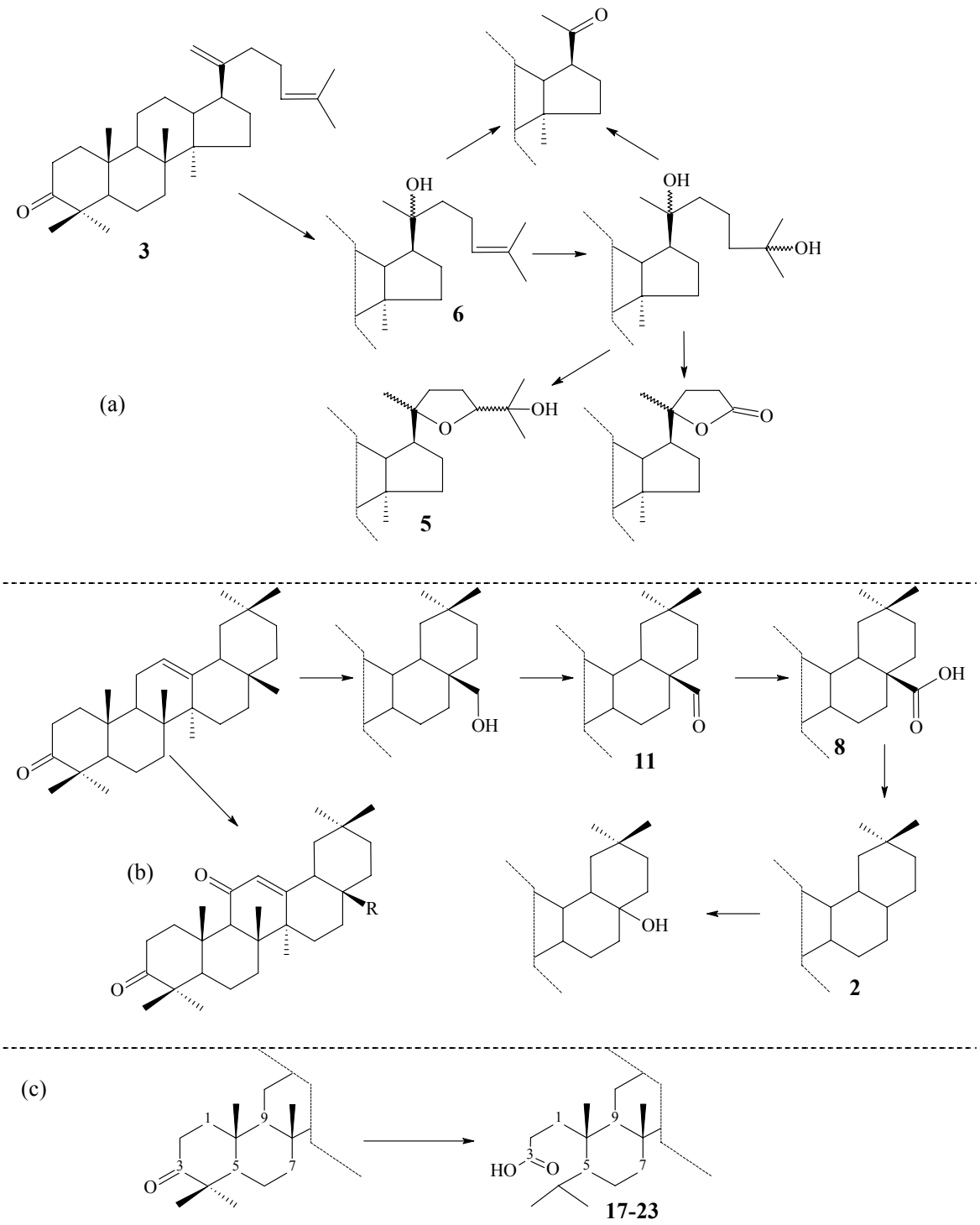

Figure 2.2.2 Oxidation stages (a) of dammarane type molecules in the side chain, (b) of oleanane type molecules and (c) of the A-ring at position C-2 of dammarane type molecules (Van der Doelen, et al. 1998a, 1998b, 2000). The figures correspond to labels in Tables 2.3.1 – 2.3.4.

2.2.1.2 Polymerisation (Crosslinking)

Figure 2.2.3 shows the radical polymerisation of the cadinene to polycadinene (Van Aarssen, *et al.* 1990) and the monoterpene (C10) molecule β-myrcene to cis-1,4-poly-β-myrcene (Van den Berg, *et al.* 1998), which are the polymers of dammar and mastic respectively. Both polycadinene and cis-1,4-poly-β-myrcene are not soluble in alcohol and are present in the teardrops of the resins, when harvested under sunlight. If mastic is harvested in the dark and radical formation is suppressed in the resin, polymerisation is hindered, while light exposure at a later date does not lead to polymerisation because of the evaporation of the monoterpenoids (Dietemann 2003). According to this finding, drying of natural resins involves evaporation of monoterpenes and polymerisation.

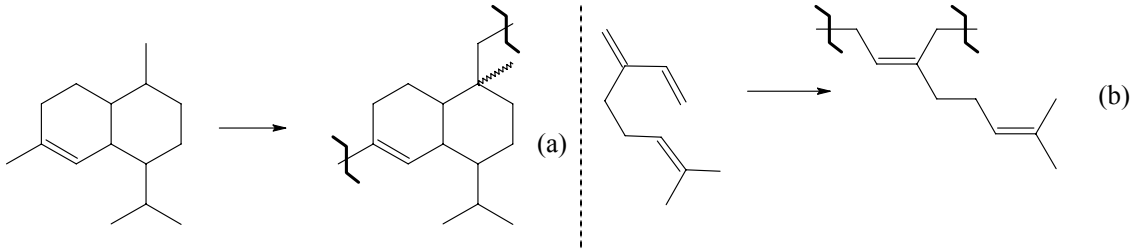

Figure 2.2.3 Radical polymerisation of cadinene (204 Da) to polycadinene (a) and β-myrcene to cis-1,4-poly-β-myrcene that is 136 Da (b) corresponding to the identified polymers of dammar (Van Aarssen, et al. 1990) and mastic (Van der Berg, et al. 1998)

Accelerated ageing under xenon arc radiation excluding UV wavelengths and radiation under fluorescent tubes generate a lower degree of crosslinking than that in natural aged varnishes (Van der Doelen 1999, Scalarone, *et al.* 2003a). Ageing using xenon-arc radiation with UV wavelengths to simulate outdoor exposure under sunlight has shown that both dammar and mastic resins generate a considerable degree of condensation (Zumbühl, *et al.* 1998b, Scalarone, *et al.* 2003a). A

comparable degree of condensation to that of natural aged varnishes is also formed upon ageing in solution (Van der Doelen and Boon 2000).

2.2.1.3 Discolouration (Yellowing)

Yellowing is the most obvious visual effect of aged natural resins and is attributed to unsaturated ketones that are formed upon autoxidation and absorb in the blue (400–490 nm) (De la Rie 1988b, Van der Doelen 1999, Dietemann 2003). In experimental ageing tests, yellowing was mainly observed to develop in darkness and not under

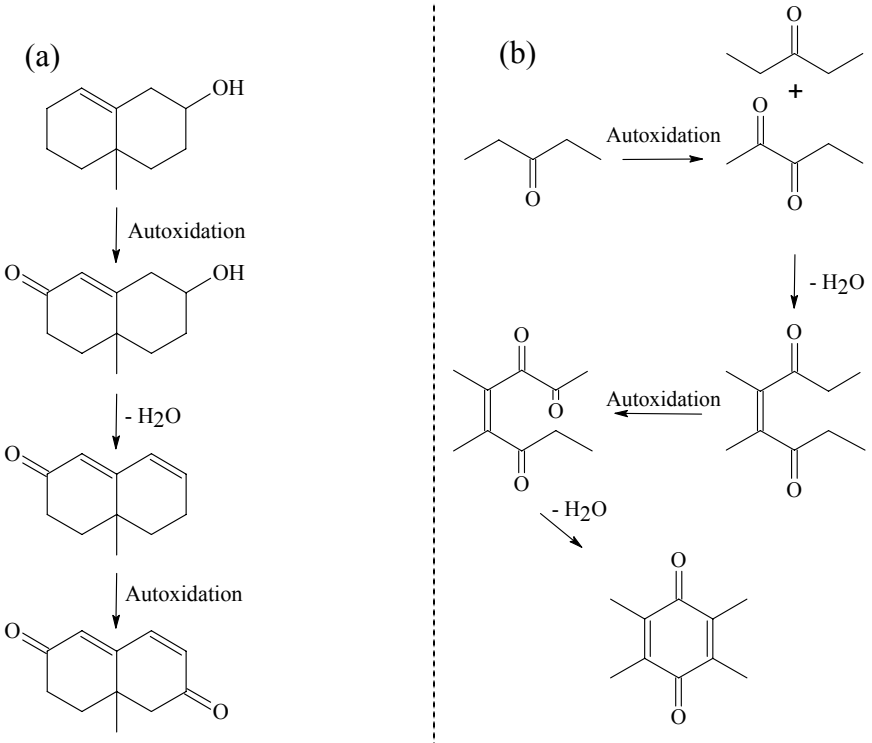

Figure 2.2.4 Unsaturated ketones formed via allylic oxidation and elimination of hydroxy groups. Subsequent autoxidation leads to (a) conjugated diketones (De la Rie 1988); and combination of condensation and autoxidation reactions leads to (b) dimerisation and cyclisation forming unsaturated quinones (Formo 1979). Both these products absorb in the blue region of electromagnetic radiation and are responsible for the yellowing effect of aged natural resins.

accelerating light exposure, in which autoxidation is much stronger (De la Rie 1988b, Feller 1994). This has been attributed to bleaching of the yellow chromophores under intense light (De la Rie 1988b). Yellow chromophores are formed in two ways

(Figure 2.2.4): (i) a two step process requiring allylic oxidation of double bonds and by elimination of hydroxy groups, which enlarges unsaturation and then leads to yellow conjugated diketones upon subsequent autoxidation (De la Rie 1988b); and, (ii) combination of condensation reactions inducing dimerisation of two ketones, which upon autoxidation generate yellow unsaturated quinones (Formo 1979b). The latter yellow products are accountable for the strong absorption of the polymeric fraction of aged triterpenoid varnishes at 400 nm (De la Rie 1988b, Boon and van der Doelen 1999). This is consistent with findings showing that yellowing is associated with the high molecular weight fraction of triterpenoid varnishes (Van der Doelen and Boon 2000). Removal of the condensed fractions of natural resins (Koller, *et al.* 1997) prior to ageing, reduces significantly the yellowing effect, although more oxygen is consumed this way (Dietemann 2003).

2.2.2 An argument for the laser cleaning of paintings

Upon chemical cleaning of paintings coated with natural resins there are indications that the polymeric fraction of the varnish is not removed by the solvent, but it rather precipitates on the painted surface (Boon and van der Doelen 1999). It is hereby suggested that this development would cause several problems. First, given that the polymers of dammar and mastic alone become extensively yellow with age (Dietemann 2003), the painting would appear more discoloured than it would be if these fragments were removed. Usually, once a varnish is removed from a painting it is replaced with a new one. It is therefore assumed that the heavily discoloured, crosslinked fragments of the old varnish would diminish the performance of the new varnish upon their integration. Evidently, the high molecular weight fragments

remaining on the surface would raise the overall MW of the new varnish. In this case the overall higher MW of the new varnish would increase the viscosity of the final coating. This indicates that the roughness of the final surface of the new varnish would be higher than it could have been without the high MW of the older varnish, rendering the coating less transparent (De la Rie 1987, Berns and De la Rie 2002, 2003). In case of a gradient, laser cleaning can then be very valuable, because the high MW fraction, being at the surface, is readily removed with a few laser pulses.

In addition, the contact of the solvent with the polymer and the volatile fraction of the varnish removed, suggests that some volatile fragments may stick to the high MW crosslinked fragments remaining on the painted surface leaving behind a considerable number of free radicals, which would speed up the oxidation process in the new varnish. This argument, however, can be also used against laser cleaning for paintings with excimer lasers, because of the interaction of the varnish with the UV laser photons. Therefore some of the aged, laser-ablated varnish should remain on the surface to prevent the UV laser photons from propagating in the paint (Zafiropulos and Fotakis 1998). Nevertheless, the fate of the irradiated organic surface mainly depends on the energy density of the photons and specific time windows, including the duration of the pulse, excitation and relaxation time frames (Bäuerle 2000, see also Chapter 1). There are indications that using optimal fluences (Zafiropulos 2002), the free radicals formed in the material, upon the generation of laser-induced desorbing photofragments, recombine efficiently to form similar structures to the parent molecule due to the so-called ‘cage effect’ (Georgiou, *et al.* 1997, Georgiou, *et al.* 1998).

2.3 An Evaluation of the aged dammar and mastic varnishes

DTMS is a rigorous technique based on thermally assisted ionisation that provides short-time analysis of complex molecular systems and requires a microscopic sample quantity without chemical processing (Boon 1992). It has been very effective in the molecular characterisation of dammar and mastic aged under various conditions (Van der Doelen, *et al.* 1998a, Van der Doelen 1999, Van der Doelen and Boon 2000, Scalarone, *et al.* 2003a). These studies showed that more than 30 identified triterpenoid molecules of moderate molecular weights (400/500 Da) are incorporated in the varnish after a considerable degree of degradation. A valuable feature of DTMS is the separation of the ionised components in apolar, polar and crosslinked fractions desorbing in the ion source at successively increasing temperature windows with an end temperature of 800 °C (Boon 1992). Given that pyrolysis is obtained online under vacuum, once the thermally dissociated products are formed they evaporate instantly and therefore the probability of secondary reactions due to molecular collisions is minimal. The apolar and polar fractions of a sample desorb at relatively low temperatures via evaporation, while high MW crosslinked material desorbs at higher temperatures owing to pyrolysis via thermally assisted bond breaking. The various groups generate apparent peaks in the order of the temperature of desorption and, hence, are readily monitored in the DTMS total ion currents (TIC's). The EI-DTMS TIC's in Figure 2.3.1 demonstrate that dammar and mastic, analysed prior to and after ageing become more polar and crosslinked with age (Van der Doelen 1999, Scalarone, *et al.* 2003a). See Section 2.3.1 for more details on the DTMS TIC's.

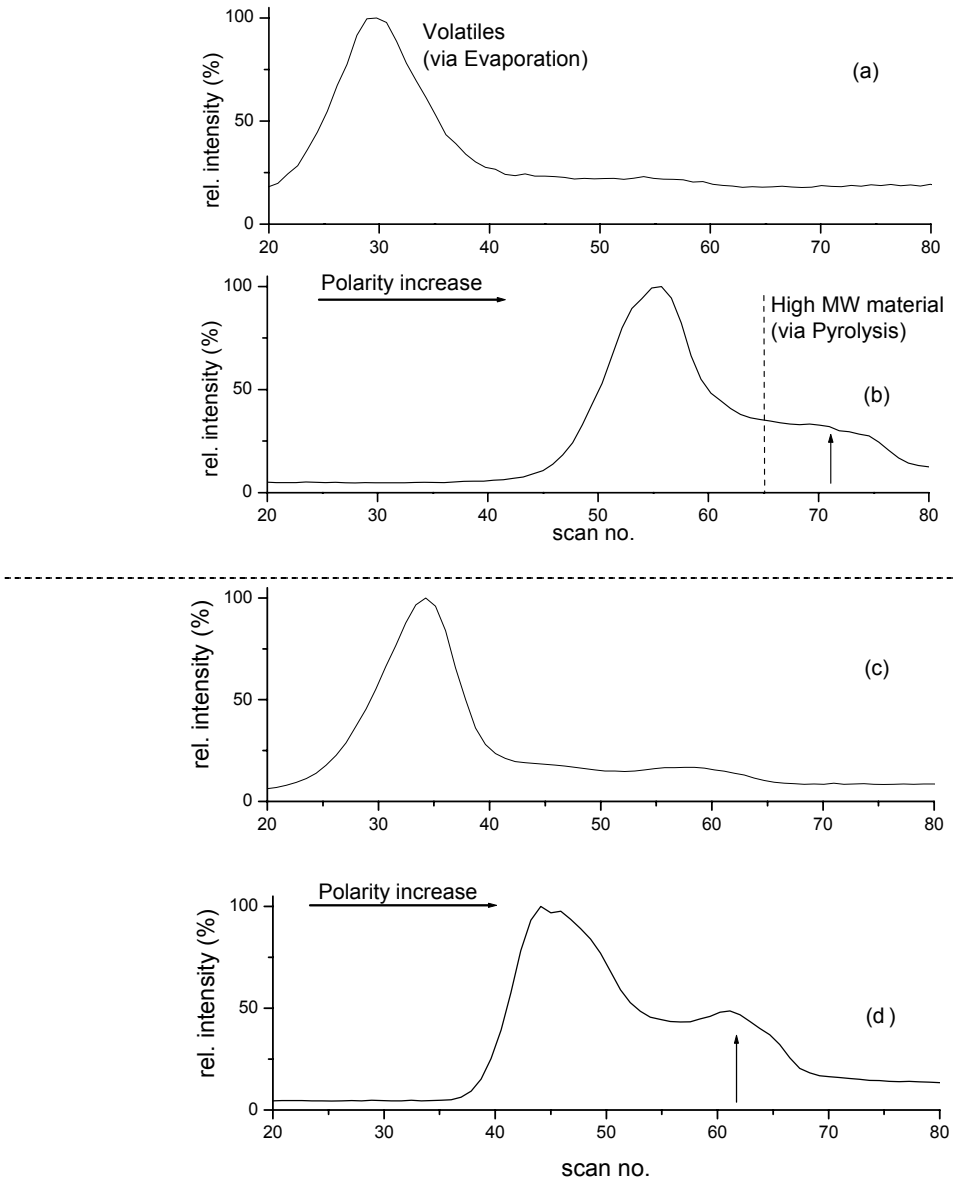

Figure 2.3.1 EI-DTMS TIC's of unaged and aged (500h, λ > 295 nm) dammar (a, b) and mastic (c, d) respectively. The shifts of the peak emerging at the lower scan numbers between unaged and aged states indicates the increased polarity, while the intensity increase of the peak emerging at the high scan numbers indicates that pyrolysed high MW species are more abundant in the aged films.

The main difficulty of DTMS is the interpretation of summation mass spectra that are produced by volatilisation and subsequent thermal degradation, because of the composition complexity of the multi-component resins. Therefore, DTMS analysis of such materials is usually carried out both under Electron Ionisation (EI) and ammonia chemical ionisation (NH_3/CI) modes (Van der Doelen 1999). Under EI ionisation

mode (16 eV) minor fragmentation of the incorporated molecules is induced, thereby yielding structural and hence more detailed information, whereas under NH_3/CI ionisation mode ammonia adduct molecular ions $[M+NH_4]^+$, $[M+H]^+$ and $[M+NH_4-H_2O]^+$ cations are obtained, thus giving molecular weight information. For the present study, interpretation of EI- and NH_3/CI-DTMS was obtained with support from earlier DTMS studies (Van der Doelen, *et al.* 1998a, Van der Doelen 1999, Van der Doelen and Boon 2000, Scalarone, *et al.* 2003a), as well as from findings based on GC/MS and HPLC-MS (Van der Doelen, *et al.* 1998a, Van der Doelen, *et al.* 1998b).

Table 2.3.1 List of Compounds found in unaged dammar resin

Label	Compound name	Mw	EI mass/charges*	NH_3/CI mass/charges
1	Nor-α-amyrone (3-oxo-28-nor-urs-12-ene)	410	**204**, 410	428
2	Nor-β-amyrone (3-oxo-28-nor-olean-12-ene)	410	**204**, 410	428
3	Dammaradienone (3-oxo-dammara-20(21),24-diene)	424	109, 205, **424**	442
4	Dammaradienol (3β-hydroxy-dammara-20,24-diene)	426	**109**, 189,207,408, 426	
5	Dammarenolic acid (20-hydroxy-3,4-seco-4(28),24-dammaradien-3-oic acid)	458	**109**, 440	476,458
6	Hydroxydammarenone (20-hydroxy-24-dammaren-3-one)	442	109, 315, 355, **424**	442
7	20,24-epoxy-25-hydroxy-dammaran-3-one	458	**143**, 399	143
8	Oleanonic acid (3-oxo-olean-12-en-28-oic acid)	454	189, **203**,248,409, 454	472
9	Ursonic acid (3-oxo-12-ursen-28-oic acid)	454	189, **203**,248,409, 454	472
11	Oleanonic aldehyde	438	**203**, 232, 409, 438	456
12	Ursonic aldehyde	438	**203**, 232, 409, 438	456
15	20,24-epoxy-25-hydroxy-3,4-seco-4(28)dammaren-3-oic acid	474	143	143

* m/z in bold correspond to the highest relative intensity of the series according to previous findings (Van der Doelen, et al. 1998a)

Table 2.3.2 List of Compounds found in unaged mastic resin

Label	Compound name	Mw	EI mass/charges	NH_3/CI mass/charges
2	Nor-β-amyrone (3-oxo-28-nor-olean-12-ene)	410	**204**, 410	428
3	Dammaradienone (3-oxo-dammara-20(21),24-diene)	424	109, 205, **424**	442
5	Dammarenolic acid (20-hydroxy-3,4-seco-4(28),24-dammaradien-3-oic acid)	458	**109**, 440	476,458
6	Hydroxydammarenone (20-hydroxy-24-dammaren-3-one)	442	109, 315, 355, **424**	442
7	20,24-epoxy-25-hydroxy-dammaran-3-one	458	**143**, 399	143
8	Oleanonic acid (3-oxo-olean-12-en-28-oic acid)	454	189, **203**,248,409, 454	472
10	(3-oxo-olean-18-en-28-oic acid)	454	**189**, 203,248,409, 454	472
11	Oleanonic aldehyde	438	**203**, 232, 409, 438	456
	(Iso)masticadienonic acid (3-oxo-13α,14β,17βH,20αH-lanosta-8,24-dien- lanosta-7,24-dien-26-oic acid)	454	439, **454**	472
14	3-O-Acetyl-3epi(iso)masticadienolic acid (3α-Acetoxy-13α,14β,17βH,20αH-lanosta-8,24-dien-26-oic acid or 3α-Acetoxy-13α,14β,17βH,20αH-lanosta-7,24-dien-26-oic acid)	498	**438**, 498	516
16	28-nor-olean-18-en-3-one	410	163, 191, 410	428

Figure 2.3.2 shows the EI-DTMS summation mass spectra of two varnishes, after solidification, prior to ageing. The NH_3/CI-DTMS are shown in Figure 2.3.3 below. The compounds detected are listed in Tables 2.3.1, for dammar and Table 2.3.2, for mastic. All the triterpenoid molecules have molecular weights somewhat larger than 400 and less than 500 Da. This is demonstrated in the EI DTMS summation mass spectra of both unaged dammar and mastic films, which produce highly abundant mass/charges between m/z 400 and 500. These peaks are attributed to triterpenoid molecular ions and radical cations $[M\text{-}H_2O]^{+\cdot}$ (Van der Doelen, *et al.* 1998a, Scalarone, *et al.* 2003a).

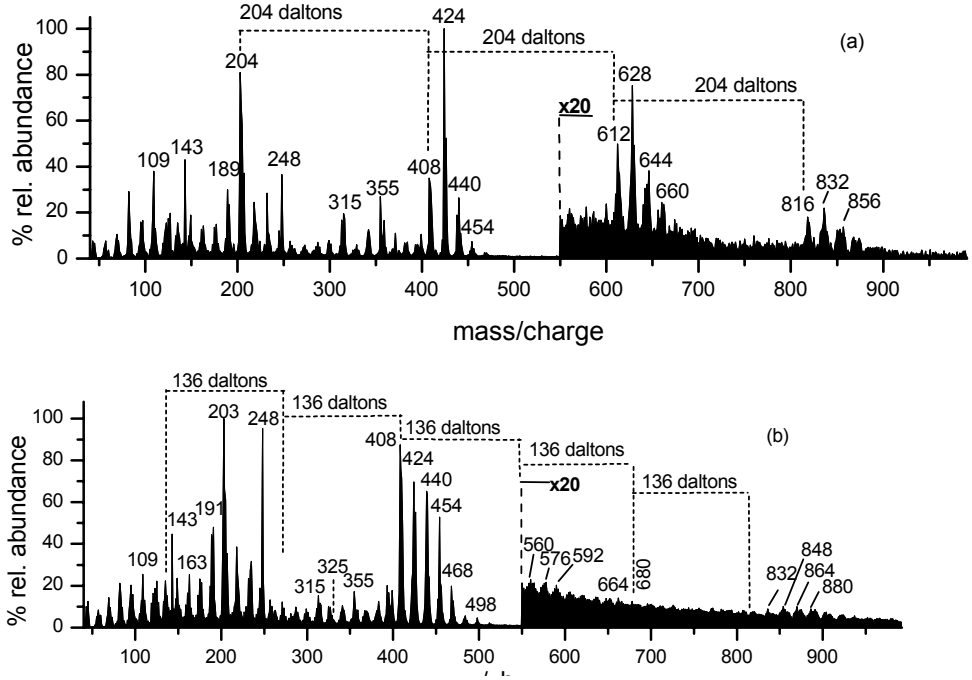

Figure 2.3.2 EI-DTMS of the unaged dammar (a) and mastic (b) films

Relative abundances of m/z 204 and 410 in the EI mode and m/z 428 in the NH_3/CI mode indicate the presence of nor-α-amyrone (**1**) and/or nor-β-amyrone (**2**) in dammar (Van der Doelen, *et al.* 1998b) confirming previous GC/MS findings (De la Rie 1988a), but only nor-β-amyrone (**2**) for mastic (Marner, *et al.* 1991, Van der Doelen, *et al.* 1998b). The presence of dammarane type molecules (Figure 2.2.1), i.e dammaradienone (**3**) (Mills and Werner 1955, Mills 1956, De la Rie 1988a), dammaradienol (**4**) (Mills and Werner 1955, Mills 1956, Poehland, *et al.* 1987, De la Rie 1988a), dammarenolic acid (**5**) and hydroxydammarenone (**6**) (Mills and Werner 1955, Poehland, *et al.* 1987, De la Rie 1988a) that have been established as constituents of fresh dammar resin (Van der Doelen, *et al.* 1998a, Van der Doelen, *et al.* 1998b, Scalarone, *et al.* 2003a), is also confirmed in the present DTMS study of the unaged dammar film. Characteristic components with the dammarane skeleton are also present in unaged mastic, i.e. **3** and **6**, which is in a good agreement with past

molecular investigations on fresh mastic resin (Marner, *et al.* 1991, Papageorgiou, *et al.* 1997, Van der Doelen, *et al.* 1998a, Van der Doelen, *et al.* 1998b, Scalarone, *et al.* 2003a). In the EI ionisation mode the mass spectra of all the dammarane type

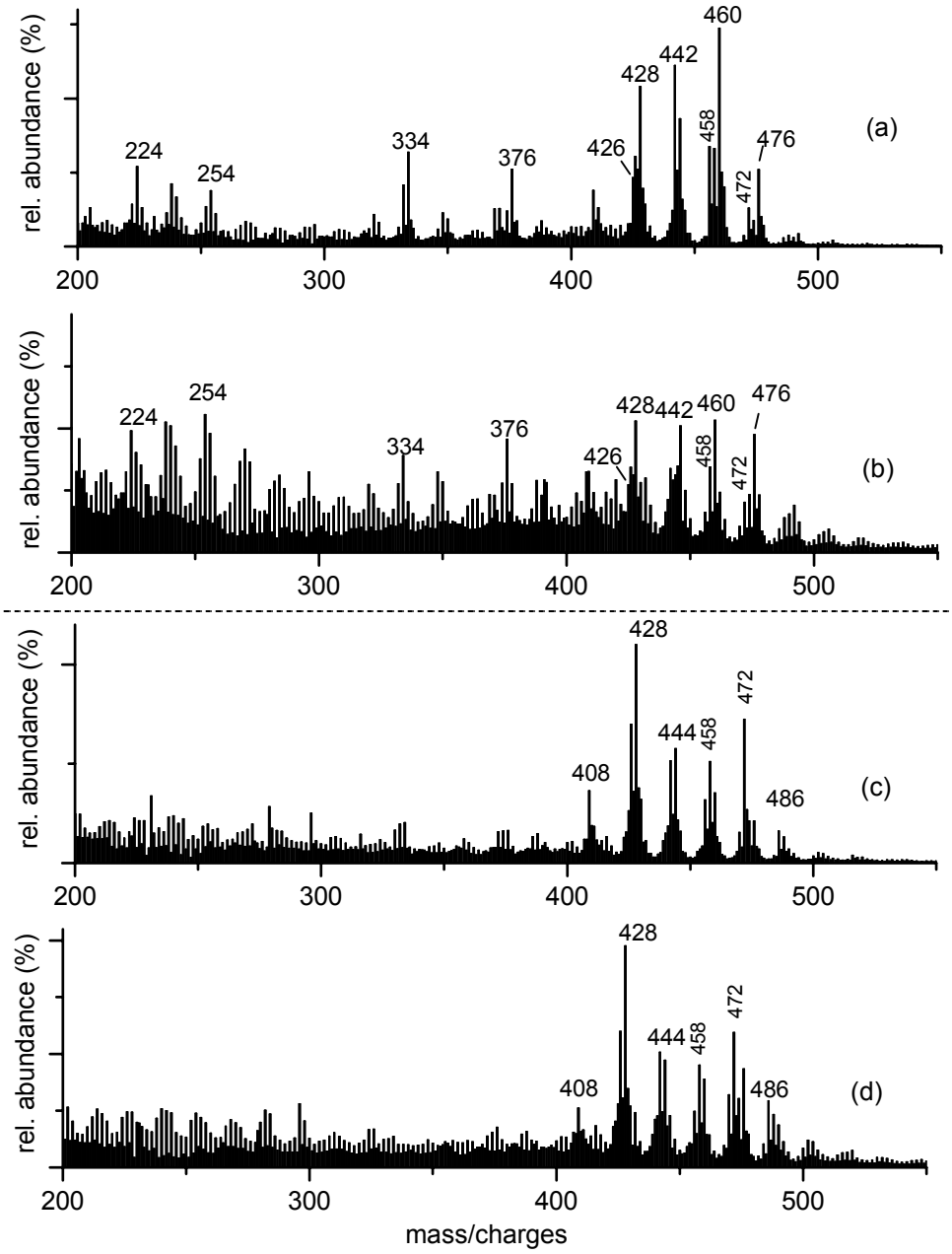

Figure 2.3.3 NH_3/CI-DTMS of dammar prior to (a) and after (b) light ageing (500h, $\lambda > 295$ nm); and mastic prior to (c) and after (d) light ageing (500h, $\lambda > 295$ nm).

molecules have a common ionic fragment at m/z 109 that results from aliphatic side-chain scission at position C-17 of the dammarane skeleton (Van der Doelen, *et al.*

1998b). The presence of **3** and **6**, which have additional ion peaks in the EI mode at m/z 424 ($[M]^{+\cdot}$), 205 and m/z 315, 355, 424 ($[M\text{-}OH]^{+}$) respectively and the same ion peaks in the NH_3/CI mode at m/z 442 ($[M+NH_4]^{+}$ corresponding to **3** and $[M\text{-}OH+NH_4]^{+}$ to **6**), signifies the molecular similarities of dammar and mastic. However, it is demonstrated that dammarane compounds are more abundant in dammar in line with previous DTMS and GC/MS studies (Van der Doelen, *et al.* 1998a, Scalarone, *et al.* 2003a).

Other compounds that were identified with the present DTMS study were molecules with oleanane and ursane skeletons. Based on previous chromatographic analytical data and DTMS analysis (Van der Doelen, *et al.* 1998a, Scalarone, *et al.* 2003a) the ionic peaks of oleanonic and ursonic acids (**8**, **9**), oleanonic and ursonic aldehydes (**11**, **12**) were confirmed in dammar and oleanonic and moronic acids and aldehydes (**8**, **10**, **11**) in mastic. The presence of **8**, **9**, **11** and **12** in dammar has been established by De la Rie (1988a), while previous studies had shown the presence of **9** (Mills and Werner 1955, Poehland, *et al.* 1987). In the case of mastic only oleanane and not ursane type molecules have been identified, i.e. **8**, **10** (Papageorgiou, *et al.* 1997) and **11** (Marner, *et al.* 1991). The moronic acid (**10**), which has the same molecular weight and ionic fragments with oleanolic acid (**8**) in both EI and NH_3/CI ionisation modes, is a characteristic and relatively stable marker for mastic (Mills and White 1994). Generally, it has been reported that oleanane molecules are more abundant in the composition of mastic than that of dammar (Van der Doelen, *et al.* 1998a, Scalarone, *et al.* 2003a).

According to the above then, practical discrimination between the mass spectra of these two resins can be obtained by comparing the ratios of the relative intensities of the characteristic dammarane masses with those attributed to oleanane molecules, e.g. [dammarane ions] > [oleanane ions] in case of dammar (Scalarone, *et al.* 2003a). In the case of mastic however, additional characteristic molecules are present. These are (iso)masticadienonic acid, **13**, (Seoane 1956, Papageorgiou, *et al.* 1997) with reported EI-DTMS mass/charges at m/z 439, 454 and NH_3/CI m/z 472 (Scalarone, *et al.* 2003a) and 3-O-acetyl-3-epi(iso)masticadienonic acid, **14**, (Papageorgiou, *et al.* 1997) corresponding to a very low relative abundance at EI m/z 438, 498, NH_3/CI m/z 516 (not shown). As Scalarone and co-workers remarked, the presence of these compounds is not very accommodating when marker compounds are sought to discriminate mastic from dammar, because the ion peaks of **13** coincide with those of compounds **8**, **9**, **10** and the ion peaks of **14** coincide with those of compounds **11**, **12** (Scalarone, *et al.* 2003a). In line with this study the ionic fragments of 28-nor-olean-18-en-3-one, **16**, at m/z 163 and 191 in the EI mode are confirmed here to be a clear marker of mastic resin.

Judging from findings based on previous DTMS studies (Van der Doelen, *et al.* 1998a, Scalarone, *et al.* 2003a), both triterpenoid resins examined here were somewhat oxidised before ageing. Dammarenolic acid, **5**, has been indicated to be the major acidic constituent in dammar (Mills and Werner 1955). This molecule with an attached carboxylic acid group at position C-2, which results from A-ring opening of the dammarane skeleton, evidently derives from oxidation of **6**. In contrast to previous analytical data, the presented mass spectra of the unaged mastic film indicate the

presence of **5**, since its characteristic ion peak at m/z 440, $[M\text{-}OH]^+$, is present in the EI mode, and in the NH_3/CI mode m/z 458 and 476 correspond to the ammonia adducts of the former ionic fragment and the molecular ion of **5**, $[M\text{-}OH+NH_4]^+$ and $[M+NH_4]^+$. The mass spectra of both resins determine the presence of the ocotillone compound **7**, which derives from oxidation of dammarane skeleton molecules with a hydroxyisopropylmethyltetrahydrofuran side chain signified by a characteristic ionic fragment at m/z 143 in both EI and NH_3/CI modes (Van der Doelen, *et al.* 1998a). Previously, LC/MS analysis of dammar has determined the presence of dammarane type degradation compound **15** that has both an A-ring oxidation site and the characteristic ocotillone group (Van der Doelen, *et al.* 1998b). Compound **15** that has not been found in unaged mastic on the basis of chromatographic mass analysis (Van der Doelen, *et al.* 1998a), was recently detected in fresh dammar resin using DTMS (Scalarone, *et al.* 2003a).

The presence of oxidised dammarane type triterpenoids even at a relatively early stage in the degradation of these resins, (see Section 2.2), is attributed to the presence of free radicals generated by sunlight when the resins were exuding from the bark of the tree and during harvesting (Koller, *et al.* 1997, Dietemann 2003). Slightly oxidised 'fresh' triterpenoid resins have also been reported by Zumbühl and co-workers (1998b). In addition, traces of some crosslinked oligomers of polycadinene (up to tetramers), which is the polymer of dammar (Van Aarssen, *et al.* 1990), and cis-1,4-poly-β-myrcene (up to pentamers) that is the polymer of mastic (Van der Berg, *et al.* 1998) (Figures 2.2.3, 2.3.2), were obvious by mass increments of 204 Da in dammar and 136 Da in mastic. Detection of cadinene in the corresponding EI-DTMS of

dammar is more precise, since the polymer is relatively abundant in the resin (Van Aarssen, *et al.* 1990). In contrast, accurate detection of poly-β-myrcene requires separation of raw mastic because of its low concentration in the resin (Van der Berg, *et al.* 1998). In case of dammar, mass/charges at m/z 204, 408, 612 and 816 correspond to the molecular ions, $[M]^{+\bullet}$, of cadinene monomers, dimers, trimers and tetramers (Scalarone, *et al.* 2003a) (Figure 2.3.2a). In line with Scalarone and co-workers, the sequence of ionic peaks at m/z 612, 628, 644, 660, 676 and m/z 816, 832 is interpreted as a partial oxidation of the starting dammar film. Similarly for mastic, following the outlined traces of poly-β-myrcene (136 Da per monomer) (Figure 2.3.2b), oligomers are expected in the ion sequence m/z 136, 272, 408, 544, 680 and 816. It is observed that at m/z 544 and around m/z 816 there is a sequence of mass increments of 16 Da, which indicates some oxygen consumption from the starting mastic film. This information along with the similar case of dammar indicates the presence of oxidised crosslinked molecules. On the other hand, the low relative abundance of the mass/charges of these oxidised molecules and the profoundly high relative abundance of the mass/charges, corresponding to the identified triterpenoid molecules (**1-16** depending on the resin), indicate that both dammar and mastic keep most of their original molecular quality.

2.3.1 DTMS of the triterpenoid resin films after artificial light ageing

DTMS summation mass spectra in both NH_3/CI (Figure 2.3.3) and EI (Figure 2.3.4) ionisation modes demonstrate that upon accelerated light ageing, the films developed some evident differences compared to their unaged state. Initially, this is obvious from the corresponding EI-DTMS TIC's shown in Figure 2.3.1. Both films become less volatile owing to a high degree of polarity caused by oxygen consumption and a considerable degree of crosslinking demonstrated by the increased intensity of the pyrolysis peak. This is the reason why the compounds of both films require higher temperatures (scan numbers) to desorb compared to the lower temperatures prior to ageing. However, some reservation should be kept for the readings of the relative intensities of the TIC's pyrolysis peaks, which represent the ionised, high molecular weight compounds. It has been remarked that the triterpenoid polymerised products, which belong to a three-dimensional covalently bonded macromolecular lattice, are not readily desorbed with DTMS (Van der Doelen 1999), since many chemical bonds must break to induce volatile matter upon pyrolysis (Boon 1992). Some reactive high MW fragments, yielding upon pyrolysis during the analysis, may recombine to form thermally stable material that is not desorbed into the ionisation chamber. The broadness and the intensity of the pyrolysis peak depend on the extent and the type of polymerisation that occurs in the investigated substance (Boon 1992). For instance, linear polymers, such as polystyrene, give an explosive depolymerisation at high temperatures leading to a sharp pyrolysis peak. In condensed materials there are several crosslinked fractions with various degrees of polymerisation, which broaden

the pyrolysis peak. At lower temperatures fewer bonds are broken while at high temperatures more thermally stable materials are detected, which corresponds to breakage of more or stronger bonds. The apex at high temperatures indicates higher thermal stability, interpreted as more crosslinks. However, the evident increase and broadening of the pyrolysis peak in both dammar and mastic upon accelerated ageing is a good indicator of the presence of polymerised and condensed material (Figure 2.3.1).

Table 2.3.3 List of additional compounds found in light aged dammar resin

Label	Compound name	Mw	EI mass/charges	NH_3/CI mass/charges
17	3,4-seco-28-nor-urs-12-en-3-oic acid	428	204, 428	446
18	3,4-Seco-28-nor-olean-12-en-3-oic acid	428	204, 428	446
19	3,4-seco-28-nor-urs-12-en-3,28-dioic acid	472	203, 248 472	490
20	3,4-seco-28-nor-olean-12-en-3,28-dioic acid	472	203, 248 472	490
21	Dihydro-dammarenolic acid (20-hydroxy-3,4-seco-24-dammaren-3-oic acid)	460	387, 456	478
24	3-oxo-25,26,27-trisnordammarano-24,20-lactone	414	95, 99, 205, 315, **414**	432
25	17-hydroxy-11-oxo-nor-β-amyrone (3,11-dioxo-17-hydroxy-28-norolean-12-ene)	440	**234**, 275, 422, 440	458
26	11-oxo-oleanonic acid (3,11-dioxo-olean-12-en-28-oic acid)	468	217, 257, **276**, 317, **482**	486
27	17-hydroxy-11-oxo-nor-α-amyrone (3,11-dioxo-17-hydroxy-28-norurs-12-ene)	440	**234**, 275, 422, 440	458
28	11-oxo-ursonic acid (3,11-dioxo-urs-12-en-28-oic acid)	468	257, 276, **317**, **482**	486

Table 2.3.4 List of additional compounds found in light aged mastic resin

Label	Compound name	Mw	EI mass/charges	NH_3/CI mass/charges
18	3,4-seco-28-nor-olean-12-en-3-oic acid	428	204, 428	446
20	3,4-seco-28-nor-olean-12-en-3,28-dioic acid	472	203, 248 472	490
22	3,4-Seco-28-nor-olean-18-en-3-oic acid	428	204, 428	446
23	3,4-seco-28-nor-olean-18-en-3,28-dioic acid	472	203, 248 472	490
24	3-oxo-25,26,27-trisnordammarano-24,20-lactone	414	95, 99, 205, 315, **414**	432
25	17-hydroxy-11-oxo-nor-β-amyrone (3,11-dioxo-17-hydroxy-28-norolean-12-ene)	440	**234**, 275, 422, 440	458
26	11-oxo-oleanonic acid (3,11-dioxo-olean-12-en-28-oic acid)	468	217, 257, **276**, 317, **482**	486

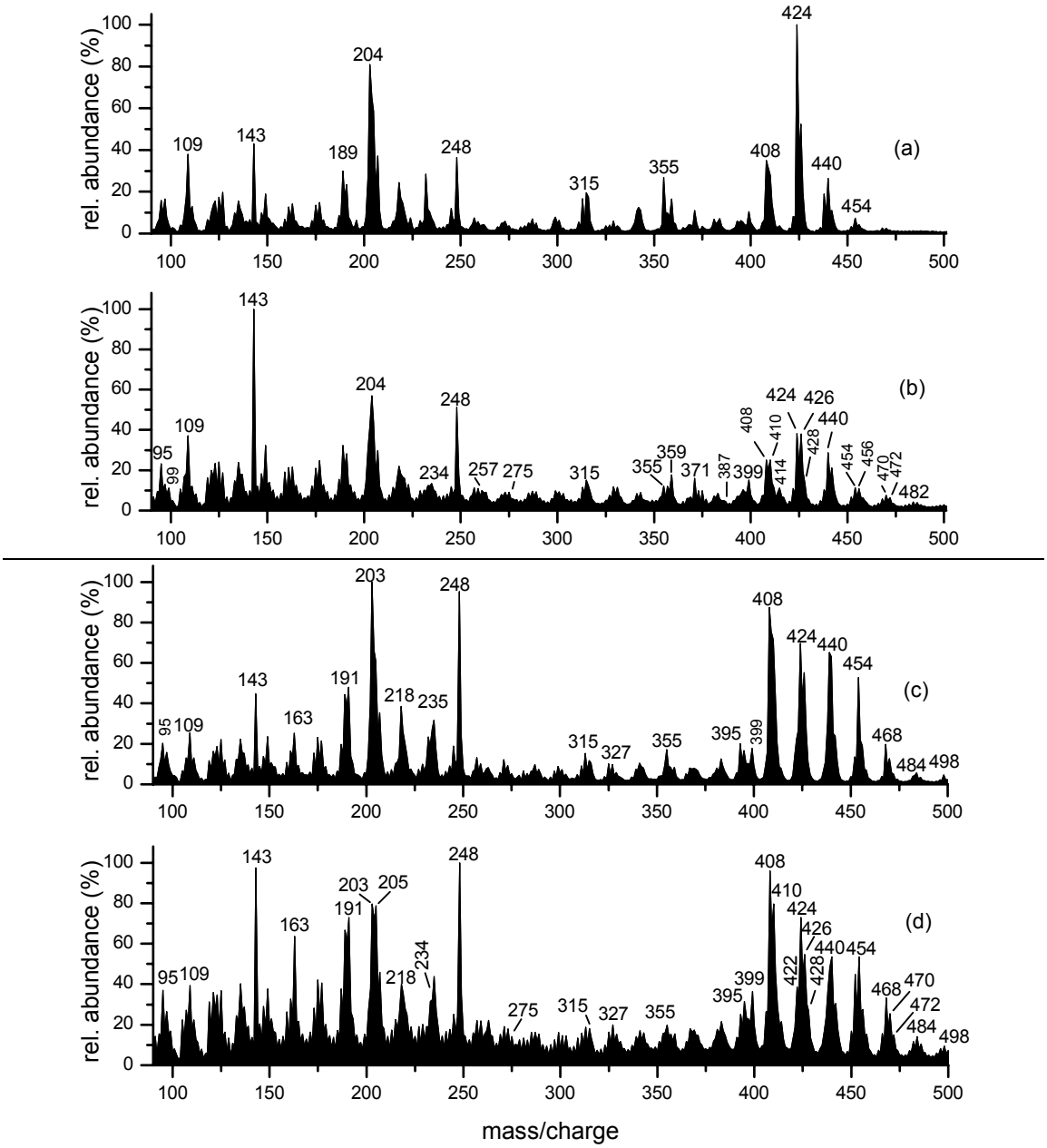

Figure 2.3.4 EI-DTMS of the unaged (a) and light (500h, λ > 295 nm) aged (b) dammar; and unaged (c) and light (500h, λ > 295 nm) aged (d) mastic.

The EI summation mass spectra of the aged films reveal a reduction in the relative abundance of the ionic fragments of dammarane (**3**, **4**, **5**, **7**, **6**) and oleanane/ursane compounds (**1**, **2**, **8, 9, 10**) with marker peaks at EI m/z 424 and 440 for the dammarane, m/z 204, 410 (**1**, **2**), m/z 454 ($[M]^{+\cdot}$ of **8, 9, 10**) and m/z 438 ($[M]^{+\cdot}$ of **11**,

12) for the oleanane/ursane type of molecules. This reduction in abundance is less intense in mastic (Figures 2.3.4d). This observation is in line with previous findings on the artificial and natural ageing of dammar and mastic resins in which a large number of specific triterpenoid carbon skeletons are preserved after ageing (Van der Doelen, *et al.* 1998a, Van der Doelen 1999, Scalarone, *et al.* 2003a).

In both cases, m/z 143, 399 at EI mode, and m/z 143 at NH_3/CI mode, indicate the presence of ion fragments of oxidised dammarane molecules with the ocotillone side chain, i.e. compounds such as **7** and **15** that are usually more abundant in dammar (Van der Doelen 1999, Van der Doelen, *et al.* 2000). In the case of mastic, no oxidation products have been reported for compounds **13** and **14**. Degradation in mastic leads to a relative decrease of the ionic peak at EI-DTMS m/z 439 that is characteristic of **13** and a simultaneous increase at m/z ~900 (Scalarone, *et al.* 2003a). It is possible that this compound is involved in crosslinking and therefore mass/charges at m/z ~900 may include dimerised **13** molecules (MW = 454 Da).

In both cases there is an abundance of peaks of moderate relative intensity corresponding to compounds **17**/ **18**, **19**/**20** and **21** for dammar and **18**/**22**, and **20**/**23** for mastic, identified by molecular ions $[M]^{+\cdot}$ at m/z 428, 460 and 472 in the EI mode and the ammonia adduct ions $[M+NH_4]^+$ at m/z 446 and 490 in the NH_3/CI mode. These seco-products have been identified in xenon arc exposed dammar under radiation that included some UV wavelengths (Van der Doelen, *et al.* 2000, Scalarone, *et al.* 2003a). Compound **21** that was found in the degraded dammar film is very similar to compound **5** showing clearly its dammarane skeleton origin. The difference between the two compounds lies in position C-5, at which **21** has an

isopropyl group and **5** an isopropenyl group (Van der Doelen, *et al.* 2000). The notable characteristic of all these degradation molecules is an oxidised A-ring with a carboxylic acid group at C-2 and an isopropyl group at C-5 (Figure 2.2.2c) (Van der Doelen 1999, Van der Doelen, *et al.* 2000). Their mass spectra include peaks such as m/z 204 for **17**, **18** and **22** and m/z 203 for **19**, **20** and **23** (Van der Doelen 1999). Compounds with these characteristic ion fragments are also present in the fresh triterpenoid resins. For example **1** and **2** have an ion fragment peaking at m/z 204 that is characteristic of the oleanane and ursane skeleton with a hydrogen at position C-17, while **8**, **9**, **10**, **11** and **12** have an ion fragment peaking at m/z 203 corresponding to the oleanane/ursane skeleton with a carboxylic acid group at C-17 (Van der Doelen 1999). This coupling clearly demonstrates that degradation products **17**-**20**, **22** and **23** derive from oleanane and ursane triterpenoids. Their formation has been attributed to Norrish type I reactions (Van der Doelen, *et al.* 2000) that commonly occur during autoxidation of triterpenoid resins (De la Rie 1988b, Scott 1993). Van der Doelen and co-workers determined that these degradation compounds are not formed in varnishes aged on paintings nor on artificially light aged dammar resins, when the radiation employed excludes UV wavelengths (Van der Doelen 1999, Van der Doelen, *et al.* 2000).

This observation points out that the aged varnishes prepared for the laser ablation experiments are very degraded with additional carboxylic acid groups, which will enhance absorptivity to the UV laser photons. Exposure under UV wavelengths was also utilised for the accelerated ageing of the triterpenoid varnishes studied in the past (De la Rie 1988b, Zumbühl, *et al.* 1998b, Van der Doelen, *et al.* 2000, Scalarone, *et*

al. 2003a). Thus, the results of the current study shed more light on established findings on the ageing of dammar and mastic. In Chapter 5 it is examined whether the UV-induced generated compounds really exist under the surface of the investigated degraded varnishes. At this point, it should kept in mind that even in their unaged state both triterpenoid resins already have a relatively high abundance of compounds **5**, **7** and **15** (dammar only), which also have an oxidised A-ring opening at the C-2 position (Mills and Werner 1955, Poehland, *et al.* 1987, De la Rie 1988a). This is the case not only for the unaged dammar and mastic films examined here but also for other unaged dammar and mastic varnishes, which were less oxidised than the starting material used for the present study (Van der Doelen, *et al.* 1998a). It has been suggested that these compounds are formed during biosynthesis of the resins or after excretion by exposure to outdoor conditions (Dietemann 2003). The presence of the seco-products in the present work therefore indicates an advanced degree of degradation induced by exposure to daylight in the laboratory.

In addition to the presence of the A-ring oxidised compounds, other oxidation products are recognised from their characteristic ion peaks in the EI mode. These are some characteristic compounds **24**, **25**, **26**, **27** and **28** in dammar and **24**, **25** and **26** in mastic. Compound **24** is the only one derived from dammarane type molecules. Compounds **25**-**28** derive from oxidation of triterpenoids with the oleanane and ursane skeleton at C-11 and C-28. The presence of these compounds has been established in 'naturally' aged varnishes on paintings by Van der Doelen and co-workers (1998a). The same compounds were reproduced by exposure under light excluding UV and by artificial ageing in solution under fluorescent radiation (Van der Doelen and Boon

2000). A comparison of the relative intensities of the most characteristic ion fragments at EI mode of both types of oxidation products indicates that the investigated films have these molecules in almost equal amounts (see Tables 2.3.5 and 2.3.6). Hence, the composition of the examined degraded varnishes, is a mixture of a few intact triterpenoid molecules (**1-16**), some oxidised molecules, which are only detected under UV-including xenon arc radiation (**17-23**) and some oxidised molecules that have been previously identified in painting varnishes and UV-excluding light ageing (**24-28**).

Table 2.3.5 A-ring oxidised compounds vs plain oxidised products in aged dammar (m/z 143, 100% rel. abundance)

A-ring Oxidised Compounds			Oxidised Compounds		
Label	Characteristic EI m/z	% Relative Abundance	Label	Characteristic EI m/z	% Relative Abundance
17/18	428	13.4	**24**	414	9
19/20	472	6.4	**25/27**	234	12
21	456	10.9	**26**	482	3.3
			28	317	9.3

Table 2.3.6 A-ring oxidised compounds vs plain oxidised products in aged mastic (m/z 248, 100% rel. abundance)

A-ring Oxidised Compounds			Oxidised Compounds		
Label	Characteristic EI m/z	% Relative Abundance	Label	Characteristic EI m/z	% Relative Abundance
18/22	428	26.9	**24**	414	21.5
20/23	472	14.9	**25**	234	32.3
			26	482	11.7

As explained in the introduction (Section 2.1), a state of advanced degradation was actually required for this work. It is known that at this stage triterpenoid varnishes obtain high levels of polarity because of the direct interaction of the oxygenated molecules with water molecules attracted from the atmosphere (Scott 1993, Boon and van der Doelen 1999). At these stages of advanced degradation, solubility of these coatings is enabled with very polar solvents, which are usually avoided in the cleaning

of paintings because they diffuse rapidly into the bulk of the films and penetrate into the underlying paint layers (Stolow 1971, 1985). There is a potential for devastating effects on the painting, because of the possible resulting degradation of the binding medium. At the same time the long exposure time under the xenon-arc radiation was intended to induce the highest levels of degradation by enabling a full three-dimensional polymer network to form, thereby increasing the possibility of truly insoluble matter generation (Feller 1964a, b). Furthermore, it has been determined that exposure under xenon-arc radiation for durations longer than 300 hours leads to depolymerisation (Zumbühl, *et al.* 1998b) and, consequently, the breakdown of the longer macromolecules at the surface results in the formation of species with low molecular weight, which is justified with the accumulation of small masses as demonstrated in the DTMS summation mass spectra. These ageing conditions produce material suitable for the use of excimer lasers, because the UV photons interact directly with the carbonyl species (Srinivasan and Braren 1989, Bäuerle 2000) attached to the degraded molecules during degradation. Admittedly, it should be noted that using the extreme ageing parameters described here, the protocols for researching the chemistry of these resins were in fact broken. This deliberate degradation however enables investigations of the possible existence of a real compositional gradient across the thickness of the films.

2.4 Part II: Formation and degradation of oil varnishes

Oil varnishes are basically mixtures of heat-bodied drying oils with resins. Initially, their use was reported in the medieval era when fabricated by pulverised sandarac with linseed oil (Merrifield 1999). In the beginning of the fifteenth century, Italian artists used oil varnishes, known as *vernice liquida*, made of heat processed incense or colophony with linseed oil, to coat tin, iron, stone objects and paintings (Merrifield 1999). In northern Europe, oil varnishes were introduced during the eighteenth century and applied on floors, furniture, baking vessels and outdoor exposed spars or other objects (Mantell, *et al.* 1949). The high viscosity, the mellow and smooth saturation of these coatings as well as their durability, justified by the fact that they were considered not to bloom or chill and less likely to crack compared to 'spirit' varnishes (Williams 1787), re-established oil varnishes in the world of paintings during the nineteenth century by contemporary artists and craftsmen (Carlyle 2001). Art painters used oil varnishes as additives to paint media (megilps), as driers for certain pigments, as intermediate layers for overpaints and as finishing varnishes, justifying a wide list of manufacturing recipes (Carlyle 2001). In the present work we will focus on their application as finishing varnishes. The most commonly used materials were poppy, nut and/or linseed oil mixed with copal, amber, sandarac and/or colophony resins, with the most popular ingredients being linseed oil and copal resin (Brommelle 1956, Mills and White 1994, Carlyle 2001).

Manufacturing of oil varnishes for paintings involved vigorous boiling of the resin with the drying oil at high temperatures in the range of 300-350 °C (Carlyle 2001).

Driers, such as lime, lead, zinc and manganese, were occasionally employed in order to control the drying time of the final film (Neil 1833, Scott Taylor 1890), while oil of turpentine was, occasionally, employed to dissolve the resin prior to the heat procedure and/or to dilute the final viscous product for the ease of eventual application (Neil 1833). From the early years of their application it was soon realised that once dried these coatings became insoluble, causing so a major problem in the conservation of paintings (Tingry 1804). The main reason for this problem is that upon drying and eventual ageing, oil varnishes develop a crosslinked polymer network incorporating ester bonded fatty acids (triacylglycerols), resin molecules and inorganic particles if driers had been used (Feller, *et al.* 1985). Besides, aged copal is polymerisable and difficult to dissolve even without being mixed with drying oils (Gettens and Stout 1966).

Such coatings have been by no means studied as meticulously as the natural varnishes described in Section 2.2. Two aspects however are evident. First, these coatings become insoluble (Brommelle 1956, Stolow 1985, Mills and White 1994, Carlyle 2001), especially if the incorporated resin belongs to the diterpenoid class, that comprises resins such as copal, amber, sandarac and/or colophony. These resins polymerise strongly (Scalarone, et al 2003a, b) even if dried without the incorporation of the oil, and thus become insoluble (Gettens and Stout 1966). Obviously, upon integration with the heat-bodied drying oil, which polymerises via the crosslinking of its component triacylglycerols (Van den Berg 2002), a very viscous, insoluble film is formed. This feature of the oil varnishes makes their study with excimer laser ablation valuable for the painting conservation point of view. Secondly, there have been two

molecular studies of oil varnishes, which showed that upon ageing the resin components reduce to trace amounts in the final crosslinked polymer of the film (Dunkerton, *et al.* 1990, Van den Berg, *et al.* 1999), making the varnish resemble stand oil films, given the vigorous heating process upon manufacturing. An allegedly 600 year old oil varnish analysed by GLC/MS, showed traces of sandaropimaric acid, indicating the presence of sandarac resin (Dunkerton, *et al.* 1990, Mills and White 1994). Using DTMS and Pyrolysis GC/MS with online derivatisation with TMAH (Py-TMAH-GC/MS), Van den Berg and co-workers (1999) showed that upon ageing the polymer of copal resin in a copal oil varnish almost disappears. In the present study we will focus on the excimer ablation and, subsequently, the properties of a copal oil varnish at successive uncovered depth steps (Chapter 3). For this reason, a short overview is provided for the linseed oil and its degradation during and after preparation, since basically the properties of the oil components are the dominant features of oil varnishes (Dunkerton, *et al.* 1990, Mills and White 1994, Van den Berg, *et al.* 1999). Some general information is also provided for diterpenoid resins.

2.4.1 Linseed oil

Linseed oil is produced from flax seeds in many regions around the world, mainly Argentina, Canada, Europe, India and the USA. The oil content of the seeds varies from 35 to 45% by weight and extraction is mainly obtained either with pressure or processing with organic solvents. Modern methods for extraction involve the incorporation of organic solvents after an initial pressing to enhance the final product (Wingard 1959, Keller 1973, Laisney 1996). Mainly, the composition of drying oils consists of glycerol, and triacylglycerols (Figure 2.4.1), which are triesters of glycerol

(1,2,3-propanetriol) with mixtures of fatty acids, as well as free fatty acids (Figure 2.4.2) up to 80% per weight (Mills and White 1994). The average content and type of the free fatty acids ranges from 0.5 to 2% per weight, and occasionally higher depending upon the origin and the extraction processing of the oil (Tawn 1969b), and reflects the constituents of the triacylglycerols.

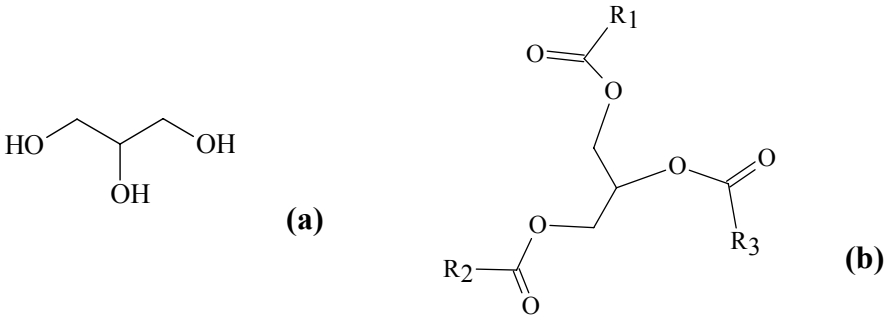

Figure 2.4.1 Glycerol (a) and a triacylglycerol (b) formed by ester bonds of a glycerol and three fatty acids. Several fatty acids may be involved (see also Figure 2.4.2) as indicated with R_1, R_2 and R_3.

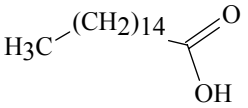

Palmitic (Hexadecanoic) acid (C16)

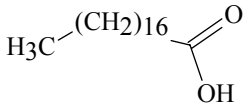

Stearic (octadecanoic) acid (C18)

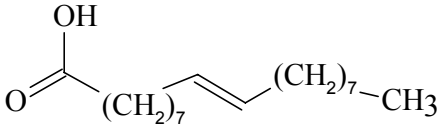

Oleic (9-Octadecenoic) acid (C18:1)

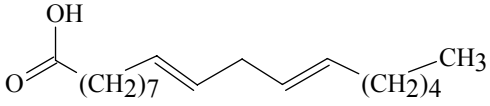

Linoleic (Z9,Z12- Octadecadienoic) acid (C18:2)

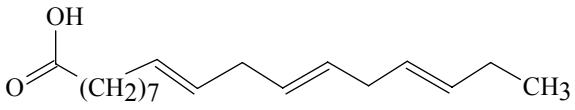

Linolenic (Z9,Z12,Z15- Octadecatrienoic) acid (C18:3)

Figure 2.4.2 The main constituent fatty acids in linseed oil. These can be found free or participate in the formation of triacylglycerols.

The principal fatty acids of linseed oil (Figure 2.4.2) are: 4-10% (by weight) palmitic (hexadecanoic, C16), 2-8% stearic (octadecanoic, C18), 10-24%, oleic (*cis*-9-

octadecenoic, C18:1), 12-24% linoleic (9,12-octadecadienoic C18:2) and 48-71% of linolenic (9,12,15-octadecatrienoic, C18:3) fatty acids depending on the origin and the extraction processing (Swern 1979, Mills and White 1994, Sultana 1996). There are however some more saturated and unsaturated fatty acids in minor proportions. These are: lauric (dodecanoic, C12), myristic (Tetradecanoic, C14), arachidic (eicosanoic, C20), behenic (docosanoic, C22) and lignoceric (tetracosanoic, C24), which are saturated, and palmitoleic (*cis*-9-hexadecenoic, C16:1), gadoleic (*cis*-9-eicosenoic, C20:1) and/or gondoic (*cis*-11-eicosenoic, C20:1) unsaturated fatty acids.

Given the variety of the principal fatty acids mainly consisting of 16 and 18 carbons, it is understandable that there are about 20 different types of triacylglycerols in the composition of the oil with unsaturation ranging from one to nine double bonds and molecular weights ranging from 851 to 889 Da per triacylglycerol (Hites 1970, Sonntag 1979a, Rezanka and Mares 1991). A comprehensive review has been recently produced (Van den Berg 2002). Linseed oil also contains 0.1-0.2% per weight water, up to 1% phosphatides and phospholipids, such as lecithin (Tawn 1969c, Sonntag 1979a, Sultana 1996). Its brownish hue is attributed to a 0.2 to 0.4% content of phytosterols, such as brassicasterol ($C_{28}H_{46}O$) and stigmasterol ($C_{29}H_{48}O$). The presence of 0.01 to 0.1% paraffins, 0.15% waxes and triterpenic alcohols, such as squalene and 0.1% of tocopherols, which act as anti-oxidants, is also reported. Traces of metals, such as iron, copper, manganese, lead, zinc and cadmium have been also identified (Schoene, *et al.* 1998), and their presence has been attributed to additives to catalyse oxidation. The proportion of these additives influences the drying rate of the oil (Mills and White 1994).

2.4.2 Processing of raw linseed oil

Raw linseed oil is commonly processed before usage to enhance its drying properties with several methods known as purification or refining processes (Keller 1973, Carlyle 2001). Purification is mainly obtained by heating up to 260 °C, so that the unwanted phosphatides and the mucilaginous material precipitate from the bulk oil via reactions with the water content (Norris 1982a, Denise 1996). In the past, refining was also carried out by chilling the oil using ice or snow (Denise 1996). As a result, the oil compounds, including the most saturated triacylglycerols and the free fatty acids, except for the undesirable mucilaginous contents freeze, so the latter were readily removed. Washing was also employed for the separation of proteins and free fatty acids, which bleached the resultant processed oil. When enhanced bleaching was intended, purification was obtained using sunlight (Norris 1982b, Denise 1996). Today, bleaching is carried out with the use of additives, such as activated carbon or Fuller's earth, which absorb the unwanted material (Norris 1982b, Wicks Jr., *et al.* 1992). In the past, breadcrumbs were used instead for the same purpose, in combination with heating under sunlight to enhance photoxidation and thus to shorten the drying time of the resultant oil (Norris 1982b). Under these conditions a thick film is formed on top of the heated oil. Depending on the intended use of the drying oil, the separated phase was either removed, resulting so in a thinned final oil, or was incorporated in the oil by regular shaking of the oil during preparation, resulting in a thickened oil.

Other popular refining techniques involve addition of acidic agents such as sulphuric acid or simply vinegar while the oil was heated. This results in the breakdown of

phosphatides and colouring substances, but this way free fatty acids are formed, which are subsequently removed by water washing afterwards (Denise 1996). Addition of caustic soda or sodium hydroxide has been also popular for the same purpose but the resulting oil has less free fatty acids than when acidic agents are used. The former refining technique is preferable by colourists and painters, since the increased proportion of free fatty acids improves the reaction of the oil with pigments (Tawn 1969a, Formo 1979a, Morgans 1990). It is also reported that past refining methods involved heating in zinc, copper or bronze vessels and/or addition of lead white (basic lead carbonate, Pb_2CO_3 $Pb(OH)_2$), yellow lead oxide (PbO), red lead oxide (Pb_3O_4), calcium oxide (CaO), zinc sulphate ($ZnSO_4$) or umber (containing iron and manganese oxides), which shortened the drying time of the resultant oil (Keller 1973). In particular, heating in a copper pan with manganese oxide additives and storage in tin or leaden vessels was recommended in the 19th century for preparing oil for varnishes (Carlyle 2001, p.341). Despite the variety of purification methods, there were no specific recommendations on which type of refining oil should be used for a subsequent pre-polymerisation towards the production of oil varnishes (Carlyle 2001).

2.4.3 Pre-polymerisation processes

According to the literature, the most popular methods for purification and refining involved heating. Heating was also popular for posterior processing, with which pre-polymerisation, i.e. increase of the oils' viscosity, was obtained that resulted in shortening the drying rate. The name of pre-polymerised (thickened or bodied) linseed oil was then bound to this posterior processing. There are three major categories of bodied linseed oils: (i) blown, (ii) boiled and (ii) stand linseed oil. (i) Blown linseed

oil was produced by blowing air to linseed oil heated up to 150 °C, resulting in increased viscosity and saturation of the brownish hue. (ii) Boiled linseed oil was produced by boiling the oil at about 150 °C in the presence of air and with addition of driers, i.e. carbonates and metal salts of organic acids, resulting in increased acidity and viscosity. (iii) Stand oils were manufactured in the presence or absence of air by heating the oil at temperatures of 300 °C or higher, resulting in decomposition of various volatile and partially inflammable products, and high viscosity. In the presence of air, the latter products were evaporated while the final product was oxidised, but in the absence of air, the stand oil retained these volatile species and became more acidic (Formo 1979a).

2.4.4 Effects on the composition of the oil during heating

From all the pre-polymerised oils described, stand oils heated in the presence of air are the matching materials that are incorporated in oil varnishes (Mantell, *et al.* 1949, Carlyle 2001). There are three principal processes that are obtained by heating, which change the fatty acyl moieties of non-oxidised unsaturated lipids (Van den Berg 2002). These are (i) hydrolysis, (ii) *cis-trans* isomerisation, and (iii) thermally induced polymerisation upon cyclisation. The presence of oxygen enhances the autoxidation processes during pre-polymerisation.

(i) Hydrolysis occurs in the glycerol ester bonds resulting in the formation of di- and monoacylglycerols, glycerol and free fatty acids (Crossley, *et al.* 1962, Paulose and Chang 1973, 1978, Frankel, *et al.* 1981). The extent of hydrolysis and the formation of these products increase with the proportion of the water content in the oil (Frilette 1946, Perrin 1996). The high amounts of free fatty acids in the oil increase

both its acid value and its oxidation rate (Privett 1959, Miyashita and Tagaki 1986, Frega, *et al.* 1999). It has been suggested that the free carboxylic acid group of these free fatty acids catalyses the decomposition of the initially formed hydroperoxides upon autoxidation (Van den Berg 2002).

(ii) The process of *cis-trans* isomerisation of double bonds occurs in fatty acids with non-conjugated double bonds in an initially *cis*-configuration. In the presence of free radicals during heating, the *cis*-configuration is transformed in the *trans*-configuration until equilibrium between the two forms is obtained. Moreover, a migration of the double bonds has been also observed (Sonntag 1979b, Martin, *et al.* 1998).

(iii) Finally, during heating dimerisation by Diels-Alder type reactions occur, which eventually leads to polymerisation (Boelhouwer, *et al.* 1967, Mills and White 1994). These are well known reactions between a conjugated diene and a compound with a single double bond resulting in cyclisation (Figure 2.4.3a). According to Mills and White (1994) isomerisation of the unconjugated double bonds resulting in conjugated dienes is a preliminary essential reaction. In addition, conjugation leads also to intermolecular cyclisation generating cyclic fatty acids (Sebedio and Grandgirard 1989).

In addition, several products are formed via thermal breakdown of acyl chains on both sides of double bonds, generating free radicals (Van den Berg 2002). These react with hydrogen and generate alkanes, alkenes and short chain unsaturated fatty acids, which form low molecular weight triacylglycerols (Nawar and Witchwood 1980). However, due to unsaturation of the low MW fatty acids the latter are expected to break down

giving rise to new radicals, which eventually may recombine to form high molecular weight species (Van den Berg 2002). In addition, saturated short chain and low molecular weight decomposition products will remain. These are volatiles however and escape the drying film in a later deterioration state.

2.4.5 Polymerisation

The most important reason leading to polymerisation of oils is recombination of long chain free radicals. Moreover, the high temperatures lead to high degrees of saturation and thermally induced polymerisation of triacylglycerols, which is readily obtained by conjugation of linoleic or linolenic acid groups (Greaves and Laker 1961), followed by Diels-Alder reactions (Figge 1971). Diels-Alder reactions may occur between two

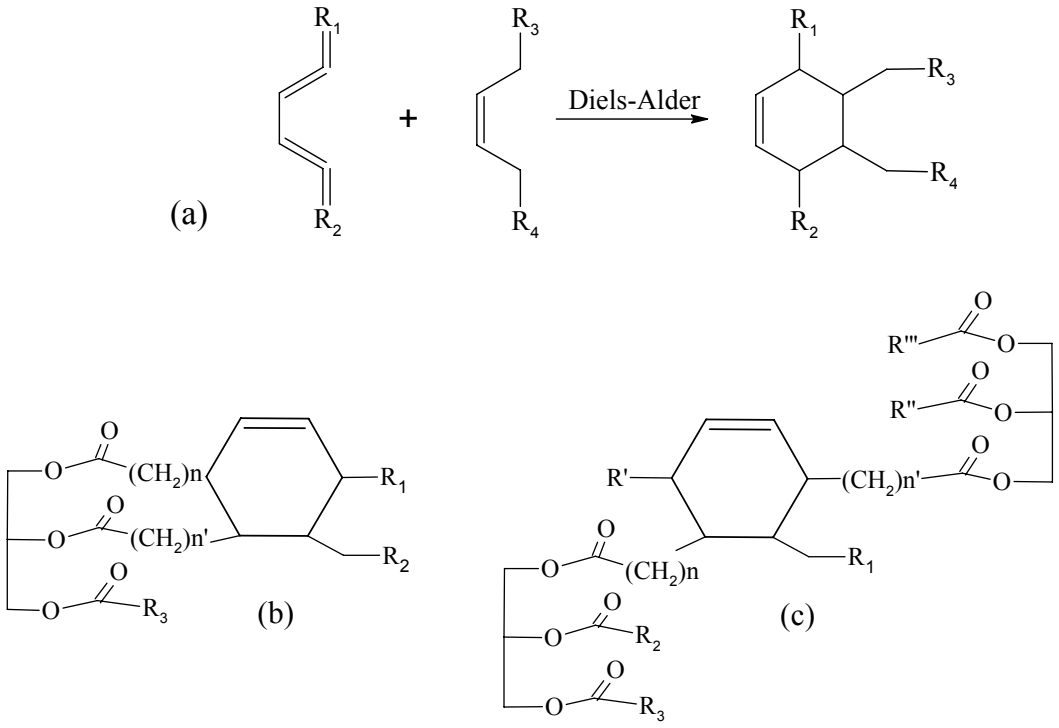

Figure 2.4.3 The Diels-Alder cyclisation reaction of a conjugated diene with a single double bond compound (a) and indicative products of two fatty acids of (b) the same triacylglycerol, and (c) of two dimerised triacylglycerols.

fatty acyl groups that are part of the same triacylglycerol, which does not lead to polymerisation at a first step (Figure 2.4.3a), but at a subsequent Diels-Alder reaction with a different triacylglycerol (Figure 2.4.3b), where two fatty acyl groups of neighbouring triacylglycerols are dimerised. The latter step is also obtained alone (Van den Berg 2002). A detailed insight on the different mechanisms and products of thermal dimerisation reactions of the unsaturated fatty acid esters is provided elsewhere (Figge 1971). Once the oil has undergone a vigorous pre-polymerisation the rate of further polymerisation upon ageing is related to the availability of unsaturated lipids, the majority of which and especially of the polyunsaturated fatty acids, have reacted away during the heat bodying (Ucciani and Debal 1996).

2.4.6 Oxidation

The presence of the atmospheric oxygen during heating catalyses autoxidation, which is enhanced by high temperatures. Autoxidation leads to the formation of free radicals, which results in the formation of hydroperoxides (Scott 1993, Feller 1994). The elevated temperatures increase the rate of decomposition of the hydroperoxides, which in turn provide highly reactive free radicals in the oil, according to the autoxidation process shown in page 81. Termination reactions involve formation of peroxides by termination step (v), reactions between two peroxyl radicals producing a tetroxide: $RO_2^{\cdot} + R'O_2^{\cdot} \rightarrow ROOOOR'$, which readily breaks down to form a ketone, a secondary alcohol and molecular oxygen (Russel 1956, 1957), and recombination of two radicals. Some of the most characteristic end products are dicarboxylic fatty acids or diacids (Figure 2.4.4). In addition, several other polar materials with hydroperoxide, epidioxide, hydroxide, epoxide, and carbonyl groups with ether and

peroxide crosslinks are generated (Frankel, *et al.* 1960, Figge 1971, Artman and Smith 1972, Ohfuji and Kaneda 1973, Whitlock and Nawar 1976, Paulose and Chang 1978, Frankel 1998).

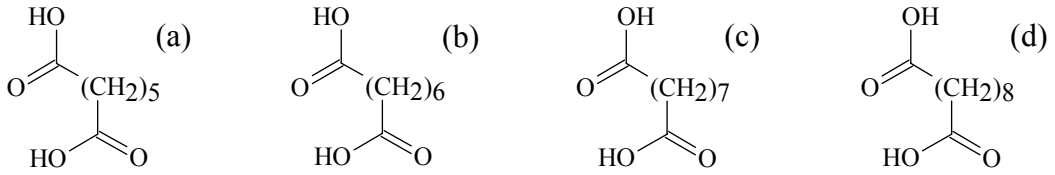

Fatty diacids: (a) Heptanedioic (Pimelic), (b) Octanedioic (Suberic), (c) Octanedioic (Suberic), and (d) Decanedioic (Sebacic) acids

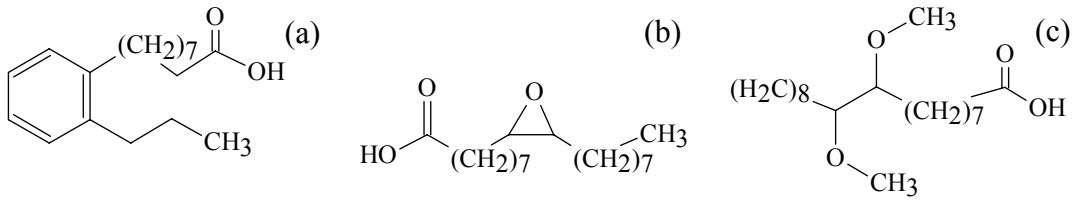

(a) 9-(2-propylphenyl)nonanoic acid, (b) 9,10-epoxy-octadecanoic acid and (c) 9,10-dimethoxy octadecanoic acid

Figure 2.4.4 Some characteristic compounds, other than the constituent C16 and C18 fatty acids (Figure 2.4.2), found by Van den Berg (2002) in a five year old stand oil

The presence of atmospheric oxygen during heating also accounts for several qualitative changes (Van den Berg 2002). When the heat rises gradually in the manufacturing pots, upon reaching a temperature of 100 °C the hydroperoxides begin to decompose to ether linked and other oxygenated polar compounds (Frankel 1998). Accordingly, decomposition of other radicals at 100 °C leads to products similar to those formed upon normal autoxidation, such as oxidised mono-, double- and tri-unsaturated lipids (Selke, *et al.* 1977, Nawar and Witchwood 1980, Silwood and Grootveld 1999). When the temperature reaches or exceeds 150 °C, even the saturated lipids undergo oxidation leading to products such as 2-alkanones, alkanals, and 1-alkanals, homologous of the fatty acids they derive from (Crossley, *et al.* 1962, Selke, *et al.* 1975, Silwood and Grootveld 1999, Van den Berg 2002). Eventual increase of

the processing temperature increases the abundance of these decomposition products. Upon heating of saturated with unsaturated lipids, most of the decomposition products derive from the unsaturated ones (Van den Berg 2002). Instead of attacking the methylene groups of a saturated chain, the alkoxy radicals are more prone to abstract a hydrogen from the (bis)allylic systems. Thus the unsaturated material acts as an antioxidant inhibiting oxidation of the saturated chains. However, once a stand oil is formed further oxidation is limited. It has been determined that raw linseed oil may consume up to 12% of oxygen by weight compared to an approximate 3% for the heat bodied oils (Mills and White 1994).

2.4.7 The copal resin component: An introduction

Copals are diterpenoid resins harvested upon exudation from trees. In general, diterpenoid resins are produced from *Coniferae* and *Leguminosae* family trees, which give their names to two large diterpenoid families (Mills and White 1994). Kauri and Manila copal resins belong to the *Coniferae* (conifer) family group. In the large family of conifer resins there are several subfamilies, such as the *Pinaceae*, *Cupressaceae*, *Araucariaceae*, *Taxodiaceae* and *Podocarpaceae* resin groups. The most significant conifer subfamilies are the first three in this order, since they yield significant amounts of resin. The two latter groups along with many other conifer subfamilies yield small amounts of resin and hence they are not very popular in mass production and general use. Kauri and Manila copal resins that have been used extensively by artists belong to the *Araucariaceae* group and are known as *Agathis* species. The main production of these resins occurs in the southern hemisphere and basically in Australia, New Zealand and the East Indies.

The various species of conifer resins consist of diterpenoid molecules that are mainly classified in three skeletal groups, namely the abietane, pimarane and labdane diterpenoids (Figure 2.4.5). While all three molecular types are found in the

Abietane Diterpenoids

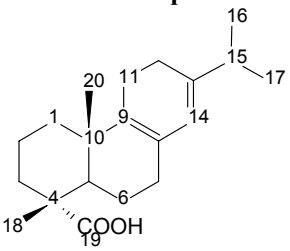

Palustric acid

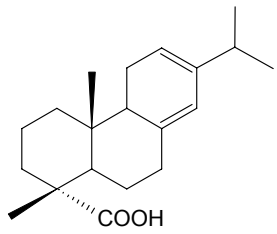

Laevopimaric acid

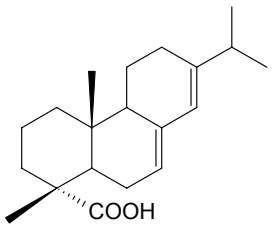

Abietic acid

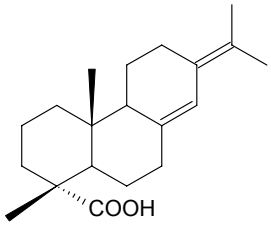

Neoabietic acid

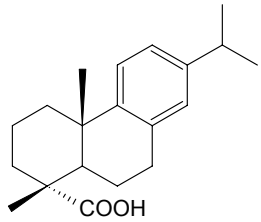

Dehydroabietic (DHA) acid

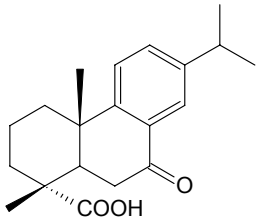

7-Oxo-DHA acid

Pimarane Diterpenoids

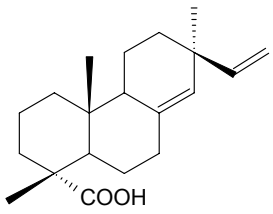

Pimaric acid

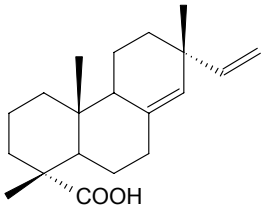

Sandaracopimaric acid

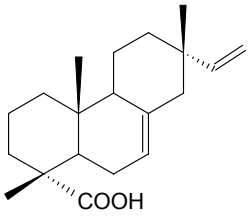

Isopimaric acid

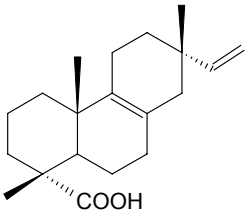

Δ8–Isopimaric acid

Labdane Diterpenoids

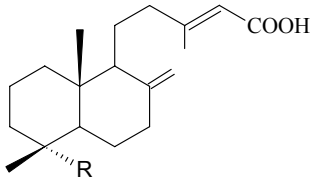

R: COOH Agathic acid

R: CH_2OH Agatholic acid

R: CH_2O Acetoxyagatholic acid

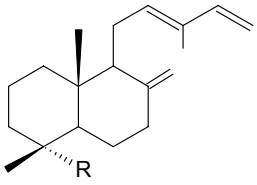

R:COOH
trans-communic acid
R:CH_2OH
trans-communol

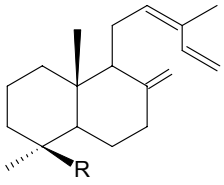

R:COOH
cis-communic acid
R:CH_2OH
cis-communol

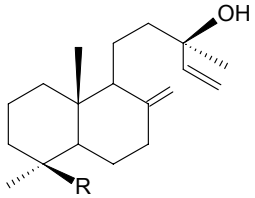

R:COOH
torulosic acid
R:CH_2OH
Torulosol

Figures 2.4.5 The characteristic abietane, pimarane and labdane type diterpenoid molecules of the conifer resins.

Araucariaceae resins, the latter are rich in labdane compounds, which polymerise rather readily to form a 'hard' varnish film that is difficult to dissolve (Gettens and Stout 1966). In particular, the communic acid types are strongly involved in the polymerisation process. When fresh, the Kauri copal contains almost the same amounts of the communol alcohol and the communic acid and therefore the polymer is actually a co-polymer of both these components (Thomas 1966). Abietic, sandaracopimaric and agathic acids as well as sandaracopimarol are also present in significant amounts, while occasionally a relatively high abundance of torulosic acid has also been reported.

Manila copal is met under a variety of names that according to Mills and White (1994) reflect the 'hardness', that is the degree of polymerisation of the component communic acid, of the resin. Less polymerised Manila copals are called 'melengket' and/or 'loba', while more degraded varieties, which are somewhat more polymerised are called 'pontianak' and/or 'boea'. The chemical mechanisms involved in the ageing of copal resins have not been studied in such detail as in the case of natural resins. However, it has been suggested that these mechanisms resemble the processes that occur upon maturing of polylabdanoid molecules in fossil resins, which have been investigated on the basis of FTIR (Beck 1986, Derrick, *et al.* 1999), ^{13}C NMR and pyrolysis-GC/MS (Anderson, *et al.* 1992, Anderson 1995). These studies showed that the aged chemical structure of the fossil resins is a complex multicyclic composition that is formed by polymerisation, isomerisation, defunctionalisation by loss of acidic groups, intermolecular and intramolecular cyclisation reactions. DTMS studies carried out by Scalarone and co-workers (2003b) indicated the occurrence of cleavage in light

aged Manila copal. This mechanism is supported by the considerable amount of volatile molecules desorbed during the DTMS analysis of the samples. Despite this fact, increased abundances of dimers and trimers of communic acid are readily detected with DTMS, which is attributed to the increased degree of polymerisation of copal with age. The polymer of copal, polycommunic acid (Figure 2.4.6), derives from communic acid, and according to the authors it can be detected in a significant number of crosslinks even prior to ageing, if the resin is examined without being mixed with oil.

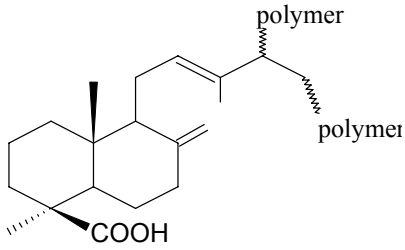

Figure 2.4.6 Polycommunic acid: the polymer of Manila copal

The most characteristic abietane type molecule detected is dehydroabietic (DHA) acid. Both communic and DHA acids are susceptible to autoxidative reactions owing to the conjugated double bonds in their skeletons (Anderson and Winans 1991, Anderson, *et al.* 1992, Pastorova, *et al.* 1997, Van den Berg, *et al.* 2000, Van der Werf, *et al.* 2000, Scalarone, *et al.* 2002, 2003b). Double bond conjugation of the communic acid occurs outside the ring configuration of the molecule (C_{12}=C_{13} and C_{14}=C_{15}), while in the DHA in the C-ring, which makes the former more susceptible to breakdown. Indeed, communic acid polymerises rapidly at two carbon-carbon double bond sites (C-8 and C-12), which along with cleavage reactions based on radical mechanisms (b- or oxidative scission) form a saturated network of bicyclic units connected by a polymer chain (Scalarone, *et al.* 2003b). The degradation fate of

polycommunate polymer is possibly the reason why its monomer cannot be effectively detected in oil varnishes fabricated with copal resins, especially when the film is somewhat aged (Van den Berg, *et al.* 1999). Certainly, the intense heat processing of copal resin with linseed oil to form the oil varnish (Mantell, *et al.* 1949, Carlyle 2001) facilitates a rigorous degradation of the communic acid. In contrast, the abietane diterpenoids, which are typical molecules of colophony and Venice turpentine, are less reactive (Anderson and Winans 1991, Anderson, *et al.* 1992, Van den Berg, *et al.* 1996, Pastorova, *et al.* 1997, Van den Berg, *et al.* 2000, Scalarone, *et al.* 2002). Upon heating, the abietane molecules isomerise giving a rich mixture of several isomers of abietic acid (Mills and White 1977).

2.5 An evaluation of the aged copal oil varnish.

The evaluation of the aged copal oil varnish was carried out with Pyrolysis TMAH GC/MS analysis. Py-TMAH-GC/MS is an online derivatisation analytical technique of advanced selectivity compared to off-line derivatisation methods (Van den Berg, *et al.* 2002). The detailed molecular information obtained by Py-TMAH-GC/MS is attributed to isomerisation and degradation of the heat- and alkali-sensitive compounds of the tested material (Kossa, *et al.* 1979, Ding, *et al.* 1997). As a result of the thermally assisted methylation several methylated derivatives are formed due to dehydration. Thus, Py-TMAH-GC/MS analysis of heat-bodied linseed oil converts some originally present fatty diacids into α-methylated and α,α-dimethylated diacids (Van den Berg and Boon 2001), while some oxidised diterpenoid acids convert into more than one derivative (Anderson and Winans 1991, Van den Berg, *et al.* 1996, Pastorova, *et al.* 1997). Despite this complication, Py-TMAH-GC/MS is a valuable

technique for the analysis of complex polymerised materials, such aged oil varnish films, although it does not determine the degree of polymerisation of the material (Van den Berg, *et al.* 1999).

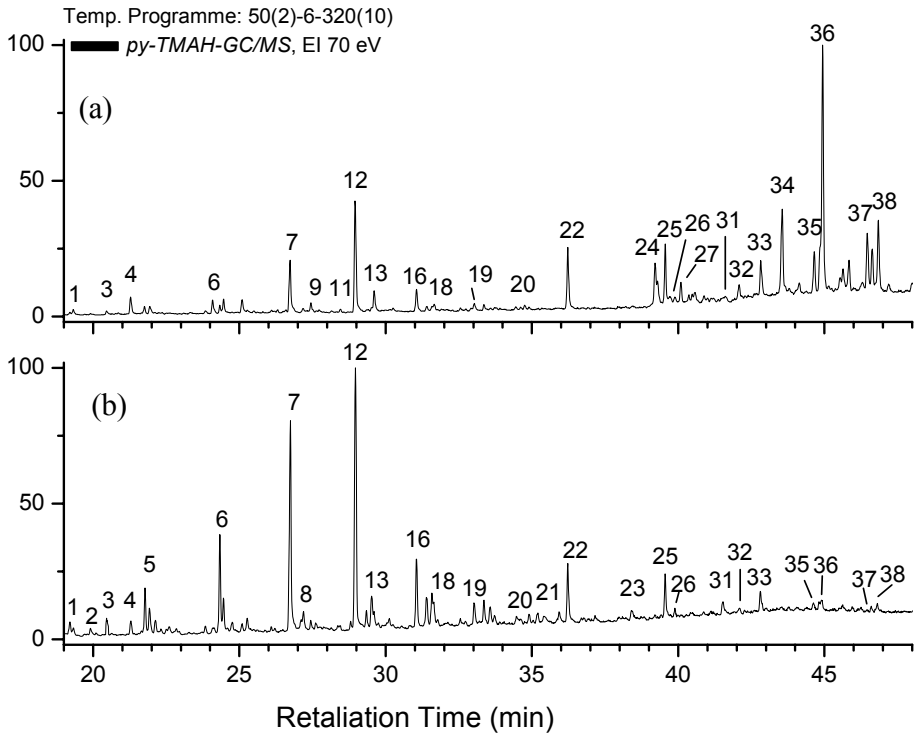

Figure 2.5.1 The Pyrolysis-TMAH-GC/MS total ion currents of the copal oil varnish film prior to (a) and after (b) 500 h under xenon arc (λ > 295 nm) exposure.

The GC/MS total ion current traces of the methylated methanol extract of the unaged and aged copal oil varnish film are shown in Figure 2.5.1 and listed in Table 2.5.1, while some of the most characteristic compounds are shown in Figure 2.4.2 and 2.4.4. The results show that most of the compounds in the film both prior to and after ageing belong to the heat-bodied linseed oil (**1**-**34**) and only compounds **35**, **36**, **37** and **38** correspond to the resin component. In particular, the concentration and the nature of the oil constituents of the examined film closely resemble a five-year-old stand oil examined by Van den Berg and co-workers (2002) on the basis of Py-TMAH-GC/MS.

Table 2.5.1 Identified methylated compounds with on-line trasmethylation using Py-GC/MS

Label	Mw	Compound
1	158	octanoic acid methyl ester
2	160	pentanedioic acid dimethyl ester
3	172	nonanoic acid methyl ester
4	174	hexanedioic acid dimethyl ester
5	186	decanoic acid methyl ester
6	188	heptanedioic acid methyl ester
7	202	octanedioic acid dimethyl ester
8	*194*	*1,2-benzenedicarboxylic acid*
9	216	α-methyl octanedioic acid dimethyl ester
10	230	α,α-dimethyl octanedioic acid dimethyl ester
11	214	dodecanoic acid methyl ester
12	216	nonanedioic acid dimethyl ester
13	230	α-methyl nonanedioic acid dimethyl ester
14	244	α,α-dimethyl nonanedioic acid dimethyl ester
15	228	tridecanoic acid methyl ester
16	230	decanedioic acid dimethyl ester
17	244	α-methyl decanedioic acid dimethyl ester
18	242	tetradecanoic acid methyl ester
19	244	undecanedioic acid dimethyl ester
20	256	pentadecanoic acid methyl ester
21	258	dodecanedioic acid dimethyl ester
22	270	hexadecanoic acid methyl ester
23	284	heptadecanoic acid methyl ester
24	296	octadecenoic acid methyl ester (cis/trans)
25	298	octadecanoic acid methyl ester
26	290	octadecatetranoic acid methyl ester (9-(-o-propylphenyl)-nonanoic acid methyl ester)
27	296	octadecenoic acid methyl ester
28	326	8-methoxy-9-octadecenoic acid methyl ester
29	326	11- methoxy-9-octadecenoic acid methyl ester
30	326	9-methoxy-10-, or 10-methoxy-8-octadecenoic acid methyl ester
31	312	9,10-epoxy-octadecanoic acid methyl ester
32	312	4-oxo-octadecanoic acid methyl ester
33	312	9-hydroxy-10-octadecenoic acid methyl ester
34	310	9-hydroxy-10-octadecenoic acid +:1, methyl ester
35	344	15-hydroxy-7-oxo-dehydroabietic (DHA) methyl ester, or 15-hydroxy-DHA methyl ether, methyl ester
36	342	7-oxo-DHA methyl ether, methyl ester
37	374	7, 15-hydroxy-DHA dimethyl ether, methyl ester
38	372	15-hydroxy-7-oxo-DHA dimethyl ether, methyl ester

The identified oil compounds arise from the crosslinked triacylglycerols either via hydrolysis or via oxidative degradation, and confirmation of their mass spectra (not

shown) has been carried out in comparison with published mass spectrometric data (Ryhage and Stenhagen 1959, 1960b, a, Christie 1998, Van den Berg, *et al.* 1999, Van den Berg, *et al.* 2002).

First, a wide range of saturated, aliphatic chain fatty acids ranging from eight to eighteen carbons in their skeleton was detected. Some long chain fatty acids identified correspond to tridecanoic (**15**), tetradecanoic (**18**), pentadecanoic (**20**), palmitic (C16, **22**), margaric (C17, **23**) and stearic (C18, **25**) acids, with the most abundant being palmitic (C16) and stearic (C18) acids. The ratios[2] of palmitic to stearic acids, 1.5 for the unaged and 1.6 for the aged film confirm that the drying oil employed originates from linseed seeds (Mills and White 1994). The identified short chain fatty acids, which have eight to twelve carbons (compounds **1**, **3**, **5** and **11**) are formed via oxidation and are likely to escape the film in a later degradation state (Privett 1959, Miyashita and Tagaki 1986, Frega, *et al.* 1999).

Mono-, double- and triple- unsaturated C18 fatty acids, and particularly *cis*-9-octadecenoic (C18:1, oleic), all-*cis*-9,12-octadecadienoic (C18:2, linoleic) and all-*cis*-9,12,15-octadecatrienoic (C18:3, linolenic) acids are significant constituents of linseed oil (Mills and White 1994). Oleic acid is detected as compounds **24** and **27** in the unaged film, while linoleic and linolenic acids are monitored only in trace amounts in the aged oil varnish. Upon processing, purification, heat-bodying and subsequent exposure under radiation, the compounds with the higher degree of unsaturation oxidise faster, and hence decrease in concentration, than those with a lower degree of unsaturation (Ucciani and Debal 1996). Therefore, the loss of

[2] All ratios presented herein correspond to peak areas measured

unsaturation especially in the unaged film signifies that C18:2 and C18:3 fatty acids have reacted away during the severe heat processing in the preparation of the oil varnish. In particular, polyunsaturated fatty acids, such as linolenic acid, react away during heat bodying generating cyclic fatty acids that are formed via Diels-Alder cyclisation (Boelhouwer, *et al.* 1967, Martin, *et al.* 1998) and/or intermolecular cyclisation of heat-induced conjugation that occurs to octadeca-dienes (Sebedio and Grandgirard 1989). For example, compound **26**, is a typical cyclic octadecanoic fatty acid, namely 9(-o-propylphenyl)-nonanoic acid, that is generated via such mechanisms (Van den Berg, et al 2002), whose presence was detected in trace amounts both prior to and after ageing. Traces of other oxygenated fatty acids, such as 9,10-epoxy octadecanoic acid (**31**) and 4-oxo-octadecanoic acid (**32**) were also present, with compound **31** peaking slightly higher in the aged oil varnish and compound **32** being more apparent in the unaged film.

Another typical group of degradation compounds detected are the saturated fatty diacids, such as pentanedioic (**2**), hexanedioic (**4**), pimelic (C7, **6**), suberic (C8, **7**), azelaic (C9, **12**), sebacic (C10, **16**), undecanedioic (**19**), dodecanedioic (**21**) acids. These are typical end products of aged oils formed upon oxidative degradation of unsaturated fatty acids via isomerisation of double bond systems (Sonntag 1979b, Martin, *et al.* 1998). The most characteristic ones are azelaic, **12**, and sebacic, **16**, acids formed readily from octadecadienoic acid (C18:2) and other conjugated dienes (Mills and White 1994). It has been postulated that the sebacic-to-azelaic ratio indicates whether the oil has undergone heat-induced polymerisation (Van den Berg, *et al.* 1999, Van den Berg, *et al.* 2002). In this case the sebacic-to-azelaic ratios are

0.5 for the unaged and 0.7 for the aged film, both being within the margins of the heat-bodied linseed oil. In addition, the typical oleic-to-palmitic and azelaic-to-stearic ratios, which are 1.1 and 1.5 in the unaged 1.6 and 3.5 in the aged, are a good indicator of the oxidative degradation of the film upon ageing (Mills and White, 1994).

Another series of oil constituents are α- and β-hydroxy diacids (Van den Berg, *et al.* 2002), the former being probably derived from dihydroxy fatty acids and the latter from epidioxides, both formed via autoxidation (Frankel, *et al.* 1990a, b). In the tested oil varnish only α-hydroxy diacids, compounds **33** and **34**, were detected, because β-hydroxy diacids are less abundant and are not detected with Py-GC/MS (Van den Berg, *et al.* 2002). Compounds **28**, **29** and **30** were identified as octadecenoic acid methyl esters substituted with a methylated hydroxy group. These compounds were also detected by van den Berg and co-workers (2002) in a five-year-old stand oil film, using both methylated and silylated extracts and analysed with GC/MS. A final series of compounds associated with the oil are α-methylated and α,α-dimethylated diacids (**9**, **10**, **13**, **14** and **17**), which are by-products formed during the transesterification reaction of the TMAH reagent with the original fatty diacids in the film (Van den Berg and Boon 2001).

Finally, peaks **35**, **36**, **37** and **38** correspond to methylated diterpenoid compounds of the copal resin. The identified compounds are dehydrogenation and oxidation products of dehydroabietic acid (DHA), which are associated with the tricyclic abietane-type molecules (Anderson and Winans 1991, Van den Berg, *et al.* 1996, Pastorova, *et al.* 1997). Since the resin incorporated in the film is copal, it was

expected that some traces of polycommunic acid would be identified, as was the case in an earlier examination of a copal oil varnish (Van den Berg, et al 1999). Earlier investigations on diterpenoids demonstrated that abietane type molecules are more stable than the labdane type molecules (Van den Berg, *et al.* 2000, Van der Werf, *et al.* 2000, Scalarone, *et al.* 2002, 2003b). As mentioned above this is probably attributed to the fact that double bond conjugation in the abietane molecules takes place inside the C-ring, while in labdane molecules outside the two-ring configuration. On the other hand, the non-detected polycommunic acid might be attributed to a possible dissolution of the resin in oil of turpentine prior to the boiling process, as commonly was the case in traditional recipes (Mantell, *et al.* 1949, Carlyle 2001). This suggestion is suitable since turpentine oil is rich in abietic acids (Scalarone, *et al.* 2002). In any case the diterpenoid molecules are present only in trace amounts in the aged copal oil varnish film prepared for the laser ablation experiments. This finding is in line with earlier investigation on aged varnishes (Dunkerton, *et al.* 1990, Van den Berg, *et al.* 1999), signifying the degradation induced in the film during the strong ageing conditions.

2.6 Conclusions

This chapter provides a review on the ageing characteristics of dammar, mastic and copal oil varnishes based on up-to-date knowledge. Moreover, it provides an insight into the specific choices made with respect to the degraded varnishes that will be studied on the basis of excimer laser ablation. Although the extreme ageing that these coatings suffered (see Appendix) may not represent moderate ageing problems, which are efficiently dealt with on the basis of chemical treatments (Hedley 1980, Stolow

1985, Phenix 1998, 2002a, b), it is expected to be indicative for cases where excimer laser ablation would provide a valuable utility for paintings' conservation.

In particular, the natural resin varnishes, which were extremely depredated, became very polar, as signified by the presence of oxidised compounds with the characteristic A-ring opening, which has been mainly detected upon artificial ageing including UV radiation (Van der Doelen, *et al.* 2000). Since some of them, such as dammarenolic acid, 20,24-epoxy-25-hydroxy-dammaran-3-one, are generated upon exposure of the resin to sunlight during harvest (Dietemann 2003), we may postulate that these products are indicators of the intense degradation of the varnishes tested. Besides, other oxidised compounds, such as those found in varnishes upon moderate (non-UV) light ageing and in painting varnishes by Van der Doelen and co-workers (1998a) were also present in almost equal proportions with the A-ring oxidised triterpenoids. It would therefore be interesting to examine whether these A-ring oxidised molecules are present across the depth profile of the natural resins, or whether they are only formed in the surface layers. This suggestion is in line with findings by Dietemann (2003), who showed that small resin 'tears' are more oxidised than large ones, harvested at the same time, which might indicate that the large 'tears' protect their bulk from radiation. This suggestion becomes firmer bearing in mind that it was shown herein that along with the oxidised compounds there are some intact triterpenoids preserved, which have not consumed oxygen. Notwithstanding oxidation, both resins generated a relatively high degree of polymerisation, delineated with the EI-DTMS-TIC's.

The copal oil varnish was examined with Py-TMAH-GC/MS. It should be noted that because of the online derivatisation process, no information about the polymerization of the film was obtained, but the existence of the high degree of polymerization in such films is already established. First it is demonstrated that upon light ageing, the concentration of the resin component in oxidised dehydroabietic acids is strongly reduced in line with earlier findings in oil varnishes (Dunkerton, *et al.* 1990, Van den Berg, *et al.* 1999). Oxidation of the heat bodied oil-resin mixture was monitored by the increasing concentration of saturated fatty diacids, including azelaic acid, over unsaturated fatty acids, such as oleic and linoleic acids (Sonntag 1979b, Martin, *et al.* 1998), which were critically reduced. Upon the heat-induced manufacture of the copal oil varnish several oxygenated fatty acids were generated from polyunsaturated fatty acids, such as linolenic acid which was not detected and traces of a cyclic octadecanoic fatty acid formed via Diels-Alder cyclisation (Boelhouwer, *et al.* 1967, Martin, *et al.* 1998) and/or intermolecular cyclisation of heat-induced conjugation (Sebedio and Grandgirard 1989). Both high degrees of polymerisation and oxidation are expected to enhance the laser ablation process.

2.7 Appendix

2.7.1 Materials:

Supplier: AP Fitzpatrick, 142 Cambridge Heath Road, Spitalfields London E1 5QJ

Kremer Pigmente® Dammar. AP Fitzpatrick Product code: 60000

Kremer Pigmente® Mastic AP Fitzpatrick Product code: 60050

Kremer Pigmente® Copal (linseed) oil varnish AP Fitzpatrick Product code: 79450

2.7.2 Experimental Methods

2.7.2.1 Varnish films preparation

Films of mastic, dammar and copal oil varnish were prepared in the chemical laboratory of the Institute of Microelectronics (IMEL) National Centre for Scientific Research (NCSR) 'Demokritos', 153 10 Athens, Greece.

Dammar and mastic varnishes were fabricated from 50% (w/v) solutions in xylene. Copal oil varnish was used as obtained by the supplier. The solutions were spin-coated on a Headway Research I-PM-1010D-CB15 Spinner at 250 to 1000 rpm on quartz substrates with dimensions 5 x 5 cm^2. A variety of film thicknesses were produced ranging from 10 to 60 μm. The thickest films of dammar and mastic varnishes were obtained two months after their dissolution in xylene. All the films dried in *vacuo***.** Evaluation of the dried films was obtained using an Ambios Technology® XP2 stylus profilometer with linear-scan stage technology and a motorised sample translation in a X-Y mechanical translator, which provided high-precision surface topography measurements and determined the thicknesses obtained. The best films were chosen for further experiments. These were: two films for each varnish, namely 15.4 and 56 μm (thick) for dammar, 16.5 and 53 μm for mastic and 14.5 and 30 μm for copal oil varnish.

2.7.2.2 Accelerated Ageing

Intense light ageing was carried out in the Department of Conservation and Technology in the Courtauld Institute of Art, Somerset House, Strand, London WC2R 0RN and involved the following:

– 500 hours of xenon-arc radiation (~ 160 Mlux.hrs) in a Sunset CPS unit (Heraeous®, Germany) equipped with a borosilicate inner filter to cut wavelengths shorter than 295 nm to imitate direct sunlight radiation. The films were regularly rotated so that to receive the same amount of radiation. A stabilised 60ºC temperature in the device was kept constant by forced air circulation. After irradiation the samples were found to be bleached.

After accelerated light ageing the samples were exposed to free oxygen conditions for 45 days, near an open window in Victoria & Albert Museum, (South Kensington, London SW7 2RL), to consume some atmospheric oxygen. Subsequently, storage in the dark (inside a drawer) at least for a month before experiments, produced some yellowing, mainly in mastic and the copal oil varnish.

2.7.3 Molecular evaluation of the ageing process

Molecular evaluation of the aged varnish films was carried out at Foundation for Fundamental Research on Matter (FOM), FOM Institute for Atomic and Molecular Physics, (AMOLF), 1009 DB Amsterdam, The Netherlands

2.7.2.3 Direct Temperature resolved Mass Spectrometry (DTMS)

Dammar and mastic films prior to and after ageing were examined with DTMS. From each sample, a thin film of approximately 4 mm^2 was subtracted, then homogenized and brought in suspension with a few drops of ethanol. A volume of 2-3 μl of the mixture was applied to a Pt/Rh (9:1) filament (100μm diameter) of a direct insertion probe, and dried *in vacuo* (using the Purevap) by evaporation of the ethanol. After insertion in the ionisation chamber a gradual temperature increase of the filament was set at a rate of 1A/min to a final temperature of approximately 800ºC, while the MS

was monitoring the evolved compounds in electron ionisation (EI) or ammonia chemical ionisation (NH_3/CI) modes. The compounds were ionised at 16 eV energy in EI mode and 250 eV in NH_3/CI mode, and analysed in a JEOL SX-102 double focusing mass spectrometer (B/E) over a mass range from 20-1000 Dalton at a cycle time of 1 s. The acceleration voltage was 8 kV. The total ion currents and summation mass spectra were examined based on previous investigations (Van der Doelen, *et al.* 1998a, Van der Doelen, *et al.* 1998b, Van der Doelen 1999, Van der Doelen and Boon 2000, Scalarone, *et al.* 2003a)

2.7.2.4 Pyrolysis-TMAH-GC/MS

About 15 μg of the unaged and light aged copal oil films, corresponding to film after complete drying and 500h exposure under xenon-arc radiation ($\lambda > 295$ nm) respectively, were applied onto a rotating 610 °C Curie-point (ferromagnetic) wire and 3-4 μl of a 2.5% methanolic solution of tetramethylammonium hydroxide (TMAH) was added before the samples were dried *in vacuo*. The ferromagnetic wire was inserted in a glass liner, flushed with argon to remove air and subsequently placed into the pyrolysis unit. Pyrolysis was performed with a FOM 5-LX pyrolysis unit (Van den Berg and Boon 2001). The ferromagnetic wire was inductively heated for 6 seconds in a 1 MHz Rf field to its Curie-point temperature (610 °C). The generated pyrolysis fragments were flushed into a SGE BPX5 column (25 m, 0.32 mm i.d., 0.25 μm film thickness) mounted in a Carlo-Erba gas chromatograph (series 8565 HRGC MEGA 2), which was coupled directly to the ion source of a JEOL SX 102A tandem mass spectrometer (B/E/B/E) via a home interface, which was kept at 280 °C. Helium was used as carrier gas at a flow rate of approximately 2 ml/min as regulated with a

CP-CF 818 pressure/flow control device (Fisons Instruments). The initial temperature of the gas chromatograph was 50 °C, which was maintained for 2 minutes. The oven temperature was programmed with a ramp of 6 °C to an end temperature of 320 °C. Ions were generated by electron impact ionisation (70 eV), accelerated to 3 KeV, mass separated and re-accelerated to 10 KeV prior to detection. The mass spectrometer was scanned across an m/z range from 40 to 700 with a cycle time of 1 second. A Jeol MS-MP-9020D data system was used for data acquisition and processing. The compounds were identified based on their 70 eV electron ionisation mass spectra (Ryhage and Stenhagen 1959, 1960b, Christie 1998, Van den Berg, *et al.* 1999, Scalarone, *et al.* 2002, Van den Berg, *et al.* 2002).

2.8 References

Anderson, K. B. and Winans, R. E., 'The Nature and Fate of Natural Resins in the Geosphere I. Evaluation of Pyrolysis-Gaschromatography-Mass Spectrometry for the Analysis of Plant Resins and Resinites', *Analytical Chemistry* **63** (1991) 2901-2908.

Anderson, K. B., Winans, R. E., and Botto, R. E., 'The nature and fate of natural resins in the geosphere-II. Identification, classification and nomenclature of resinities.' *Organic Geochemistry* **18** (1992) 829.

Anderson, K. B. 'New evidence concerning the stucture, composition and maturation of class I (polylabdanoid) resinites.' In *Amber, Resinite and Fossil Resins*, Ed. K. B. Anderson, Crelling, J.C., Vol. 617, American Chemical Society: Washington, DC, (1995), 105-129.

Arigoni, D., Barton, D. H. R., Bernasconi, R., Djerassi, C., Mills, J. S., and Wolff, R. E., 'The constituents of dammarenolic and nyctanthic acid', *Journal of the Chemical Society* (1960) 1900-1905.

Artman, N. R. and Smith, D. E., 'Systematic isolation and identification of minor components in heated and unheated fat', *Journal of American Oil Chemists' Society* **49** (1972) 318-326.

Barton, D. H. R. and Seoane, E., 'Triterpenoids. Part XXII. The constitution and stereochemistry of masticadieonic acid', *Journal of the Chemical Society* (1956) 4150-4157.

Bäuerle, D. *Laser Processing and Chemistry, Third, revised and enlarged edition*, Springer-Verlag, Berlin, Heidelberg, New York, 2000.

Beck, C. W., 'Spectroscopic investigations of amber', *Applied Spectroscopy Reviews* **22** (1986) 57.

Berns, R. S. and De la Rie, E. R. 'The relative importance of surface roughness and refractive index in the effects of varnishes on the appearance of painitngs'. In *Preprints of the 13th triennial meeting of the ICOM Committee for Conservation*, Ed. V. R., Vol. I, James & James (Science Publishers) Ltd, Rio de Janeiro, (2002), 211-216.

Berns, R. S. and De la Rie, E. R., 'The effect of the refractive index of a varnish on the appearance of oil paintings', *Studies in Conservation* **48** (2003) 251-262.

Boar, R. B., Couchman, L. A., Jaques, A. J., and Perkins, M. J., 'Isolation from Pistacia resins of a bicyclyc triterpenoid representing an apparent trapped intermediate of squalene 2,3-epoxide cyclization', *Journal of the American Chemical Society* (1984) 2476-2477.

Boelhouwer, C., Knegtel, J. T., and Tels, M., 'On the mechanism of the thermal polymerization of linseed oil', *Fette, Seifen, Anstrichmittel* **69** (1967) 432-436.

Boon, J. J., 'Analytical pyrolysis mass spectrometry: new vistas opened by temperature-resolved in-source PYMS', *International Journal of Mass Spectrometry and Ion Processes* **118/119** (1992) 755-787.

Boon, J. J. and van der Doelen, G. A. 'Advances in the current understanding of aged dammar and mastic triterpenoid varnishes on the molecular level'. In *Firnis: Material - Aesthetik - Geschichte, International Kolloquium, Braunschweig, 15-17 Juni 1998*, Ed. A. Harmssen, Hertog-Anton-Ulrich-Museum, Braunschweig, (1999), 92-104.

Brewis, S. and Halsall, T. G., 'The chemistry of triterpenes and related compounds. Part XXXYIII. The acidic constituents of dammar resin.' *Journal of Chemical Society* (1961) 646-650.

Brewis, S., Halsall, T. G., Harrison, H. R., and Hodder, O. J. R., 'Crystallographic structure determination of a triterpene dimethyl ester epsilon-lactone from dammar resin', *Journal of Chemical Society D* (1970) 891-892.

Brommelle, N., 'Material for a history of conservation', *Studies in Conservation* **2** (1956) 176-186.

Carlyle, L., Binnie, N., Van der Doelen, G. A., Boon, J. J., McLean, B., and Ruggles, A. 'Traditional painting varnishes project: preliminary report on natural and artificial aging and a note on the preparation of cross-sections.' In *Firnis, Material Aesthetik Geschichte, International Kolloquium*, Braunschweig, (1998), 110-127.

Carlyle, L. A. *The artist's assistant: Oil painting Instruction manuals and handbooks in Britain 1800-1900: with reference to selected eighteenth century sources*, Archetype Publications, London, 2001.

Cerny, J., Vystrcil, A., and Huneck, S., 'Uber ein neues triterpen aus dammarhartz', *Chemische Berichte* (1963) 3021-3023.

Christie, W. W., 'Gas chromatography-mass spectrometry methods from structural analysis of fatty acids', *Lipids* **33** (1998) 343-353.

Coppen, J. J. W. 'Damar'. In *Gums, resins and latexes of plant origin* Vol. 6, Food and Agricalture Organization of the United Nations, Nonwood Forest Productions, Rome, (1995), 65-73.

Cove, S., 'Mixing and mingling: John Constable's oil paint mediums c.1802-37, including the analysis of the 'Manton' paint box'. In *IIC Congress, Painting Techniques, History, Materials and Studio Practice*, Eds. R. Ashok and P. Smith, Dublin, 7-11 September, (1998), London, 211-216.

Crossley, A., Heyes, T. D., and Hudson, B. J. F., 'The effect of heat on pure triglycerides', *Journal of American Oil Chemists' Society* **39** (1962) 9-14.

De la Rie, E. R., 'The influence of varnish on the appearance of paintings', *Studies in Conservation* **32** (1987) 1-13.

De la Rie, E. R., 'Stable Varnishes for Old Master Paintings', PhD Thesis University of Amsterdam, (1988a).

De la Rie, E. R., 'Photochemical and thermal degradation of films of dammar resin', *Studies in Conservation* **33** (1988b) 53-70.

De la Rie, E. R., 'Old Master Paintings: A study of the Varnish Problem', *Analytical Chemistry* **61** (1989) 1228A.

Denise, J. 'Fats refining'. In *Oils & Fats Manual*, Eds. A. Karleskind and J.-P. Wollf, Vol. 2, Intercept, Ltd., Andover, (1996), 807-895.

Derrick, M. R., Stulick, D., and Landry, J. M. *Infrared spectroscopy in conservation science*, Getty Cnservation Institute: Los Angeles, CA, 1999.

Dietemann, P., 'Towards more stable natural resin varnihses for painintgs', PhD Thesis Swiss Federal Institute of Technology, Zurich, (2003).

Ding, J.-K., Jing, W., Zou, T.-Z., Song, M., and Yu, X.-G., 'The effect of isomerisation and degradation of polyunsaturated fatty acids from oils by different volume proportions of tetramethylammonium hydroxide in thermally assisted hydrolysis and methylation', *Journal of Analytical and Applied Pyrolysis* **42** (1997) 1-8.

Dunkerton, J., Kirby, J., and White, R. 'Varnish and early Italian tempera paintings'. In *Cleaning, Retouching and Coatings. Preprints of the Brussels Congress, 3-7 September*, IIC, London, (1990), 63-67.

Feller, R. L., 'The deteriorating effect of light on museums objects', *Museum News Technical Supplement* (1964a) i-viii.

Feller, R. L., 'A note on the exposure of dammar and mastic varnishes to fluorescent lamps', *Bulletin of the IIC-American Group* **4** (1964b) 12-14.

Feller, R. L., Stolow, N., and Jones, E. H. 'On picture varnishes and their solvents.' Revised and enlarged edition 1985. Washington DC: National Gallery of Art., (1985).

Feller, R. L. 'Solubility and removability of aged polymeric films'. In *On picture varnishes and their solvents.*, Eds. R. L. Feller, N. Stolow, and E. H. Jones, Revised and enlarged edition 1985. Washington DC: National Gallery of Art., (1985), 202-210.

Feller, R. L. 'Accelerated Aging: Photochemical and Thermal Aspects', Ed. D. Berland, The Getty Conservation Institute, Los Angeles, USA, (1994).

Figge, K., 'Dimeric fatty acid [1-^{14}C]methyl esters. I. Mechanisms and products of thermal and oxidative-thermal reactions of unsaturated fatty acid esters - Literature review', *Chemistry and Physics of Lipids* **6** (1971) 164-182.

Formo, M. W. 'Paints, varnishes, and related products'. In *Baile's Industrial Oil and Fat Products*, Ed. D. Swern, Vol. 1, John Wiley & Sons, New York, (1979a), 687-817.

Formo, M. W. 'Paints, varnishes and related products: Discolouration'. In *Baile's Industrial Oil and Fat Products*, Ed. D. Swern, Vol. 1, John Wiley & Sons, New York, (1979b), 722-724.

Frankel, E. N., Evans, C. D., and Cowan, J. C., 'Thermal dimerization of fatty ester hydroperoxides', *Journal of American Oil Chemists' Society* **37** (1960) 418-424.

Frankel, E. N., Neff, W. E., and Selke, E., 'Analysis of autoxidized fats by gas chromatography - mass spectrometry: VII. Volatile thermal decomposition products of pure hydroperoxides from autoxidized and photosensitized oxidized mehtyl oleate, linoleate and linolenate', *Lipids* **16** (1981) 279-292.

Frankel, E. N., Neff, W. E., and Miyashita, K., 'Autoxidation of polyunsaturated triacylglycerols. I. Trilinoleoylglycerol', *Lipids* **25** (1990a) 33-39.

Frankel, E. N., Neff, W. E., and Miyashita, K., 'Autoxidation of polyunsaturated triacylglycerols. II. Trilinolenoylglycerol', *Lipids* **25** (1990b) 40-47.

Frankel, E. N. 'Lipid Oxidation'. In *Oily Press Lipid Library* Vol. 10, The Oily Press Ltd, Dundee, (1998), 227-248.

Frega, N., Mozzon, M., and Lercker, G., 'Effects of free fatty acids on oxidative stability of vegetable oil', *Journal of American Oil Chemists' Society* **76** (1999) 325-329.

Frilette, V. J., 'Drying oil and oleoresinous varnish films', *Industrial and Enginering Chemistry Research* **38** (1946) 493.

Georgiou, S., Koubenakis, A., Syrrou, M., and Kontoleta, P., 'The importance of the plume ejection time for the fragmentation yieds observed in the UV ablation of molecular van der Waals films. Ablation of chlorobenzene films at 248 nm', *Chemical Physics Letters* **270** (1997) 491-499.

Georgiou, S., Zafiropulos, V., Tornari, V., and Fotakis, C., 'Mechnistic Aspects of Excimer Laser Restoration of Painted Artworks', *Laser Physics* **8** (1998) 307-312.

Gettens, R. and Stout, G. *Painting materials: a short encyclopaedia*, Dover Publications, New York, 1966.

Greaves, J. H. and Laker, B., 'Estimation of unreacted acids during polymerization of linseed oil', *Chemistry & Industry (London)* (1961) 1709-1710.

Harrison, H. R., Hodder, O. J. R., Brewis, S., and Halsall, T. G., 'Chemistry of triterpenes and related compounds XLVII. Crystal and molecular structure of 'compounds B', a triterpene dimethyl ester epsilon-lactone from dammar resin', *Journal of Chemical Society C* (1971) 2525-2529.

Hedley, G., 'Solubility parameters and varnish removal: a survey.' *The Conservator* **4** (1980) 12-18. (Re-printed, with corrections, in Measured Opinions (1993), ed. C. Villers. London: United Kingdom Institute for Conservation: 128-134).

Hites, R. A., 'Quantitative analysis of triglyceride mixtures by mass spectrometry', *Analytical Chemistry* **42** (1970) 1736-1740.

Jones, R., Townsend, J., and Boon, J. J., 'A technical assessment of eight portraits by Reynolds being considering for conservation'. In *ICOM Committee for Conservation 12th Triennial Meeting Lyon, France*, (1999), 375-380.

Keller, R., 'Leinol als malmittel', *Maltechnik* **2.** (1973) 74-105.

Koller, J., Baumer, U., Grosser, D., and Schmid, E. 'Mastic'. In *Baroque and Rococo Lascquers*, Eds. K. Walch and J. Koller, Vol. 81, Arbeitshefte des Bayerischen Landesamtes fuer Denkmalpflege, Karl M. Lipp Verlag, Muenchen, (1997), 347-358.

Kossa, W. C., MacGee, J., Ramachandran, S., and Webber, A. J., 'Pyrolytic methylation / gas chromatography: a short review', *Journal of Chromatographic Science* **17** (1979) 177-187.

Laisney, J. 'Processes for obtaining oils and fats'. In *Oils and fats manual*, Eds. A. Karleskind and J.-P. Wolff, Vol. 1, Intercept Ltd., Andover, (1996), 715-799.

Luk'yanchuk, B., Bityurin, N., Anisimov, S., and Bäuerle, D. 'Photophysical Ablation of Organic Polymers'. In *Excimer Lasers*, Ed. L. D. Laude, Kluwer Academic Publishers, The Netherlands, (1994), 59-77.

Mantell, C. L., Kopf, C. W., Curtis, J. L., and Rogers, E. M. 'Oil Varnishes'. In *The technology of natural resins*, John Wiley & Sons, Inc., (1949), 265-319.

Marner, F.-J., Freyer, A., and Lex, J., 'Triterpenoids from gum mastic, the resin of Pistacia Lentiscus', *Phytochemistry* **30** (1991) 3709-3712.

Martin, J. C., Nour, M., Lavillonniere, F., and Sebedio, J. L., 'Effects of fatty acid positional distribution and triacylglycerol composition on lipid by-products formation during heat treatment: II *Trans* isomers', *Journal of American Oil Chemists' Society* **75** (1998) 1073-1078.

Merrifield, M. P. *Medieval and Renaissance Treatises on the Arts of Painting*, Dover, New York, 1999.

Mills, J. S. and Werner, A. E. A., 'The chemistry of dammar resin', *Journal of Chemical Society* (1955) 3132-3140.

Mills, J. S., 'The constitution of the natural, tetracyclic triterpenes of dammar resin', *Journal of Chemical Society* (1956) 2196-2202.

Mills, J. S. and White, R., 'Natural resins of art and archaeology, their sources, chemistry and identification', *Studies in Conservation* **22** (1977) 12-31.

Mills, J. S. and White, R. *The Organic Chemistry of Museum Objects*, 2nd edition, Butterworth-Heinemann, Oxford, 1994.

Miyashita, K. and Tagaki, T., 'Study on the oxidative rate and proxidant activity of free fatty acids', *Journal of American Oil Chemists' Society* **63** (1986) 1380-1384.

Morgans, W. M. 'Drying oils, driers and drying'. In *Outlines of paint technology*, Ed. E. Arnold, London, (1990), 158-179.

Nawar, N. N. and Witchwood, A. 'Autoxidation of oils and fats at elevated temperatures'. In *Autoxidation in food and biological systems*, Eds. M. G. Simic and M. Karel, Plenum Press, New York, (1980).

Neil, J. W. 'The art of making copal and spirit varnishes, Transactions of the Society Instituted at London for the Encouragement of Arts, Manufacturers and Commerce' Vol. XLIX, Part II, Society's House, Housekeeper, London, (1833), 33-87 (cited by L. Carlyle 2001 p. 317).

Norris, F. A. 'Extraction of fat and oils'. In *Bailey's industrial oil and fat products*, Ed. D. Swern, Vol. 2, John Wiley & Sons, New York, (1982a), 175-251.

Norris, F. A. 'Refining and bleaching'. In *Bailey's industrial oil and fat products*, Ed. D. Swern, Vol. 2, John Wiley & Sons, New York, (1982b), 253-314.

Ohfuji, T. and Kaneda, T., 'Characterization of toxic compound in thermally oxidized oil', *Lipids* **8** (1973) 353-359.

Papageorgiou, V. P., Sagredos, A. N., and Moser, R., 'GLC-MS computer analysis of the essential oil of mastic gum', *Chimica Chronika, new series* **10** (1981) 119-124.

Papageorgiou, V. P., Bakola-Christianopoulou, M. N., Apazidou, K. K., and Psarros, E. E., 'Gas chromatographic-mass spectrometric analysis of the acidic triterpenic fraction of mastic gum', *Journal of Chromatography A* **769** (1997) 263-273.

Pastorova, I., van der Berg, K. J., Boon, J. J., and Verhoeven, J. W., 'Analytisis of oxidised diterpenoid acids using thermally assisted methylation with TMAH', *Journal of Analytical and Applied Pyrolysis* **43** (1997) 41-57.

Paulose, M. M. and Chang, S. S., 'Chemical reactions involved in deep fat frying of foods: VI. Characterization of nonvolatile decomposition products of trilinolein', *Journal of American Oil Chemists' Society* **50** (1973) 147-154.

Paulose, M. M. and Chang, S. S., 'Chemical reactions involved in deep fat frying of foods: VIII. Characterization of nonvolatile decomposition products of triolein', *Journal of American Oil Chemists' Society* **55** (1978) 375-380.

Perikos, J. *The Chios Gum Mastic*, Print All Ltd., Athens, 1993.

Perrin, J. L. 'Chemical and physical changes in edible fats'. In *Oils & fats manual*, Eds. A. Karleskind and J.-P. Wollf, Vol. 2, Intercept Ltd., Andover, (1996), 1025-1042.

Phenix, A., 'Solubility parameters and the cleaning of paintings: an update and review', *Zeitschrift fór Kunsttechnologie und Konservierung* **12** (1998) 387- 409.

Phenix, A., 'The swelling of artists' paints in organic solvents Part 1 - a simple method for measuring the in-plane swelling of unsupported paint films', *Journal of the American Institute for Conservation* **41** (2002a) 43-60.

Phenix, A., 'The swelling of artists' paints in organic solvents Part 2 - comparative swelling powers of selected organic solvents and solvent mixtures', *Journal of the American Institute for Conservation* **41** (2002b) 61-90.

Poehland, B. L., Carte, B. K., Francis, T. A., Hyland, L. J., Allaudeen, H. S., and Troupe, N., 'In vitro antiviral activity of dammar resin triterpenoids', *Journal of Natural Products* **50** (1987) 706-713.

Privett, O. S., 'Autoxidation and autoxidative polymerisation', *Journal of American Oil Chemists' Society* **36** (1959) 505-512.

Rezanka, T. and Mares, P., 'Determination of plant triacylglycerols using capillary gaschromatography, high-performance liquid chromatography and mass-spectrometry', *J. Chrom.* **542** (1991) 145-159.

Russel, G. A., 'The rates of oxidation of aralkyl hydrocarbons. Polar effects in free radical reactions', *J Am.Chem. Soc.* **78** (1956) 1047-1054.

Russel, G. A., 'Deuterium-isotope effects in the autoxidation of aralkyl hydrocarbons. Mechanism of the interaction of peroxy radicals', *J. Am. Chem. Soc.* **79** (1957) 3871-3877.

Ryhage, R. and Stenhagen, E., 'Mass spectrometric studies III. Esters of saturated dibasic acids', *Ark. Kemi* **14** (1959) 497-509.

Ryhage, R. and Stenhagen, E., 'Mass spectrometry in lipid research', *Journal of Lipid Research* **1** (1960a) 361-391.

Ryhage, R. and Stenhagen, E., 'Mass spectrometric studies. VI. Methyl esters of normal chain oxo-, hydroxy-, methoxy- and epoxy-acids', *Ark. Kemi* **15** (1960b) 545-574.

Scalarone, D., Lazzari, M., and Chiantore, O., 'Ageing behaviour and pyrolytic characterisation of diterpenic resins used as art materials: colophony and Venice turpentine', *Journal of Analytical Applied Pyrolysis* **64** (2002) 345-361.

Scalarone, D., van der Horst, J., Boon, J. J., and Chiantore, O., 'Direct-temperature mass spectrometric detection of volatile terpenoids and natural terpenoid polymers in fresh and artifficially aged resins', *Journal of Mass Spectrometry* **38** (2003a) 607-617.

Scalarone, D., Lazzari, M., and Chiantore, O., 'Ageing behaviour and analytical pyrolysis characterisation of diterpenic resins used as art materials: Manila copal and sandarac', *Journal of Analytical Applied Pyrolysis* **68-69** (2003b) 115-136.

Schoene, F., Fritsche, J., Bargholz, J., Leiterer, M., Jahreis, G., and Matthaeus, B., 'Zu den Veranderungen von Rapsol und Leinol wahrend der Verarbeitung', *Fett/Lipid* **100** (1998) 539-545.

Scott, G. *Atmospheric oxidation and antioxidants*, Elsevier Science Publishers B.V, Amsterdam, 1993.

Scott Taylor, J. 'Oil Painting'. In *Modes of Painting Described and Classified*, Winsor and Newton, Ltd, London, (1890), 38-39 (cited by L.Carlyle 2001 p. 321).

Sebedio, J. L. and Grandgirard, A., 'Cyclic fatty acids: natural sources, formation during heat treatment, synthesis and biological properties', *Progress in Lipid Research* **28** (1989) 303-336.

Selke, E., Rodwedder, W. K., and Dutton, H. J., 'Volatile components from tristearin heated in air', *Journal of American Oil Chemists' Society* **52** (1975) 232-235.

Selke, E., Rodwedder, W. K., and Dutton, H. J., 'Volatile components from triolein heated in air', *Journal of American Oil Chemists' Society* **54** (1977) 62-67.

Seoane, E., 'Further crystalline constituents of gum mastic', *Journal of the Chemical Society* (1956) 4158-4160.

Shepherd, R. "A conservator's note". In *George Stubbs 1724-1806*, Ed. J. Egerton, Tate Gallery, London, (1984), 20-21.

Silwood, C. J. L. and Grootveld, M., 'Application of high-resolution, two-dimensional ^{1}H and ^{13}C nuclear magnetic resonance techniques to the characterisation of lipid oxidation products in autoxidized linoleoyl/linoleneoylglycerols', *Lipids* **34** (1999) 741-756.

Sonntag, N. O. V. 'Structure and composition of oil and fats'. In *Bailey's industrial oil and fat products*, Ed. D. Swern, Vol. 1, John Wiley & Sons, New York, (1979a), 45-83.

Sonntag, N. O. V. 'Reactions of fats and fatty acids'. In *Bailey's industrial oil and fat products*, Ed. D. Swern, Vol. 1, John Wiley & Sons, New York, (1979b), 158-164.

Srinivasan, R. and Braren, B., 'Ultraviolet laser ablation of organic polymers', *Chemical Reviews* **89** (1989) 1303-1316.

Srinivasan, R. 'Interaction of laser radiation with organic polymers'. In *Laser Ablation: Principles and Applications*, Ed. J. C. Miller, Vol. 28, Springer Series of Material Science, Springer, Berlin, Heidelberg, (1994), 107.

Stolow, N. 'Part II: Solvent Action'. In *On picture varnishes and their solvents.*, Eds. R. L. Feller, N. Stolow, and E. H. Jones, Revised edition 1971. Cleveland, Ohio: Case Western Reserve University. Revised and enlarged edition 1985. Washington DC: National Gallery of Art., (1985).

Sultana, C. 'Oleaginous flax'. In *Oils & Fats Manual*, Eds. A. Karleskind and J.-P. Wolff, Vol. 1, Intercept Ltd., Andover, (1996), 154-168.

Sutherland, K. R., 'Solvent extractable components of oil paint films', PhD Thesis University of Amsterdam, (2001).

Swern, D. 'Bailey's industrial oil and fat products' Vol. 1, John Wiley & Sons, New York, (1979).

Swicklik, M. 'French painting and the use of varnish, 1750-1900'. In *Conservation Research*, National Gallery of Art, Washington DC, (1993), 157-174.

Tawn, A. R. H. 'Solvents, oils, resins and driers'. In *Paint technology manuals*, Ed. A. R. H. Tawn, Vol. 2, Chapman and Hall, London, (1969a), 31-57.

Tawn, A. R. H. 'Solvents, oils, resins and driers'. In *Paint technology manuals*, Ed. A. R. H. Tawn, Vol. 2, Chapman and Hall, London, (1969b), 113-141.

Tawn, A. R. H. 'Solvents, oils, resins and driers'. In *Paint technology manuals*, Ed. A. R. H. Tawn, Vol. 2, Chapman and Hall, London, (1969c), 142-156.

Thomas, B. R., 'The bled resins of *Agathis Australis*', *Acta Chem. Scand.* **20** (1966) 1074-1081.

Tingry, P. F. 'The Painter and Varnisher's Guide', J. Taylor, Black-Horse-Court, London, (1804), 138 (cited by L. Carlyle 2001 p.327).

Torquebiau, E., 'Man-made dipterocarp forest in Sumatra', *Agroforestry Systems* **2** (1984) 103-127.

Ucciani, E. and Debal, A. 'Chemical properties of fats'. In *Oils & Fats Manual*, Eds. A. Karleskind and J.-P. Wolff, Vol. 1, Intercept Ltd., Andover, (1996), 325-443.

Van Aarssen, B. G. K., Cox, H. C., Hoogendoorn, P., and De Leeuw, J. W., 'A cadinene biopolymer present in fossil and extant dammar resins as a source for cadinanes and bicadinanes in crude oils from Southern Asia', *Geochimica et Cosmochimica Acta* **54** (1990) 3021-3031.

Van den Berg, J. D. J. and Boon, J. J., 'Unwanted alkylation during direct methylation of fatty (di)acids using tetramethylammonium hydroxide reagent in a Curie-point pyrolysis unit', *Journal of Analytical Applied Pyrolysis* **61** (2001) 45-63.

Van den Berg, J. D. J., 'Analytical chemical studies on traditional linseed oil paints', PhD Thesis University of Amsterdam, (2002).

Van den Berg, J. D. J., Van den Berg, K. J., and Boon, J. J., 'Identification of non-cross-linked compounds in methanolic extraxts of cured and aged linseed oil-based paint films using gass chromatography - mass spectrometry', *Journal of Chromatography A* **950** (2002) 195-211.

Van den Berg, K. J., Pastorova, I., Spetter, L., and Boon, J. J., 'State of oxidation of diterpenoid *Pinaccae* resins in varnish, wax lining material, 18th century resin oil paint, and a recent copper resinate glaze'. In *Preprints ICOM Committee for Conservation 11th Triennial Meeting, Edinburgh, Scotland, 1- 6 September 1996*, Ed. J. Bridgland, Vol. 2, James & James, (1996).

Van den Berg, K. J., van der Horst, J., Boon, J. J., and Sudmeijer, O. O., 'Cis-1,4-poly-b-myrcene; the structure of the polymeric fraction of mastic resin (Pistacia lentiscus L.) elucidation', *Tetrahedron Letters* **39** (1998).

Van den Berg, K. J., Van der Horst, J., and Boon, J. J., 'Recognition of copals in aged resin paints and varnishes'. In *Preprints ICOM Committee for Conservation 12th Triennial Meeting, Lyon, France, 29 Aug. - 3 September 1999*, Vol. II, James & James, London, (1999), 855-861.

Van den Berg, K. J., Boon, J. J., Pastorova, I., and Spetter, L. F. M., 'Mass spectrometric methodology for the analysis of highly oxidized diterpenoid acids of Old Master paintings', *Journal of mass Spectrometry* **35** (2000) 512-533.

Van der Doelen, G. A., van der Berg, K. J., and Boon, J. J., 'Comparative chromatographic and mass spectrometric studies of triterpenoid varnishes: fresh material and aged samples from paintings', *Studies in Conservation* **43** (1998a) 249-264.

Van der Doelen, G. A., Van der Berg, K. J., Boon, J. J., Shibayama, N., De la Rie, E. R., and Genuit, W. J. L., 'Analysis of fresh triterpenoid resins and aged triterpenoid varnishes by high-performance liquid chromatography-atmospheric pressure chemical ionisation (tandem) mass spectrometry', *Journal of Chromatography A* **809** (1998b) 21-37.

Van der Doelen, G. A., 'Molecular studies of fresh and aged triterpenoid varnishes', PhD Thesis University of Amsterdam, (1999).

Van der Doelen, G. A., Van den Berg, K. J., and Boon, J. J., 'A comparrison of weatherometer aged dammar varnish and aged varnishes from paintings'. In *Art Chimie: La Couleur: Actes du Congres*, Eds. J. Goupy and J.-P. Mohen, CNRS Editions, Paris, (2000), 146-149.

Van der Doelen, G. A. and Boon, J. J., 'Artificial ageing of varnish triterpenoids in solution', *Journal of Photochemistry and Photobiology A: Chemistry* **134** (2000) 45-57.

Van der Werf, I. D., Van den Berg, K. J., Schmitt, S., and Boon, J. J., 'Molecular characterization of copaiba balsam as used in painting techniques and restoration procedures', *Studies in Conservation* **45** (2000) 1-18.

Wenders, E., 'Dammar als Gemaldefirnis', *Zeitschrift fór Kunsttechnologie und Konservierung* **15** (2001) 133-162.

Whitlock, C. B. and Nawar, N. N., 'Thermal oxidation of mono-unsaturated short chain fatty acids: I. ethyl 3-hexanoate', *Journal of American Oil Chemists' Society* **53** (1976) 586-591.

Wicks Jr., Z. W., Jones, F. N., and Pappas, S. P. 'Drying oils'. In *Organic coatings: science and technology* Vol. 1: Film formation, components, and appearance, John Wiley & Sons, Inc., New York, (1992), 133-143.

Williams, W. 'An Essay on the Mechanic of Oil Colours', Printed by P. Hazard, Bath, (1787), 196-197 (cited by L. Carlyle 2001 p 184).

Wingard, M. R., ', "Extraction methods for drying oils', *Journal of American Oil Chemists' Society* **36** (1959) 483-490.

Zafiropulos, V. and Fotakis, C. 'Lasers in the Conservation of painted Artworks'. In *Laser in Conservation: an Introduction*, Ed. M. Cooper, Butterworth Heineman, Oxford, (1998), 79.

Zafiropulos, V. 'Laser ablation in cleaning of artworks'. In *Optical Physics, Applied Physics and Material Science: Laser Cleaning*, Ed. B. S. Luk'yanchuk, World Scientific, Singapure, New Jersey, London, Hong Kong, (2002), 343-392.

Zumbühl, S., Knochenmuss, R. D., and Wülfert, S., 'Rissig und blind werden in relativ kurzer Zeit alle Harzessenzfirnisse', *Zeitschrift für Kunsttechnologie und Konservierung* **12** (1998a) 205-219.

Zumbühl, S., Knochenmuss, R., Wülfert, S., Dubois, F., Dale, M. J., and Zenobi, R., 'A graphite-assisted laser desorption/ionisation study of light-induced ageing in triterpene dammar and mastic varnishes.' *Analytical Chemistry* **70** (1998b) 707-715.

3. *Optimisation Process of Excimer Laser Ablation for Painting Coatings*

Abstract

The ablation properties of artificially aged triterpenoid dammar and mastic films and a copal oil varnish were investigated using KrF excimer laser ablation. Depth-step formation was carried out with a step-by-step scanning process proposed for the laser 'cleaning' of paintings. At first, optimisation was possible across the whole thickness of the copal oil varnish film and the surface layers of the triterpenoid films. In the aged triterpenoid varnish films there were ablation rate variations between surface and whole thickness studies indicating gradual changes of the ablation mechanisms across the depth profile of these films. Indeed, 'optimal' fluences yielded from mean laser ablation rate studies on the surface yielded different ablation steps in surface and bulk layers. The changes of the excimer laser ablation mechanisms of the aged natural resin varnishes are in line with determined compositional gradients across the depth-profile of aged triterpenoid varnishes. The constant ablation step across the depth profile of the aged copal oil varnish tested indicated that the film was saturated in terms of absorption. The differences in three aged varnishes and the changes across the depth profiles of the

natural resin films were outlined (a) by analysis of the ablation plume emission using laser-induced breakdown spectroscopy (LIBS) and (b) by measurements of the etched depth-steps generated with the proposed laser cleaning procedure. Details on the precise methodology for the laser cleaning process are presented. The experimental data demonstrate that the proposed laser cleaning process provides predictable step removal combining both submicron-scale precision per pulse and an excellent quality of the uncovered surfaces per step.

3.1 Introduction

The laser cleaning of old master paintings, and/or other works of art coated with aged and deteriorated varnishes requiring removal, has been proposed since 1993 (Hontzopoulos, *et al*. 1993, Morgan 1993, Fotakis 1995). This method is based on UV pulsed (excimer) lasers, providing a superior selectivity based on a stepwise, micron-scale varnish removal. From the early stages of investigations, it was obvious that the work should concentrate on the excimer laser ablation of aged varnish coatings and at the same time, the protection of the coated (underlying) sustainable layers from the UV laser photons (Fotakis, *et al*. 1997, Zafiropulos, *et al*. 1997, Zergioti, *et al*. 1997). Upon UV laser irradiation, paints discolour devastatingly (Athanassiou, *et al*. 2000, Hill, *et al*. 2000, Zafiropulos, *et al*. 2001), which is a problem caused in the presence of inorganic pigments only (Castillejo, *et al*. 2002, Castillejo, *et al*. 2003), and in particular in the uppermost layers of the irradiated inorganic pigment particles (Luk'yanchuk and Zafiropulos 2002). Given the irreversibility of such damage, two reasonable ways have been proposed to avoid it: first, using online control of the laser ablation process by employing techniques that monitor the plume emission, such as

Laser-Induced Fluorescence (LIF), Laser-Induced Breakdown Spectroscopy (LIBS), and/or monitor the treated surface with means of reflectography (Zafiropulos, *et al*. 1997, Zergioti, *et al*. 1997, Zafiropulos and Fotakis 1998, Scholten, *et al*. 2000, Teule, *et al*. 2003); and second, keeping a thin film of the ablated varnish on the surface to prevent irradiation of the underlying, usually photosensitive, surface (Zafiropulos and Fotakis 1998, Zafiropulos 2002).

Leaving a thin layer of varnish on the surface basically permits the control of the application by optimising the parameters that influence the excimer laser ablation of the coating (Zafiropulos 2002). Excimer laser ablation of polymerised films with intense absorption in the UV, such as the aged and discoloured natural varnishes (De la Rie 1988b, Van der Doelen 1999, Dietemann 2003), is a complex interaction based on various factors. These include: (a) the ambient atmosphere in which ablation takes place, as it regulates the pressure applied on the material and the ablation products (Bäuerle 2000); (b) the UV laser wavelength, which influences the extent of the photochemical and/or thermal interaction mechanisms in the ablated surface and the desorbed photofragments (Bäuerle 2000); (c) the duration of the laser pulses, which influences the extent of electronic excitations both spatially and qualitatively, with the longer pulse durations increasing the risks for thermal modifications both of the irradiated spot and the surrounding area (Luk'yanchuk, *et al*. 1994, Srinivasan 1994, Bäuerle 2000, Georgiou and Koubenakis 2003); (d) the pulse energy, which affects the size of the laser beam profile that can be utilised, bearing in mind that higher pulse energies allow for sufficient irradiation of larger spots that are essential for sufficient laser cleaning of large surfaces (Bäuerle 2000); (e) the energy density or fluence per

pulse, which controls the intensity of the interaction in the irradiated surface (Luk'yanchuk, *et al*. 1994, Srinivasan 1994, Bäuerle 2000); (f) the optical density and the optical absorption length of the ablated organic film in the laser wavelength, which controls the type and the depth of the electronic excitations per pulse; and finally (g) the degree of polymerisation of the ablated material, which controls the extent of bond-breakage along the optical absorption length (Srinivasan and Braren 1989, Zafiropulos 2002).

Notwithstanding the diverse factors influencing excimer laser ablation, several requirements have been taken into account for the proposed laser cleaning method (Zafiropulos and Fotakis 1998, Zafiropulos 2002). First, it has been proposed that laser clearing should be performed under normal ambient conditions (Zafiropulos and Fotakis 1998) to provide direct access to the object during application. It is determined that the best commercially available laser for cleaning applications in terms of efficiency (ablated volume per photon), speed and safety of the irradiated varnished works of art is KrF excimer laser[1] (Zafiropulos 2002, Madden, *et al*. 2005). KrF excimer laser emits a monochromatic beam at 248 nm (5 eV photon energy), with pulse duration in the nanosecond scale (10 - 30 ns), and has a pulse energy maximum of 2 Joule. At 248 nm, despite some negligible thermal effects, the ablation process is mainly photochemical and therefore removal of aged varnishes is obtained upon laser-induced bond-breakage (Srinivasan and Braren 1989, Luk'yanchuk, *et al*. 1994,

[1] ArF excimer laser (193 nm, 6.4 eV, ns) induces neat photochemical ablation, but has a small pulse energy maximum of 0.8 Joule, which makes laser cleaning extremely lengthy (Zafiropulos and Fotakis 1998). XeCl excimer laser (308 nm, 4 eV, ns) has a pulse energy maximum at 3 Joule, but accounts for strong thermal effects, which causes melting of the ablated surface (Bäuerle 2000, Zafiropulos 2002).

Srinivasan 1994, Bäuerle 2000). In addition, the nanosecond pulse duration allows for spatially and chemically stoichiometric ablation with virtually no damage to the surrounding material, in particular for heat sensitive coatings and multi-component substrates (Bäuerle 2000). Finally, the high pulse energy permits work with an enlarged laser spot, which is essential for the scanning procedure of the proposed laser cleaning method (Zafiropulos and Fotakis 1998, Zafiropulos 2002, Section 3.3.3). Consequently, having an aged varnish and a KrF excimer laser, the only adjustable measure which controls the ablation rate per pulse and the interaction mechanisms is the fluence (Zafiropulos 2002).

The choice of an 'optimum' fluence via common laser ablation rate studies (Zafiropulos and Fotakis 1998, Zafiropulos 2002) allows work in a regime, in which the photochemical interaction between the laser photons and the ablated surface predominate (Srinivasan and Braren 1989, Zafiropulos 2002). Working with lower or higher fluences several risks are posed. Low fluences near the ablation threshold maximise the transmission of laser light through the varnish into the underlying paint film (Zafiropulos 2002), and increase the thermal effects via an Arrhenius type behaviour (Luk'yanchuk, *et al*. 1994, Srinivasan 1994, Bäuerle 2000), causing melting, changes of the optical density of the irradiated varnish and generation of free radicals, which will eventually undergo autoxidative degradation. Higher than 'optimal' fluences, although better than the near threshold fluence, are reported to lead to oxidation of the varnished substrate, as was found in a dammar varnish – linseed oil paint system, using KrF excimer laser and GC/MS analysis (Zafiropulos, *et*

al. 2000b). Very high fluences may cause strong photomechanical effects, which may lead to detachments of the ablated varnish with its substrate (Zafiropulos 2002).

The type of trend of the resulting laser ablation rate per pulse as a function of fluence for varnishes, using KrF excimer lasers, is suggested to be similar to that for polymers (Zafiropulos and Fotakis 1998, Zafiropulos 2002), such as poly(methylmethacrylate) (PMMA), polyimide (PI) and polyurethane (PU) (Srinivasan, *et al*. 1986b, Sutcliffe and Srinivasan 1986, Srinivasan, *et al*. 1987, Küper, *et al*. 1993, Pettit and Sauerbrey 1993, Luk'yanchuk, *et al*. 1994, Srinivasan 1994, Zafiropulos, *et al*. 1995, Luk'yanchuk, *et al*. 1996). However, in the case of aged natural varnishes there are indications for the existence of gradients in the degrees of oxidation and polymerisation as a function of depth. In particular, aged dammar films investigated by means of KrF excimer laser etching and subsequent UV spectrophotometry and FTIR spectroscopy were found to reduce their absorption as a result of depth-wise carbonyl elimination and were found to have a reduced number of crosslinks monitored by ratios of methyl versus methylene groups across the reducing thickness of the laser ablated film (Zafiropulos, *et al*. 2000a). Unidentified aged varnishes processed with a KrF excimer laser were found to have a decreasing depth-dependent polarity, which is also associated with oxidation and absorption (Theodorakopoulos and Zafiropulos 2003). Another example showed that upon ablation at 248 nm, the intensity of carbon dimer emission, monitored with LIBS, reduces as ablation proceeded into deeper layers of an aged film, indicating that less bonds were broken (Section 1.4), which is in line with depth-dependent polymerisation gradients (Chapters 4 and 5, Zafiropulos, *et al*. 2000a). Since the optical properties and the

degree of polymerisation of a film influence ablation (Srinivasan and Braren 1989, Zafiropulos 2002), these gradients are expected to play a crucial role in the laser cleaning of varnished objects.

This chapter deals with the optimisation of an ablation procedure, similarly to the method proposed for the laser cleaning of paintings (Zafiropulos and Fotakis 1998), using a set of thick and thin dammar, mastic and copal oil varnishes, which have been extremely aged to justify the requirement of using a laser (Chapter 2). First, the ablation rate per pulse as a function of fluence is tested with (a) shallow and (b) randomly chosen etching depths in the thick films and the results are compared with ablation rate studies of the thin films. LIBS was employed to monitor the ablation plume emission per pulse, analysed as a function of the depth profiles of the films. Finally the ablation step at different depth-steps of the three case studies was examined.

3.2 Experimental Methods

Both laser ablation rate studies and laser cleaning have been carried out on the prototype experimental system for laser cleaning applications of paintings, configured at IESL/FORTH (Gobernado-Mitre, *et al*. 1997, Maravelaki, *et al*. 1997, Zergioti, *et al*. 1997). A simplified schematic representation of the system is shown in Figure 3.2.1.

Photoablation was carried out with a Lamda Physic®, COMPex series, KrF excimer laser (248 nm, 25 ns) at a constant energy mode of the order of 380 mJ and repetition rate as short as 5 Hz to avoid cumulative heating effects on the films. Upon emission

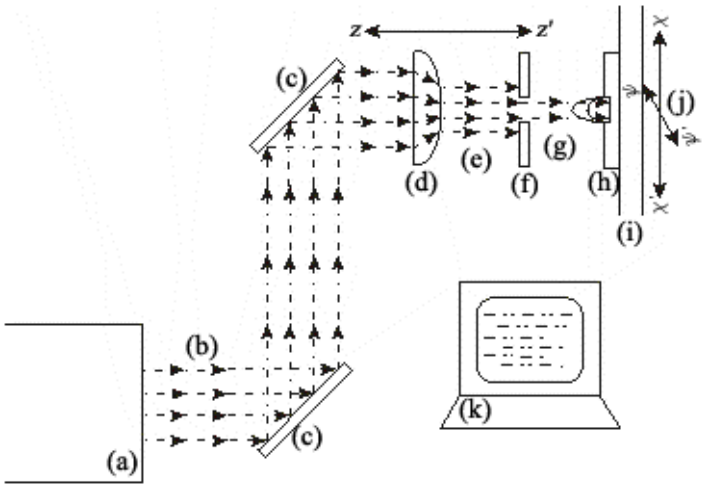

Figure 3.2.1 Schematic representation of the prototype experimental setup employed for laser ablation rate studies and the final laser cleaning. Components: (a) KrF excimer laser source; (b) 248 nm laser beam; (c) mirrors; (d) cylindrical plano-convex lens, f= +300 mm; (e) focused beam; (f) slit opening at the yy' direction only; (g) modified and shaped laser beam; (h) ablated sample; (i) quartz substrate; (j) x-y-z mechanical translator; (k) computational control over triggering and the translator movement.

from the output of the device and reflection by two UV mirrors (Melles Griot®), the 248 nm beam was directed parallel and above an optical bench on which a cylindrical plano-convex quartz lens of focal length f = +300 mm (Melles Griot®, high-grade quartz) and a slit were adjusted to face the beam normally. The beam was directed to propagate vertically and through the centre of the lens via manual alignment of all optics prior to application. In addition, the axes of the cylindrical lens and the opening of the slit were parallel to the direction of the top-hat profile of the laser beam. Consequently, the laser irradiation beyond the slit was both focused and homogenously shaped, for distances up to the focal point of the lens. The effective power of the laser pulses was measured after the modified beam propagated through the slit, with a 10.1 mV/mJ pyroelectric energy meter connected to a digital oscilloscope (LeCroy® 9400 Dual, 125MHz). Calibration of the output pulse energy and the effective pulse energy incident on the sample was occasionally required and

conducted using the energy meter. The accuracy of the energy measurements was dependent upon the error estimation of the energy meter that was ≤ 10%.

Upon the irradiance of a single laser pulse, fluence (J/cm^2) was measured initially from the dimensions of the rectangular spots marked on PVC sheets that were placed at the exact position of the samples (Figure 3.2.2). Maintaining the laser energy and the slit opening constant throughout the experiments, fluence was only dependent upon the lens-sample distance, d. By increasing the lens-sample distance, focusing became more intense, increasing so the laser fluence. A variety of fluences were determined on the PVC sheets for d ranging between 17 and 28 cm.

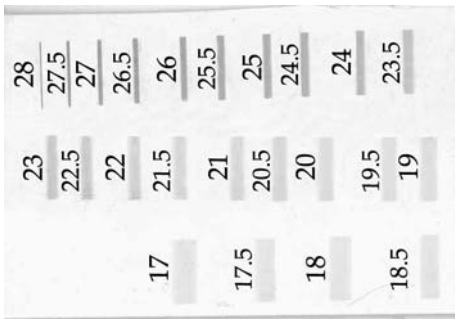

Figure 3.2.2 PVC sheet with a series of spots marked with KrF excimer laser pulses for a range of distances marked on the left of each spot (in cm). The waist of the spots varied between 0.17 and 3.5 mm corresponding to fluences of 3 to 0.15 J/cm^2 in that order.

The samples were placed to face the laser pulses vertically on their surface. For each fluence tested, a certain number of pulses were fired on the same spot of the films under investigation. A mechanical stylus profilometer, Perthometer® S5P, was employed to measure both the longitudinal and transverse dimensions of the etched spots. The measured beam waist was plotted against the distance from the lens and their relation was determined to be almost linear, away from the focal point, verifying the initial measurements on the PVC sheet, as shown in Figure 3.2.3. The corresponding fluences, calculated from the fitted beam waist values, were increasing

when approaching the focal point of the lens (Figure 3.2.4). By these means, the measurements on the PVC and subsequently the values of laser fluence were corrected. Experimentally, the fluence was controlled via adjustment of the sample-lens distance according to Figure 3.2.4.

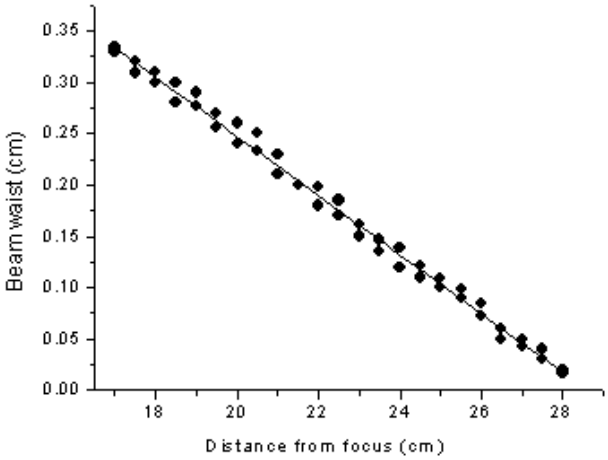

Figure 3.2.3 The KrF excimer laser beam waist, as measured from the transverse dimension of the etched spots, against the distance from the focal point of the lens.

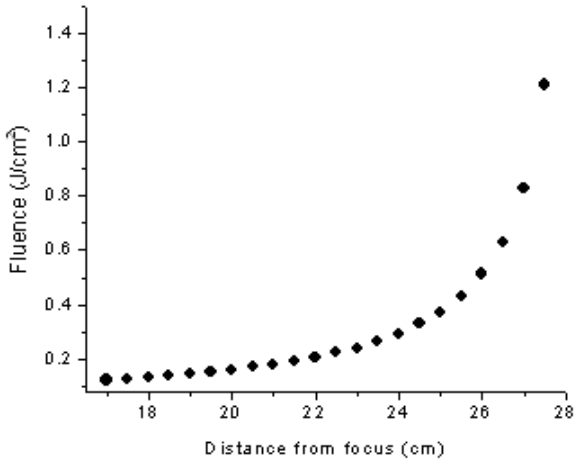

Figure 3.2.4 The laser fluence, calculated by the fitted values of the beam waist, against the distance from the focal point of the lens. The estimated error is ≤ 10%, depending upon the energy measurements

Figure 3.2.5 shows the plan and the three-dimensional profile of the Gaussian front of a KrF excimer laser pulse at the output before passing through the optics. The bottom of each etched spot acquired the Gaussian front at the transverse (xx') direction. Therefore, determination of the mean depth of the spots was essential in order to

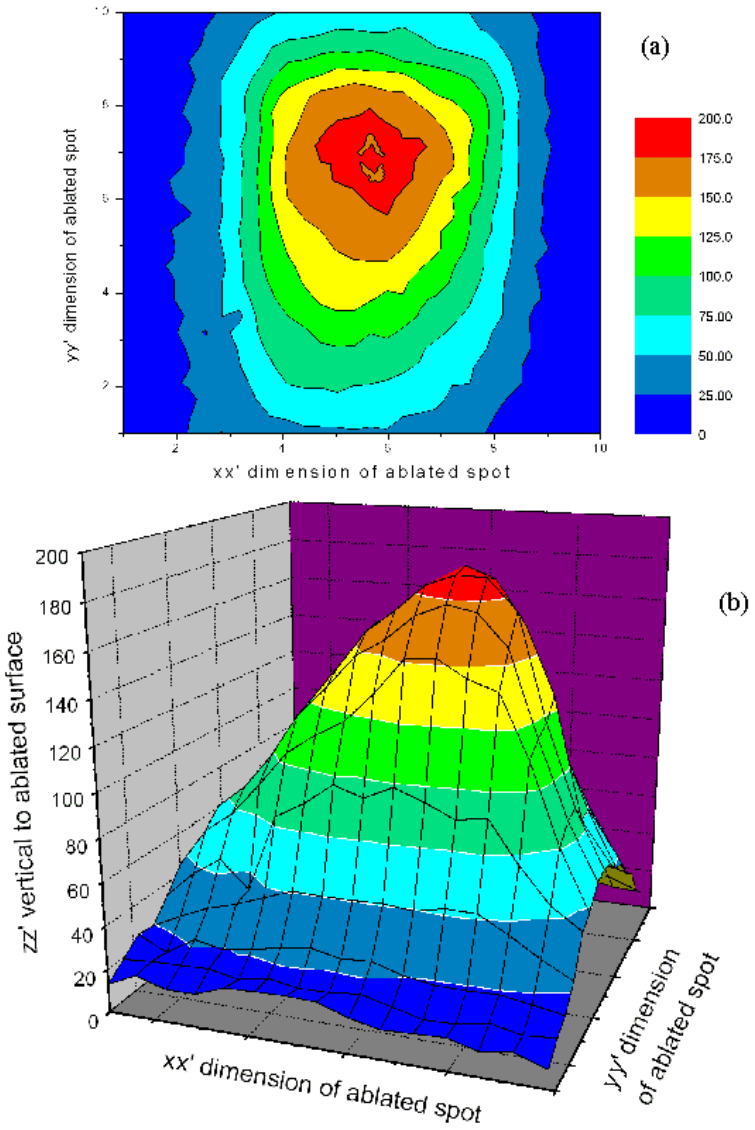

Figure 3.2.5 The plan (a) and the 3-d profile (b) of the KrF excimer laser as captured on the output of the laser source. After passing through the cylindrical lens and the slit the beam had a top-hat profile along the yy' axis.

obtain representative values for the ablation yield. Three profile measurements were carried out on each etched spot and the profile areas were integrated. The resulting area values of each profile were then divided by the width of the spot in order to calculate the mean etched depth. This procedure was repeated three times for each spot so that the final error is the standard deviation of these three values. The measured depths were divided by the number of pulses fired for each fluence tested.

By these means the mean laser ablation rate versus fluence for each artificially aged varnish film was determined separately. Measurements of the energy fluence and the ablation rate enabled the calculation of the exact ablated volume per incident photon. This elaborate process is rather common and is essential in order to define the best possible parameters for controlled photoablation of the tested organic coatings (Zafiropulos 2002).

3.3 Results

3.3.1 Laser ablation rate studies: Introduction

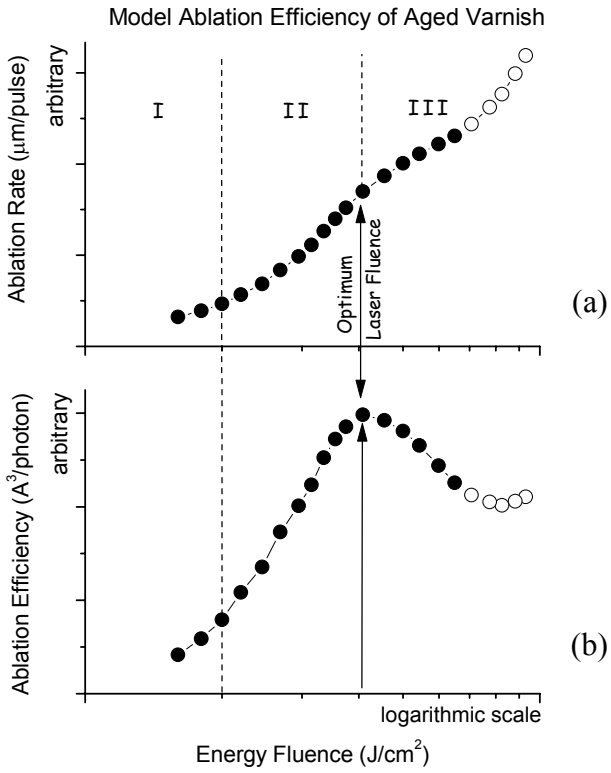

Figure 3.3.1 Model laser ablation rate (a) and efficiency (b) dependence versus laser fluence.

Figure 3.3.1 introduces a model of mean ablation rate (a) and the corresponding efficiency (b) against fluence. The delineated trends are similar to those yielded from typical laser ablation rate studies of aged triterpenoid resin films (Zafiropulos and

Fotakis 1998, Zafiropulos 2002) carried out with KrF excimer lasers. The selectivity provided by the KrF excimer laser is evident from the ~ 0.1 μm/pulse ablation rate of aged resins obtained with the lowest fluence (Zafiropulos 2002). Even at the highest fluences, the ablation rate hardly exceeds a maximum of ~ 1 μm/pulse, although, commonly, 'optimal' fluences yield ablation rates shorter than 1 μm/pulse. Such minor etching capacities, which are typical of excimer laser ablation, are not feasible by any other application related to varnish removal from paintings.

The 'lazy S' shape of the ablation rate curve, up to a certain fluence (sections I, II and III), that is observed in the case of aged resins, has been determined for the laser ablation of polymers (Srinivasan and Braren 1989). Commonly, the horizontal axis of the graph is set in a logarithmic scale in order to demonstrate the linear response of the 'variable' ablation rates versus the logarithm of the examined fluence values, especially at a relatively low fluence range (section II). As observed experimentally, the exact function of the laser ablation rate against the fluence is case-specific upon the film's composition and mainly upon different types and degrees of degradation. Consequently, the graph in Figure 3.3.1 represents only the ablation rate versus fluence of a typical varnish for a certain degree of ageing.

At the lowest fluence range (section I), the ablated material is influenced by thermal dissipation of excited species that remain in the material, owing to incubation effects (Sutcliffe and Srinivasan 1986, Küper and Stuke 1988, Meyer, *et al*. 1988, Chuang and Tam 1989, Bäuerle 2000). According to Srinivasan and Braren (1989) the molecular weight of the laser desorbed photofragments may span between 200 and 10,000 Daltons. The authors reported that, after expulsion into the air, part of the

highest molecular weight fraction precipitates on the sides of the etched surface. The closer the utilised fluence is to the ablation threshold, the more significant this phenomenon becomes, because of the profoundly higher temperatures that are generated in this regime (Bäuerle 2000). Essentially, because of the increased photothermal effects within the low fluence regime the mean etching depth per pulse is effectively less than the corresponding etched depth obtained with neat photochemical ablation. Therefore, the ablation rate yield within this regime does not respond linearly to the logarithm of fluence, but contributes to an asymptotic approach of the curve with the horizontal axis of the plot. This response starts at fluences below the ablation threshold, where the process is exclusively thermal and characterised by an Arrhenius-type behaviour (Luk'yanchuk, *et al*. 1994). Thus, the ablation rate curve obtained with low fluences just above the ablation threshold is commonly referred to as the Arrhenius tail (Bäuerle 2000). Due to the asymptotic approach of the curve with the horizontal axis, the exact threshold fluence cannot be accurately defined (Srinivasan 1994). Nevertheless, determination of threshold fluences is far beyond the scope of laser cleaning of aged and polymerised coatings applied on painted surfaces. Even the fluences just above the ablation threshold are unsuitable for 'safe' photoablation, because of the non-desorbed free radicals generated within the excited surface, resulting in incubation (Bäuerle 2000). In that case, laser irradiation may initiate free radical chain reactions within the films, which leads to autoxidation and crosslinking, thereby inducing further the deterioration of the already degraded films via established degradation processes (Al-Malaika 1993, Scott 1993). Consequently, low fluences should be never used for the ablation of varnishes (Zafiropulos 2002). The response of the ablation rate versus fluence in the second part of the curve

(section II) is discussed in the next paragraph. In the high fluence regime (section III), the density of the desorbed photofragments increases, resulting in screening effects (Brannon, *et al*. 1985, Keyes, *et al*. 1985, Srinivasan, *et al*. 1986a, Sutcliffe and Srinivasan 1986, Küper and Stuke 1988, Mahan, *et al*. 1988, Sauerbrey and Pettit 1989, Futzikov 1990, Cain, *et al*. 1992, Soberhart 1993, Georgiou, *et al*. 1998). In this regime, the high concentration of ablation products absorb, reflect and scatter the laser beam before termination of the pulse preventing the laser energy reaching the ablated surface.

Figure 3.3.1 (b) demonstrates the corresponding efficiency of the same fluence range, that is the desorbed volume per photon given in $Å^3$/photon units. Such curves are commonly employed for the determination of 'optimal' fluences for the laser cleaning of aged varnishes (Zafiropulos and Fotakis 1998, Zafiropulos 2002, Theodorakopoulos, *et al*. 2005). 'Optimum' fluences correspond to the highest ablation rate within section II and maximise the efficiency across the whole range of fluences tested, as shown in Figure 3.3.1 (b). Consequently, the 'optimum' fluence offers the advantage of selective varnish removal at an ablation rate, which is less than 1 μm/pulse (usually 0.3 to 0.6 μm/pulse) (Zafiropulos and Fotakis 1998). Applications with optimal fluences also minimise the potential of laser-induced oxidation of the underlying paint media (Zafiropulos, *et al*. 2000b). Efficiency, in the high fluence regime (section III) may undergo a second increase as shown in Figure 3.3.1 (b) with the white data points. This phenomenon has been attributed to 'vaporisation' and suggests that in this range photomechanical effects such as thermoelastic stresses and shock wave formation take place (Zafiropulos 2002). These effects may cause

delaminations on the ablated surface that lead to flake ejection or detachments to the underlying layers (Tornari, *et al.* 2003). The long-term effects of high fluence excimer ablation on the structural layers of paintings are still under investigation (Tornari, *et al*. 1998).

3.3.2 Influence of depth on the laser ablation rate

A full laser ablation rate study was carried out for the three artificially aged films tested, i.e. dammar, mastic and copal oil varnish. The laser energy that finally reached the substrate was first measured behind the slit. The slit was adjusted to an ~1 cm opening centred to the incident 248 nm laser radiation. While keeping the longitudinal (yy') dimensions of the spots constant to ~1 cm, the Gaussian beam waist, i.e. the transverse (xx') dimension, varied depending on the distance from the lens, thereby changing the spot size and thus the energy fluence. Initially a random number of pulses were fired for a first series of spots and the ablated depths of the etchings were found to vary with the fluence and the number of pulses fired per spot. Some of the spots were shallow in the surface layers and others were deep into the bulk of the films. Once the mean ablation rates were determined, the exact number of pulses were established (Figure 3.3.2.1) for the ablation of a second series of spots only at the surface layers of the films. This enabled an investigation of the response of KrF excimer ablation over the depth profile of the aged films. In the case of the triterpenoid resin films, the results were verified with ablation rate studies on thinner films of the same substances aged with the same parameters.

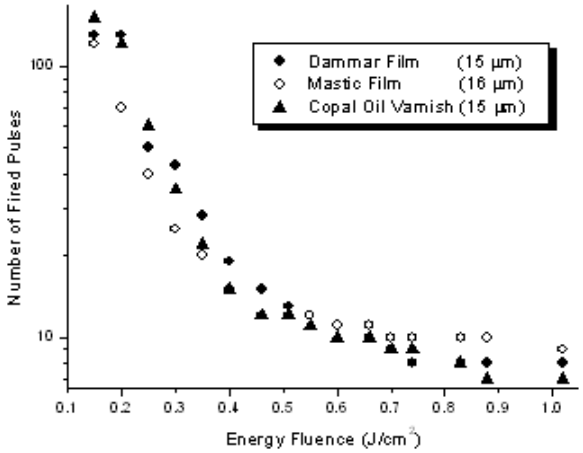

Figure 3.3.2.1 The number of pulses fired onto the surfaces of the investigated films to produce etchings of the same depth versus the range of fluence employed for the laser ablation rate studies, using a KrF excimer laser (248 nm, 25 ns)

3.3.2.1 Dammar

The thick film of dammar was about 56 microns. The data obtained with a wide range of fluences and a random number of pulses for each spot are demonstrated in Table 3.3.2.1. The corresponding ablation rate study graph is presented in Figure 3.3.2.2, (white symbols). The etched spots spanned between 15 and 43 microns, as a result of different number of pulses fired for each energy fluence tested. The ablation rate curve shows an obvious step between fluences 0.55 and 0.7 J/cm^2, which causes the ablation rate to jump from 0.4 to 1 μm/pulse. The data in the study show that the etching obtained with 0.7 J/cm^2 was ~ 17 μm deeper than that with 0.55 J/cm^2 and therefore the step in the ablation rate curve reflects the increase of the etching depth.

This provides initial evidence that ablation is affected by chemical changes across the depth profile of the dammar film for this study. The mean efficiency curve was separated in two 'groups'. The first 'group' belongs to laser fluence values up to 0.6 J/cm^2, corresponding to ablation efficiency spanning from 27 Å^3 to 69 Å^3 per photon and the second to higher values of fluence that generated ablation efficiency between

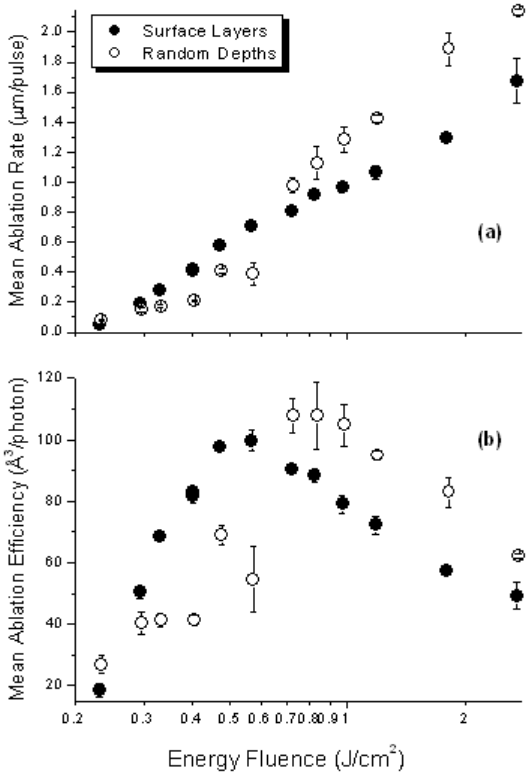

Figure 3.3.2.2 The double mean laser ablation rate plot (a) and the corresponding mean ablation efficiency (b) of artificially aged dammar with spots etched in random depths (white symbols) and surface layers (black symbols), using a KrF excimer laser.

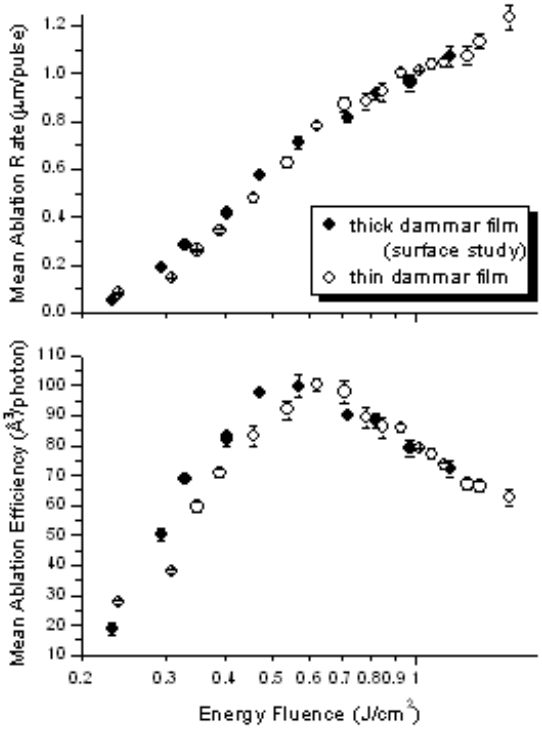

Figure 3.3.2.3 Laser ablation rate study of a 15 μm thick dammar film plotted with data of the surface study of the 56 μm thick dammar film, with KrF excimer laser.

108 Å^3 and 62 Å^3 per photon. The resulted curve in Figure 3.3.2.2 (b) points to an 'optimum' fluence of 0.7 J/cm^2, that maximized the ablation efficiency at 108 Å^3 per photon corresponding to an ablation rate of 1 μm/pulse. However, the plots deviate from the standard laser ablation rate and efficiency trends that were determined for aged dammar films in recent investigations (Zafiropulos and Fotakis 1998, Zafiropulos 2002). In contrast to the referred studies, a fluence of 0.7 J/cm^2 is far too high for controlled KrF excimer laser ablation of aged dammar films. In addition, the fluctuations of the ablation rate and efficiency curves indicate an impaired interaction between the laser and the resin film. In view of these considerations, a second ablation

rate study on the very-top surface layers of the same dammar film with etching spots not deeper than ~ 10 μm from surface. The data of this second study are presented in Table 3.3.2.2 and Figure 3.3.2.2 (black symbols).

The difference between the two studies is obvious. Both ablation rate and efficiency trends were higher in the surface study for the fluence range 0.3 to 0.6 J/cm^2, and decreased for the set of higher fluences (> 0.6 J/cm^2). In this case, both the ablation rate and the efficiency curves for the uppermost surface layers retained a trend similar to the corresponding trends of polymers and resins tested on the basis of KrF excimer laser ablation in previous studies (Srinivasan and Braren 1989, Zafiropulos, *et al*. 1995, Zafiropulos and Fotakis 1998, Zafiropulos 2002, Theodorakopoulos, *et al*. 2005). In the surface ablation rate study, the lowest fluence at 0.23 J/cm^2 yielded a 0.05 μm/pulse, which was half the ablation rate obtained in the study with the deeper etching spots. The 'optimum' fluence was shifted to 0.55 J/cm^2 yielding an ablation rate of 0.7 μm/pulse that maximised the efficiency with a 100 Å^3 per photon yield. Figure 3.3.2.3 shows that the results compare well with the laser ablation rate study carried out on a much thinner dammar film of the order of 15 μm that was aged with the same conditions as the 56 μm thick dammar film. The 'optimum' fluence in this case was somewhat increased to 0.57 J/cm^2 (Table 3.3.2.3). The observed 20 mJ/cm^2 shift of the lower fluences up to the 'optimum' fluence was within the 10% experimental error given for the pyroelectric power meter employed for the energy measurements.

Table 3.3.2.1: Random Depth – Laser Ablation Rate Study for Dammar (Total Thickness: 56μm)

Fluence (J/cm^2)	Fired pulses	Depth of etched spot (μm)	Mean ablation rate (μm/pulse)	Ablation efficiency ($Å^3$/photon)
1.82	20	38 ± 2.2	1.88 ± 0.11	83 ± 4.8
1.19	25	35 ± 0.6	1.42 ± 0.02	95 ± 1.6
0.98	25	32 ± 2.13	1.29 ± 0.08	105 ± 6.9
0.83	30	34 ± 3.3	1.12 ± 0.11	107.5 ± 10.9
0.72	40	39 ± 1.9	0.98 ± 0.05	108 ± 5.5
0.55	60	23.5 ± 4.4	0.39 ± 0.08	55 ± 10.6
0.48	70	29 ± 1.2	0.41 ± 0.02	69 ± 3.1
0.41	150	32 ± 1.3	0.21 ± 0.01	41 ± 1.8
0.33	150	26 ± 1.4	0.17 ± 0.01	41.5 ± 2.4
0.29	100	15 ± 1.25	0.15 ± 0.01	40 ± 3.7
0.23	200	16 ± 1.44	0.08 ± 0.01	27 ± 2.9

Table 3.3.2.2: Surface Layer – Laser Ablation Rate Study for Dammar (Deepest etching spot 12μm approximately)

Fluence (J/cm^2)	Fired pulses	Depth of etched spot (μm)	Mean ablation rate (μm/pulse)	Ablation efficiency ($Å^3$/photon)
1.79	3	3.9 ± 0.04	1.29 ± 0.01	57 ± 0.57
1.18	4	4.3 ± 0.26	1.07 ± 0.04	72 ± 2.97
0.97	4	3.8 ± 0.14	0.95 ± 0.03	79 ± 2.81
0.83	5	4.6 ± 0.11	0.91 ± 0.02	88 ± 2.19
0.72	6	4.9 ± 0.06	0.81 ± 0.01	90 ± 1.11
0.55	15	10.7 ± 0.4	0.71 ± 0.03	100 ± 3.65
0.47	14	8.1 ± 0.08	0.57 ± 0.01	97 ± 0.93
0.40	28	11.7 ± 0.05	0.42 ± 0.01	83 ± 0.39
0.34	34	9.6 ± 0.1	0.28 ± 0.01	69 ± 0.74
0.29	40	7.4 ± 0.28	0.18 ± 0.01	50 ± 1.92
0.23	76	4.1 ± 0.44	0.05 ± 0.01	18 ± 2

Table 3.3.2.3: Laser Ablation Rate Study for a 15 μm Dammar film

Fluence (J/cm^2)	Fired pulses	Depth of etched spot (μm)	Mean ablation rate (μm/pulse)	Ablation efficiency ($Å^3$/photon)
1.57	8	9.9 ± 0.4	1.23 ± 0.05	62.6 ± 2.5
1.36	8	9.1 ± 0.26	1.13 ± 0.03	66.4 ± 1.9
1.28	8	8.7 ± 0.31	1.07± 0.04	67 ± 1.6
1.14	8	8.4 ± 0.13	1.05± 0.02	73.4 ± 1.1
1.08	9	9.3 ± 0.2	1.04± 0.02	77 ± 1.6
1.02	10	10.1 ± 0.02	1.01± 0.00	78.8 ± 0.2
0.93	11	11 ± 0.18	1.00± 0.02	85.8 ± 1.4
0.85	12	11 ± 0.44	0.92± 0.04	86.2 ± 3.5
0.79	13	11.5 ± 0.46	0.88± 0.04	89.3 ± 3.6
0.71	15	13 ± 0.49	0.87± 0.03	97.8 ± 3.6
0.57	19	14.9 ± 0.29	0.78± 0.02	100 ± 2
0.54	22	13.8 ± 0.46	0.63± 0.02	91.9 ± 3.1
0.46	25	12 ± 0.47	0.48± 0.02	83.1 ± 3.3
0.39	30	10.3 ± 0.16	0.34± 0.01	70.9 ± 1.1
0.35	45	11.7 ± 0.32	0.26± 0.00	59.4 ± 1.6
0.31	90	13 ± 0.24	0.14± 0.00	37.8 ± 0.7
0.24	130	10.5 ± 0.31	0.08± 0.00	27.5 ± 0.8

3.3.2.2 Mastic

The thick film of mastic was about 53 microns. The depths of the first set of spots for the ablation rate study were randomly distributed between 24 to 50 microns, depending on the number of pulses fired. The results of this study are presented in Table 3.3.2.4 and in Figure 3.3.2.4 (white symbols). The lowest energy fluence tested was 0.23 J/cm^2 yielding 0.1 μm/pulse. This point is near the ablation threshold and belongs to the Arrhenius tail of the ablation rate curve (Bäuerle 2000). Similarly to the case of dammar, there was a step jump between fluences 0.6 and 0.7 J/cm^2 corresponding to a 15 μm depth difference between the etchings. It is also observed

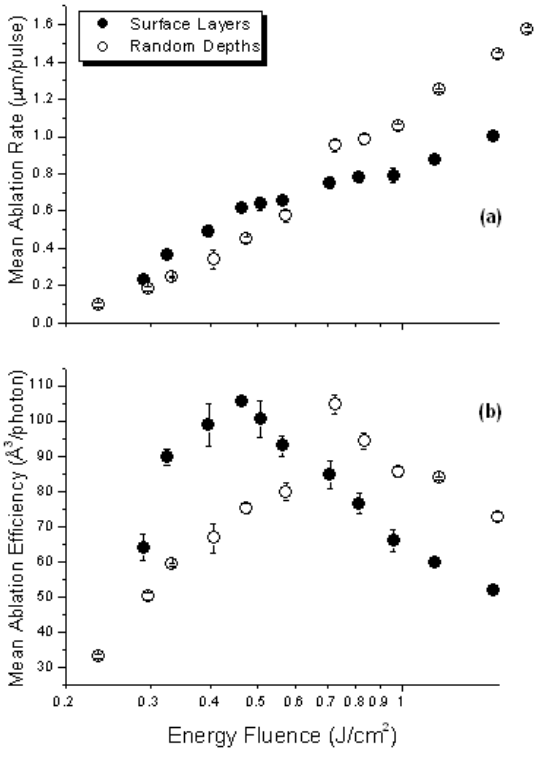

Figure 3.3.2.4 The double mean laser ablation rate (a) and ablation efficiency study (b) of artificially aged mastic in random depths (white symbols) and surface layers (black symbols); KrF excimer laser, 25 ns.

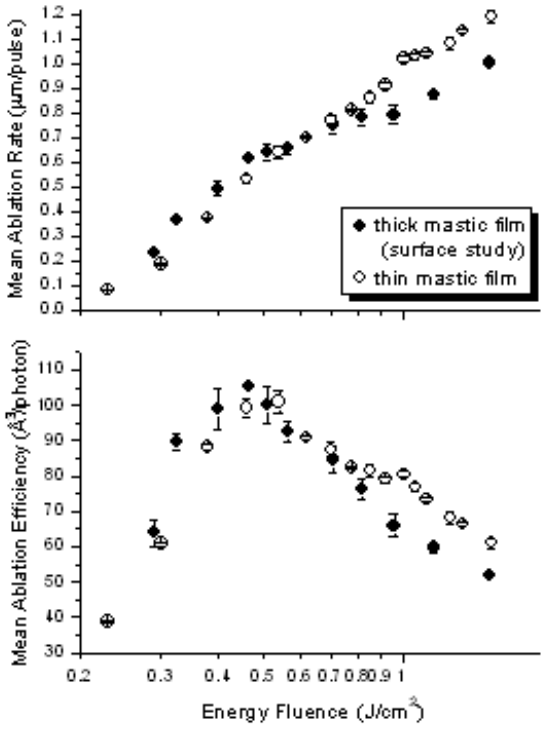

Figure 3.3.2.5 Laser ablation rate study of the 15 μm thick mastic film in comparison with data of the surface study of the 53 μm thick mastic film, with KrF excimer laser.

that as the fluence increases, the ablation rates increase up to unusually high values. Moreover, the maximum efficiency is observed at unexpectedly high fluence values for aged mastic (Zafiropulos 2002).

The laser ablation rate study at the surface of the same mastic film is demonstrated in Figure 3.3.2.4 (black symbols) and Table 3.3.2.5. The depths of the spots etched for this particular study were not deeper than 9 μm from the surface. The difference between the two studies, in both ablation rate and efficiency trends, is evident. In the surface study the ablation rate slope increases sharply with increasing fluences up to 0.45 J/cm^2.

After this point the linear dependence on the logarithm of fluence is terminated. This is a first indication that 0.45 J/cm^2 corresponds to the 'optimum' fluence, which was confirmed in the ablation efficiency graph. This fluence produces the maximum ablation efficiency and is consistent with findings of previous ablation rate studies on artificially aged mastic (Zafiropulos 2002). Fluences higher that 1 J/cm^2, however, do not increase linearly the ablation rate, suggesting mainly screening effects (Brannon, *et al*. 1985, Keyes, *et al*. 1985, Srinivasan, *et al*. 1986a, Sutcliffe and Srinivasan 1986, Küper and Stuke 1988, Mahan, *et al*. 1988, Sauerbrey and Pettit 1989, Futzikov 1990, Cain, *et al*. 1992, Soberhart 1993, Georgiou, *et al*. 1998).

The laser ablation rate study of a 16.5 thick mastic film, which was aged identically as the thicker film, is demonstrated in Figure 3.3.2.5 and Table 3.3.2.6. The optimum fluence was shifted by almost 50 mJ/cm^2 that is about 10% higher than the previous study. Compared to the ablation rates on the surface of the thick film, some increase

in the ablation rates obtained in the high fluence regime (> 0.8 J/cm^2) is observed. However this is still within the limits of the experimental error.

Table 3.3.2.4: Random Depth – Laser Ablation Rate Study for Mastic (Total Thickness: 53μm)

Fluence (J/cm^2)	Fired pulses	Depth of etched spot (μm)	Mean ablation rate (μm/pulse)	Ablation efficiency (Å^3/photon)
1.82	30	47.29 ± 0.35	1.58 ± 0.01	69 ± 1
1.58	35	50.31 ± 0.6	1.44 ± 0.02	72.5 ± 1.4
1.19	40	50 ± 0.4	1.25 ± 0.01	84 ± 0.3
0.98	40	42.08 ± 0.7	1.05 ± 0.02	86 ± 1.4
0.83	40	39.33 ± 1.15	0.98 ± 0.03	94 ± 2.3
0.72	43	40.83 ± 1.4	0.95 ± 0.03	105 ± 2.7
0.57	45	25.83 ± 1.4	0.57 ± 0.03	80 ± 2.6
0.48	54	24.17 ± 0.9	0.45 ± 0.02	75 ± 1.4
0.41	72	24.37 ± 3.8	0.34 ± 0.05	67 ± 4.2
0.33	120	29.58 ± 0.7	0.25 ± 0.01	59 ± 0.5
0.29	150	27.92 ± 1.8	0.19 ± 0.01	50 ± 1
0.23	300	28.96 ± 2.5	0.09 ± 0.01	33 ± 0.7

Table 3.3.2.5: Surface Layer – Laser Ablation Rate Study for Mastic (Deepest etching spot 9μm approximately)

Fluence (J/cm^2)	Fired pulses	Depth of etched spot (μm)	Mean ablation rate (μm/pulse)	Ablation efficiency (Å^3/photon)
1.55	4	4 ± 0.05	1.00 ± 0.01	51.7 ± 0.59
1.17	5	4.4 ± 0.09	0.87 ± 0.02	59.8 ± 1.28
0.96	6	4.7 ± 0.23	0.79 ± 0.04	65.9 ± 3.2
0.81	6	4.7 ± 0.18	0.78 ± 0.03	76.5 ± 3.01
0.71	6	4.5 ± 0.21	0.75 ± 0.03	84.8 ± 3.95
0.56	10	6.3 ± 0.2	0.65 ± 0.02	92.7 ± 2.83
0.51	9	5.9 ± 0.3	0.64 ± 0.03	100.4 ± 5.28
0.45	10	6.2 ± 0.04	0.61 ± 0.01	105.4 ± 0.69
0.40	18	8.8 ± 0.54	0.49 ± 0.03	98.9 ± 6.02
0.32	23	8.4 ± 0.21	0.36 ± 0.01	89.6 ± 2.26
0.29	32	7.5 ± 0.43	0.23 ± 0.01	63.9 ± 3.69

Table 3.3.2.6: Laser Ablation Rate Study for a 15 μm thick Mastic film

Fluence (J/cm^2)	Fired pulses	Depth of etched spot (μm)	Mean ablation rate (μm/pulse)	Ablation efficiency (Å^3/photon)
1.56	9	10.7 ± 0.24	1.19 ± 0.03	61.1 ± 1.4
1.35	10	11.3 ± 0.1	1.13 ± 0.01	66.6 ± 0.6
1.27	10	10.8 ± 0.24	1.08 ± 0.02	68.3 ± 2
1.13	10	10.4 ± 0.11	1.04 ± 0.01	73.4 ± 0.8
1.07	10	10.3 ± 0.13	1.03 ± 0.01	76.9 ± 0.9
1.01	11	11.3 ± 0.14	1.02 ± 0.01	80.6 ± 1
0.92	11	10.1 ± 0.12	0.91 ± 0.01	79.2 ± 0.9
0.85	12	10.4 ± 0.22	0.86 ± 0.02	81.4 ± 1.8
0.78	12	9.7 ± 0.06	0.81 ± 0.0	82.4 ± 0.5
0.70	12	9.2 ± 0.21	0.77 ± 0.02	87.5 ± 2
0.62	15	10.5 ± 0.06	0.70 ± 0.00	90.7 ± 0.5
0.54	20	12.8 ± 0.44	0.64 ± 0.02	95.0 ± 3.3
0.46	25	13.3 ± 0.35	0.53 ± 0.01	93.3 ± 2.4
0.38	40	14.6 ± 0.15	0.37 ± 0.00	76.2 ± 0.8
0.30	70	13.0 ± 0.15	0.19 ± 0.00	48.8 ± 0.6
0.23	120	9.4 ± 0.16	0.08 ± 0.00	26.8 ± 0.5

3.3.2.3 Copal Oil Varnish

The thickness of the copal oil varnish film was of the order of 30 μm. As in the case of the triterpenoid resin films, a wide range of fluences was tested and the etchings were obtained at random depths between 14 and 25 μm from surface. The results are presented in Table 3.3.2.7 and Figure 3.3.2.6 (white symbols). In contrast to the ablation rate studies on the triterpenoid films, the ablation rate and efficiency curves did not seem to be influenced by the depth of the film, in line with corresponding slopes described for PMMA, PI and PU films (Srinivasan, *et al*. 1986b, Sutcliffe and Srinivasan 1986, Srinivasan, *et al*. 1987, Srinivasan and Braren 1989, Küper, *et al*. 1993, Pettit and Sauerbrey 1993, Luk'yanchuk, *et al*. 1994, Srinivasan 1994, Zafiropulos, *et al*. 1995, Luk'yanchuk, *et al*. 1996). It is demonstrated that a fluence of

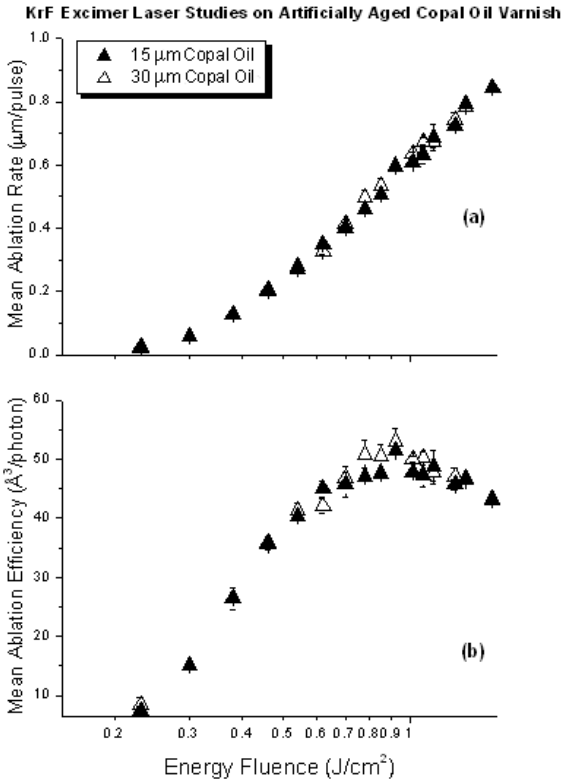

Figure 3.3.2.6 Laser ablation rate (a) and efficiency (b) at 248 nm against fluence for artificially aged copal oil varnish films.

0.9 J/cm^2, which corresponds to a mean laser ablation rate of 0.6 μm/pulse, yields the maximum efficiency at 53 Å^3 per photon.

Table 3.3.2.7: Random Depth – Laser Ablation Rate Study for Copal Oil Varnish (Total Thickness: 30 μm)

Fluence (J/cm^2)	Fired pulses	Depth of etched spot (μm)	Mean ablation rate (μm/pulse)	Ablation efficiency (Å^3/photon)
1.55	16	14 ± 0.18	0.84 ± 0.005	43 ± 0.55
1.35	25	20 ± 0.12	0.78 ± 0.02	46 ± 0.28
1.28	18	13.5 ± 0.41	0.74 ± 0.01	47 ± 1.43
1.15	30	20.5 ± 0.37	0.68 ± 0.02	48 ± 0.87
1.08	20	13.4 ± 0.31	0.67 ± 0.01	50 ± 1.16
1.01	24	15.5 ± 0.16	0.63 ± 0.02	49.9 ± 0.52
0.91	24	15 ± 0.61	0.59 ± 0.02	53 ± 2.16
0.85	26	14 ± 0.6	0.53 ± 0.02	50 ± 2.14
0.78	44	22 ± 0.62	0.49 ± 0.01	51 ± 1.44
0.71	35	14 ± 0.45	0.41 ± 0.01	47 ± 1.51
0.62	43	13 ± 0.38	0.33 ± 0.01	42 ± 1.23
0.55	50	14 ± 0.44	0.27 ± 0.01	41 ± 1.29
0.45	110	22 ± 0.37	0.20 ± 0.003	35 ± 0.59
0.38	150	19 ± 1.33	0.13 ± 0.01	26 ± 1.82
0.31	300	17 ± 0.89	0.06 ± 0.003	15 ± 0.79
0.23	1000	25 ± 2.39	0.02 ± 0.003	8 ± 0.76

Table 3.3.2.8: Laser Ablation Rate Study for a 15 μm thick Copal oil film

Fluence (J/cm^2)	Fired pulses	Depth of etched spot (μm)	Mean ablation rate (μm/pulse)	Ablation efficiency (Å^3/photon)
1.55	7	6 ± 0.03	0.84 ± 0.005	43 ± 0.22
1.35	7	5.5 ± 0.03	0.79 ± 0.004	47 ± 0.26
1.27	8	6 ± 0.07	0.72 ± 0.01	46 ± 0.54
1.14	9	6 ± 0.36	0.69 ± 0.04	49 ± 2.94
1.07	9	6 ± 0.26	0.63 ± 0.03	47 ± 2.04
1.01	10	6 ± 0.04	0.61 ± 0.004	47 ± 0.31
0.92	10	6 ± 0.42	0.59 ± 0.04	51 ± 3.57
0.85	11	5.5 ± 0.06	0.50 ± 0.01	48 ± 0.52
0.78	12	5.5 ± 0.04	0.46 ± 0.004	47 ± 0.34
0.70	12	5 ± 0.22	0.40 ± 0.02	46 ± 2.02
0.62	15	5 ± 0.15	0.35 ± 0.01	45 ± 1.35
0.55	22	6 ± 0.02	0.27 ± 0.001	40 ± 0.13
0.45	35	7 ± 0.2	0.20 ± 0.01	36 ± 1.03
0.38	60	7.5 ± 0.25	0.13 ± 0.004	26 ± 0.87
0.30	120	7 ± 0.37	0.06 ± 0.003	15 ± 0.79
0.23	150	3 ± 0.26	0.02 ± 0.002	7.5 ± 0.65

Because of these trends of both ablation rate and efficiency, a second ablation rate study was not carried out on the surface of this particular film, but on a 15 μm copal oil varnish film aged under the same conditions as the previous film (Chapter 2). The spots generated for the latter study spanned between 3 and 10 μm, as demonstrated in

Table 3.5.2.8. The trends of the mean ablation rate and efficiency curves, shown in Figure 3.3.2.6, demonstrate that there is virtually no change in the interaction of the particular varnish with the KrF excimer laser across the whole range of fluences tested, regardless of the depth of the etched spots or the thickness of the film. The differences between the two curves are minor and insignificant and are well within the experimental error. Both studies demonstrated that the 'optimum' fluence for KrF excimer laser cleaning is 0.9 J/cm^2, yielding a mean laser ablation rate of 0.6 μm/pulse and mean efficiency of the order of 50 Å^3/photon.

3.3.3 Ablation rate in the bulk of the triterpenoid resin films

The changes determined in the ablation rate studies of natural resin varnishes signify the change in the interaction of the 248 nm pulses with the films as ablation propagates into the bulk. As shown below, in Section 3.3.5, the ablation of the films maintained constant at the uppermost 15 μm and beyond this depth the interaction was altered compared with the copal oil varnish, whose ablation was stable down to 30 μm from surface. Having studied the mean ablation rates with spots whose depths spanned between surface and bulk layers (Tables 3.3.2.1 and 3.3.2.4), the ablation rates in the bulk of the two natural resin films were calculated (Figure 3.3.3.1).

The process did not involve area measurements of transversal profiles as described above in Section 3.2. Instead, the required number of pulses for the ablation of 15 μm steps was calculated for each fluence of the tested range, using the data from the surface ablation rate studies (Tables 3.3.2.2 and 3.3.2.5). The number of pulses remaining to reach the depths obtained during the initial studies (Tables 3.3.2.1 and

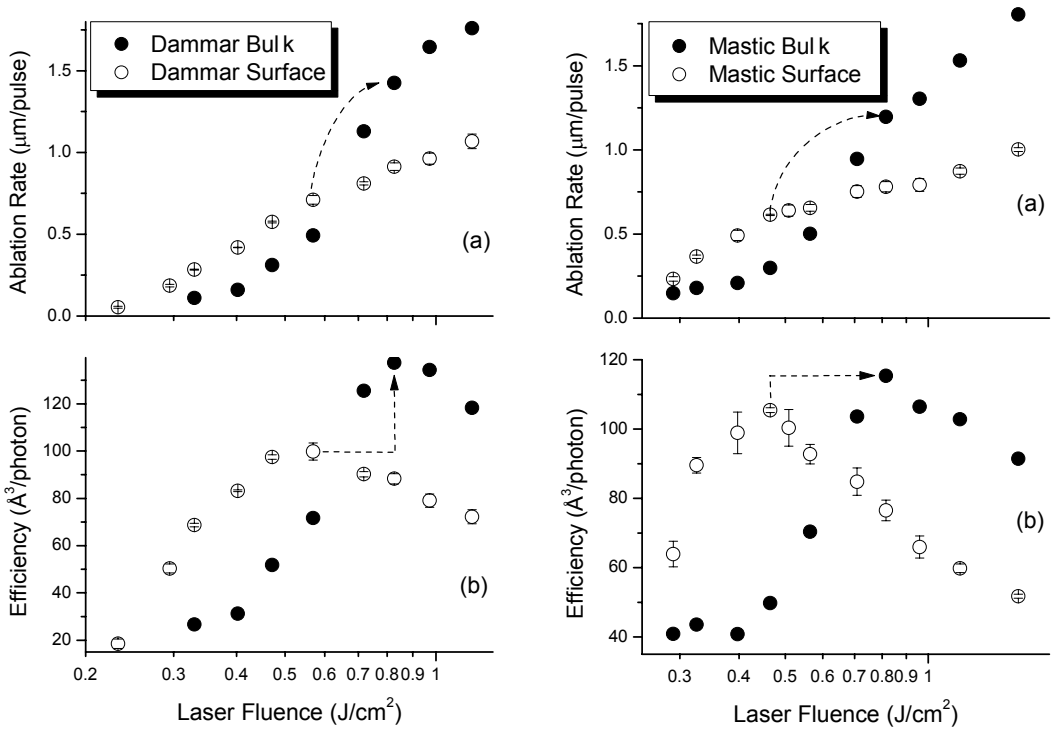

Figure 3.3.3.1 Determined laser ablation rates (a) and the corresponding efficiencies (b) in the bulk of the thick dammar and mastic films at 248 nm. The error is expected to be less than 10%. The corresponding rates at the surface of the same films have been plotted for comparison reasons. The dashed arrows delineate the change of the 'optimum' fluence from the surface towards the bulk of the films.

3.3.2.4) was determined for each etching spot separately. Hence, the residual number of pulses and the remaining depth, i.e. (d-15) μm, where d represents the depth of the random etched depth spot range, were taken into account to calculate both the ablation rate and the efficiency of the bulk. In case of d ≤15 μm, no residual depth could be determined. This was in particular the case for the lowest fluences tested when the ablation yield was low. However, there were sufficient data points to produce the ablation rate curves shown in Figure 3.3.3.1. Certainly, these curves would have been more accurate if all the deep spots had the same depth. However, the absence of fluctuations, as was the case in the initial ablation rate studies (Figures 3.3.2.2 and 3.3.2.4), demonstrates that the response of the bulk to the 248 nm laser photons

provides some reliability. The errors in the calculated laser ablation rates and the corresponding efficiency are not shown, because no accurate calculation could be made having used the mean ablation rate values of Tables 3.3.2.1, 3.3.2.2, 3.3.2.4 and 3.3.2.5. Nevertheless, it should be expected that the error of the ablation rate studies in the bulk is comparable with that of the latter studies, which generally was less than 10%.

The plots reveal that the ablation yield of the bulk is lower than that of the surface up to fluences 0.6 J/cm^2 for dammar and 0.7 J/cm^2 for mastic. In the high fluence regime the opposite situation occurs with the ablation rates increasing significantly compared to the ablation rates at the surface of the films. Both cases obtained 'optimal' fluences at 0.8 J/cm^2, although different fluences maximised the ablation efficiency at the surface of the films, i.e. 0.55 J/cm^2 and 0.45 J/cm^2 respectively. Despite the differences in the ablation rates at the surfaces, the bulk of both films produced similar rates although efficiency is somewhat higher in the case of dammar. The overall trend of the curves in the bulk indicates that upon 248 nm laser irradiation with fluences up to 0.6 – 0.7 J/cm^2 the thermal effects occurring on the remaining films are higher than these at the surface. This is justified by the low ablation rate and efficiency yield in this fluence regime (Srinivasan and Braren 1989). Hence, it is plausible to suggest that upon successive pulses in this fluence regime in the bulk, a significant fraction of the desorbed photofragments precipitates in the ablated etching spots (Srinivasan and Braren 1989), as was previously determined for lower fluences than these. According to Srinivasan and Braren (1989) this fraction contains the photofragments with the highest molecular weight. Thus, only the most vulnerable

molecular fragments are desorbed into the gas phase. On the contrary, by increasing the fluence further than the 0.6 – 0.7 J/cm^2 threshold the intense ablation rate increase in the bulk implies that some photomechanical effects may have contributed to the ablation process, such as ejection of clusters of both excited and unreacted species (Srinivasan 1994, Bäuerle 2000).

3.3.4 Laser-Induced Breakdown Spectroscopy (LIBS) across the ablated depth-profiles

The changes in the ablation rates across the depth profile of the natural resin films and the difference in the ablation of these with the copal oil varnish, all aged under the same conditions (Chapter 2), were expected to be detected in the ablation plume. One of the techniques providing analysis of ablation plume is laser-induced breakdown spectroscopy (LIBS) (Anglos 2001). LIBS is a virtually non-destructive, atomic emission spectroscopic technique mainly for elemental analysis, which provides qualitative information for multi-element samples (Anglos 2001). Owing to its selectivity, requiring minimal sample quantities in the order of a few ng, LIBS has been proposed for the on-line monitoring and *in situ* control at all stages of laser cleaning applications on diverse objects, such as limestone (Gobernado-Mitre, *et al*. 1997), marble (Maravelaki, *et al*. 1997), sandstone, stained glass (Klein, *et al*. 1999) and painted works of art (Zafiropulos and Fotakis 1998).

The principle of online monitoring is based on spectroscopic identification of the plume emission, pulse after pulse, during the ablation process (Scholten, *et al*. 2000, Zafiropulos 2002). In addition, one should keep in mind that a thin layer of the ablated varnish should remain on the surface to prevent the laser beam from penetrating the

paint layers (Zafiropulos and Fotakis 1998). Therefore, LIBS can be only applied online with laser cleaning to monitor the plume emission of the ablated varnish down to a depth of the same varnish film, at which ablation should be terminated. For the present work, LIBS was employed in order to observe the plume emission upon successive laser pulses in the three ablated films. The generated plume of neat organic films is characterised by the abundance of CO groups, representing the absorption of the ablated films at 248 nm, and carbon dimers representing the amount of carbon-carbon bonds ceased per pulse and hence the degree of polymerisation of the films (Zafiropulos 2002).

While testing a range of fluences, which would provide clear LIBS spectra, it was observed that the detectable onset of the plume emission commenced when 'optimal' fluences were employed. This phenomenon, which was also reported by Zafiropulos (2002), requires further investigations. Nevertheless, the noise-to-signal ratios using 'optimal' fluences were low and therefore higher fluences were employed for sufficient plume analysis. These were 0.9 J/cm^2 for the aged dammar film, 0.8 J/cm^2 for mastic and 1.2 J/cm^2 for the copal oil varnish. The most intense bands of neat organic material are the Ångsrtöm system corresponding to CO emission, due to $B^1\Sigma - A^1\Pi$ electronic transitions, and the Swan system, due to $A^3\Pi_g - X'^3\Pi_u$ transitions, for C_2 (Huber and Hertzberg 1979). In particular, the most intense peaks of the CO Ångsrtöm system are at ~ 560 nm ($\Delta v = -3$), ~ 520 nm ($\Delta v = -2$), ~ 485 nm ($\Delta v = -1$), and ~ 450 nm ($\Delta v = 0$). Some characteristic C_2 Swan band system peaks emerge between 547 nm and 565 nm ($\Delta v = -1$), 516 nm and 510 nm ($\Delta v = 0$), as well as 469 nm and 474 nm ($\Delta v = +1$). Therefore, LIBS was set to monitor the spectral region of

400-600 nm. In all cases, the CO peaks were overlapped with the broader C_2 emission peaks and when some CO emission was observed the intensity of the characteristic Ångsrtöm bands was low for a clear discrimination, in contrast to the intense emission of carbon dimers. The clearest signals of carbon dimer emission emerged at two broad peaks at ~ 470 nm and ~ 515 nm and a shorter one at ~ 550 nm. An example is shown for mastic in Figure 3.3.4.1.

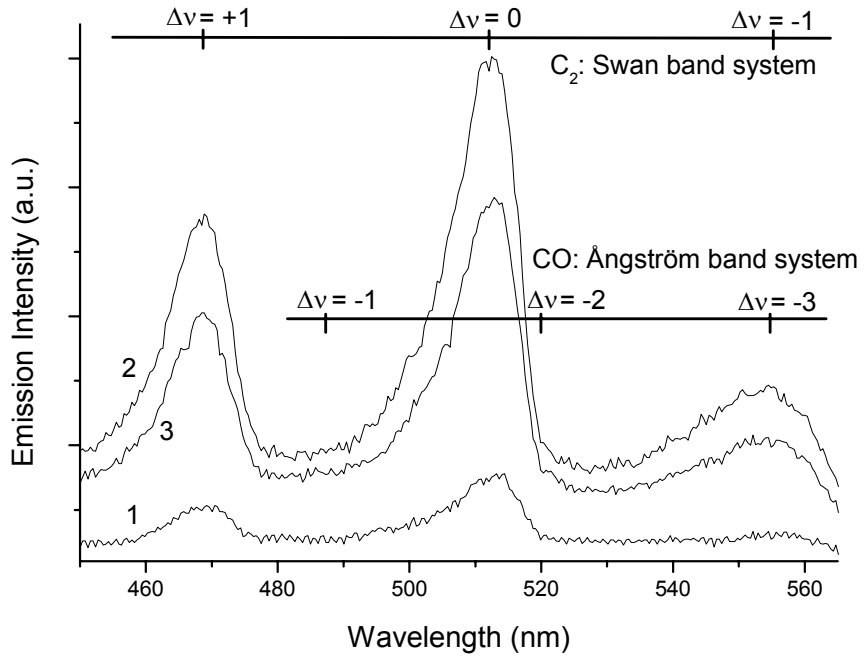

Figure 3.3.4.1 LIBS spectra of light aged mastic using KrF excimer laser at ~ 0.8 J/cm^2, resulting in 0.78 μm/pulse ablation rate (surface). The emissions illustrated correspond to pulses one (1), thirteen (2) and twenty-third (3) yielding 0.78 μm, 10.15 μm and 18.77 μm etchings respectively.

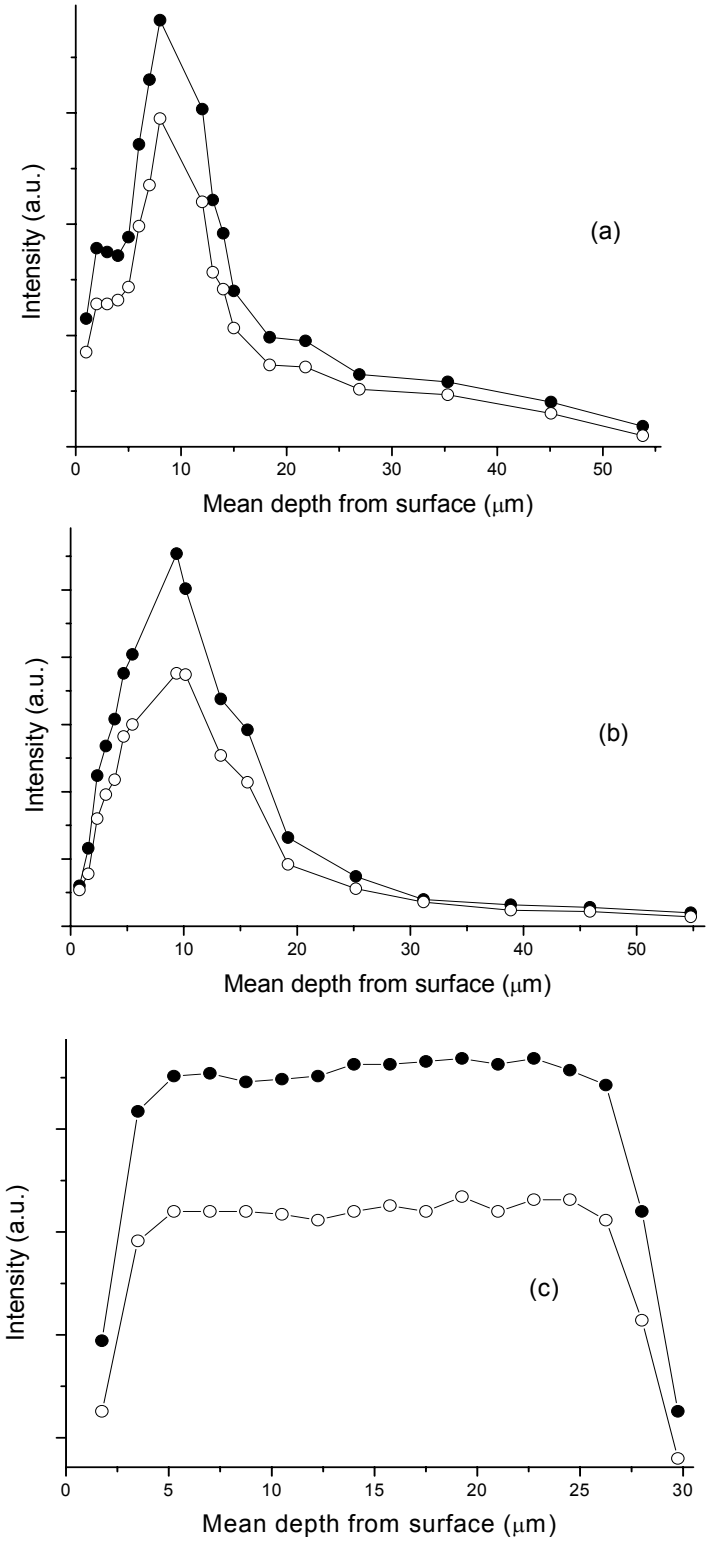

Figure 3.3.4.2 Intensity of characteristic C_2 Swan band system peaks at ~ 515 nm (●) and ~ 470 nm (○) versus mean depth from surface for light aged dammar (a), mastic (b) and copal oil varnish (c). The data were extracted from LIBS spectra using a KrF excimer laser and fluences of 0.9 J/cm^2 (a), 0.8 J/cm^2 (b) and 1.2 J/cm^2 (c).

The intensity of the highest peaks at ~ 415 nm and ~ 470 nm was observed pulse after pulse. Figure 3.3.4.2 shows that there was a clear difference in the intensity of carbon dimer emission in the three varnishes as a function of depth upon ablation with successive pulses. A common characteristic in all cases was that the first pulses produced low intensities. This is consistent with previous findings indicating that the first few pulses somewhat change the optical properties of the ablated film prior to sufficient desorption of photofragments in the gas phase (Srinivasan and Braren 1989, Bäuerle 2000). Thereafter, ablation proceeds at a rate that is characteristic of each material. Thus, observing the relative intensities of carbon dimer emission upon successive pulses, and therefore across the decreasing thickness of the films, it was possible to monitor the amount of species desorbed via the laser induced carbon-carbon bond-breakage as a function of depth, which according to Zafiropulos (2002) is characteristic of the degree of polymerisation across the depth profiles of the ablated films.

Based on this association, the degree of polymerisation across the depth profiles of the aged triterpenoid films seems to be higher in the surface layers, approximately 15 μm from surface. In contrast, the copal oil varnish seems to be polymerised identically all the way down to the lowest layers. This finding is in a very good agreement with the response of the films to changes in laser ablation rate and in the laser cleaning process discussed below in the Section 3.3.5. Namely, the ablation rate per pulse seems to be stable as long as the treated film is highly polymerised. Previous findings indicating that excimer laser ablation is significantly dependent on polymerisation are herein supported (Srinivasan and Braren 1989, Zafiropulos 2002). Further evidence on this

particular aspect is provided in Chapter 4. Finally, it is observed that the carbon dimer emission at the lowest layers decreases gradually and not abruptly, as may have been expected, as soon as the last pulse divests the last microns remaining on the substrate. This is in particular apparent in the copal oil varnish, whose emission is identical at all depths down to the lowest ~ 3 μm of residual film. This phenomenon is associated with the Gaussian beam profile of the KrF excimer laser (Figure 3.2.5). At these depths the centre of the Gaussian beam profile etches deeper than the mean depth measurements indicate, resulting to faster elimination of material in the centre of the etched spot at each consecutive laser pulse. Therefore, at the very end of the film the quartz substrate is first uncovered at the centre of the etched spot, while there is still some material left at the sides of the spot, resulting in reduced plume emission monitored as reduced intensity of the final LIBS spectra.

3.3.5 Laser 'Cleaning'

The laser 'cleaning' of aged organic films is based on a process, in which the laser is employed to irradiate the surface step by step, based on a scanning process (Zafiropulos and Fotakis 1998). The final result requires uncovering a surface a few microns below the original film surface, on which the marks of the ablative laser beam should not be visible. This is critical because the smoother the treated varnish surface will be after application the more saturated the underlying paint in the case of an artwork will appear (De la Rie 1987, Berns and De la Rie 2002). Therefore, some processing utilising the homogeneous beam of excimer lasers, having stable Gaussian versus Top-hat profiles (Bäuerle 2000), is performed. This processing involves overlapping of the beam trace on the varnish surface (Zafiropulos and Fotakis 1998).

For large areas, it has been determined that 80% and 15% spot-by-spot overlap across the transverse (Gaussian) and longitudinal (top-hat) directions respectively during scanning produces the optimum result. Therefore, the appearance of the final scanned surface depends on the accuracy of the preceding measurements and especially that of the fluence, which depends on the spot size.

The 80% scanning overlap across the Gaussian beam profile results in a decrease of the spatial depth resolution compared to the mean depth that is obtained by a single shot with the same fluence (Zafiropulos and Fotakis 1998). With this setting the laser beam passes five times over each point on the irradiated surface. Therefore the ablation rate per scan becomes five times the corresponding ablation rate per pulse. In particular, using the 'optimal' fluences obtained on the surfaces of the tested dammar, mastic and copal oil varnishes, i.e. 0.55, 0.45 and 0.9 J/cm^2 respectively, the ablation rate across the Gaussian profile of the laser became 3.5 and 3 μm per scan for the surface of the natural varnishes and 3 μm per scan for the copal oil varnish. With these settings a fixed number of depth-step zones were produced similar to previous reported work (Theodorakopoulos and Zafiropulos 2003). Overlapping across the Top-hat profile was not essential because the amplitude of the zones was left deliberately equal to the longitudinal dimension of the incident pulses. A schematic representation of a section of the films after the laser cleaning process is demonstrated in Figure 3.3.5.1. In order to avoid heat accumulation during the scanning process onto the ablated surfaces the repetition rate was kept low at 5 Hz. The shallowest depth-step zone was obtained with one pulse per position of step per motor (scan) for the given fluence. For the deeper zones more pulses were employed as shown in Table

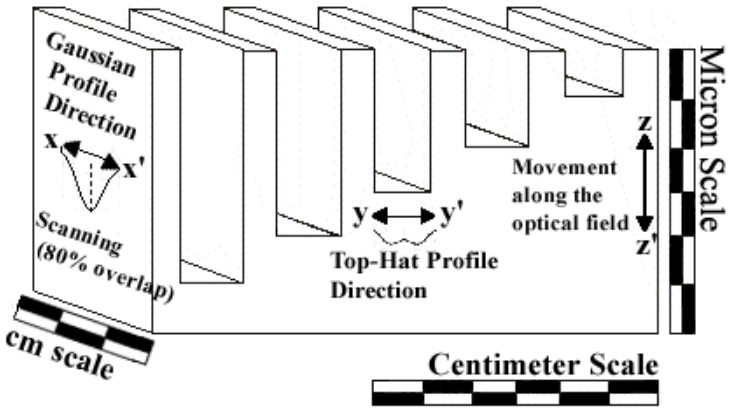

Figure 3.3.5.1 Axonometric scheme of the depth-step zones etched on the films with the KrF excimer laser. The delineated dimensions facilitate the representation of the sample processing but are not accurate. For the clarity of the illustration the resin depth along the zz' axis of the optical field has been exaggerated into a micron scale. Orientations of the Gaussian (xx') and Top-Hat (yy') beam profiles are shown.

3.3.5.1. In the experiment it was judged that the best surface quality was obtained by scanning several times along the deep zones by one pulse per scan rather than more pulses for each scan. This way the scanned film surfaces were allowed to relax before a subsequent intervention with the laser.

Another question considered was the maximum depth of the deepest zone. Photochemical ablation is characterised by reproducing the macro-roughness of the surface after successive pulses (Galyfianaki 1999). Although, the investigated films were spin-coated (Chapter 2), which mainly produces smooth surfaces, surface roughness in the sub-micron scale might have been generated (Figure 3.3.5.2) from minor shocks or deposition of dust particles during drying of the films. Subsequently, in the case shown in Figure 3.3.5.2 sketch b rather than c was the desirable state in which the process should terminate.

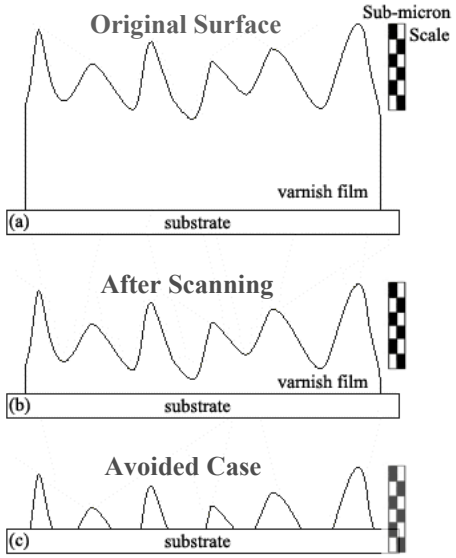

Figure 3.3.5.2 Representation of surface roughness before (a) and after (b) scanning. Situation in (c) was avoided.

Prior to the laser 'cleaning' tests, the number of zones that were to be formed within each film was calculated, taking into account the spatial dimensions (5 x 5 cm^2) and the thickness of the films. Each zone was about 1 cm wide, corresponding to the opening of the slit in front of the cylindrical plano-convex quartz lens (Figure 3.2.1), i.e. the longitudinal dimension of the final spot, and 4 cm long. The depths of the zones were calculated prior to ablation on the basis of the ablation rate data of the surface studies and the reported linear function of the etching depth against the number of incident pulses (Srinivasan and Braren 1989).

As shown in Figure 3.3.5.3 only the aged copal oil varnish preserved this relation across the whole ablated depth from 3 to 27 μm. The aged triterpenoid films produced an obvious change in the ablation step after the removal of the uppermost ~15 μm, determining a different response to the interaction between surface and bulk layers. This change was determined above using the information obtained from the laser

ablation rate studies (Sections 3.3.2 and 3.3.3) and the plume emission (Section 3.3.4) (Theodorakopoulos, *et al*. 2005).

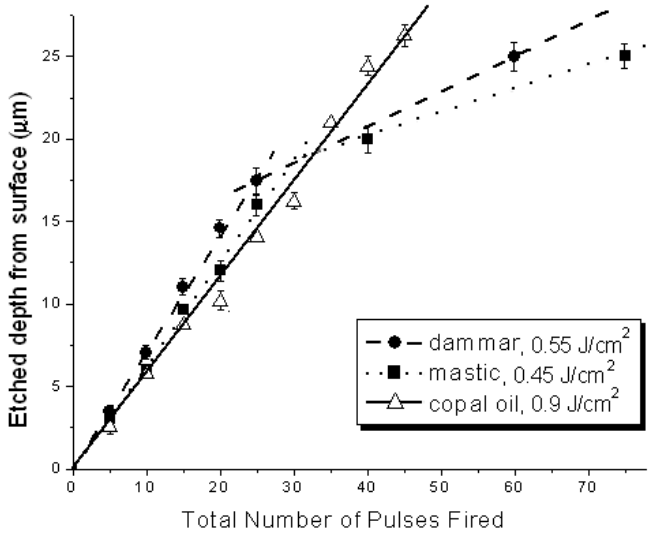

Figure 3.3.5.3 Plot of etched depth as a function of the total number of pulses per spot fired using the 'optimal' fluences for each case, using a KrF excimer laser (248 nm, 25 ns)

Table 3.3.5.1 Laser Cleaning Data for calculated and measured etching

Zone No	Fluence (J/cm^2)	Mean ablation rate (μm/pulse)	Laser Cleaning Rate (μm/scan)	Number of scanning	Calculated* depth (μm)	Calculated** depth (μm)	Measured depth (μm)
Aged Dammar							
1	0.55	0.71	3.55	1	3.55	3.55	3.5
2				2	7.1	7.1	7
3				3	10.65	10.65	11.5
4				4	14.2	14.2	15
5				6	21.3	18.1	17
6				12	42.6	29.6	25
Aged Mastic							
1	0.45	0.61	3.05	1	3.05	3.05	3
2				2	6.1	6.1	6
3				3	9.15	9.15	10
4				4	12.2	12.2	12
5				5	15.25	15.25	16
6				8	24.4	20.35	20
7				15	45.75	32.25	25
Aged Copal Oil Varnish							
1	0.91	0.59	2.95	1	2.95		2.5
2				2	5.9		5.8
3				3	8.85		8.7
4				4	11.8		10.2
5				5	14.75		14
6				6	17.7		16.2
7				7	20.65		21
8				8	23.6		24.3
9				9	26.55		26.2

* According to the surface ablation rate data, i.e. Tables 3.3.2.2, 3.3.2.5 and 3.3.2.8

** According to the random depth ablation rate data, i.e. Tables 3.3.2.1 and 3.3.2.4, of the triterpenoids

3.4 Discussion

3.4.1 Excimer laser ablation of aged varnishes

As shown in Sections 3.2, the interaction of a KrF excimer laser (248 nm, 25 ns) with aged varnishes can be tested using an elaborate yet simple, and for some empirical, way. It is shown that the mechanisms that participate in this interaction can be modified to some extent by changing the fluence between 0.1 and 1 J/cm^2. The influence of the laser fluence has been discussed in Section 3.3.1. As it was determined in earlier investigations, excimer laser ablation of aged varnishes is optimised using fluences that maximize the laser ablation efficiency, measured in Å^3/photon units (Zafiropulos and Fotakis 1998, Zafiropulos 2002). Therefore, the analysis of the results herein is concentrated on the ablation process, having kept all the parameters of the KrF excimer laser, which are the pulse duration, the energy, the waist of the beam profile and consequently the fluence, constant. Consequently, the changes in the interaction between the three case studies and across the depth profile of the natural resin films are associated with their chemistry. Thus, a comprehensive insight of the interaction requires an understanding of the chemistry across the depth-profile of the ablated varnishes. In particular, the ablated films are clearly separated in two groups: (a) the natural varnishes, dammar and mastic, which upon ageing produce a depth-dependent gradient in absorption (owing to a gradient in oxidation) and in crosslinking, that is examined in Chapters 4 and 5; and, (b) the tested copal oil varnish, which did not generate gradient characteristics as a function of depth, because it is optically saturated as shown in Chapters 4 and 6.

It should be realised that upon the release of a UV laser pulse there is a sequence of consecutive actions that participate in the ablation process (Section 1.3.2). During the laser irradiation, the 248nm photons are absorbed first (a) causing electronic excitations down to the depth determined by the optical absorption length, which in turn causes (b) shock waves, that is photochemical and photomechanical action in the irradiated area that instantly swells because of mechanical stresses and pressure among the excited compounds leading to (c) bond-breakage and desorption of excited species into the gas phase (Luk'yanchuk, *et al*. 1993a, Bäuerle 2000). This sequence of actions (Figure 1.3.3.1a, b, c) occurs in a time window spanning from some femto- to a few nanoseconds (10^{-15} – 10^{-9} sec), which leads to the conclusion that in some point of the nanosecond ablation during the release of the pulse, all these processes coexist (Bäuerle 2000). Absorption of the laser wavelength is evidently the main process that determines the subsequent actions (Figure 1.3.3.1a). Because of the gradient in absorption (Chapter 4, Zafiropulos, *et al*. 2000a), and the distribution of different amounts and types of chromophores across depth (Chapter 5), the mechanisms that cause the ablation of natural resin films are gradually altered as the thickness of the films is eventually reduced. In the surface, the high degree of polymerisation (Zafiropulos, *et al*. 2000a, Chapters 4 and 5) and the increased numbers of carbonyl groups attached to oxygenated products, such as ketones, lactones, aldehydes and carboxylic acids (De la Rie 1988a, Van der Doelen 1999) and in particular the latter, which absorb intensively the 248 nm laser wavelength (Srinivasan and Braren 1989), guarantee higher photochemical action than in the bulk of the films.

Because of the depth-dependent gradient in absorption, the average number of electronic excitations per unit volume caused at 248 nm (5 eV) (Luk'yanchuk, *et al*. 1994, Srinivasan 1994, Bäuerle 2000, Bityurin, *et al*. 2003) is expected to decrease with depth (Pettit and Sauerbrey 1993). According to the literature, the type of electronic excitations partly determines the type of ablation. It has been reported that in photochemical ablative decomposition, electronic transitions from ground states to elevated excited states S_1 predominate, leading subsequently to desorption prior to relaxation (Section 1.3.3.1, Luk'yanchuk, *et al*. 1994, Srinivasan 1994, Bäuerle 2000, Bityurin, *et al*. 2003). If the excited compounds at the S_1 state fall to internal conversions or to a triplet state T_1 prior to desorption, vibrational energy of the relaxing excited species leads to some thermal decomposition in the irradiated surface (Bäuerle 2000). At 248 nm, due to the longer lifetime of the triplet T_1 than the singlet state S_1, the excited compounds may absorb a second photon, which causes elevation to higher electronic states, i.e. S_2, T_2, leading to rapid decomposition (Srinivasan 1994). Two-photon excitations have been determined for small organic molecules (Koplitz and McVey 1985) and are suggested to occur for the ablation of aged triterpenoid varnishes of small thicknesses (< 10-15 μm) (Georgiou, *et al*. 1998).

Thus, electronic excitations are the consequent actions following absorption and are the preceding actions prior to the generated shock waves (Koren 1988, Kelly, *et al*. 1992) (Figure 1.3.3.1b). Shock waves are mechanical stresses and pressure among the excited compounds initiating by a first step of bond-breakage and a moderate temperature rise, leading to localised surface swelling that finally results in volume explosion (Section 1.3.3, Bäuerle 2000). At the same time, the excitation-induced

mechanical stresses and pressure are dependent on the number of covalent bonds that are involved in the preliminary stages of the bond-breakage process (Srinivasan and Braren 1989). Since the degree of polymerisation decreases with depth (Zafiropulos, *et al*. 2000a, Chapters 4 and 5), the intensity of these actions is expected to be affected accordingly. The two parallel gradients in the degrees of excitations and bond-breakage determine that shock waves are reducing both qualitatively and quantitatively across depth. This is understandable because as the thickness is reduced, upon the same dose of irradiation, that is to say the same number of laser photons per pulse, less photons are absorbed and at the same time, due to the decreased degree of polymerisation, less covalent bonds are contributing to the generated stresses prior to their cleavage. This finally results in desorption of less excited species into the gas phase (Figure 1.3.3.1c). The latter has been experimentally proved, as shown by the reduced emission of carbon dimers as a function of depth (Figure 3.3.4.2 a and b) and the reducing ablation step (Figure 3.3.5.3). In Section 3.3.3 it is shown that the same effect can be identified with laser ablation rate studies of surface and bulk layers (Figure 3.3.3.1). Thus, there is an excess of 248 nm photons, whose action is not clearly described simply from the measurement of the depth of the etchings. These photons are either contributing to collisions with the photofragments resulting in (a) screening effects and ionisation, (b) reflected away from the surface, (c) provide surface excitation leading to thermal dissipation in the material, or (d) transmitted through the remaining film along the optical absorption length (Srinivasan, *et al*. 1986b, Luk'yanchuk, *et al*. 1993a, b, Srinivasan 1994, Luk'yanchuk, *et al*. 1996). In case of films with a perfectly homogenous depth-profile, all the mechanisms of excimer laser ablation evidently

remain constant across depth, as is the case in regular polymers. Hence, screening, ionisation in the gas phase and effects in the irradiated film such as thermal dissipation and transmission along the optical absorption length would remain unchanged if the same laser parameters were kept constant.

3.4.2 The fate of the remaining varnish after the KrF excimer laser ablation

The question remaining is the fate of the irradiated residual surface of the ablated films. Especially for the natural resins, some suggestions can be made based on earlier findings on excimer laser ablation. Upon ablation of surface layers, relaxation of excited compounds is mainly obtained in the gas phase, while in the bulk some excited species are expected to relax in the film resulting in thermal dissipation in the film (Luk'yanchuk, *et al*. 1994, Srinivasan 1994, Bäuerle 2000). The same effect has been termed 'vaporisation' by Zafiropulos (2002) and is attributed to the lack of polymerisation in the bulk. This is justified since in the absence of an efficient number of crosslinks to be cleaved and to contribute to the laser induced shock waves, relaxation and thermal dissipation in the material will lead to vaporisation of the irradiated surface. This was observed during the experiments in the laboratory, since upon ablation of deeper layers the remaining surfaces obtained a slightly melting texture. At the surface of the films this phenomenon was not observed because of the high degrees of absorption and polymerisation (Chapters 4 and 5), which, according to findings determined by Srinivasan (1994), leads to melting of the desorbed photofragments in the gas phase rendering the latter in a 'liquid' phase, a few μs after the incidence of the pulse (Figure 1.3.3.1d).

The excess of 248 nm photons, which are not involved either in the ablation process or in reflections and collisions in the gas phase, are transmitted across the remaining film onto the substrate. This action has been recorded upon ablation of PI (Pettit, *et al*. 1994) and on ablation of an aged mastic varnish (Zafiropulos 2002) on quartz substrates, while transmission was measured pulse-after-pulse at the back of such samples using a pyroelectric power-meter. Further investigations on online transmission upon ablation of the tested films are described in Chapter 4, but it should be stressed here that a 'safe' laser cleaning requires taking this property into account, in order to protect light-sensitive substrates. Thus, the maintenance of a thin layer of the ablated varnish to filter the transmitted laser photons is essential for successful laser cleaning of a varnish-photosensitive substrate system.

A significant concern is that the propagation of the UV photons through the remaining film results in the generation of reactive free radicals (Georgiou, *et al*. 1998). Since no laser-induced oxidative deterioration of the ablated films was detected, Georgiou and co-workers (1998) suggested that due to the compressed energy of the transmitted photons these radicals rapidly recombine to form the parent molecule or a similar compound. This action, which was termed 'cage' effect, has been also observed upon ablation of chlorobenzene films at 248 nm (Georgiou, *et al*. 1997). The theory of the 'cage' effect is herein fully supported, because molecular studies of the remaining films of dammar and mastic (after ablation) using DTMS and MALDI-TOF-MS revealed that only the established triterpenoid compounds are present in these films (Chapter 5). The results are also supported with a DTMS study of the ablated copal oil

varnish, which detected no variations in the concentration of the expected lipids and resin molecules in the film (Chapter 6).

On the other hand, it has been noted that upon excimer laser ablation the optical properties of the irradiated surface are somewhat altered (Bäuerle 2000). The findings presented above and in chapters 4, 5 and 6 suggest that this should be a minor change. It is herein suggested that, despite this minor change, the outlined optical properties upon ablation are similar to the original optical properties across the depth-profile of the material prior to ablation. In Section 1.4 some preliminary results on gradients in polarity and yellowing were described (Theodorakopoulos and Zafiropulos 2003). Because of absorption between photons and carbonyl groups in the remaining film, transmission and 'cage' effects, the former observations could be attributed to changes of the optical properties of the ablated films. Increased polarity is caused by the attraction of water molecules with oxygenated molecules, while yellowing is caused by the absorption of blue light (400–490 nm) by unsaturated ketones and quinones (Formo 1979, De la Rie 1988b) that are generated via autoxidation. The yellow chromophores are present in the high MW fraction of the resins (De la Rie 1988b, Boon and van der Doelen 1999, Dietemann 2003), as described in Chapter 2. It could be suggested that the UV laser ablation leads to reduction of polar groups, defunctionalisation and bleaching of the yellow compounds. However, the fact that polarity and yellowing have been observed to eliminate gradually with depth (Theodorakopoulos and Zafiropulos 2003) indicates that the laser contribution is not significant, or at least that it does not induce abrupt changes of the properties of the varnish. Even in case of laser-induced bleaching, this could be considered as a

positive side-effect. Thus, accepting that some minor contribution of the UV laser photons to the degree of polarity and yellowing occur, these actions are suggested to be equivalent to the minor optical modification of the irradiated material (Bäuerle 2000).

3.4.3 Laser cleaning based on KrF excimer laser ablation

The practice of laser cleaning is bound to the interaction of the varnish to be removed with the UV pulsed laser. A significant difference between laser ablation and laser cleaning experiments is that in 'cleaning' 80% overlapping across the Gaussian beam profile are employed to optimise the resulting texture of the scanned surface (Section 3.3.5, Zafiropulos and Fotakis 1998). This way, ablation of one scan etches the same depth of material as ablation of five consecutive pulses (Section 3.3.5). Laser cleaning should aim at keeping a balance between (a) the 'violent' laser-induced photochemical and photomechanical action of surface layers of the varnish and (b) the protection of the underlying layers, which should not be affected by the ablation process of the surface of the varnish. Therefore, the aged varnish must be regarded as a barrier capable of preserving this balance. This approach is facilitated by the minute resolution in the etching step with a KrF excimer laser (Section 3.3.1).

It is hereby proposed that in the case of aged natural varnish with gradient characteristics, such as the aged dammar and mastic tested, laser cleaning should be terminated as soon as the highly deteriorated surface layers are removed. In practice, the end point becomes evident, because at a certain depth from surface there is a change in the ablation yield. This change can be identified by differences either in the ablation rate per pulse (Figure 3.3.3.1), in the intensity of the carbon dimer (Figure

3.3.4.2) and CO emission per pulse (Zafiropulos 2002) and/or in the ablation step (Figure 3.3.5.3) (Theodorakopoulos *et al*. 2005). Since a preliminary investigation of the interaction based on laser ablation rate studies is essential prior to laser cleaning (Zafiropulos 2002, Section 3.3), any change across depth is readily monitored. Therefore, by recording the mean ablation rate per pulse as a function of fluence and having determined the exact depth of the generated spots, a laser cleaning strategy for a certain film can be planned to provide a fully controlled pulse-to-pulse removal, the rate of which can be fully predictable prior to the laser cleaning procedure.

Following removal of the highly deteriorated surface layers of aged natural varnishes with gradient characteristics, the optical absorption length of the remaining varnish increases, which leads to increasing transmission of the laser photons towards the underlying layers (Chapter 4, Zafiropulos 2002). The depth-wise reduction of optical density (Zafiropulos *et al*., 2000a) and polarity (Theodorakopoulos and Zafiropulos 2003) signifies that once the highly polar material is ablated the remaining varnish can be either preserved (given that the degree of discolouration is also eliminated with depth) or removed with apolar or medium polarity organic solvents based on the 'traditional' chemical cleaning applications (Hedley 1980, Stolow 1985, Phenix 1998). In cases such as the copal oil varnish tested, which did not develop a gradient upon the certain ageing process (Chapters 4 and 6), a different approach should be considered. In this case, given that the optical density does not change with depth (across a 30 μm depth profile), the protection of the underlying layers depends almost exclusively on the optical absorption length that can be measured on the surface of the film. Thus, the remaining varnish thickness must be at least as short as the optical

absorption length of the specific varnish. The process may be somewhat complicated when several varnishes are layered one on top of the other. In this case the protection of the substrate depends on the optical properties of the older varnish lying between the substrate and the surface coatings. This is also the case in the laser ablation of overpaintings painted on top of varnishes. A representative example on the advances of excimer laser cleaning, was the selective layer-by-layer removal of multi-layered black overpaints from a black solvent-sensitive painting (McGlinchey, et al. 2005). In this particular case, LIBS was employed prior to laser cleaning for identification of the thickness and the content of the subsequent layers, while the final cleaning was carried out using a KrF excimer laser.

3.5 Conclusions

The excimer laser ablation at 248 nm of three artificially aged varnishes, dammar, mastic and copal – linseed oil varnish was studied using standard laser ablation rate studies (Srinivasan and Braren 1989, Zafiropulos 2002), plume emission upon successive pulses until total ablation of the films using LIBS (Anglos 2001, Zafiropulos 2002) and a laser cleaning method proposed for the cleaning of paintings (Zafiropulos and Fotakis 1998). Based on their ablation characteristics, the three case studies were clearly separated into two groups: aged natural resins and copal oil varnish.

The copal oil varnish was laser ablated using the ‘optimum’ fluence obtained from the ablation rate study, which was identical at all depths of a 30 μm film and a 15 μm film. Moreover, the intensity of the carbon dimers emitted per pulse of the aged copal

oil varnish was constant across its ablated depth profile. The stability of the ablation step was also delineated by the linear function of the etched depth versus the number of pulses fired. From that point of view the excimer laser ablation of this film is comparable with that of the well-studied PMMA, PI and PU polymers (Srinivasan, *et al*. 1986b, Sutcliffe and Srinivasan 1986, Srinivasan, *et al*. 1987, Küper, *et al*. 1993, Pettit and Sauerbrey 1993, Luk'yanchuk, *et al*. 1994, Srinivasan 1994, Zafiropulos, *et al*. 1995, Luk'yanchuk, *et al*. 1996). These findings on the laser ablation of the specific copal oil varnish, aged under the intense and prolonged UV including xenon arc radiation that was described in Chapter 2, demonstrate that the depth profile of the film had a uniform chemical state, including the degrees of absorption, oxidation and polymerisation as shown in Chapters 4 and 6. Given these findings, it could be suggested that the film was saturated in terms of absorption.

In contrast, the excimer laser ablation of the aged natural varnishes tested was affected by the depth-dependent gradients in oxidation, and therefore absorption, and polymerisation (Chapters 4 and 5, Zafiropulos, *et al*. 2000a, Theodorakopoulos, *et al.* 2005). The ablation rate curves of these varnishes changed after removal of the 15 μm uppermost layers. This was evident from a range of spots ablated at random depths and calculated curves of ablation rate per pulse as a function of fluence for the bulk of the films. The carbon dimer emission of the films showed an evident reduction in their intensity after ablation of 15 μm, which is clearly associated with the gradient in polymerisation (Zafiropulos 2002). Laser cleaning based on the described scanning method was employed with the 'optimal' fluences determined for the surface of the aged films. After removal of the uppermost 15 mm layers there was a clear step in the

function of the etched depth versus the number of pulses fired, which reflected the change of the interaction and hence the change of the chemistry of these materials across their depth profile.

These findings dictate a certain strategy with respect to the cleaning approach of varnished objects, especially if the substrate is photosensitive as in the case of a painting. In particular, laser cleaning of homogeneous varnishes could aim at the removal of most of the coating leaving a film as thin as its optical absorption length to absorb the transmitted UV laser photons. In the case of natural resins laser cleaning could be employed to remove the uppermost very deteriorated layers, while the remaining varnish could be left on the substrate given that yellowing and polarity are significantly reduced because of the gradient in oxidation (Theodorakopoulos and Zafiropulos 2003). This way the depth transmission of the UV laser photons would be shorter than the optical absorption length, which becomes longer with depth because of the gradient in absorption (Chapters 4 and 5, Zafiropulos, *et al*. 2000a), bearing in mind that the optical absorption length would not be readily determined at the surface of the films. In multi-layered coated objects, where all the coatings require removal, laser cleaning should be dependent on the optical properties of the lowest coating.

3.6 References

Al-Malaika, S. 'Autoxidation'. In *Atmospheric oxidation and antioxidants*, Ed. G. Scott, Vol. I, Elsevier Science Publishers B.V., Amsterdam, (1993), 45 - 82.

Anglos, D., 'Laser-Induced Breakdown Spectroscopy in Art and Archaeology', *Applied Spectroscopy* **55** (2001) 186A-205A.

Athanassiou, A., Hill, A. E., Fourrier, T., Burgio, L., and Clark, R. J. H., 'The effects of UV laser light radiation on artist's pigments', *Journal of Cultural Heritage (Suppl. 1)* **1** (2000) s209-s213.

Bäuerle, D. *Laser Processing and Chemistry, Third, revised and enlarged edition*, Springer-Verlag, Berlin, Heidelberg, New York, 2000.

Berns, R. S. and De la Rie, E. R. 'The relative importance of surface roughness and refractive index in the effects of varnishes on the appearance of painitngs'. In *Preprints of the 13th triennial meeting of the ICOM Committee for Conservation*, Ed. V. R., Vol. I, James & James (Science Publishers) Ltd, Rio de Janeiro, (2002), 211-216.

Boon, J. J. and van der Doelen, G. A. 'Advances in the current understanding of aged dammar and mastic triterpenoid varnishes on the molecular level'. In *Firnis: Material - Aesthetik - Geschichte, International Kolloquium, Braunschweig, 15-17 Juni 1998*, Ed. A. Harmssen, Hertog-Anton-Ulrich-Museum, Braunschweig, (1999), 92-104.

Brannon, J. H., Lankard, J. R., Baise, A. I., Burns, F., and Kaufman, J., 'Excimer laser etching of polyimide', *Journal of Applied Physics* **58** (1985) 2036-2043.

Cain, S. R., Burns, F. C., and Otis, C. E., 'On single-photon ultraviolet ablation of polymeric materials', *Journal of Applied Physics* **71** (1992) 4107-4117.

Castillejo, M., Martin, M., Oujja, M., Silva, D., Torres, R., Manousaki, A., Zafiropulos, V., van den Brink, O. F., Heeren, R. M. A., Teule, R., Silva, A., and Gouveia, H., 'Analytical study of the chemcial and physical changes induced by KrF laser cleaning of tempera paints', *Analytical Chemistry* **74** (2002) 4662-4671.

Castillejo, M., Martin, M., Oujja, M., Santamaria, J., Silva, D., Torres, R., Manousaki, A., Zafiropulos, V., van den Brink, O. F., Heeren, R. M. A., Teule, R., and Silva, A., 'Evaluation of the chemical and physical changes induced by KrF laser irradiation of tempera paints', *Journal of Cultural Heritage (Suppl. 1)* **4** (2003) 257s-263s.

Chuang, M. C. and Tam, A. C., 'On the saturation effect in the picosecond near ultraviolet laser ablation of polyimide', *Journal of Applied Physics* **65** (1989) 2591-2595.

De la Rie, E. R., 'The influence of varnish on the appearance of paintings', *Studies in Conservation* **32** (1987) 1-13.

De la Rie, E. R., 'Stable Varnishes for Old Master Paintings', PhD Thesis University of Amsterdam, (1988a).

De la Rie, E. R., 'Photochemical and thermal degradation of films of dammar resin', *Studies in Conservation* **33** (1988b) 53-70.

Dietemann, P., 'Towards more stable natural resin varnihses for painintgs', PhD Thesis Swiss Federal Institute of Technology, Zurich, (2003).

Formo, M. W. 'Paints, varnishes and related products: Discolouration'. In *Baile's Industrial Oil and Fat Products*, Ed. D. Swern, Vol. 1, John Wiley & Sons, New York, (1979), 722-724.

Fotakis, C., 'Lasers for art's sake', *Optics and Photonics News* **6** (1995) 30-35.

Fotakis, C., Zafiropulos, V., Anglos, D., Balas, C., Fandidou, D., Georgiou, S., Tornari, V., Zergioti, I., and Doulgeridis, M., 'Lasers in the Conservation of Painted Artworks,' *submitted in Restauratorenblätter, Sonderband, for the proceedings of Lacona II (this extra volume of the journal was never published)* (1997).

Futzikov, N. P., 'Approximate theory of highly absorbing polymer ablation by nanosecond laser pulses', *Applied Physics Letters* **56** (1990) 1638-1640.

Galyfianaki, A., 'Laser cleaning of artworks with short-pulsed lasers', University of Crete, Physics Department, Herakleion, Greece, (1999).

Georgiou, S., Koubenakis, A., Syrrou, M., and Kontoleta, P., 'The importance of the plume ejection time for the fragmentation yieds observed in the UV ablation of molecular van der Waals films. Ablation of chlorobenzene films at 248 nm', *Chemical Physics Letters* **270** (1997) 491-499.

Georgiou, S., Zafiropulos, V., Tornari, V., and Fotakis, C., 'Mechanistic Aspects of Excimer Laser Restoration of Painted Artworks', *Laser Physics* **8** (1998) 307-312.

Georgiou, S. and Koubenakis, A., 'Laser-Induced Material Ejection from Model Molecular Solids and Liquids: Mechanisms, Implications, and Applications', *Chemical Reviews* **103** (2003) 349-393.

Gobernado-Mitre, I., Prieto, A. C., Zafiropulos, V., Spetsidou, Y., and Fotakis, C., 'On-line monitoring of laser cleaning of limestone by laser induced breakdown spectroscopy', *Applied Spectroscopy* **51** (1997) 1125-1129.

Hedley, G., 'Solubility parameters and varnish removal: a survey.' *The Conservator* **4** (1980) 12-18. (Re-printed, with corrections, in Measured Opinions (1993), ed. C. Villers. London: United Kingdom Institute for Conservation: 128-134).

Hill, A. E., Athanassiou, A., Fourrier, T., Anderson, J., and Whitehead, C., 'Progress in the use of excimer lasers to clean easel paintings'. In *Proceedings of the 5th International Conference on Optics Within Life Sciences (OWLS V)*, Eds. C. Fotakis,

T. G. Papazoglou, and C. Kalpouzos, Springer Verlag, Aghia Pelagia, Crete, Greece, 1998, (2000), 203-207.

Hontzopoulos, E. I., Fotakis, C., and Doulgeridis, M., 'Excimer laser in art restoration'. In *SPIE; 9th International Symposium on Gas Flow and Chemical Lasers*, Eds. C. Fotakis, C. Kalpouzos, and T. G. Papazoglou, Vol. 1810, Bellingham, Washington, (1993), 748-751.

Huber, K. P. and Hertzberg, G. *Molecular Spectra and Molecular Structure. IV. Constants of Diatomic Molecules*, Van Nostrand/Reinhold, New York, 1979.

Kelly, R., Miottello, A., Braren, B., and Otis, C. E., 'On the debris phenomenon with laser sputtered polymers', *Applied Physics Letters* **60** (1992) 2980-2982.

Keyes, T., Clarke, R. H., and Isner, J. M., 'Theory of photoablation and its implications for laser phototherapy', *Journal of Physical Chemistry* **89** (1985) 4194-4196.

Klein, S., Stratoudaki, T., Zafiropulos, V., Hildenhagen, J., Dickmann, K., and Lehmkuhl, T., 'Laser-induced breakdown spectroscopy for on-line control of laser cleaning of sandstone and stained glass', *Applied Physics A* **69** (1999) 441-444.

Koplitz, B. D. and McVey, J. K., 'Fragment power dependence in the laser-induced ionization of benzene-d6', *Journal of Physical Chemistry* **89** (1985) 4196-4200.

Koren, G., *Appl. Phys B* **46** (1988) 147.

Küper, S. and Stuke, M., 'Femtosecond UV excimer laser ablation', *Applied Physics B* **44** (1988) 199-201.

Küper, S., Brannon, J., and Brannon, K., 'Threshold Behavior in Polyimide Photoablation: Single-Shot Rate Measurements and Surface-Temperature Modeling', *Applied Physics A 56* **56** (1993) 43-50.

Luk'yanchuk, B., Bityurin, N., Anisimov, S., and Bauelre, D., 'The role of excited species in UV-Laser Material Ablation, Part I: Photophysical Ablation of Organic Polymers', *Applied Physics A* **57** (1993a) 367-374.

Luk'yanchuk, B., Bityurin, N., Anisimov, S., and Bauelre, D., 'The role of excited species in UV-Laser Material Ablation, Part II: The stability of the ablation front', *Applied Physics A* **58** (1993b) 449-455.

Luk'yanchuk, B., Bityurin, N., Anisimov, S., and Bäuerle, D. 'Photophysical Ablation of Organic Polymers'. In *Excimer Lasers*, Ed. L. D. Laude, Kluwer Academic Publishers, The Netherlands, (1994), 59-77.

Luk'yanchuk, B., Bityurin, N., Anisimov, S., Arnold, N., and Bauelre, D., 'The role of excited species in UV-Laser Material Ablation, Part III: Non-stationary regimes in ablation', *Applied Physics A* **62** (1996) 397-401.

Luk'yanchuk, B. and Zafiropulos, V. 'On the theory of discolouration effect in pigments at laser cleaning'. In *Optical Physics, Applied Physics and Material Science: Laser Cleaning*, Ed. B. S. Luk'yanchuk, World Scientific, Singapure, New Jersey, London, Hong Kong, (2002), 393-414.

Madden, O., Abraham, M., Scheerer, S., and Werden, L., 'The effects of laser radiation on adhesives, consolidants and varnishes', In *Lacona V Proceedings, Osnabrück, Germany, September 15-18, 2003*, Eds. K. Dickmann, C. Fotakis, and J. F. Asmus, Springer Proceedings in Physics, Vol. 100, Springer-Verlang, Berlin Heidelberg, (2005), 247-254.

Mahan, G. D., Cole, H. S., Liu, Y. S., and Philipp, H. R., 'Theory of polymer ablation', *Applied Physics Letters* **53** (1988) 2377-2379.

Maravelaki, P. V., Zafiropulos, V., Kylikoglou, V., Kalaitzaki, M. P., and Fotakis, C., 'Laser induced breakdown spectroscopy as a diagnostic technique for the laser cleaning of marble', *Spectrochimical Acta B* **52** (1997) 41-53.

McGlinchey, C., Stringari, C., Pratt, E., Abraham, M., Melessanaki, K., Zafiropulos, V., Anglos, D., Pouli, P., and Fotakis, C., 'Evaluating the Effectiveness of Lasers for the Removal of Overpaint from a 20th C Minimalist Painting', In *Lacona V Proceedings, Osnabrück, Germany, September 15-18, 2003*, Eds. K. Dickmann, C. Fotakis, and J. F. Asmus, Springer Proceedings in Physics, Vol. 100, Springer-Verlang, Berlin Heidelberg, (2005), 209-216.

Meyer, J., Feldeman, D., Kutzner, J., and Welge, K., *Appl Phys B* **45** (1988) 7.

Morgan, N., 'Excimer lasers restore 14th century icons', *Opto and Laser Europe* **7** (1993) 36-37.

Pettit, G. H. and Sauerbrey, R., 'Pulsed Ultraviolet Laser Ablation', *Applied Physics A* **56** (1993) 51-63.

Pettit, G. H., Ediger, M. N., Hahn, D. W., Brinson, B. E., and Sauerbrey, R., 'Transmission of polyimide during pulsed ultraviolet laser irradiation', *Appl. Phys. A* **58** (1994) 573.

Phenix, A., 'Solubility parameters and the cleaning of paintings: an update and review', *Zeitschrift fór Kunsttechnologie und Konservierung* **12** (1998) 387- 409.

Sauerbrey, R. and Pettit, G. H., 'Theory of the etching of organic materials by ultraviolet laser pulses', *Applied Physics Letters* **55** (1989) 421-423.

Scholten, J. H., Teule, J. M., Zafiropulos, V., and Heeren, R. M. A., 'Controlled laser cleaning of painted artworks using accurate beam manipulation and on-line LIBS-detection', *Journal of Cultural Heritage (Suppl. 1)* **1** (2000) s215-s220.

Scott, G. 'Autoxidation and antioxidants: historical perspective'. In *Atmospheric oxidation and antioxidants*, Ed. G. Scott, Vol. I, Elsevier Science Publishers B.V., Amsterdam, (1993), 1 - 44.

Soberhart, J. R., 'Polyamide ablation using intense laser beams', *Journal of Applied Physics* **74** (1993) 2830-2833.

Srinivasan, R., Braren, B., Seeger, D. E., and Dreyfus, R. W., 'Photochemical cleavage of a polymeric solid: details of the ultraviolet laser ablation of poly(methyl methacrylate) at 193 nm and 248 nm', *Macromolecules* **19** (1986a) 916-921.

Srinivasan, R., Braren, B., and Dreyfus, R. W., 'Ultraviolet laser ablation of polyimide films', *Journal of Applied Physics* **61** (1987) 372-376.

Srinivasan, R. and Braren, B., 'Ultraviolet laser ablation of organic polymers', *Chemical Reviews* **89** (1989) 1303-1316.

Srinivasan, R. 'Interaction of laser radiation with organic polymers'. In *Laser Ablation: Principles and Applications*, Ed. J. C. Miller, Vol. 28, Springer Series of Material Science, Springer, Berlin, Heidelberg, (1994), 107.

Srinivasan, V., Smrtic, M. A., and Babu, S. V., 'Excimer laser etching of polymers', *Journal of Applied Physics* **59** (1986b) 3861-3867.

Stolow, N. 'Part II: Solvent Action'. In *On picture varnishes and their solvents.*, Ed. E. H. Jones, Revised edition 1971. Cleveland, Ohio: Case Western Reserve University. Revised and enlarged edition 1985. Washington DC: National Gallery of Art., (1985).

Sutcliffe, E. and Srinivasan, R., 'Dynamics of UV laser ablation of organic polymer surfaces', *Journal of Applied Physics* **60** (1986) 3315-3322.

Teule, R., Scholten, H., van den Brink, O. F., Heeren, R. M. A., Zafiropulos, V., Hesterman, R., Castillejo, M., Martin, M., Ullenius, U., Larsson, I., Guerra-Librero, F., Silva, A., Gouveia, H., and Albuquerque, M. B., 'Controlled UV laser cleaning of painted artworks: a systematic effect study on egg tempera paint samples', *Journal of Cultural Heritage (Suppl. 1)* **4** (2003) 209s-215s.

Theodorakopoulos, C. and Zafiropulos, V., 'Uncovering of scalar oxidation within naturally aged varnish layers.' *Journal of Cultural Heritage (Suppl. 1)* **4** (2003) 216s-222s.

Theodorakopoulos, C., Zafiropulos, V., Fotakis, C., Boon, J. J., van der Horst, J., Dickmann, K., and Knapp, D., 'A study on the oxidative gradient of aged traditional triterpenoid resins using 'optimum' photoablation parameters', In *Lacona V Proceedings, Osnabrück, Germany, September 15-18, 2003*, Eds. K. Dickmann, C. Fotakis, and J. F. Asmus, Springer Proceedings in Physics, Vol. 100, Springer-Verlang, Berlin Heidelberg, (2005), 255-262.

Tornari, V., Fantidou, D., Zafiropulos, V., Vainos, N. A., and Fotakis, C., 'Photomechanical effects of laser cleaning: a long-term nondestructive holographic interferometric investigation on painted artworks'. In *Third International Conference on Vibration Measurements by Laser Techniques: Advances and Applications*, Ed. E. P. Tomasini, Vol. 3411, SPIE, (1998), 420-430.

Tornari, V., Bonarou, A., Zafiropulos, V., Fotakis, C., Smyrnakis, N. and Stassinopoulos, S., 'Structural evaluation of restoration processes with holographic diagnostic inspection'. Journal of Cultural Heritage 4 (2003) 347s-354s.

Van der Doelen, G. A., 'Molecular studies of fresh and aged triterpenoid varnishes', PhD Thesis University of Amsterdam, (1999).

Zafiropulos, V., Petrakis, J., and Fotakis, C., 'Photoablation of polyurethane films using UV laser pulses', *Optical and Quantum Electronics* **27** (1995) 1359-1376.

Zafiropulos, V., Maravelaki, P., and Fotakis, C., 'Ablation Rate studies and LIBS as an on-line control technique in the removal of unwanted selected layers', *submitted in Restauratorenblätter, Sonderband, for the proceedings of Lacona II (this extra volume of the journal was never published)* (1997).

Zafiropulos, V. and Fotakis, C. 'Lasers in the Conservation of painted Artworks'. In *Laser in Conservation: an Introduction*, Ed. M. Cooper, Butterworth Heineman, Oxford, (1998), 79.

Zafiropulos, V., Manousaki, A., Kaminari, A., and Boyatzis, S., 'Laser Ablation of aged resin layers: A means of uncovering the scalar degree of aging', *ROMOPTO: Sixth Conference on Optics, Vlad V. I. (Ed.), SPIE Vol. 4430 (SPIE The International Society for Optical Engineering, Washington, (2001) 181-185.* (2000a).

Zafiropulos, V., Galyfianaki, A., Boyatzis, S., Fostiridou, A., and Ioakimoglou, E. 'UV-laser ablation of polymerised resin layers and possible oxidation process in oil-based painting media'. In *Optics and Lasers in Biomedicine and Culture*, Ed. G. von Bally, Springer-Verlag, Berlin, (2000b), 115.

Zafiropulos, V., Stratoudaki, T., Manousaki, A., Melesanaki, K., and Orial, G., 'Discoloration of pigments induced by laser irradiation', *Surface Engineering* **17** (2001) 249-253.

Zafiropulos, V. 'Laser ablation in cleaning of artworks'. In *Optical Physics, Applied Physics and Material Science: Laser Cleaning*, Ed. B. S. Luk'yanchuk, World Scientific, Singapure, New Jersey, London, Hong Kong, (2002), 343-392.

Zergioti, I., Petrakis, A., Zafiropulos, V., and Fotakis, C., 'Laser applications in paintings conservation', *LACONA I, Restauratotenblaetter Sonderband, Wien, Austria* (1997) 57-60.

4. Spectroscopic investigations of light aged, laser-ablated natural varnishes and a copal oil varnish

Abstract

The optical properties of aged dammar, mastic and copal oil varnish films were examined on the basis of laser-induced transmission upon KrF excimer laser ablation, and subsequently with UV/VIS spectrophotometry and Attenuated Total Reflection (ATR)-FTIR of successive laser-ablated depth-steps across the films. UV laser pulsed ablation with optimal fluences, which maximise the ablation yield per laser photon (in $Å^3$/photon units), also minimises the transmission of laser light across the residual films. The laser-induced transmission at 248 nm was different across the surface layers and across the bulk layers of the natural resin films, indicating chemical changes across the depth profile of these particular aged varnishes.

UV/VIS and ATR-FTIR measurements determined these changes as well as the spectroscopic differences between the aged natural resin films and the copal oil varnish film. In particular, UV/VIS spectra of the remaining films after laser ablation indicated that the optical densities of the aged natural resin films undergo a depth-dependent gradient, while the aged copal oil varnish tested was optically saturated and absorbed equally at all depths the ambient radiation across an available wavelength range (λ > 250 nm).

ATR-FTIR showed that both absorption due to C=O stretching vibration and ratios corresponding to bending vibrations of CH_3 to CH_2 gradually decrease with depth in the aged natural resins, while these remain constant at all depths of the aged copal oil varnish film. These findings indicate that oxidation and crosslinking undergo a depth-dependent gradient across the aged natural resin films tested and are constant across the depth profile of the copal oil varnish.

The reason for these sharp differences is that natural resin films absorb the UV wavelengths of the ambient radiation in their exposed surfaces down to a depth d < 10 μm, whereas the copal oil varnish film allowed the UV wavelengths to penetrate as deep as 30 μm. In addition, the ATR-FTIR measurements on the remaining surfaces showed that there is virtually no oxidative contribution of the KrF excimer laser to the ablated varnishes.

4.1 Introduction

Nanosecond excimer laser ablation is employed for the laser cleaning of aged varnish films coating photosensitive substrates (Zafiropulos and Fotakis 1998, Zafiropulos 2002). In case of aged natural resin varnishes, such as dammar and mastic films of considerable thickness, the ablation yield per incident laser photon ($Å^3$/photon units) is eventually reduced as soon as the surface layers are removed with successive laser pulses (Theodorakopoulos, *et al.* 2005, Chapter 3). In sharp contrast, the ablation of a copal oil varnish film, aged under the same parameters as the natural varnishes tested (Section 2.7), was constant at all depths across the 30 μm film thickness. Unlike common studies on excimer laser ablation of polymers, which aim at an insight of the

interaction of the UV laser photons with organic materials (Srinivasan and Braren 1989, Luk'yanchuk, *et al.* 1993, Srinivasan 1994), laser cleaning investigations of varnish-photosensitive substrate systems aim to protect the substrate at the same time the uppermost layers of the aged coating are photoablated. If the substrate is paint, there are certain risks posed upon UV laser irradiation. In particular, the paint undergoes discolouration (Athanassiou, *et al.* 2000, Hill, *et al.* 2000, Scholten, *et al.* 2000, Zafiropulos, *et al.* 2001), which is attributed to the sharp temperature dependence in the nucleation rate on the irradiated part of the pigment particles (Luk'yanchuk and Zafiropulos 2002). Despite early suggestions implying that discolouration is also caused in the binding medium, this phenomenon has not been proved experimentally, while discolouration was observed only when inorganic pigments are incorporated in the paint (Castillejo, *et al.* 2002, Castillejo, *et al.* 2003).

During preliminary experiments for the present work (Section 1.4), it was observed that paint discolouration commenced when deep parts of an aged coating were laser ablated prior to total removal of the coating. This phenomenon indicates transmission of increasing laser light intensity through the reducing film thickness towards the substrate (Pettit, *et al.* 1994). Hence recommendations are supported, according to which a thin layer of the aged varnish must be preserved on the surface of the laser-ablated object to inhibit the transmission of the UV laser photons towards the paint (Georgiou, *et al.* 1998, Zafiropulos and Fotakis 1998, Zafiropulos 2002). In view of the potential risks, determination of transmission during excimer laser ablation has been studied alongside laser ablation rate studies of aged varnishes (Zafiropulos 2002). According to the latter work, the principle objective of such a study is the

quantification of the transmitted photon energy and the determination of the appropriate laser parameters to minimise it. Accordingly, it was determined that upon KrF excimer laser ablation of a light aged, thin mastic varnish film, the minimum transmission as a function of depth was obtained when the fluence that maximised the ablation yield per incident laser photon was employed (Zafiropulos 2002).

Taking into account early findings on excimer laser ablation of polymers, it is understood that transmission following ablation is highly depended on the degree of the excess of energy remained in the irradiated surface after the laser-induced photochemical action and the final desorption of the photofragments (Srinivasan and Braren 1989, Luk'yanchuk, *et al.* 1993, Pettit, *et al.* 1994, Srinivasan 1994). The extent of this energy excess is therefore related to the sequence of processes that determine the ablation of the material during a nanosecond laser pulse (Section 1.3.3). These processes are: (i) the degree of absorption of the laser wavelength (Luk'yanchuk, *et al.* 1993), (ii) the degree of electronic excitations in the irradiated surface (Luk'yanchuk, *et al.* 1993, Bäuerle 2000), and (iii) the extent of bond-breakage that is generated while contributing to the laser-induced shockwaves following surface excitation (Koren 1988, Kelly, *et al.* 1992, Bäuerle 2000). Besides the significance of absorption of the laser photons for the initiation of the ablation processes, it has been indicated that the extent of the laser-induced bond-breakage depends on the degree of crosslinking of the irradiated surface (Srinivasan and Braren 1989, Zafiropulos 2002).

The differences between the excimer laser ablation of aged dammar, mastic and copal oil varnish films and the ablation dissimilarities of surface and bulk layers determined

in dammar and mastic resin films (Theodorakopoulos, *et al.* 2005, Chapter 3), open up two mutually dependent aspects to be addressed, namely the excimer laser ablation and the chemistry of the material of the three case studies across their depth-profile. Since the protection of the substrate is, in practice, the principal objective for a successful laser cleaning, ablation herein is studied on the basis of laser-induced transmission through the remaining films. Therefore, quartz substrates were used. In particular, an online transmission study was carried out with the same experimental set-up, on which the dependence of laser light transmission on fluence in light aged mastic varnish films was determined (Zafiropulos 2002). In the present work, this study is employed to support the fluences chosen for the ablation of the films (Chapter 3) and subsequently to test the transmission of laser light upon ablation of surface and bulk layers using a variety of fluences.

The chemistry across the depth of the films is tested with UV/VIS spectrophotometry and Attenuated Total Reflection FTIR (ATR-FTIR). Since absorption in the UV determines the laser induced electronic excitations (Bäuerle 2000), which affect both ablation and laser-induced transmission, UV/VIS measurements across consecutive photoablated depth-steps are utilised to uncover the absorption profile of the three case studies versus depth. Finally, ATR-FTIR analysis was employed to shed some light on the micro-chemistry of the ablated surfaces across the consecutive depth-steps etched on the films. These investigations were carried out bearing in mind that absorption and crosslinking of dammar films had been observed to undergo a depth-dependent gradient (Zafiropulos, *et al.* 2000a), as was also indicated upon KrF excimer laser ablation of aged natural resin films (Chapter 3). In contrast, ablation of

the aged copal oil varnish indicated that the film was optically saturated. Online transmission and UV/VIS measurements result in mean absorption values for the remaining thicknesses, while detection of UV absorbing bands or other structural information with ATR-FTIR result in absolute values, since analysis is carried out directly on the investigated surfaces (Pemble 2000). Thus, the resulting data are expected to provide a comprehensive overview of the laser-ablated depth-profile of the tested films.

4.2 Experimental

4.2.1 On-line Transmission

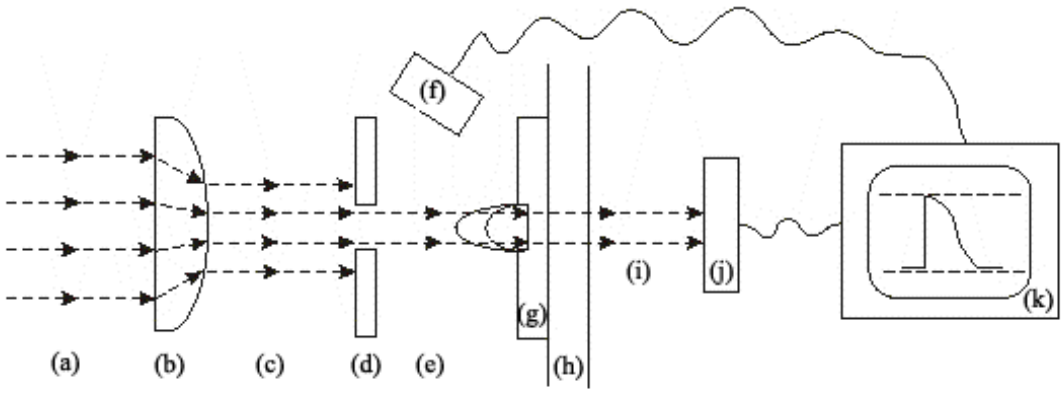

Figure 4.2.1 A schematic representation of the configuration employed for the transmission studies. The abbreviations correspond to: (a) the 248 nm laser beam emitted straight from the source; (b) the cylindrical plano-convex lens, f = + 300 mm; (c) the focused 248 nm beam; (d) the slit employed to regulate the spot size; (e) the modified laser light intensity I_0; (f) a fast photodiode; (g) the ablated aged coating; (h) the non-absorbing quartz substrate; (i) the transmitted light of intensity I_{trans}; (j) the sensitive pyroelectric energy meter; (k) the oscilloscope for the final transmission reading

A schematic representation of the configuration employed for the transmission studies is shown in Figure 4.2.1. This set-up is a simplified version of the corresponding set-up that was employed for transmission investigations on PI films (Pettit, *et al.* 1994) and is identical to the one employed by Zafiropulos (2002) for transmission experiments upon KrF excimer laser ablation of thin aged mastic films. Here, the

components of the experimental set-up were a KrF excimer laser (Lamda Physic®, COMPex series), a cylindrical plano-convex lens, f = +300 mm (Melles Griot®, high-grade quartz), a slit facing normally the laser beam, a 10.1 mV/mJ pyroelectric energy meter connected to a digital oscilloscope (LeCroy® 9400 Dual, 125MHz) and a fast photodiode to induce triggering. The substrates of the investigated samples were quartz sheets which do not absorb the transmitted laser light. The laser beam intensity behind the slit (I_o) was measured prior to positioning of the samples.

Prior to the experiment, full ablation rate studies were performed and the thickness of the films had been determined (Chapter 3). Thus, the exact number of pulses required to remove the whole film for the tested fluences was known. Upon the release of a single laser pulse, the energy of laser light transmitted (I_{trans}) was measured. For a chosen fluence, within a range of 0.25 to 1.2 J/cm^2, transmission was measured pulse after pulse in the same spot until ablation of the entire film. The transmission profile of the film was determined by plotting the transmitted energy as a function of the reducing thickness. When the entire film was laser ablated, the energy of the laser light transmitted did not coincide with the laser light intensity I_o as measured behind the slit mainly owing to reflections on the quartz substrate. This energy loss was taken into account for the final determination of transmission.

4.2.2 UV/VIS Spectrophotometry

The varnish film – quartz systems were placed in a Perkin-Elmer Lambda-19 spectrophotometer and UV/VIS spectra were determined on the aged, unaged and laser ablated depth steps of 15 μm thick films (Chapter 3) over a wavelength range of 190-600 nm. The resulting spectra of the thinnest films were reliable up to absorbance

(A) units of 2 and wavelengths longer than 250 nm. Noise in the spectra of the thickest films (10-15 μm, surface and surface steps) was generated in the 190-300 nm range, where A units were higher than 2. Mean absorption coefficients of all samples were determined at 320 nm were all the UV/VIS spectra had a clear signal.

4.2.3 Attenuated Total Reflection Fourier Transformed Infrared Spectroscopy

IR absorption was determined with a Bio-Rad FTS-6000 FTIR spectroscope connected to a Bio-Rad UMA-500 IR microscope. Single point spectra were recorded at a 4 cm^{-1} spectral resolution, an undersampling ratio (UDR) of 2 and a mirror speed of 5 kHz. A Bio-Rad slide-on ATR crystal connected to a standard 15x Cassegrain objective was employed in order to determine the IR absorption of the surfaces (aged, unaged and laser ablated steps).

4.3 Results and Discussion

4.3.1 Part I: On-line Transmission

4.3.1.1 Introduction to laser induced transmission studies

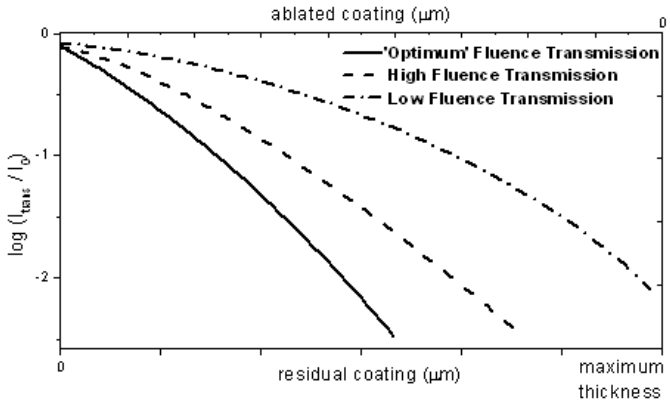

Figure 4.3.1.1 Schematic representation of characteristic plots of log (I_{trans}/I_0) versus remaining thickness or ablated material.

Figure 4.3.1.1 presents a schematic representation of transmission versus the remaining film thickness (low horizontal axis) and the ablated films thickness (upper

horizontal axis). The terms ‘low’ and ‘high’ fluences in the following text describe the fluences that are below and above the optimal fluences, as these were determined using data obtained by mean ablation rate studies (Chapter 3). Irradiation with low fluences leads to ablation of less material per incident laser photon than ablation with optimal fluences although the energy of the laser pulse remains the same (Chapter 3). Therefore, even though photochemical effects predominate upon ablation at 248 nm, using low fluences the thermal dissipation of the excited species in the irradiated surface becomes significant (Srinivasan 1994, Bäuerle 2000) and the remaining film consumes high amounts of the laser energy (Pettit, *et al.* 1994). Thus, irradiation with low fluences leads to deposition of an excess of laser photon energy in the film, which results in high transmission towards the bulk (Zafiropulos 2002). Ablation with high fluences accounts for a different problem. Increasing the fluence above the optimum increases the screening effects in the gas phase (Srinivasan, *et al.* 1986, Sutcliffe and Srinivasan 1986, Küper and Stuke 1988, Sauerbrey and Pettit 1989, Futzikov 1990, Soberhart 1993, Zafiropulos, *et al.* 1995, Zafiropulos, *et al.* 2000b). Thus, the laser light intensity that finally reaches the surface of the ablated material is significantly less than the light intensity measured on the surface prior to ablation. Hence, the surface is actually irradiated with less laser energy than in the case of optimal fluences resulting in low desorption per excited volume, while the overall low consumption of laser light leads to low transmission. However, ablation with optimal fluences leads to even lower transmission, because irradiation with these fluences maximises desorption per incident laser photon (Chapter 3) and at the same time thermal dissipation becomes significant in the desorbed photofragments rather than in the surface (Srinivasan 1994).

Zafiropulos (1999) employed Beer's Law to demonstrate the transmission of laser photon energy online with excimer laser ablation, using the following equation:

$$A = \log [(I_o - I_p) / I_{trans}] = \alpha_{mean} \cdot d \qquad (4.3.1.1)$$

where, A is the absorbance of the ablated film (in the laser wavelength); I_p the light intensity dissipated in the ablation process, the reflections on the ablated surface and the reflections on the substrate; α_{mean} the mean absorption coefficient or optical density (in the laser wavelength); and d the thickness of the irradiated film including both the ablated portion and the remaining film. Equation 4.3.1.1 becomes:

$$\log (I_{trans} / I_o) = \log [1 - (I_p / I_o)] - \alpha_{mean} \cdot d \qquad (4.3.1.2)$$

Accordingly, $\log (I_{trans} / I_o)$ is characteristic of the light transmitted to the substrate of the film (Zafiropulos 1999, 2002). Equation 4.3.1.2 indicates that the transmission slope, i.e. $\log (I_{trans} / I_0)$ versus the reducing film thickness, is negative, as also delineated in Figure 4.3.1.1. Regardless of the fluence used, the $\log (I_{trans} / I_o)$ factor is maximised when the whole film is ablated, i.e. A = 0. Because of the influence of I_p in the measured pulse-to-pulse transmission virtually none of the measurements reaches this maximum (Zafiropulos 1999). An alternative representation of a similar study has been presented for light aged dammar, mastic and copal oil varnishes, using an XeCl excimer laser in order to find the optical absorption length for the particular films (Hill, *et al.* 1999). In that case the vertical axis represented absorption of the film in the form of transmitted power and the trends had an opposite slope, which was suggested to be characteristic of the absorption coefficient of the films at 308 nm. However, it has been determined that upon ablation at 308 nm thermal effects play a

significant role in ablation of organic films (Luk'yanchuk 2002) and therefore the photochemical action is limited compared to ablation at 248 nm (Bäuerle 2000). For this reason laser ablation and online transmission in the present work are studied with a KrF excimer laser producing 25 ns pulses at 248 nm.

4.3.1.2 On-line transmission measurements at 248 nm

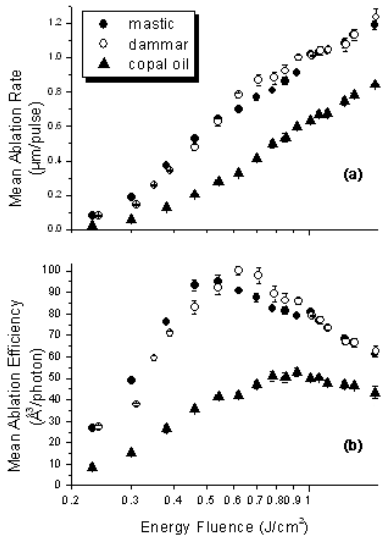

Figure 4.3.1.2.1 Laser ablation rate (a) and efficiency (b) versus fluence for 15 μm thick films of artificially aged mastic, dammar and copal oil films with KrF excimer laser. Maximum efficiency was obtained at 0.5, 0.55 and 0.9 J/cm^2 respectively (Chapter 3).

Because of the intense absorbance of the aged films in the UV (De la Rie 1988c, Van der Doelen 1999, Dietemann 2003), the initial transmission signals upon the incidence of a 248 nm laser pulse onto thick films (triterpenoids: ~ 55 μm, copal oil varnish: ~ 30 μm) were recorded after a significant amount of the films was laser ablated. The changes in the excimer laser ablation across the depth profile of the natural resins (Chapter 3) indicate that there should be significant changes in the absorption properties of these particular films, which would influence the transmission of the laser light accordingly. Hence, the presented studies were carried out to determine: (a) transmission upon ablation of 15 μm thin films representing the transmission across the surface layers, and (b) transmission upon ablation of the bulk layers using the thick samples. Figure 4.3.1.2.1 shows the mean ablation rate per pulse versus fluence of the 15 μm thin films, which was identical to that of the surface layers of the thicker films (Chapter 3). The results of the transmission studies of the 15 μm thin films are

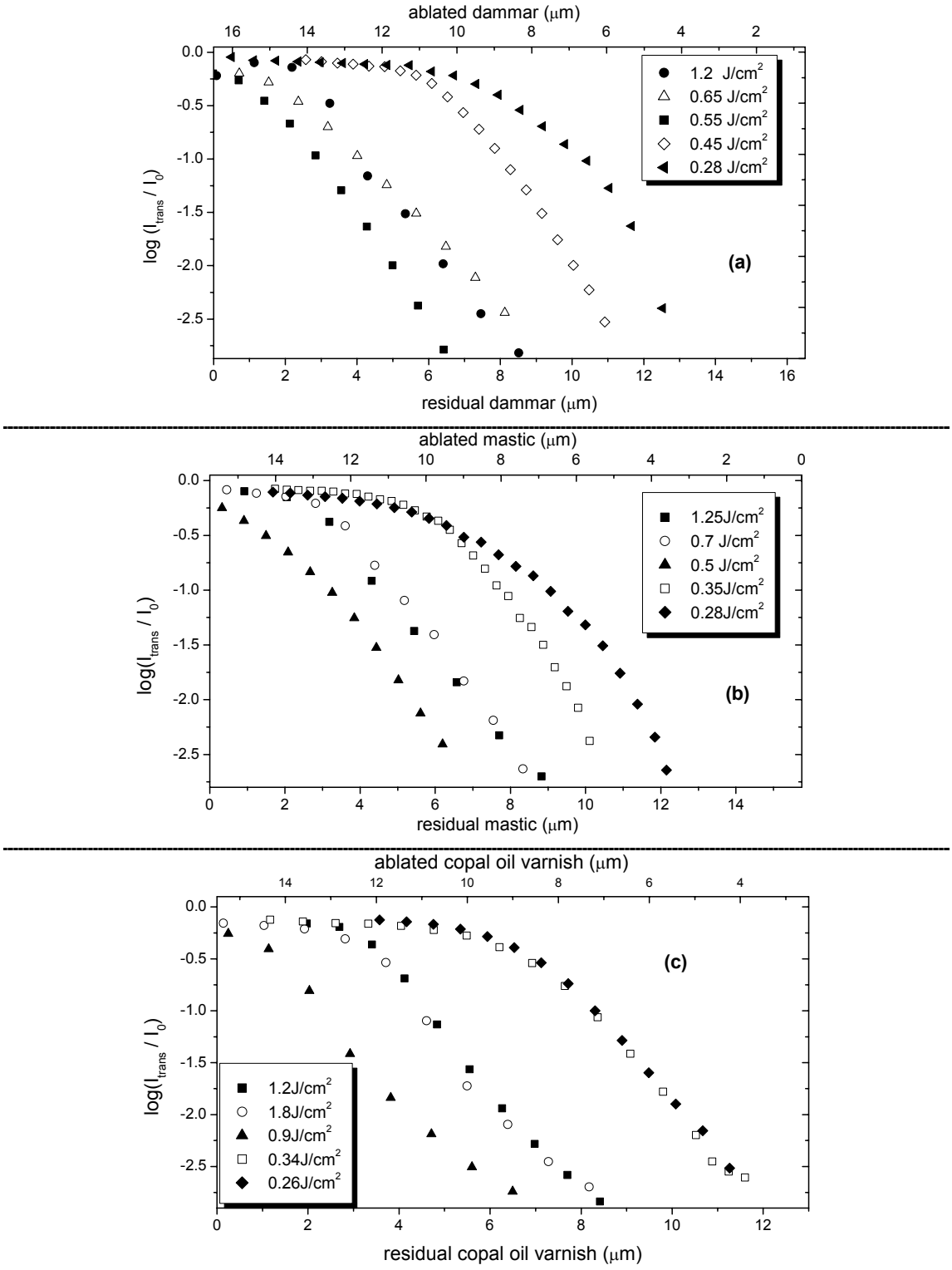

Figure 4.3.1.2.2 Transmission studies with KrF excimer laser on the artificially aged thin films of dammar (a), mastic (b) and copal oil varnish (c). The experimental error is less than 5% for the energy measurements, and consistent with the error of the ablation rate versus fluence (Figure 4.3.2.1)

presented in Figure 4.3.1.2.2. It can be observed that even the 15 μm films were thicker than required to record the first transmission signal at the first pulse. As the thickness of the films is gradually reducing the transmitted laser light intensity per pulse follows a trend that depends significantly on the optical properties across the depth of the film (Pettit, *et al.* 1994). The presented data agree with earlier findings by Zafiropulos (2002) on thin mastic films. The lowest transmission at all depths is obtained upon ablation with optimal fluences (maximum desorbed material per incident laser photon), which were 0.55, 0.52 and 0.91 J/cm^2 for the tested dammar, mastic and copal oil varnish films respectively (Figure 4.3.1.2.1b). Upon ablation with these fluences the first detectable transmission signals commenced deeper in the films (after removal of ~ 9 μm) than upon ablation with any other fluence tested. Transmission corresponding to ablation with low fluences commenced after only ~ 4 μm had been removed, while using high fluences the first transmission signal was recorded after removal of about 7 μm. Low fluences yielded increased transmission signals at all depths with broad slopes, which were gradually bending until total removal of the films. According to Zafiropulos (2002), this observation indicates the contribution of incubation effects, which cause changes of the optical properties of the ablated films (Sutcliffe and Srinivasan 1986, Küper and Stuke 1988, Meyer, *et al.* 1988, Chuang and Tam 1989, Bäuerle 2000). The trends of transmission with optimal and high fluences were similar, although the latter obtained higher transmission at all depths. Ablation with high fluences results in screening effects (Srinivasan, *et al.* 1986, Sutcliffe and Srinivasan 1986, Küper and Stuke 1988, Sauerbrey and Pettit 1989, Cain, *et al.* 1992) and maximises the photomechanical action in the surface (Srinivasan 1994, Bäuerle 2000). These effects are associated with high transmission

compared to those obtained with optimal fluences, since high fluences eventually result in low ablation yield per incident laser photon, despite the high ablation yield per pulse (Figure 4.3.1.2.1). Thus, transmission is low only when optimal fluences are used. This is also demonstrated in Figure 4.3.1.2.3, which shows the dependence of transmission, I_{trans}/I_o, on fluence for different thicknesses of dammar, mastic and copal oil varnish films. The largest remaining thicknesses showing in Figure 4.3.1.2.3 correspond to the depth-steps at which the first transmitted signal was recorded upon ablation with optimal fluences.

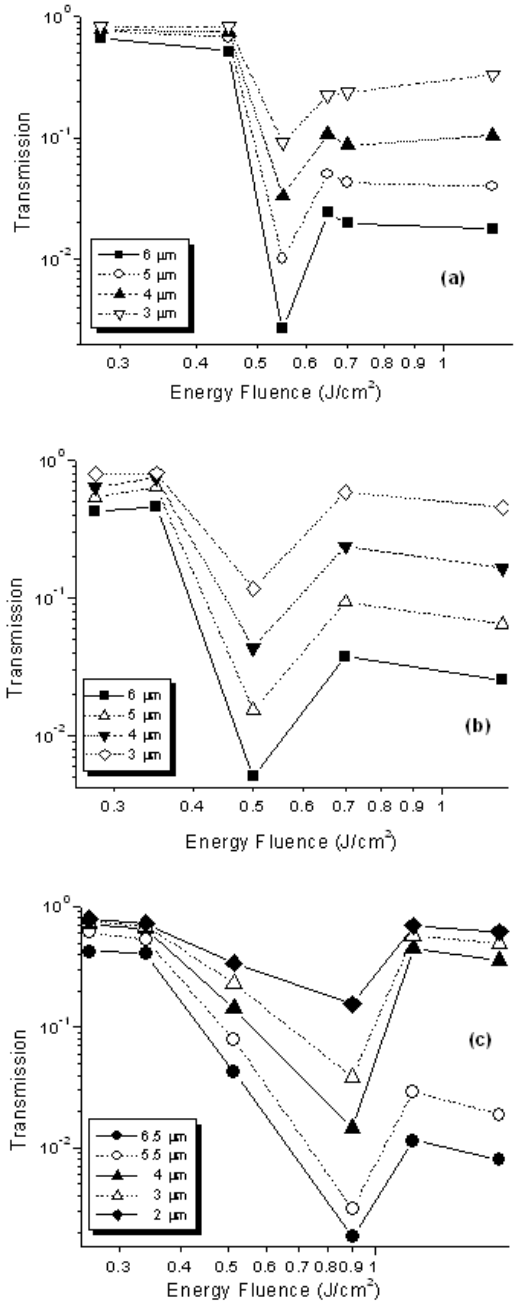

Figure 4.3.1.2.3 The logarithm of transmission versus fluence with decreasing thickness during ablation of aged dammar (a), mastic (b) and copal oil varnish (c).

Figure 4.3.1.2.4 presents the 248 nm laser light transmission as a function of depth upon ablation of ~ 55 μm thick dammar and mastic films, which were aged under the same conditions as the thinner films (Chapter 2). Transmission by the 30 μm thick copal oil varnish film was similar to that of the 15 μm shown in Figure 4.3.1.2.2c. As shown below, the latter film was optically saturated,

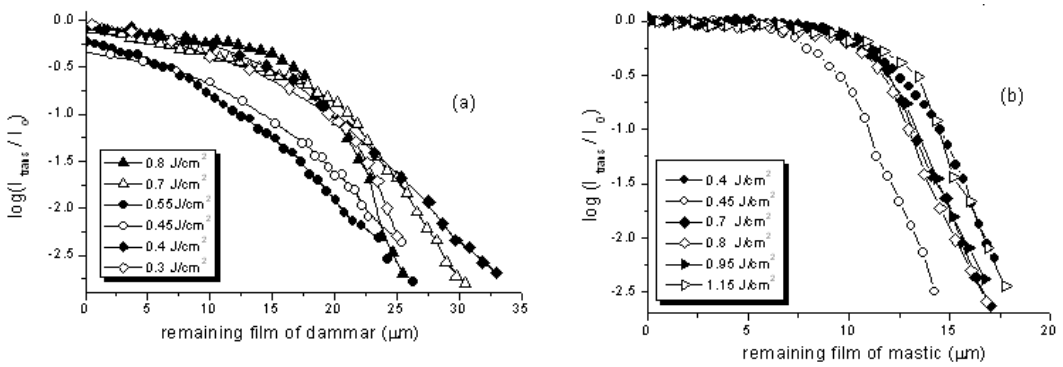

Figure 4.3.1.2.4 Transmission studies with KrF excimer laser on the artificially aged films of dammar (a), mastic (b) and copal oil varnish (c).

which explains why both ablation (Chapter 3) and transmission remain identical at the surface and in the bulk. For the thick natural resin films, it is shown that 22 and 37 μm, or 40% and ~ 70% of the original film thicknesses of dammar and mastic respectively had to be removed before any transmission signal was recorded. Thus, the results show that transmission upon ablation in the bulk of the tested films is significantly different from that upon ablation of the surface layers, in line with findings on the ablation rate (Section 3.3.3) and the ablation step (Figure 3.3.5.3). It is also observed that ablation in the bulk results in almost similar transmission slopes regardless of the fluence employed. All the transmission slopes increase abruptly as the remaining film thickness is gradually reduced. The differences compared to the surface of the films are related to the factors that change the interaction of the KrF excimer laser with the surface and bulk layers (Chapter 3). As shown below, these factors are associated with depth-dependent gradients in absorption and crosslinking in the natural resin varnish films after ageing.

4.3.2 Part II: Spectroscopic investigations on the ageing properties across depth

4.3.2.1 UV/VIS spectrophotometry across the laser ablated depth profile

UV/VIS spectrophotometry was employed to determine the optical properties of the aged dammar, mastic and copal oil varnish films, prior to and after the accelerated ageing process (Chapter 2), as well as across the consecutive laser ablated depth-steps (Chapter 3). For this particular analysis several technical and practical difficulties were encountered. First, the 55 μm and 30 μm films were too thick for sufficient light transmission across their thicknesses, which resulted in distorted absorbance spectra in the near UV wavelength range (especially in the surface and the short depth-steps of the 55 μm thick triterpenoid films). Consequently, the UV/VIS study was carried out in the ~ 15 μm thick films. The results are shown in Figures 4.3.2.1, 4.3.2.2 and 4.3.2.3. It can be seen that even these films prior to ageing were thick enough to result in high absorbencies at 250 nm, namely 2.4 for dammar, 2.9 for mastic and about 2.5 for copal oil varnish. This observation had two consequences. First, given that the maximum linear response of the spectrophotometer to absorbance was of the order of 2, after ageing the reliable readings were reduced towards longer wavelengths, since the limit of $A < 2$ was exceeded even at $\lambda < 310$ nm. Second, the resulting absorption spectra could not be strictly associated with the oxygen consumption across depth, because oxidation products, such as alcohols, ethers, saturated acids and esters absorb light with $\lambda < 250$ nm (Silverstein, *et al.* 1991). The latter case has been also encountered elsewhere (De la Rie 1988c, Dietemann 2003) and therefore such UV/VIS spectra are commonly employed for the study of yellowing, corresponding to $\lambda > 400$ nm (Chapter 2). The objective herein is the examination of the absorption

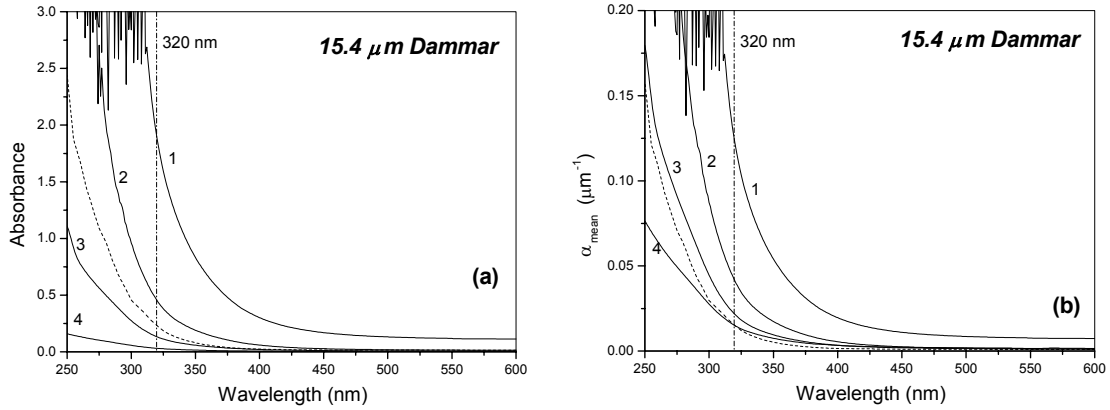

Figure 4.3.2.1 Absorbance (a) and the mean optical densities (b) of the 15.4 μm aged dammar film (1), and after KrF excimer laser ablation of 4.41 μm (2), 9.24 μm (3) and 13.33 μm (4) from the surface. Dashed lined spectra correspond to the absorption properties of the unaged film.

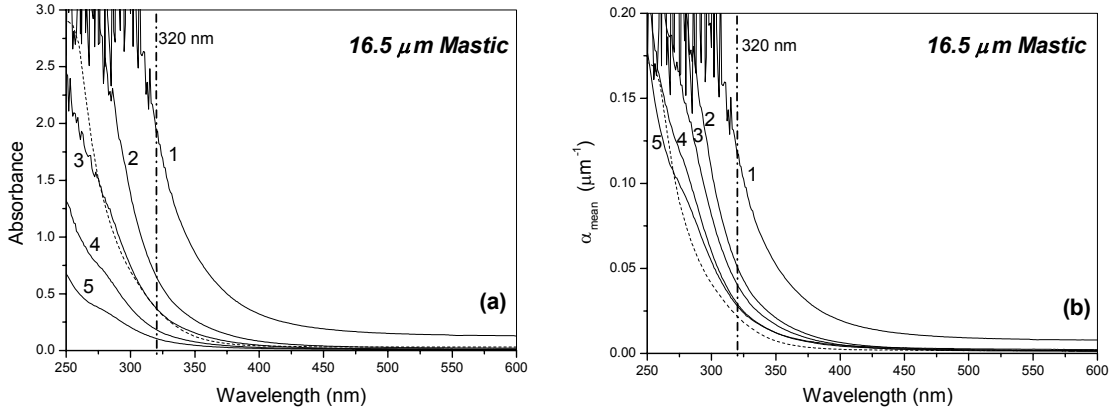

Figure 4.3.2.2 UV/VIS spectra (a) and the mean optical densities (b) of the 16.5 μm aged mastic film (1), and after KrF excimer laser ablation of 3.7 μm (2), 7.32 μm (3), 10.2 μm (4) and 12.7 μm (5) from surface. A and α_{mean} of the film before ageing is plotted in a dashed line.

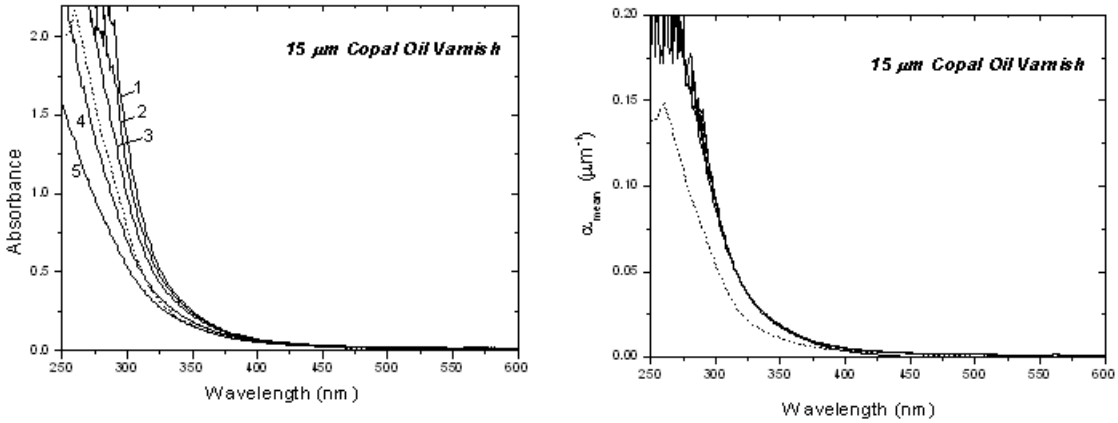

Figure 4.3.2.3 UV/VIS spectra (a) and the mean optical densities (b) of the 15 μm aged copal oil varnish film (1), and after KrF excimer laser ablation of 1.6 μm (2), 3.3 μm (3), 6 μm (4) and 7.7 μm from surface. Dashed lined spectra correspond to the absorption properties of the unaged film.

profile of the aged resin films and the copal oil varnish film as a function of depth along the range of the available wavelengths. Given the results of the excimer laser ablation (Chapter 3), the former films were expected to reveal a depth-wise gradient of their optical densities (Figures 4.3.2.1b, 4.3.2.2b), similar to findings on light aged dammar films by Zafiropulos and co-workers (2000a). In contrast, given the constant ablation step at all depths of the copal oil varnish film (Chapter 3), the latter was expected to be saturated in terms of absorption.

Starting from the unaged films, it has been demonstrated that the triterpenoid varnishes begin to absorb increasingly at $\lambda < 400$ nm. Absorption in the blue (400–490 nm) causes discolouration (De la Rie 1988c, Van der Doelen 1999, Dietemann 2003). This is attributed to unsaturated ketones and quinones that are generated during autoxidative degradation (Formo 1979). It has been determined that yellow chromophores are oxidative products (see also Section 2.2.1.3), which are present in the high MW fraction of the aged natural varnishes (De la Rie 1988c, Boon and van der Doelen 1999, Dietemann 2003). Hence, yellowing is a good indication for both oxidation and crosslinking. It is shown below that the natural resin films tested prior to ageing did not absorb significantly in the blue. In contrast, the unaged copal oil varnish absorbed increasingly from about 450 nm justifying the yellow and brownish hue of the film prior to the ageing procedure. The oxidative state of the unaged copal oil varnish and its discolouration is mainly attributed to the vigorous heat-induced (300-350 °C) pre-polymerisation process (Chapter 2), which is employed for the preparation of the oil varnish (Mantell, *et al.* 1949, Carlyle 2001). In the presence of oxygen the process leads to significant autoxidative degradation causing oxidation,

isomerisation, polymerisation, condensation and cyclisation of the oil component (Van den Berg 2002) and at the same time integration, polymerisation and rupture of the diterpenoid resin molecules (Van den Berg, *et al.* 1999). The presence of phytosterols in the oil (0.2 to 0.4% in row linseed oil) accounts for the original brownish hue (Tawn 1969, Sonntag 1979, Sultana 1996), which upon ageing becomes stronger owing to the production of yellow compounds.

After accelerated ageing, absorbencies of all the films increased for the whole range of wavelengths shown. Notably in the case of the two natural resin films, the increase in absorption in the near UV region was very pronounced, in line with the generation of highly absorbing carbonyl groups at $\lambda < 250$ nm (Silverstein, *et al.* 1991), which results in a general rise of absorption even at $\lambda > 250$ nm. At 320 nm, tails of the carbonyl groups of hydroperoxides, aliphatic acids and aldehydes affect the UV absorption of the films due to $n \rightarrow \pi^*$ transitions (Silverstein, *et al.* 1991). This is reflected in the shoulder peak at 300 – 330 nm in the UV/VIS spectra of the unaged triterpenoid films (Figures 4.3.2.1a and 4.3.2.2a) that is more pronounced in dammar. De la Rie (1988c) suggested that α,β-unsaturated carbonyl groups, which absorb between 300 and 350 nm, are present in unaged dammar. These compounds are important photoinitiators, owing to the decomposition of carbonyl and peroxide groups under the influence of UV, which then break down to free radicals (De la Rie 1988b, Scott 1993). The general rise of absorbencies along the visible wavelength range indicates scattering that is attributed to microcracking. The copal oil varnish seems to be more resistant to cracking than the resin films, since no scattering was detected in the former case. This property of oil varnishes had been rated as a

significant advantage over resin varnishes during the nineteenth century, when these oil varnishes were frequently used on paintings (Carlyle 2001). It is shown also that the overall increase in absorbance of the aged copal oil varnsh was low (Figure 4.3.2.3a), suggesting that the film was somewhat saturated even prior to ageing. It should be stressed that in all cases there should be some reservation with respect to the absorption in the blue and the extent at which this corresponds to the actual degree of ageing of the tested films. Basically, because of the intense light ageing (Chapter 2), a significant amount of yellow chromophores is bleached upon irradiation (De la Rie 1988c, Carlyle, *et al.* 1998, Dietemann 2003), although some were reformed upon storage in the dark (Chapter 2), as determined for varnishes (De la Rie 1988c, Carlyle, *et al.* 1998, Dietemann 2003) and oil media (Carlyle, *et al.* 2002).

The absorption profile across depth of the three aged films tested was studied on the laser-ablated consecutive depth-steps (Chapter 3). UV/VIS spectra were determined for the remaining 11 μm, 6 μm and 2 μm films of dammar, 13 μm, 9 μm, 6 μm and 4 μm films of mastic and 13 μm, 11 μm, 9 μm and 7 μm films of the remaining copal oil varnish film (Figures 4.3.2.1, 4.3.2.2 and 4.3.2.3). The mean absorption coefficients or optical densities, α_{mean} = A/d, at the available wavelength range across the remaining film thicknesses, d, follow two different trends (Figures 4.3.2.1b, 4.3.2.2b and 4.3.2.3b). In particular, there is a gradual reduction of the optical densities with depth in the aged dammar and mastic films. In a sharp contrast, the optical densities of the remaining copal oil varnish films remain constant regardless of the reduced thicknesses (Figure 4.3.2.3b). An example of the different trends of the optical densities at 320 nm as a function of depth is shown in Figures 4.3.2.4 and 4.3.2.5 and

Table 4.3.2.1. It is demonstrated that the gradient in the optical densities across the depth of the aged natural resin films is almost logarithmic, which is in a good agreement with earlier results (Zafiropulos, *et al.* 2000a). On the contrary, the copal oil varnish film is optically saturated.

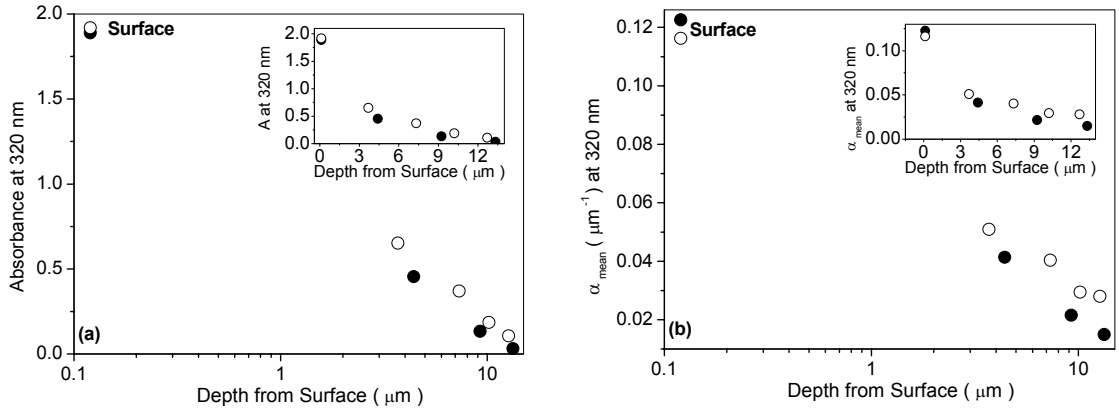

Figure 4.3.2.4 The linear decrease of absorbance (a) and mean absorption coefficients (b) at 320 nm to the logarithm of the laser ablated depth-profiles of dammar (●) and mastic (○). In the inlets A and α_{mean} at 320 nm are plotted against the uncovered depths in a linear scale. Note the optical change between the aged surfaces and the first depth-steps. All values are extracted from the UV/VIS spectra uncorrected.

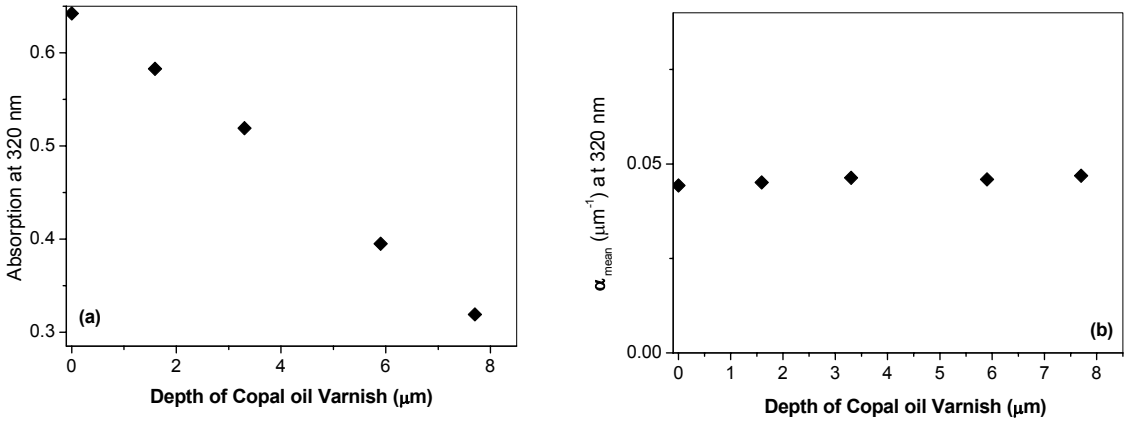

Figure 4.3.2.5 Linear absorbance decrease (a) and stable mean absorption coefficients (b) as a function of depth for the laser ablated copal oil varnish at 320 nm. The first point at 0 μm corresponds to the optical properties at the surface. The constant α_{mean} at all depths indicates optical saturation.

Table 4.3.2.1 Absorption trends of unaged, aged and laser ablated varnishes at 320 nm

Varnish	Ablated material (μm)	Thickness (μm)	Absorbance at 320 nm	Mean Absorption coefficient (μm^{-1})
Dammar	13.3	2.1	0.03	0.015
	0 (after ageing)	15.4	1.89	0.123
	4.4	11	0.45	0.041
	9.2	6.2	0.13	0.022
	0 (before ageing)	15.4	0.23	0.015
Mastic	0 (after ageing)	16.5	1.92	0.116
	3.7	12.8	0.65	0.051
	7.3	9.2	0.37	0.040
	10.2	6.3	0.18	0.029
	12.7	3.8	0.11	0.028
	0 (before ageing)	16.5	0.37	0.022
Copal Oil Varnish	0 (after ageing)	14.5	0.64	0.044
	1.6	12.9	0.58	0.045
	3.3	11.2	0.52	0.046
	5.9	8.6	0.39	0.046
	7.7	6.8	0.32	0.047
	0 (before ageing)	14.5	0.37	0.025

These trends are indicative of the optical absorption lengths ($\ell_\alpha = 1/\alpha_{mean}$) of the various wavelengths in the aged films (Figure 4.3.2.6) and the intensity of light that is transmitted across depth. Assuming the absence of gradients, the optical absorption lengths were determined from the UV/VIS spectra of the films prior to ablation (Figures 4.3.2.1b, 4.3.2.2b and 4.3.2.3b; spectra label: 1). The most reliable data corresponded to $\lambda > 320$ nm, although ℓ_α of $\lambda > 250$ nm are shown. At 320 nm the optical absorption length of the aged dammar and mastic films is of the order of 5 μm, while in copal oil varnish it is ~ 20 μm. At 350 nm, ℓ_α becomes 18 μm for dammar, 19 μm for mastic and more than 30 μm for the copal oil varnish, which is the thickness of the thick film. Light is transmitted almost intact across the total thickness of the aged thick (~ 55 μm) natural resin films at $\lambda > 400$ nm, indicating that the yellow products are either sparsely distributed across the films' depth profiles, or bleached upon the UV pulsed ablation.

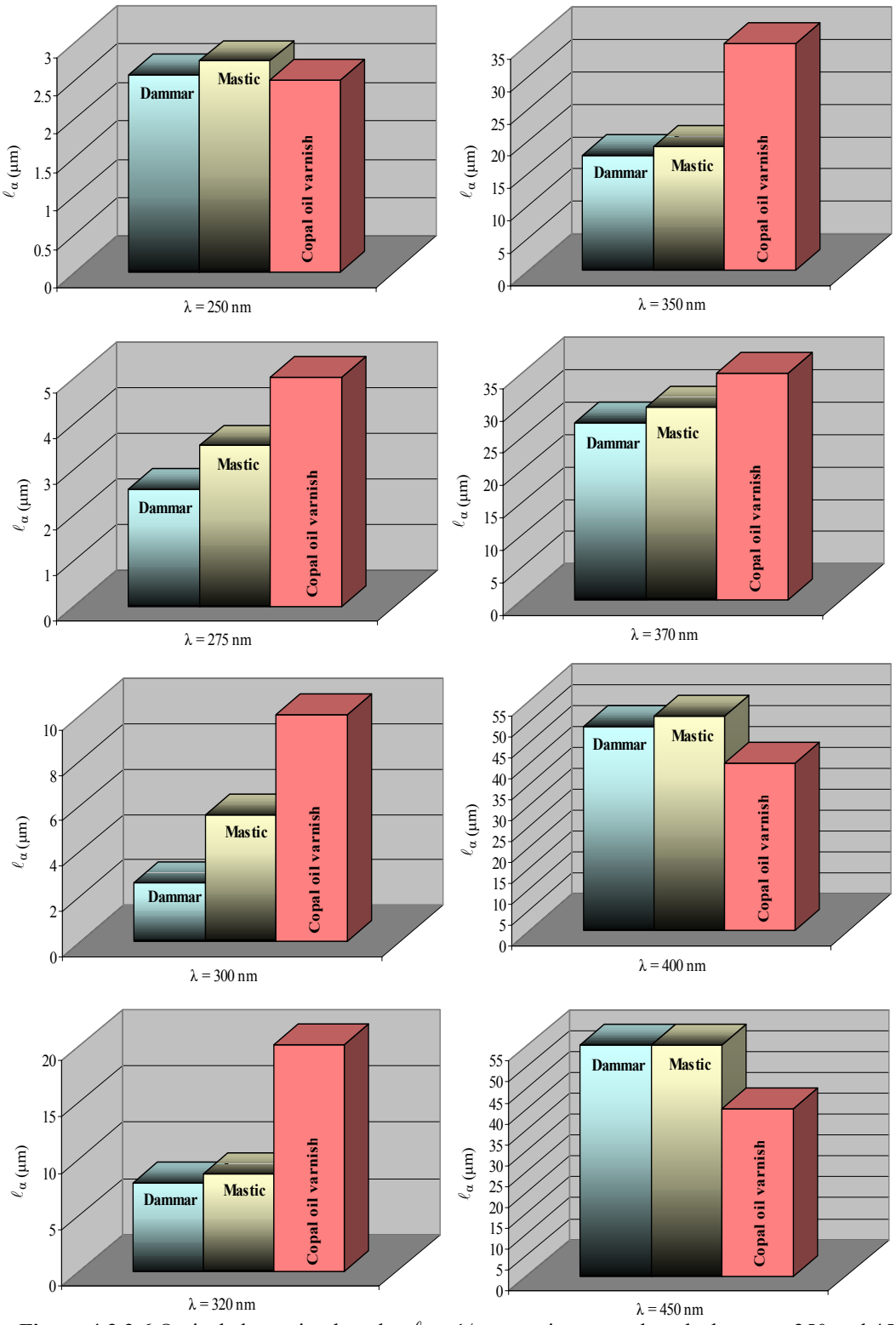

Figure 4.3.2.6 Optical absorption lengths, $\ell_\alpha = 1/\alpha$, at various wavelengths between 250 and 450 nm for the aged dammar, mastic and copal oil varnish films tested. Wavelengths λ > 320 nm provide more reliable information than λ < 320 nm. Values of α_{mean} were extracted from the UV/VIS data of ~ 15 μm films. Values of ℓ_α are shown here up to the total thicknesses of aged ~55 μm dammar and mastic and the ~ 30 μm copal oil varnish film. **The corresponding optical absorption lengths of the 248 nm laser are one order of the magnitude shorter** (Zafiropulos, et al 2000a).

The results on the natural resin films provide only an estimation of ℓ_α, since both α_{mean} and the intensity of light transmitted reduce with depth. In contrast, the ℓ_α values of the tested copal oil varnish film are more reliable since the optical densities are the same at all depths. According to these findings then, it must be highlighted that Beer's Law should not be valid for aged dammar and mastic films, if their absorption coefficients are considered to be constant across depth. Beer's Law for these particular films can only be used if their optical densities are considered as variables dependent on the depth-dependent optical gradient, as determined by Zafiropulos and co-workers (2000a).

4.3.2.2 Surface examination of the laser ablated films by Attenuated Total Reflection Fourier Transformed Infrared Spectroscopy (ATR -FTIR)

The trends determined for laser-induced transmission and UV/VIS measurements indicate that the distribution of carbonyl groups across the depths of triterpenoid resins and copal oil varnish is different. Infrared spectroscopy was required to quantify this difference and to determine the extent of absorption from the different groups, especially those containing carbonyls, which are responsible for the absorption of the 248 nm laser photons. In the present study FTIR spectra were carried out with Attenuated Total Reflection (ATR), because of the simplicity in application, requiring only contact of the ATR crystal with the investigated films (Pemble 2000). ATR-FTIR provided an investigation of the laser-ablated surfaces at the successive depth-steps. In line with earlier FTIR investigations in resins (De la Rie 1988c, Dietemann 2003) all the spectra were normalised at the ~2950 cm^{-1} peak, where absorption is attributed to the C–H stretching vibration of methylene groups. A

list of the tentative frequency assignments of the absorbing bands is presented in Table 4.3.2.2. Interpretation of the peaks was carried out using a BIO-RAD® IR-mentor pro 2.0 digital database and data by (Silverstein, *et al.* 1991).

Table 4.3.2.2 Tentative frequency assignments of the IR absorption bands in all films (aged, unaged and depth-steps)

Wavenumbers (cm^{-1})	Frequency assignment	Dammar	Mastic	Copal Oil Varnish
3400-3200	O–H stretching	√	√	√
2969-2958	C–H stretching of CH_3			√
2950, 2936, 2930	C–H stretching of CH_2	√	√	√
2870-2860	C–H stretching of CH_2	√	√	√
2380-2310	C=O asymmetric stretching of atmospheric carbon dioxide	√	√	√
1709, 1712	C=O stretching of aldehydes, ketones and carboxylic acids	√	√	
1733	C=O stretching of esters, carboxylic acids and diacids			√
1655-1640	C=C stretching of *cis* –C=C–	√	√	√
1458-1450	C–H bending of CH_2 and CH_3	√	√	√
1440-1395 and 960-875	O–H bending	√	√	√
1392-1379	C–H bending of CH_3	√	√	√
1340,1300	C–H bending of CH	√	√	√
1250	C–C stretching vibration, C–H bending in ring	√	√	
1280, 1125, 1110	C–H bending in ring	√	√	
1100	C–O stretching			√
1175	C–H bending in ring, C–O stretching in esters, C–C stretching in alkanes	√	√	
1168	C–O stretching in esters			√
1148	C–H bending in ring, C–C stretching in alkanes	√	√	
1080, 1040, 1032	C–H bending in ring, C–O stretching	√	√	
1031	C–O stretching			√
990	*trans* C–H out-of-plane deformation	√	√	
971	*cis* C–H out-of-plane deformation	√	√	√
950, 922	C–H out-of-plane deformation, (one only H attached to ring)	√	√	
891	C–H out-of-plane deformation, (two adjacent H attached to ring)	√	√	

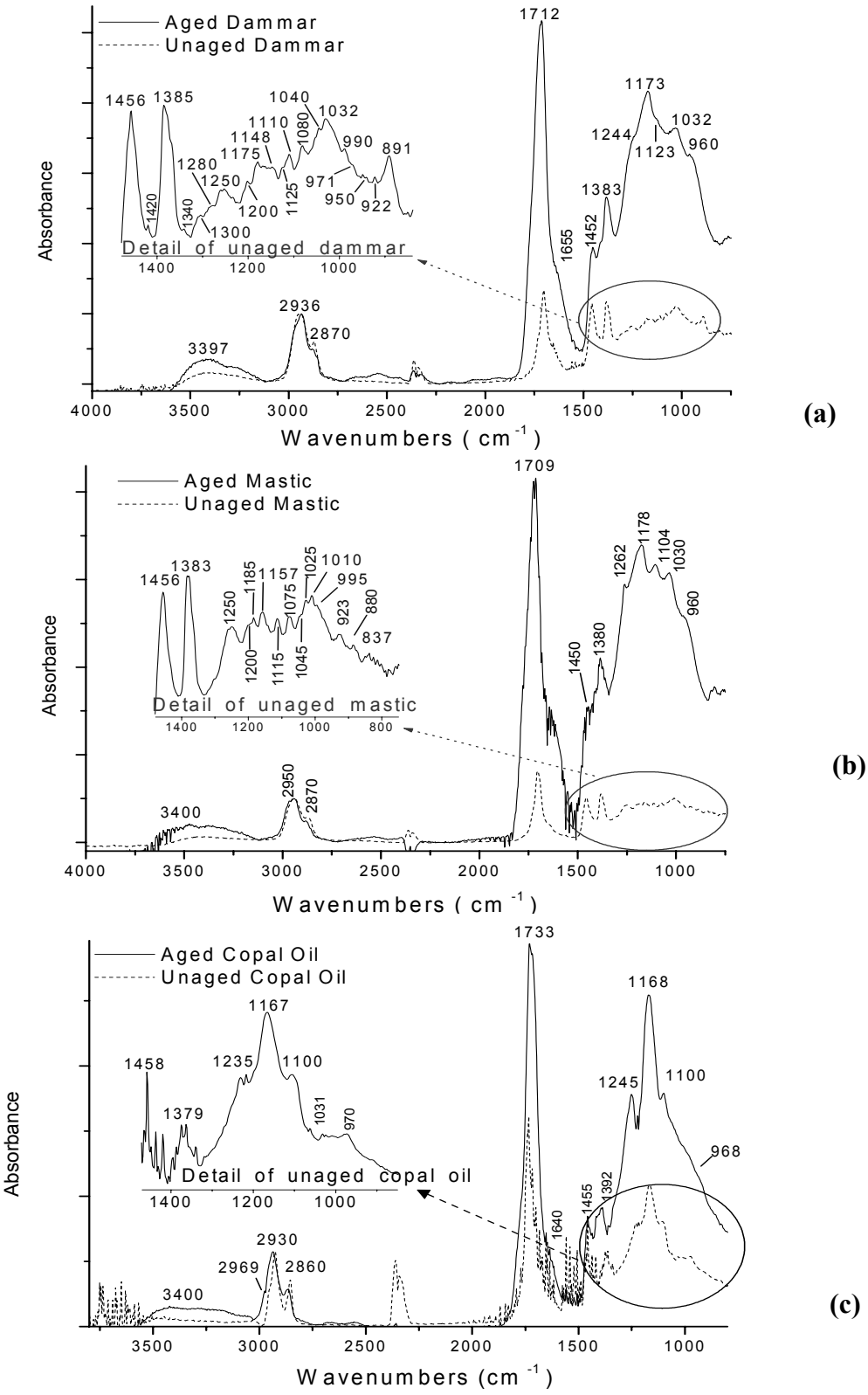

Figure 4.3.2.7 ATR-FTIR of the surfaces of the aged and unaged films of dammar (a), mastic (b) and copal oil varnish (c)

Figure 4.3.2.7a and b shows the FTIR spectra of the surface of the unaged and aged triterpenoid films prior to laser ablation. Both films show an intense increase of the ~ 1710 cm^{-1} peak, where the C=O stretching vibration of carbonyl groups of aldehydes, ketones and carboxylic acids is monitored. Ageing results in further changes of the films, as already shown on the molecular level (Chapter 2). The increase of the broad absorption band at 3400-3200 cm^{-1} attributed to O–H stretching, and at 1440-1395 and 960-875 cm^{-1} attributed to O–H bending vibrations indicates the polarity increase of both films. It should be noted that the instrument was very sensitive to humidity variations in the laboratory. Measurements were carried out in ambient conditions, and thus O–H readings were influenced accordingly. Nevertheless, the increased polarity of the films is supported by the strong peaks at 1080, 1040 and 1032 cm^{-1}, which indicate C–O stretching vibration in alcohols. The double peak at 2380-2310 cm^{-1} that is ascribed to the asymmetric stretching of C=O of the atmospheric carbon dioxide varies in intensity and broadness depending on the atmospheric conditions in the lab. Structural information for the incorporated hydrocarbon skeletons are given at peaks 1456-1450 cm^{-1} due to C–H bending vibration of methylene and methyl groups, 1385-1380 cm^{-1} due to C–H bending of CH_3, 1340 and 1300 cm^{-1} owing to CH bending, 990 and 971 cm^{-1} ascribed to *trans* and *cis* CH out-of-plane deformation respectively. In addition, absorbance peaks at 1655 and 1645 point to unsaturation, i.e. C=C stretching of *cis* –C=C–, while 1148, 1175 and 1250 cm^{-1} to C–C stretching vibrations. The latter peaks can be also ascribed to C–H bending in aromatic rings that are generally increasing upon ageing. C–H bending in rings is also detected at 1280, 1125, 1110, 1080, 1040, 1032 cm^{-1}. Peaks at 950 and 922 cm^{-1} indicate C–H out-of-

plane deformation of a hydrogen attached to aromatic rings, while 891 cm^{-1} points to C–H out-of-plane deformation of two hydrogen atoms in aromatic rings.

Changes are monitored also in the aged copal oil varnish (Table 4.3.2.2, Figure 4.3.2.7c). The spectra show that in the fingerprint region < 1300 cm^{-1} there are less peaks compared to the triterpenoids indicating lower aromaticity than in the triterpenoids. The aged film has an increased peak at 1733 cm^{-1}, which is attributed to C=O stretching frequency of carbonyl groups of esters and carboxylic acid groups of mono- and di-carboxylic acids. Some unsaturation is indicated due to a shoulder peak at 1640 cm^{-1} ascribed to *cis* –C=C– stretching. Peaks at 1458 cm^{-1} (unaged) and 1455 cm^{-1} (aged) are attributed to C–H bending of methylene and methyl groups, while peaks at ~1380 (unaged) and ~1390 cm^{-1} (aged) to C-H bending of CH_3. At peak 970 cm^{-1} a *cis* C–H out-of-plane deformation is indicated. Peaks at 1100, 1168, 1031 cm^{-1} are attributed to absorption from carbonyls. All these peaks increase significantly with age, although this increase is not as intense as in the case of the triterpenoids.

In all, the characteristic changes induced upon accelerating light ageing involve increase in polarity, formation of aromatic hydrocarbons in the triterpenoids resins, increased absorption in the UV due to the increased functionalisation, and increase in crosslinking that is detectable by comparison of peaks at ~ 1450 cm^{-1} (ascribed to CH bending of methyl and methylene groups) with peaks at 1380 cm^{-1} (due to bending of methyl groups) (Zafiropulos 2002). Figure 4.3.2.8, shows that the absorption of the various bands, which increased upon ageing, eventually decreases with depth in the aged natural resin films. This finding indicates that the composition of aged triterpenoid varnish films is shifted gradually towards a less deteriorated state with

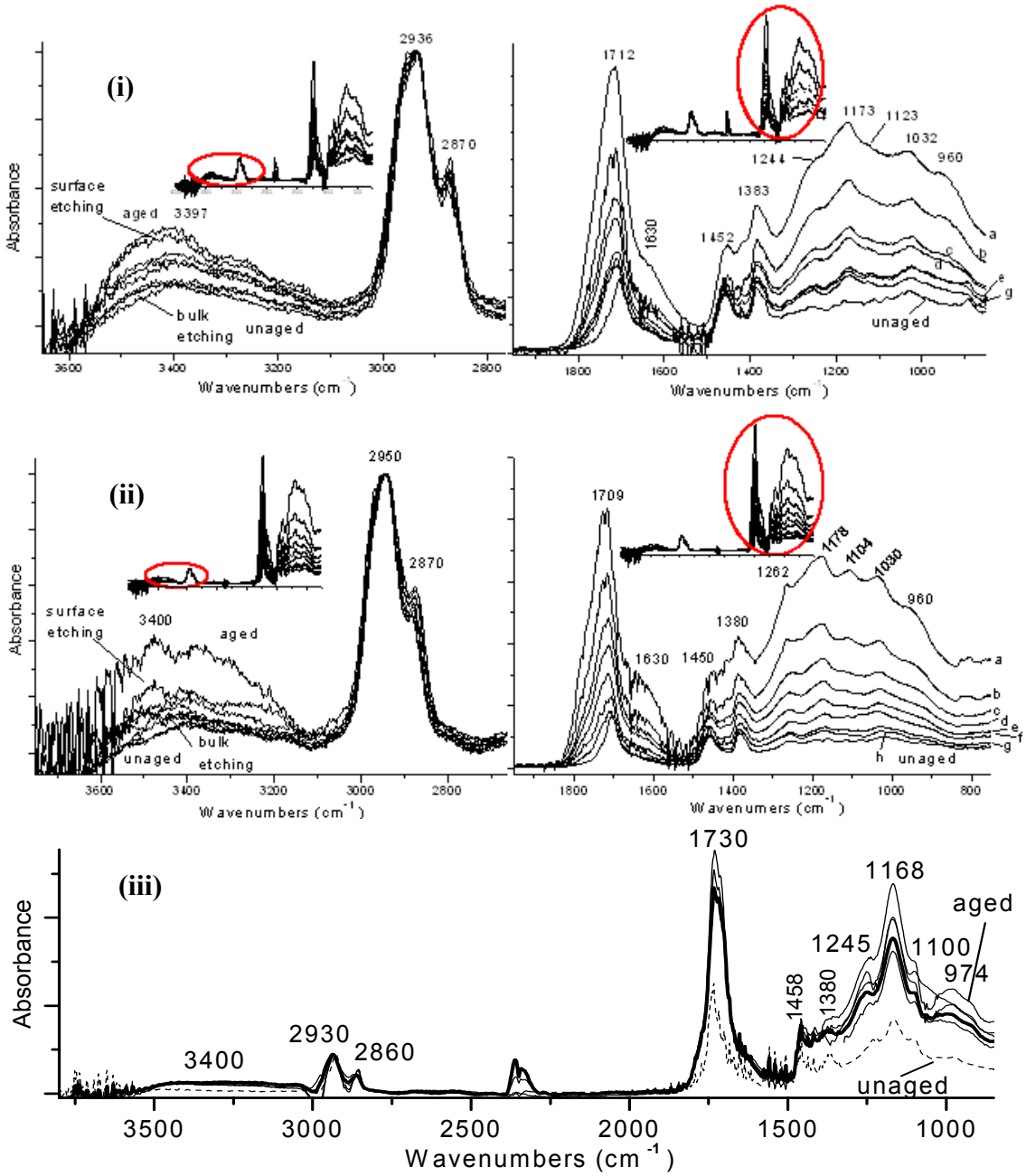

Figure 4.3.2.8 ATR-FTIR spectra of aged dammar (i), mastic (ii) and copal oil varnish (iii) on the KrF excimer laser ablated surfaces, normalised at 3100-2800 cm^{-1}. The sequence of the spectra corresponds to the aged surfaces (a), and surfaces after removal of 3.5 and 3 μm (b), 7 and 6 μm (c), 11.5 and 10 μm (d), 15 and 12 μm (e), 20 and 16 μm (f), 25 and 20 μm (g) for dammar and mastic respectively and 25 μm (h) for mastic. The spectra of the unaged surfaces are shown for comparison reasons. In copal oil varnish (iii) only the FTIR spectra of the surface and the unaged surface are discriminated clearly, while the spectra of the laser ablated surfaces coincide regardless of the thickness of the material removed.

increasing depth. Hence, recent findings on compositional gradients across the depth profile of aged resin films are supported (Zafiropulos, *et al.* 2000a,

Theodorakopoulos, *et al.* 2001, Theodorakopoulos and Zafiropulos 2003, Theodorakopoulos, *et al.* 2005). The gradual reduction of the absorbance intensities of carbonyl species that are assigned to the 1710 cm^{-1} peak reflects the changes in the absorption and transmission characteristics across the depth profile of the aged dammar and mastic films tested. In contrast, ATR-FTIR does not show significant changes across the depth profile of the aged copal oil varnish film. As shown in Figure 4.3.2.8iii there is a slight decrease in absorption in the fingerprint region < 1800 cm^{-1} at 2.95 μm below the aged surface. From that depth onwards the bulk absorption is stabilised and hence the ATR-FTIR spectra of the successive laser-ablated depth levels coincided. The different trends of the three case studies are graphically delineated in the 3D graphs of the successive FTIR spectra versus the depth-profile of each case (Figure 4.3.2.9).

The structural differences across depth of the three case studies can be also determined by comparison of peaks that are attributed to characteristic frequencies of carbonyls, methyl and methylene groups. This approach was recently published to determine the gradient of a 'naturally' aged varnish film that was laser ablated at 248 nm and analysed by micro-FTIR in a reflectance mode (Zafiropulos 2002). In that work, peaks attributed to stretching frequencies of carbonyl groups were compared with peaks attributed to bending vibrations of methyl and methylene groups. Moreover, a gradient in crosslinking of light aged (Hg-Xe radiation) dammar films with controlled thicknesses was demonstrated by comparing stretching vibrations of methyl to that of methylene groups using FTIR transmission (Kaminari 2000, Zafiropulos, *et al.* 2000a).

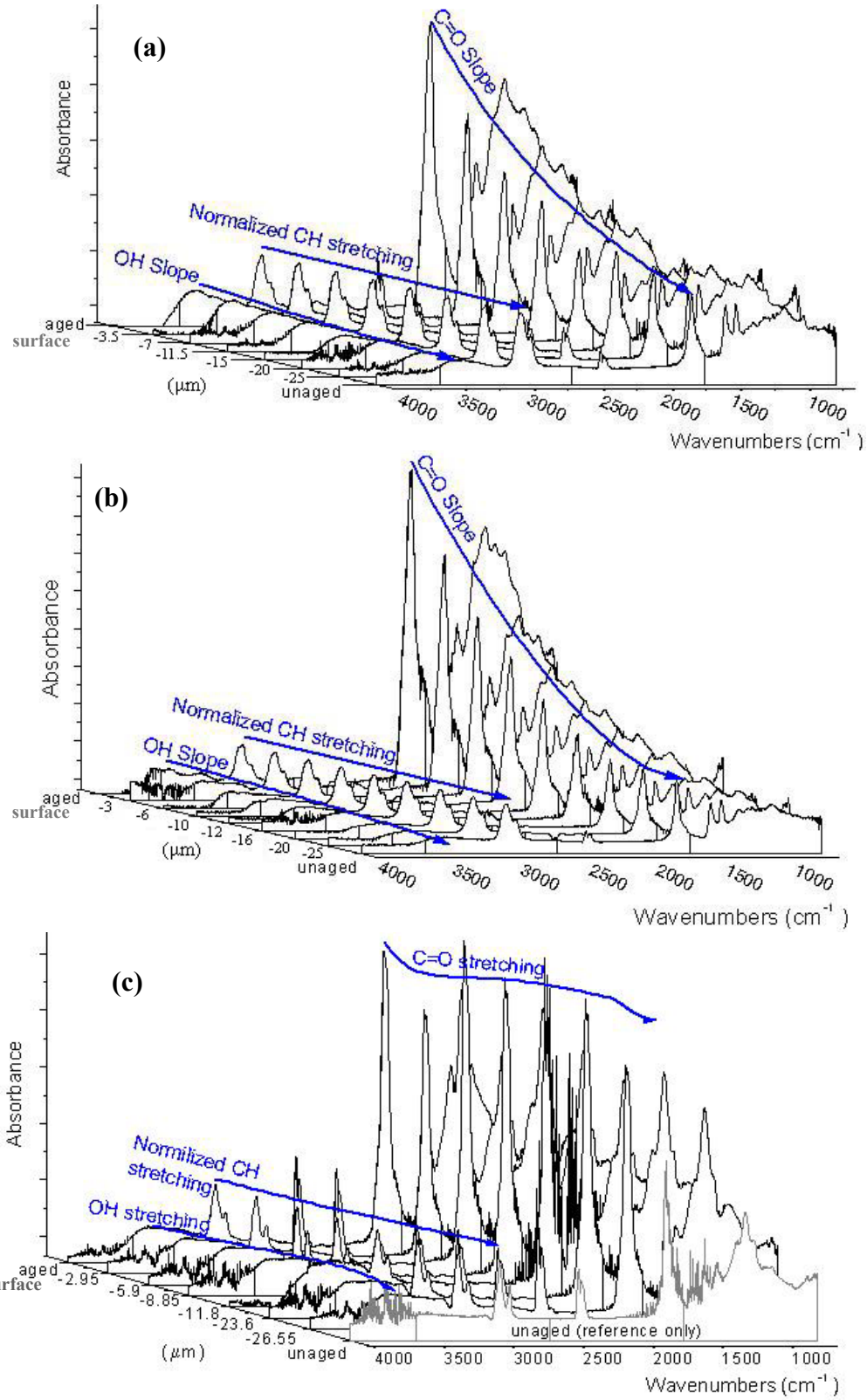

Figure 4.3.2.9 Three-dimensional plots of the ATR-FTIR spectra of dammar (a), mastic (b), and copal oil varnish (c) versus their laser ablated depth-profiles

Comparison of the C=O stretching vibrations (~1710 cm^{-1} for the triterpenoids and ~ 1730 cm^{-1} for copal oil varnish) with the normalised peaks of C–H stretching vibrations (2860-2950 cm^{-1} for the triterpenoids and 2860-2970 cm^{-1} for copal oil varnish) was carried out to illustrate the gradient in absorption. The corresponding gradient in crosslinking was illustrated by comparison of peaks at 1390-1380 cm^{-1}, where the C–H bending vibration of methyl groups is ascribed, versus peaks at 1460-1450 cm^{-1} that are attributed to C–H bending vibration of methylene groups. This way the ratio for the less crosslinked material produces a larger value than that of the highly crosslinked material due to the higher abundance of methyl than methylene groups in the former case (Zafiropulos, *et al.* 2000a). For the ease of the graphical illustration the opposite ratios were calculated for the present study, i.e. CH_2 : CH_3. Processing of the peaks involved determination of the peak areas and ratio comparison to define the relative percentages that are shown in Figure 4.3.2.10.

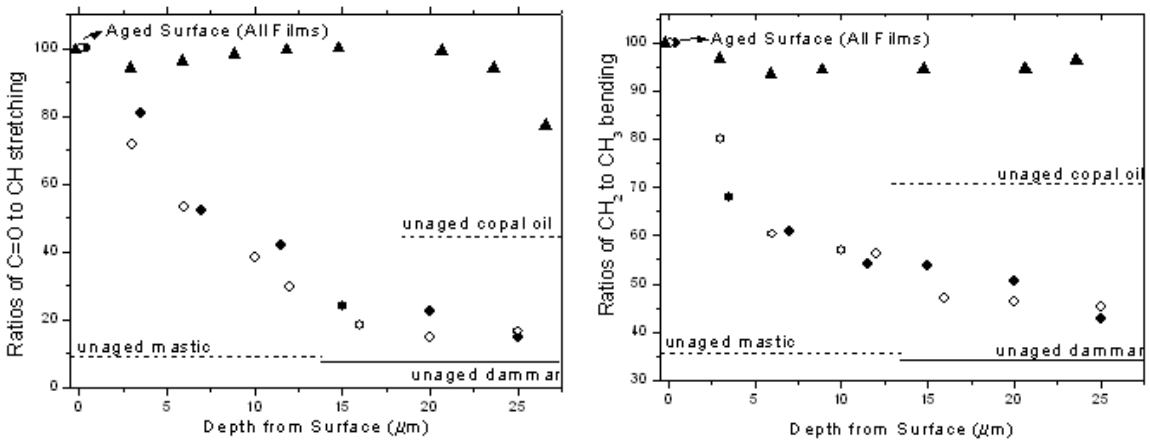

Figure 4.3.2.10 ATR-FTIR peak ratios of carbonyl groups to CH stretching vibrations (a) and CH bending of CH_2 to CH_3 (b) as a function of depth of light aged dammar (●), mastic (○) and copal oil varnish (▲). The horizontal lines delineate the corresponding ratios of the films prior to ageing.

4.4 Conclusions

KrF excimer laser ablation across the depth profile of light aged dammar, mastic and copal oil varnish films was examined on the basis of online transmission, and the optical properties of the films were determined with UV/VIS and ATR-FTIR measurements. The presented findings show that the ablated films are clearly separated in two groups as seen above in the mean laser ablation rate studies (Sections 3.3.2 and 3.3.3), the plume emission upon successive 248 nm laser pulses using LIBS (Section 3.3.4), and measurements of the etched depth-steps using laser cleaning parameters (Section 3.3.5). Namely these are the natural varnishes, dammar and mastic, which upon ageing generated a depth-dependent gradient in absorption (Figures 4.3.2.1b, 4.3.2.2b, 4.3.2.4b and 4.3.2.9a, b and 4.3.2.10a) and in crosslinking (Figure 4.3.2.10b) and a copal oil varnish film, which upon ageing (Chapter 2) did not generate gradient characteristics as a function of depth because it was optically saturated (Figures 4.3.2.3b, 4.3.2.5b, 4.3.2.9c and 4.3.2.10).

4.4.1 Laser-induced transmission at 248 nm

The results of the laser-induced transmission studies were in a good agreement with earlier findings determining that the lowest transmission at all depths is obtained using optimal fluences, which maximise the ablation yield per incident laser photon. Hence the use of optimal fluences is an essential condition for the maximum protection of the underlying layers. Since the highest transmission at all depths, regardless of the film chemistry, is obtained upon ablation with low fluences, it has been pointed out that laser cleaning at 248 nm is preferable to be carried out at high fluences, if it is not possible to determine the optimum fluence for a certain case

(Zafiropulos 2002). However, it must be stressed that much higher than the optimal fluences may cause detachments at the interface of the ablated varnish with the substrate (Zafiropulos 2002), because of the increased photomechanical action onto the irradiated surface (Srinivasan 1994, Bäuerle 2000). It is herein determined that depending on the initial film thickness and using optimal fluences, a significant portion of the thickness of the aged coatings can be removed with no transmission towards the substrate (Figures 4.3.1.2.2 and 4.3.1.2.3). Using other fluences and especially lower fluences than the optimal ones, transmission signals were obtained upon ablation of layers closer to the surface. Ablation of the aged natural resin films showed that transmission of laser light towards the bulk becomes more intense as soon as the highly absorbing and condensed surface layers are removed. Because of the significant decrease in the degrees of absorption and crosslinking with depth, which are responsible for the reduction of laser-induced bond-breakage, shockwaves and desorption of the excited photofragments (Koren 1988, Srinivasan and Braren 1989, Kelly, *et al.* 1992, Luk'yanchuk, *et al.* 1993, Srinivasan 1994, Bäuerle 2000), transmission upon ablation of the bulk is almost identical at all fluences tested (Figure 4.3.1.2.4).

In contrast, laser-induced transmission of the aged copal oil varnish using optimal fluences commenced when the remaining thickness of the film was of the order of 6.5 μm in two films tested, which had initial thicknesses of ~ 15 and ~ 30 μm. It was observed that the trends of transmission across the depth-profile of the aged copal oil varnishes with the tested range of fluences were similar to those presented upon ablation of the 15 μm thin film (Figure 4.3.1.2.2c), regardless of the initial film

thickness. This observation indicated that the copal oil varnish absorbed equally the 248 nm laser photons at all depths. Given that carbonyls of carboxylic acid groups absorb highly at 248 nm (Silverstein, *et al.* 1991), it is concluded that oxidation products with carboxylic acids (Section 2.5) were equally distributed across the whole thickness of the specific copal oil varnish, whereas the abundance of the corresponding oxidation products with carboxylic acids across the thickness of the aged dammar and mastic films (Section 2.3) decreased with depth. The data obtained with UV/VIS and ATR-FTIR were in particular enlightening.

4.4.2 Ageing properties with depth

UV/VIS measurements across the depth-profiles of the aged natural resin films showed that the existence of a depth-dependent gradient of the mean absorption coefficients at least for wavelengths longer than 250 nm (Figures 4.3.2.1 and 4.3.2.2). Although important oxygenated compounds of aged natural resins (Poehland, *et al.* 1987, De la Rie 1988a, Marner, *et al.* 1991, Koller, *et al.* 1997, Papageorgiou, *et al.* 1997, Van der Doelen, *et al.* 1998a, Van der Doelen, *et al.* 1998b, Boon and van der Doelen 1999, Van der Doelen, *et al.* 2000, Dietemann 2003, Chapter 2), such as alcohols, ethers, esters and saturated acids, absorb mainly UV light with $\lambda < 250$ nm (Silverstein, *et al.* 1991), the depth-wise changes observed at 250 – 400 nm are not irrelevant with the optical properties the films (De la Rie 1988c). In particular, α,β-unsaturated aldehydes and ketones containing conjugated carbonyl groups are responsible for the absorption across the 300 – 350 nm wavelength range (Scott 1993). At 320 nm, where the depth-dependent gradient of the mean absorption coefficients across the aged dammar and mastic films was shown (Figure 4.3.2.4),

tails of the carbonyl groups of hydroperoxides, aliphatic acids and aldehydes affect the UV absorption via $n \rightarrow \pi^*$ transitions (Silverstein, *et al.* 1991). These compounds are important photoinitiators, owing to the decomposition of carbonyl and peroxide groups under the influence of UV, which then break down to free radicals (De la Rie 1988b, Scott 1993). It is indicated herein that these compounds absorb most of the ambient light at the surface of the dammar and mastic films, reducing both the intensity and the UV wavelengths transmitted towards the bulk. Besides being UV absorbers, oxygenated compounds are products of autoxidative degradation (Scott 1993, Section 2.2.1), that is the formation of free radicals via photoinitiation and reaction with the oxygen molecules available from the ambient atmosphere (Thomson 1965, 1979, Feller 1994a). Because of the requirement of initiation reactions for the production of free radicals, it is suggested that the propagation of light in the material is the most influential factor with respect to the final oxidation and absorption profile of aged films (Feller 1994b). This is graphically delineated in the variety of the optical absorption lengths, ℓ_α, across a wavelength range spanning from 250 nm to 450 nm (Figure 4.3.2.6). The presented findings are supported by earlier findings:

- De la Rie (1988c) found that upon a similar accelerated ageing process of dammar, films with d > 10 μm were less deteriorated than thinner films.
- Boon and Van der Doelen (1999) proposed a theoretical model on the ageing of natural resins using molecular analytical data indicative of the existence of gradient. This model indicated that, owing to the strong light intensity and the abundant presence of oxygen in the surface, most of the oxidative products are

generated in the surface, while the limited presence of oxygen in the bulk results in termination reactions of free radicals producing non-oxidative crosslinks.

– Zafiropulos and co-workers (2000a) showed that the optical densities of a wide range of identically aged dammar films increased with decreasing thickness.

– Solubility tests of laser ablated, naturally aged varnishes on paintings using a KrF excimer laser and a mixture of cleaning solvents showed that polarity decreases as a function of depth (Theodorakopoulos and Zafiropulos 2003, Section 1.4).

– Dietemann (2003) determined that the abundance of free radicals in fresh mastic resin teardrops, harvested in the same period, increases as the teardrops decrease in size, indicating that mastic blocks the propagation of light in the bulk.

Since the propagation of light and especially of the UV wavelengths across the depth-profile of natural resins is limited in the surface layers, condensation reactions leading to polymerisation and crosslinking are also reduced with depth. This is indicated by findings based on ATR-FTIR measurements showing that apart from the decreasing intensities of C=O stretching vibrations with depth (Figures 4.3.2.9a, b and 4.3.2.10a), there is also a gradual reduction of ratios corresponding to bending vibrations of CH_2 to CH_3 with depth (Figure 4.3.2.10b). This finding is in a very good agreement with earlier results on a wide range of dammar films examined by Zafiropulos and co-workers (2000a). The fact that the depth-dependent gradient characteristics of the aged dammar and mastic films, and especially the reducing trends of absorption, were determined with ATR-FTIR (Pemble 2000) directly on the surfaces of the consecutive

laser-ablated depth-steps, indicates that the films were not degraded further upon the interaction with the UV laser photons.

As mentioned above, the copal oil varnish film tested was optically saturated (Figures 4.3.2.3c, 4.3.2.5b, 4.3.2.9c and 4.3.2.10a), while the degree of polymerisation remained unchanged for the largest part of its thickness (Figure 4.3.2.10b). It is suggested that this phenomenon is based on the pre-polymerisation process employed for oil varnishes requiring vigorous boiling at strong temperatures (300-350 °C) (Mantell, *et al.* 1949, Carlyle 2001). Thus, the starting film is already polymerised and oxidised (Section 2.5) and its absorption properties do not actually change significantly upon ageing (Figure 4.3.2.3c). Measuring the light penetrating the aged film (Figure 4.3.2.6) it is shown that wavelengths longer than 320 nm abundantly penetrated the thickest film tested, while the natural resins absorbed light with $\lambda < 350$ nm in their uppermost 15 μm. These observations show that the oil varnish apart from being saturated is also a weak UV absorber, indicating that compared to natural resin varnishes, oil varnishes provide poor protection from UV wavelengths of the ambient radiation to the substrate.

In conclusion, ageing of natural resin films leads to formation of absorption and crosslinking gradients across depth. This has been determined by the laser light transmitted upon ablation with a KrF excimer laser as well as by UV/VIS and ATR-FTIR measurements on the ablated depth-steps. These findings indicate that natural resin varnishes protect the underlying substrate from the ambient UV wavelengths if they are thicker than 10-15 μm. For the excimer laser cleaning of paintings varnished with natural resins, it must be highlighted that laser-induced transmission becomes

stronger as ablation proceeds onto deep parts of the varnish, and longer than indicated by the optical absorption length measured at the deteriorated surfaces. In order to protect photosensitive substrates, laser cleaning must be terminated as soon as the highly degraded surface layers are removed. The pre-polymerisation process and the subsequent ageing of the copal oil varnish tested resulted in a low absorbing coating that was optically saturated and almost equally polymerised at all depths. In terms of laser light transmission it was shown that despite the overall low absorbing properties of the film, a layer of thickness equivalent to the constant optical absorption length is enough to filter the laser photons when optimal fluences are used.

4.5 References

Athanassiou, A., Hill, A. E., Fourrier, T., Burgio, L., and Clark, R. J. H., 'The effects of UV laser light radiation on artist's pigments', *Journal of Cultural Heritage (Suppl. 1)* **1** (2000) s209-s213.

Bäuerle, D. *Laser Processing and Chemistry, Third, revised and enlarged edition*, Springer-Verlag, Berlin, Heidelberg, New York, 2000.

Boon, J. J. and van der Doelen, G. A. 'Advances in the current understanding of aged dammar and mastic triterpenoid varnishes on the molecular level'. In *Firnis: Material - Aesthetik - Geschichte, International Kolloquium, Braunschweig, 15-17 Juni 1998*, Ed. A. Harmssen, Hertog-Anton-Ulrich-Museum, Braunschweig, (1999), 92-104.

Cain, S. R., Burns, F. C., and Otis, C. E., 'On single-photon ultraviolet ablation of polymeric materials', *Journal of Applied Physics* **71** (1992) 4107-4117.

Carlyle, L., Binnie, N., Van der Doelen, G. A., Boon, J. J., McLean, B., and Ruggles, A. 'Traditional painting varnishes project: preliminary report on natural and artificial aging and a note on the preparation of cross-sections.' In *Firnis, Material Aesthetik Geschichte, International Kolloquium*, Braunschweig, (1998), 110-127.

Carlyle, L., Binnie, N., Kaminska, E., and Ruggles, A. 'The yellowing/bleaching of oil paints and oil paint samples, including the effect of oil processing, driers and mediums on the colour of lead white paint'. In *Preprints of the 13th triennial meeting of the ICOM Committee for Conservation*, Ed. R. Vontobel, Vol. I, James & James Ltd, Rio de Janeiro, (2002), 328-337.

Carlyle, L. A. *The artist's assistant: Oil painting Instruction manuals and handbooks in Britain 1800-1900: with reference to selected eighteenth century sources*, Archetype Publications, London, 2001.

Castillejo, M., Martin, M., Oujja, M., Silva, D., Torres, R., Manousaki, A., Zafiropulos, V., van den Brink, O. F., Heeren, R. M. A., Teule, R., Silva, A., and Gouveia, H., 'Analytical study of the chemcial and physical changes induced by KrF laser cleaning of tempera paints', *Analytical Chemistry* **74** (2002) 4662-4671.

Castillejo, M., Martin, M., Oujja, M., Santamaria, J., Silva, D., Torres, R., Manousaki, A., Zafiropulos, V., van den Brink, O. F., Heeren, R. M. A., Teule, R., and Silva, A., 'Evaluation of the chemical and physical changes induced by KrF laser irradiation of tempera paints', *Journal of Cultural Heritage (Suppl. 1)* **4** (2003) 257s-263s.

Chuang, M. C. and Tam, A. C., 'On the saturation effect in the picosecond near ultraviolet laser ablation of polyimide', *Journal of Applied Physics* **65** (1989) 2591-2595.

De la Rie, E. R., 'Stable Varnishes for Old Master Paintings', PhD Thesis University of Amsterdam, (1988a).

De la Rie, E. R., 'Polymer Stabilizers. A survey with reference to possible applications in the conservation field', *Studies in Conservation* **33** (1988b) 9-22.

De la Rie, E. R., 'Photochemical and thermal degradation of films of dammar resin', *Studies in Conservation* **33** (1988c) 53-70.

Dietemann, P., 'Towards more stable natural resin varnihses for painintgs', PhD Thesis Swiss Federal Institute of Technology, Zurich, (2003).

Feller, R. L. 'Depth of Penetration of Light into Coatings; and Influence of Sample Thickness and Oxygen Diffusion'. In *Accelerated Aging: Photochemical and Thermal Aspects*, Ed. D. Berland, The Getty Conservation Institute, USA, (1994a), 56-61 and 135-137.

Feller, R. L. 'Depth of Penetration of Light into Coatings'. In *Accelerated Aging: Photochemical and Thermal Aspects*, Ed. D. Berland, The Getty Conservation Institute, USA, (1994b), 56 - 61.

Formo, M. W. 'Paints, varnishes and related products: Discolouration'. In *Baile's Industrial Oil and Fat Products*, Ed. D. Swern, Vol. 1, John Wiley & Sons, New York, (1979), 722-724.

Futzikov, N. P., 'Approximate theory of highly absorbing polymer ablation by nanosecond laser pulses', *Applied Physics Letters* **56** (1990) 1638-1640.

Georgiou, S., Zafiropulos, V., Tornari, V., and Fotakis, C., 'Mechanistic Aspects of Excimer Laser Restoration of Painted Artworks', *Laser Physics* **8** (1998) 307-312.

Hill, A. E., Fourrier, T., Anderson, J., Athanassiou, A., and Whitehead, C., 'Measurement of the light absorption length of 308nm pulsed laser light in artificially aged varnishes'. In *ICOM Commitee for Conservation*, (1999), 299-303.

Hill, A. E., Athanassiou, A., Fourrier, T., Anderson, J., and Whitehead, C., 'Progress in the use of excimer lasers to clean easel paintings'. In *Proceedings of the 5th International Conference on Optics Within Life Sciences (OWLS V)*, Eds. C. Fotakis, T. G. Papazoglou, and C. Kalpouzos, Springer Verlag, Aghia Pelagia, Crete, Greece, 1998, (2000), 203-207.

Kaminari, A. A., 'Determination of polymerisation in dammar, with the assistance of laser-induced removal, in artifically aged samples of controlled thickness.' Diploma Dissertation, Department of conservation of Antiquities and Artworks, Technological Educational Institute, Athens, (2000).

Kelly, R., Miottello, A., Braren, B., and Otis, C. E., 'On the debris phenomenon with laser sputtered polymers', *Applied Physics Letters* **60** (1992) 2980-2982.

Koller, J., Baumer, U., Grosser, D., and Schmid, E. 'Mastic'. In *Baroque and Rococo Lascquers*, Ed. J. Koller, Vol. 81, Arbeitshefte des Bayerischen Landesamtes fuer Denkmalpflege, Karl M. Lipp Verlag, Muenchen, (1997), 347-358.

Koren, G., *Appl. Phys B* **46** (1988) 147.

Küper, S. and Stuke, M., 'Femtosecond UV excimer laser ablation', *Applied Physics B* **44** (1988) 199-201.

Luk'yanchuk, B., Bityurin, N., Anisimov, S., and Bauelre, D., 'The role of excited species in UV-Laser Material Ablation, Part I: Photophysical Ablation of Organic Polymers', *Applied Physics A* **57** (1993) 367-374.

Luk'yanchuk, B. and Zafiropulos, V. 'On the theory of discolouration effect in pigments at laser cleaning'. In *Optical Physics, Applied Physics and Material Science: Laser Cleaning*, Ed. B. S. Luk'yanchuk, World Scientific, Singapure, New Jersey, London, Hong Kong, (2002), 393-414.

Luk'yanchuk, B. S. Optical Physics, Applied Physics and Material Science: Laser Cleaning, World Scientific, Singapure, New Jersey, London, Hong Kong (2002).

Mantell, C. L., Kopf, C. W., Curtis, J. L., and Rogers, E. M. 'Oil Varnishes'. In *The technology of natural resins*, John Wiley & Sons, Inc., (1949), 265-319.

Marner, F.-J., Freyer, A., and Lex, J., 'Triterpenoids from gum mastic, the resin of Pistacia Lentiscus', *Phytochemistry* **30** (1991) 3709-3712.

Meyer, J., Feldeman, D., Kutzner, J., and Welge, K., *Appl Phys B* **45** (1988) 7.

Papageorgiou, V. P., Bakola-Christianopoulou, M. N., Apazidou, K. K., and Psarros, E. E., 'Gas chromatographic-mass spectrometric analysis of the acidic triterpenic fraction of mastic gum', *Journal of Chromatography A* **769** (1997) 263-273.

Pemble, M. 'Vibrational Spectroscopy form Surfaces'. In *Surface Analysis*, Ed. J. C. Vickerman, John Willey & Sons, (2000), 273-275.

Pettit, G. H., Ediger, M. N., Hahn, D. W., Brinson, B. E., and Sauerbrey, R., 'Transmission of polyimide during pulsed ultraviolet laser irradiation', *Appl. Phys. A* **58** (1994) 573.

Poehland, B. L., Carte, B. K., Francis, T. A., Hyland, L. J., Allaudeen, H. S., and Troupe, N., 'In vitro antiviral activity of dammar resin triterpenoids', *Journal of Natural Products* **50** (1987) 706-713.

Sauerbrey, R. and Pettit, G. H., 'Theory of the etching of organic materials by ultraviolet laser pulses', *Applied Physics Letters* **55** (1989) 421-423.

Scholten, J. H., Teule, J. M., Zafiropulos, V., and Heeren, R. M. A., 'Controlled laser cleaning of painted artworks using accurate beam manipulation and on-line LIBS-detection', *Journal of Cultural Heritage (Suppl. 1)* **1** (2000) s215-s220.

Scott, G. 'Autoxidation and antioxidants: historical perspective'. In *Atmospheric oxidation and antioxidants*, Ed. G. Scott, Vol. I, Elsevier Science Publishers B.V., Amsterdam, (1993), 1 - 44.

Silverstein, R. M., Bassler, G. C., and Morrill, T. C. 'Ultraviolet Spectrometry'. In *Spectrometric Identification of Organic Compounds, 5th edition*, John Wiley and Sons, Inc., USA, (1991), 289-315.

Soberhart, J. R., 'Polyamide ablation using intense laser beams', *Journal of Applied Physics* **74** (1993) 2830-2833.

Sonntag, N. O. V. 'Structure and composition of oil and fats'. In *Bailey's industrial oil and fat products*, Ed. D. Swern, Vol. 1, John Wiley & Sons, New York, (1979), 45-83.

Srinivasan, R., Braren, B., Seeger, D. E., and Dreyfus, R. W., 'Photochemical cleavage of a polymeric solid: details of the ultraviolet laser ablation of poly(methyl methacrylate) at 193 nm and 248 nm', *Macromolecules* **19** (1986) 916-921.

Srinivasan, R. and Braren, B., 'Ultraviolet laser ablation of organic polymers', *Chemical Reviews* **89** (1989) 1303-1316.

Srinivasan, R. 'Interaction of laser radiation with organic polymers'. In *Laser Ablation: Principles and Applications*, Ed. J. C. Miller, Vol. 28, Springer Series of Material Science, Springer, Berlin, Heidelberg, (1994), 107.

Sultana, C. 'Oleaginous flax'. In *Oils & Fats Manual*, Ed. J.-P. Wolff, Vol. 1, Intercept Ltd., Andover, (1996), 154-168.

Sutcliffe, E. and Srinivasan, R., 'Dynamics of UV laser ablation of organic polymer surfaces', *Journal of Applied Physics* **60** (1986) 3315-3322.

Tawn, A. R. H. 'Solvents, oils, resins and driers'. In *Paint technology manuals*, Ed. A. R. H. Tawn, Vol. 2, Chapman and Hall, London, (1969), 142-156.

Theodorakopoulos, C., Zafiropulos, V., and Phenix, A. 'UV Aging of Varnish: Gradient in Degradation'. In *Cost Action G7 Workshop*, Heraklion, Crete 18 - 21 October, (2001).

Theodorakopoulos, C. and Zafiropulos, V., 'Uncovering of scalar oxidation within naturally aged varnish layers.' *Journal of Cultural Heritage (Suppl. 1)* **4** (2003) 216s-222s.

Theodorakopoulos, C., Zafiropulos, V., Fotakis, C., Boon, J. J., van der Horst, J., Dickmann, K., and Knapp, D., 'A study on the oxidative gradient of aged traditional triterpenoid resins using 'optimum' photoablation parameters', In *Lacona V Proceedings, Osnabrück, Germany, September 15-18, 2003*, Eds. K. Dickmann, C. Fotakis, and J. F. Asmus, Springer Proceedings in Physics, Vol. 100, Springer-Verlang, Berlin Heidelberg, (2005), 255-262.

Thomson, G. 'Topics in the conservation chemistry of surface.' In *Application of Science in Examination of Works of Art*, Museum of Fine Arts, Boston, (1965), 78 - 85.

Thomson, G., 'Penetration of Radiation into Paint Films', *National Gallery Technical Bulletin* **Vol. 3** (1979) 25 -33.

Van den Berg, J. D. J., 'Analytical chemical studies on traditional linseed oil paints', PhD Thesis University of Amsterdam, (2002).

Van den Berg, K. J., Van der Horst, J., and Boon, J. J., 'Recognition of copals in aged resin paints and varnishes'. In *Preprints ICOM Committee for Conservation 12th Triennial Meeting, Lyon, France, 29 Aug. - 3 September 1999*, Vol. II, James & James, London, (1999), 855-861.

Van der Doelen, G. A., van den Berg, K. J., and Boon, J. J., 'Comparative chromatographic and mass spectrometric studies of triterpenoid varnishes: fresh material and aged samples from paintings', *Studies in Conservation* **43** (1998a) 249-264.

Van der Doelen, G. A., Van der Berg, K. J., Boon, J. J., Shibayama, N., De la Rie, E. R., and Genuit, W. J. L., 'Analysis of fresh triterpenoid resins and aged triterpenoid varnishes by high-performance liquid chromatography-atmospheric pressure chemical ionisation (tandem) mass spectrometry', *Journal of Chromatography A* **809** (1998b) 21-37.

Van der Doelen, G. A., 'Molecular studies of fresh and aged triterpenoid varnishes', PhD Thesis University of Amsterdam, (1999).

Van der Doelen, G. A., Van den Berg, K. J., and Boon, J. J., 'A comparison of weatherometer aged dammar varnish and aged varnishes from paintings'. In *Art Chimie: La Couleur: Actes du Congres*, Ed. J.-P. Mohen, CNRS Editions, Paris, (2000), 146-149.

Zafiropulos, V., Petrakis, J., and Fotakis, C., 'Photoablation of polyurethane films using UV laser pulses', *Optical and Quantum Electronics* **27** (1995) 1359-1376.

Zafiropulos, V. and Fotakis, C. 'Lasers in the Conservation of painted Artworks'. In *Laser in Conservation: an Introduction*, Ed. M. Cooper, Butterworth Heineman, Oxford, (1998), 79.

Zafiropulos, V., 'Internal IESL-FORTH report for "Advanced Workstation for Controlled laser Cleaning of Artworks" ENV4-CT98-0787', (1999).

Zafiropulos, V., Manousaki, A., Kaminari, A., and Boyatzis, S., 'Laser Ablation of aged resin layers: A means of uncovering the scalar degree of aging', *ROMOPTO: Sixth Conference on Optics, Vlad V. I. (Ed.), SPIE Vol. 4430 (SPIE The International Society for Optical Engineering, Washington, (2001) 181-185.* (2000a).

Zafiropulos, V., Galyfianaki, A., Boyatzis, S., Fostiridou, A., and Ioakimoglou, E. 'UV-laser ablation of polymerised resin layers and possible oxidation process in oil-based painting media'. In *Optics and Lasers in Biomedicine and Culture*, Ed. G. von Bally, Springer-Verlag, Berlin, (2000b), 115.

Zafiropulos, V., Stratoudaki, T., Manousaki, A., Melesanaki, K., and Orial, G., 'Discoloration of pigments induced by laser irradiation', *Surface Engineering* **17** (2001) 249-253.

Zafiropulos, V. 'Laser ablation in cleaning of artworks'. In *Optical Physics, Applied Physics and Material Science: Laser Cleaning*, Ed. B. S. Luk'yanchuk, World Scientific, Singapure, New Jersey, London, Hong Kong, (2002), 343-392.

5. *A molecular study on the depth-dependent oxidation and condensation gradients of aged dammar and mastic varnish films*

Abstract

The depth-dependent oxidation and condensation gradients of extremely aged, ~ 55 μm thick dammar and mastic films are studied on the molecular level. Direct Temperature-resolved MS (DTMS), Matrix-Assisted Laser Desorption/Ionisation Time-Of-Flight MS (MALDI-TOF-MS) and High Performance Size Exclusion Chromatography (HP-SEC) were employed to analyse the films after 248 nm laser-induced removal of 3.5, 7, 11.5, 15, 20, 25 μm and 3, 6, 10, 12, 16, 20, 25 μm from the aged dammar and mastic films respectively. Electron ionisation (16 eV) DTMS total ion currents indicated that polarity and condensation decrease depth-wise, since lower temperature is required to volatilise the incorporated polar compounds and to induce pyrolysis of the high MW condensed fraction as the thickness of both films reduces. The relative abundance of oxidised dammarane, oleanane and ursane type triterpenoids gradually decreases with depth. Multivariant Factor Discriminant Analysis (DA) quantified the oxidative gradient and showed that a depth of 15 μm from surface of the aged films is the threshold between highly and poorly deteriorated

material. MALDI-TOF-MS showed that UV-induced oxidation resulting in A-ring openings at position C-2 of the oleanane / ursane type molecules stops at the 15 μm below the surface. The upper layers completely absorb radiation with λ < 350 nm. HP-SEC determined that the high molecular weight fraction becomes less prominent as a function of depth. All the data presented establish the depth-dependent compositional gradients and determine that deep layers in the bulk of aged dammar and mastic films remain unaffected from autoxidative degradation processes. The fact that non-UV-induced oxidation and unaffected material were detected in the bulk of the laser ablated varnish films indicates that excimer laser ablation at 248 nm is a non-oxidative process.

5.1 Introduction

Ageing of triterpenoid resins, such as dammar and mastic, under light, is in principle an oxidative process, leading, as a first step, to the conversion of triterpenoid hydrocarbon type carbon skeletons (Figure 2.2.1) to carbon skeletons with oxygen containing functional groups (Figure 2.2.2) (De la Rie 1988a, Van der Doelen 1999). Today, it is understood that these changes are only the beginning of an oxidative process leading to radical polymerisation (crosslinking or condensation), oxidative modifications in the side chain or in the functional groups on the tetra- or the pentacyclic ring structures, shortening of the side chain, especially in triterpenoid compounds with the dammarane skeleton (Van der Doelen, et al. 1998a, Van der Doelen, et al. 1998b), and probably to eventual defunctionalisation, bond breaking and disintegration of the triterpenoid carbon skeleton (Boon and van der Doelen 1999).

As already described above (Section 2.2), the extent of oxidative degradation is significantly affected by the presence or absence of UV wavelengths in the incident radiation. The main difference is that UV wavelengths lead to an opening of the A-ring at position C-2 of dammarane and oleanane/ursane type molecules (Figure 2.2.2c) (Van der Doelen, et al. 2000), while in the absence of UV wavelengths most of the oxidative products are associated with oleanane and ursane type triterpenoids oxidised at positions C-11 and C-28 (Figure 2.2.2b) (Van der Doelen, et al. 1998a). UV wavelengths have been employed for various studies on the ageing of the triterpenoid varnishes (De la Rie 1988b, Zumbühl, et al. 1998, Van der Doelen, et al. 2000, Scalarone, et al. 2003). It has been determined, herein, that for the study of extremely aged varnishes, UV wavelengths are essential during the ageing process (Section 2.3). Even freshly harvested triterpenoid resins, having been irradiated by sunlight during exudation from the bark of the resin trees (Koller, et al. 1997), contain dammarenolic acid and 20,24-epoxy-25-hydroxy-dammaran-3-one (Mills and Werner 1955, Poehland, et al. 1987, De la Rie 1988a, Van der Doelen, et al. 1998a, Van der Doelen, et al. 1998b, Scalarone, et al. 2003), both having oxidised A-rings. The presence of these highly degraded molecules in 'fresh' resins is explicable by the free radical chain reactions which were initiated in the resin teardrops during the harvesting period (Dietemann 2003). A DTMS study of 55 μm thick dammar and mastic films, aged under intense, accelerated deteriorative conditions[1], showed that both films contain a mixture of a few intact triterpenoid molecules, some oxidised triterpenoids with A-ring openings, evidently produced upon UV irradiation, and

[1] 500 h xenon arc exposure ($\lambda > 295$ nm) at 60°C, 45 days near an open window and over a month storage in the dark

some oxidised oleanane/ursane type molecules generated upon non-UV irradiation (Section 2.3). It is should be stressed that UV-induced and non-UV-induced oxidised triterpenoids were found to be almost in equal relative amounts in the investigated films (Table 2.3.5).

In Section 4.3.2 it was demonstrated that the distribution of carbonyl groups is not random in the thickness of the films but influenced by the optical absorption lengths at the various wavelengths contained in the incident light. In particular, upon ageing dammar and mastic films absorb completely wavelengths with $\lambda < 350$ nm at the uppermost 10-15 μm surface layers, wavelengths with $\lambda > 350$ nm penetrate deeper and wavelengths $\lambda > 400$ nm fully penetrate the 55 μm films tested (Figure 4.3.2.6). A theoretical model based on earlier GC/MS findings on aged dammar and mastic indicated that, owing to the strong light intensity and the abundant presence of oxygen in the surface, most of the oxidative products are generated in the surface, while the reduced amounts of oxygen in the bulk result in termination reactions of free radicals producing non-oxidative crosslinks (Boon and van der Doelen 1999). In other words, it is suggested that the oxidative deterioration of aged dammar and mastic films reduces with depth. The most apparent clues towards this conclusion are that:

– aged dammar films thicker than 10 μm were found to be less deteriorated than thinner dammar films aged under the same conditions (De la Rie 1988b).

– solubility tests of laser ablated, naturally aged varnishes on paintings using a KrF excimer laser and a mixture of cleaning solvents showed that polarity decreases as a function of depth (Theodorakopoulos and Zafiropulos 2003, Section 1.4).

– the amount of free radicals in fresh mastic resin teardrops, harvested in the same period, increases as the teardrops decrease in size, indicating that mastic blocks the propagation of light in the bulk (Dietemann 2003).

These findings are supported by theoretical models on the ageing of various organic materials. Thomson suggested the presence of unreacted substance across depth of light aged organic films and based on Beer's Law postulated that the abundance of this unreacted material should increase with increasing distance from the surface (Thomson 1965, 1979). Other models have shown that the consumption of oxygen across depth is dependent upon a reducing rate of diffusion, which leads to 'oxygen starvation' in the bulk (Thomson 1978, Cunliffe and Davis 1982, Fukushima 1983). The integration of data resulting from reducing light propagation into films and from the reduction of oxygen availability with depth produced models showing that the overall degradation of organic substrates is reduced as a function of depth (Schoolenberg and Vink 1991). A comprehensive review about depth-dependent degradation in various materials due to light propagation and oxygen diffusion has been already provided (Feller 1994a). Heat-bodied oil coatings, such as a thick copal oil varnish film tested, are the exception of this rule, because of the pre-polymerisation process (Mantell, et al. 1949, Mills and White 1994, Carlyle 2001), which leads to high degrees of saturation both in terms of absorption (Sections 2.4, 2.5 and 4.3.2) and in terms of bonding of the incorporated molecular structures (Chapter 6).

The depth-dependent gradients in oxidation and crosslinking across the thickness of aged dammar and mastic films have been determined experimentally by the changes

in the interaction of these films at consecutive depths with a KrF excimer laser (Zafiropulos, et al. 2000, Theodorakopoulos and Zafiropulos 2003, Theodorakopoulos, et al. 2005, Chapters 1 and 3). In particular, it was shown that (a) the ablation rate per pulse and the ablation yield per incident laser photon (Section 3.3.2), (b) the carbon dimers emitted in the ablation plume monitored by LIBS (Section 3.3.4), (c) the ablation step obtained using a common laser cleaning method (Section 3.3.5) and (d) the laser light transmitted towards the underlying substrate (Section 4.3.1.2), gradually change across the reducing thickness of the ablated films. UV/VIS and ATR-FTIR measurements established the decreasing gradients in absorption, oxidation, and crosslinking as a function of depth (Section 4.3.2), and the results were in a good agreement with earlier findings (Zafiropulos, et al. 2000). Moreover, evidence was provided about the non-oxidative contribution of the 248 nm pulses of the KrF excimer laser to the remaining films, as has been also determined elsewhere (Castillejo, et al. 2002). The latter finding shows that the determined gradients are not a result of the interaction of the resin films with the UV laser photons but a genuine characteristic of aged dammar and mastic films.

This chapter aims at the establishment of the compositional gradients of aged dammar and mastic films on the molecular level. The evaluation of the dammar and mastic films prior to and after ageing (Section 2.3) enables a comparison with the degradation state of the films across their depth profiles. The following work is based on Direct Temperature-resolved MS (DTMS), Matrix-Assisted Laser Desorption/Ionisation Time-Of-Flight MS (MALDI-TOF MS) and High Performance – Size Exclusion Chromatography (HP-SEC). Analytical data from earlier studies in

particular of aged and unaged natural resins, based on HPLC-MS, GC/MS and DTMS, are employed for an efficient interpretation of the complex DTMS summation mass spectra (De la Rie 1988a, Papageorgiou, et al. 1997, Van der Doelen, et al. 1998a, Scalarone, et al. 2003). Quantification of the DTMS data is enabled with Multivariant Factor Discriminant Analysis. MALDI-TOF-MS is employed to provide complementary molecular information on the ablated surfaces and interpretation of the MS is enabled by comparison with related analytical data (Zumbühl, et al. 1998, Dietemann 2003). Finally, SEC is employed to determine the molecular weight modifications across depth to support findings based on excimer laser ablation (Chapter 3) and ATR-FTIR (Section 4.3.2). Interpretation of the SEC traces was based on previous molecular weight studies of aged dammar films (De la Rie 1988b, Van der Doelen and Boon 2000).

5.2 Experimental

5.2.1 Direct temperature-resolved mass spectrometry

The laser-ablated zones were examined with DTMS in order to investigate the potential molecular variation across the depth profile. From each zone a thin film of approximately 4 mm^2 was mechanically subtracted, then homogenized and brought in suspension with a few drops of ethanol. A volume of 2-3 μl of the mixture was applied to a Pt/Rh (9:1) filament (100μm diameter) of a direct insertion probe, and dried *in vacuo* (using the Purevap) by evaporation of the ethanol. After insertion of the probe in the ionisation chamber a gradual temperature increase of the filament was set at a rate of 1A/min to a final temperature of approximately 800ºC, while the MS was monitoring the evolved compounds in electron ionisation (EI) or ammonia

chemical ionisation (NH_3/CI) modes. The compounds were ionised at 16 eV energy in EI mode and 250 eV in NH_3/CI mode, and analysed in a JEOL SX-102 double focusing mass spectrometer (B/E) over a mass range from 20-1000 Dalton at a cycle time of 1 s. The acceleration voltage was 8 kV. The total ion currents and summation mass spectra were examined.

5.2.2 Factor discriminant analysis (DA)

EI-DTMS summation mass spectra were numerically analysed by factor discriminant analysis coupled with the FOMpyroMAP multivariate analysis program, that is a modified version of the ARHTUR package from Infometrix Inc. (Seattle, USA; 1978 release) and with FOM developed Matlab® (The Mathworks Inc., Natick, MA, USA) toolbox ChemomeTricks. The discrimination was based on a double stage component analysis (PCA) that is described elsewhere (Hoogerbrugge, et al. 1983). Mass spectra of triplicate (at least) measurements for each sample were inserted in the aforementioned software to enable discrimination. To minimise variance in the data due to variance in the mass spectrometer readings, the DT mass spectra of the same films were measured on the same day prior to DA analysis.

5.2.3 Matrix-assisted laser desorption/ionisation Time-Of-Flight mass spectrometry (MALDI-TOF-MS)

Sampling was enabled with ethanol wetted minute TLC plates coated with cellulose that were simply brought in contact with the surface of the aged, unaged and laser ablated films. The samples were coated with a thin layer of 2,5-dihydroxybenzoic acid (DHB, Aldrich, Steinheim, Germany). A sample of neat DHB coating was also prepared for reference. The TLC plates were attached on the stainless steel MALDI

probe, which was then placed on the x-y-z translator of the TOF-MS system (Brucker-Franzen Analytik, Bremen, Germany) for the appropriate orientation into the ionisation chamber (10^{-7} mbar) of the system. The ion source consists of positively or negatively charged metal electrode that is the MALDI probe and a grounded accelerating grid at a ~ 2 cm distance. The accelerating potential was 19.9 kV in the reflex mode. As soon as the vacuum lock was fastened the probe was in position to face the laser beam at an angle of 60º with respect to the surface normal. The nitrogen discharge (N_2) laser (337 nm) used had a 4 ns pulse duration and a repetition rate of 1-2 Hz (Photon Technology PL2300). Manipulation of the sample was enabled by monitoring the ion source via a CCD camera. Processing was carried out with Bruker software (DataAnalysis for TOF 1.6.g).

5.2.4 High Performance Size Exclusion Chromatograph (HP-SEC)

The study of the molecular weight changes, across the depth profiles of the light aged, laser ablated resin films was carried out with High Performance Size Exclusion Chromatography (HP-SEC). Unaged, aged and laser ablated samples were dissolved in THF (~10mg/μl) and centrifuged. An amount of 20 μl was analysed on a Shimadzu HP-SEC system, consisting of a SCL-10AD *vp* control panel, an LP-10AD *vp* pump, a DGU-14A degasser, a SIL-10AD *vp* autoinjector, a CTO-10AS column oven and a FRC-10A fraction collector (Shimadzu Benelux, 's-Hertogenbosch, The Netherlands). Two different detectors connected in series were used for the signal detection. These were a Shimadzu SPD-10A *vp* UV/VIS detector operated at 240 nm and a Shimadzu RID-10A refractive index detector in combination with a Shimadzu Class *vp* 5.03 software. The temperature in the system was 40ºC and the flow rate was 1ml/min.

Finally, calibration was carried out with polystyrene standards (Polymer Laboratories) with an average mass ranging from 580 to 370,000 Daltons.

5.3 Results and Discussion

5.3.1 DTMS of the laser-ablated depth-profiles of the aged dammar and mastic films

Tables 5.3.1.1 and 5.3.1.2 present the lists of identified compounds in the aged and laser ablated dammar and mastic films with DTMS. It should be noted that because of the sampling and the subsequent dissolution of the aged films in ethanol for the technical requirements of sampling for DTMS, the final mass spectra provide average readings with respect to the abundance of these compounds across depth. Both the aged ~ 55 μm dammar and mastic films (Appendix 2.7) are basically a mixture of triterpenoids with oxidised A-rings at position C-2 (**5**, **7**, **15**[2], **17**-**20**, **22** and **23**), oxidised oleanane/ursane type triterpenoids at positions C-11 and C-28 (**24**-**28**) and a series of unreacted triterpenoids (**1**-**16**). According to the optical absorption lengths at various wavelengths (Figure 4.3.2.6), this mixture indicates that the aged dammar and mastic films can be divided in three different parts in their thicknesses; namely a surface section that absorbed the UV wavelengths of the incident radiation, a deeper part that absorbed only the visible radiation and an underlying part in the bulk at which the transmitted visible light was of low intensity, which combined with the absence of oxygen did not lead to the destruction of the triterpenoid molecules.

[2] Compounds **5**, **7** and **15** are typical oxidised dammarane type molecules with an A-ring opening at C-2 (Mills and Werner 1955, Poehland, et al. 1987, De la Rie 1988a) and are present in triterpenoid resin films even prior to ageing (Van der Doelen, et al, 1998a, Dietemann 2003).

Table 5.3.1.1 List of Compounds found in aged and laser ablated dammar resin films

Label	Compound name	Mw	EI mass/charges*	NH_3/CI mass/charges
1	Nor-α-amyrone (3-oxo-28-nor-urs-12-ene)	410	**204**, 410	428
2	Nor-β-amyrone (3-oxo-28-nor-olean-12-ene)	410	**204**, 410	428
3	Dammaradienone (3-oxo-dammara-20(21),24-diene)	424	109, 205, **424**	442
4	Dammaradienol (3β-hydroxy-dammara-20,24-diene)	426	**109**, 189,207,408, 426	444
5	Dammarenolic acid (20-hydroxy-3,4-seco-4(28),24-dammaradien-3-oic acid)	458	**109**, 440	476,458
6	Hydroxydammarenone (20-hydroxy-24-dammaren-3-one)	442	109, 315, 355, **424**	442
7	20,24-epoxy-25-hydroxy-dammaran-3-one	458	**143**, 399	143
8	Oleanonic acid (3-oxo-olean-12-en-28-oic acid)	454	189, **203**,248,409, 454	472
9	Ursonic acid (3-oxo-12-ursen-28-oic acid)	454	189, **203**,248,409, 454	472
11	Oleanonic aldehyde	438	**203**, 232, 409, 438	456
12	Ursonic aldehyde	438	**203**, 232, 409, 438	456
15	20,24-epoxy-25-hydroxy-3,4-seco-4(28)dammaren-3-oic acid	474	143	143
17	3,4-seco-28-nor-urs-12-en-3-oic acid	428	204, 428	446
18	3,4-Seco-28-nor-olean-12-en-3-oic acid	428	204, 428	446
19	3,4-seco-28-nor-urs-12-en-3,28-dioic acid	472	203, 248 472	490
20	3,4-seco-28-nor-olean-12-en-3,28-dioic acid	472	203, 248 472	490
21	Dihydro-dammarenolic acid (20-hydroxy-3,4-seco-24-dammaren-3-oic acid)	460	387, 456	478
24	3-oxo-25,26,27-trisnordammarano-24,20-lactone	414	95, 99, 205, 315, **414**	432
25	17-hydroxy-11-oxo-nor-β-amyrone (3,11-dioxo-17-hydroxy-28-norolean-12-ene)	440	**234**, 275, 422, 440	458
26	11-oxo-oleanonic acid (3,11-dioxo-olean-12-en-28-oic acid)	468	217, 257, **276**, 317, **482**	486
27	17-hydroxy-11-oxo-nor-α-amyrone (3,11-dioxo-17-hydroxy-28-norurs-12-ene)	440	**234**, 275, 422, 440	458
28	11-oxo-ursonic acid (3,11-dioxo-urs-12-en-28-oic acid)	468	257, 276, **317**, **482**	486

*m/z in bold correspond to the highest relative intensity of the series according to previous findings (Van der Doelen, et al. 1998a)

Table 5.3.1.2 List of Compounds found in aged and laser ablated mastic resin

Label	Compound name	Mw	EI mass/charges	NH_3/CI mass/charges
2	Nor-β-amyrone (3-oxo-28-nor-olean-12-ene)	410	**204**, 410	428
3	Dammaradienone (3-oxo-dammara-20(21),24-diene)	424	109, 205, **424**	442
5	Dammarenolic acid (20-hydroxy-3,4-seco-4(28),24-dammaradien-3-oic acid)	458	**109**, 440	476,458
6	Hydroxydammarenone (20-hydroxy-24-dammaren-3-one)	442	109, 315, 355, **424**	442
7	20,24-epoxy-25-hydroxy-dammaran-3-one	458	**143**, 399	143
8	Oleanonic acid (3-oxo-olean-12-en-28-oic acid)	454	189, **203**,248,409, 454	472
10	Moronic acid (3-oxo-olean-18-en-28-oic acid)	454	**189**, 203,248,409, 454	472
11	Oleanonic aldehyde	438	**203**, 232, 409, 438	456
13	(Iso)masticadienonic acid (3-oxo-13α,14β,17βH,20αH-lanosta-8,24-dien-26-oic acid or 3-oxo-13α,14β,17βH,20αH-lanosta-7,24-dien-26-oic acid)	454	439, **454**	472
14	3-O-Acetyl-3epi(iso)masticadienolic acid (3α-Acetoxy-13α,14β,17βH,20αH-lanosta-8,24-dien-26-oic acid or 3α-Acetoxy-13α,14β,17βH,20αH-lanosta-7,24-dien-26-oic acid)	498	**438**, 498	516
16	28-nor-olean-18-en-3-one	410	163, 191, 410	428
18	3,4-seco-28-nor-olean-12-en-3-oic acid	428	204, 428	446
20	3,4-seco-28-nor-olean-12-en-3,28-dioic acid	472	203, 248 472	490
22	3,4-Seco-28-nor-olean-18-en-3-oic acid	428	204, 428	446
23	3,4-seco-28-nor-olean-18-en-3,28-dioic acid	472	203, 248 472	490
24	3-oxo-25,26,27-trisnordammarano-24,20-lactone	414	95, 99, 205, 315, **414**	432
25	17-hydroxy-11-oxo-nor-β-amyrone (3,11-dioxo-17-hydroxy-28-norolean-12-ene)	440	**234**, 275, 422, 440	458
26	11-oxo-oleanonic acid (3,11-dioxo-olean-12-en-28-oic acid)	468	217, 257, **276**, 317, **482**	486

*m/z in bold correspond to the highest relative intensity of the series according to previous findings (Van der Doelen, et al. 1998a)

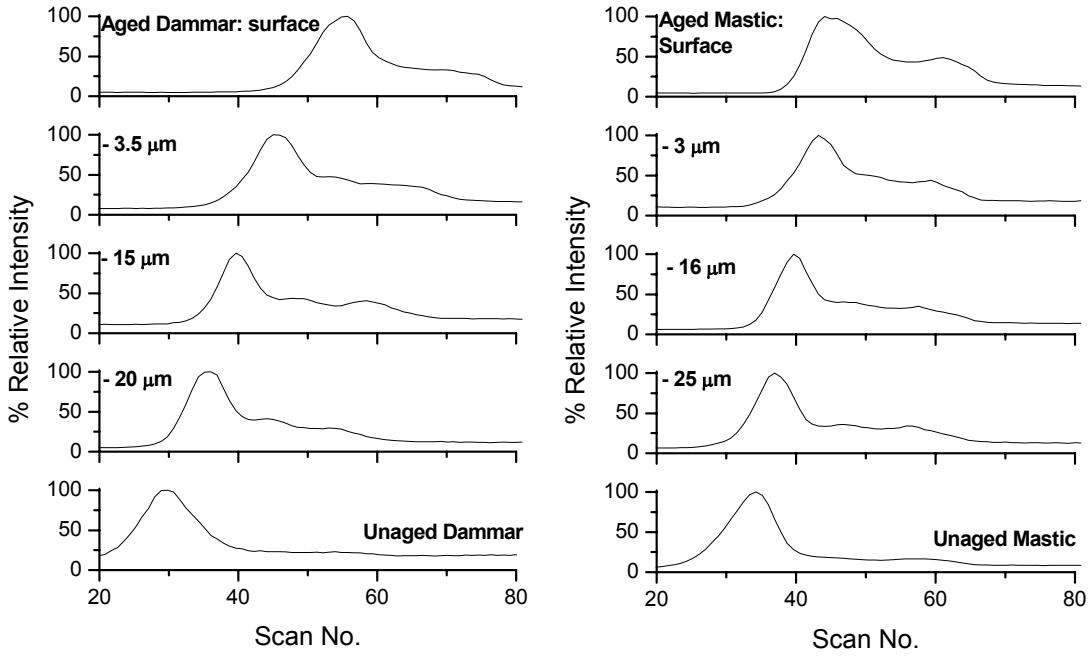

Figure 5.3.1.1 EI-DTMS TIC's of laser-ablated depth steps of (a) aged dammar and (b) aged mastic

Figure 5.3.1.1 presents the electron ionisation (16 eV) total ion currents (EI-DTMS-TIC's) of the aged films prior to ablation and that of the laser ablated depth-steps after removal of 3.5, 15 and 20 μm from the aged dammar film and 3, 16 and 25 μm from the aged mastic film. The EI-DTMS-TIC's of the unaged films are also presented for comparison reasons. The major shifts towards lower scan numbers across the successive depth-steps and especially of the volatile fraction that is desorbed via evaporation (Boon 1992) demonstrate that lower temperatures are required for sufficient desorption with depth. Consequently, the more material is removed from the surface of both aged varnish films the more volatile the remaining films become. The apparent shifts are so intense that after removal of 20 μm from the aged dammar and 25 μm from the aged mastic films the corresponding volatile fractions are evaporated with ~ 80% less heating compared to the temperatures that induced evaporation in the unaged and aged films prior to ablation. As discussed in Section 2.3, such shifts are

related to changes in the polarity (Figure 2.3.1) (Van der Doelen 1999, Scalarone, et al. 2003).

Moreover, the lower peak that emerges at high scan numbers represents the high molecular weight, crosslinked and condensed fraction of the analysed samples that desorbs in the ionisation chamber via pyrolysis at high degrees of temperature (i.e. T > 450°C) (Boon 1992). In both cases, pyrolysis occurs at lower temperatures, while the corresponding peaks become weaker with depth indicating that the high MW fraction becomes less polar and is reduced as a function of depth. It should be noted that the pyrolysis peak gives only an estimation of the high MW fraction, because at high temperature windows (> ~500°C) thermally stable material is formed corresponding to breakage of more or stronger bonds (Boon 1992) (see also Section 2.3). Despite this complexity the pyrolysis event is used often as a good indicator of the high MW fraction of aged dammar and mastic resins (Van der Doelen 1999, Scalarone, et al. 2003). According to the EI-DTMS TIC's then, light ageing of dammar and mastic films leads to lower degrees of oxidation, polarity and condensation or crosslinking as a function of depth.

With regards to polarity this finding supports preliminary results across the laser ablated depth profile of hundred-year-old natural resin varnishes, according to which solubility increases as a function of depth (Section 1.4, Theodorakopoulos and Zafiropulos 2003). In this particular example, the polarity of the remaining varnish across the laser ablated depth-steps was reducing almost logarithmically in the deeper parts of the tested varnishes (Figure 1.4.1). A similar phenomenon is observed here. Figure 5.3.1.2 shows the % volatilisation shifts against the logarithm of the laser-

ablated depth-steps (lower xx' axis) and the remaining film thickness (upper xx' axis) (Table 5.3.1.3). The scan number of the EI-DTMS-TIC volatilisation peaks of the films prior to laser ablation was set as the maximum (100%). The corresponding plots quantify the shifts in the temperature windows that are responsible for the evaporation of the volatile fraction. An estimation of the degree of crosslinking versus depth is also provided based on the apex and broadness of the pyrolysis peak of the EI-DTMS-TIC's. However, the corresponding SEC traces are more accurate with respect to the molecular weight modifications across depth (Section 5.3.4). Given that both intensity and broadness of the pyrolysis peaks enclose significant information about molecular weight, the areas of the pyrolysis peaks were measured. The plots of the pyrolysed high MW condensed fractions as a function of depth are presented in Figure 5.3.1.3. It is observed that the crosslinking gradient performs two apparent trends with depth in both films tested. The first trend is terminated at 15 μm from surface and from that point inwards new trends commence, which tend to reach the degree of pyrolysis determined prior to ageing. The outlined jump in the plots after removal of 15 μm from surface coincides with the change of the ablation step using a KrF excimer laser

Table 5.3.1.3 Data extracted from EI-DTMS TIC's

depth steps	Laser ablated depth-steps. Measured from surface (μm)		% Volatilization (Normalized with scan no of aged surface)		% Pyrolysis yield (Normalized with %area of aged surface)	
	dammar	**mastic**	**dammar**	**Mastic**	**dammar**	**mastic**
Surface	0	0	100	100	100	100
1	3.5	3	80	98	86.44	85.13
2	7	6	77	95	81.76	82.59
3	11.5	10	73	94	80.42	79.64
4	15	12	71	92	78.96	78.79
5	20	16	66	89	50.68	78.35
6	25	20	62	88	46.79	59.61
7	–	25	–	84	–	58.52
Unaged	0	0	54	77	41.80	53.24

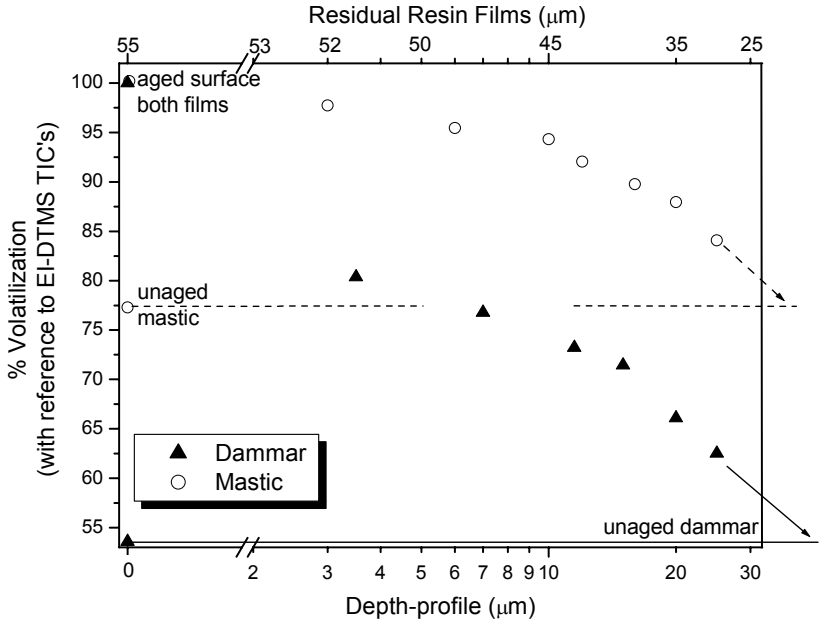

Figure 5.3.1.2 Gradient in volatilisation across depth.

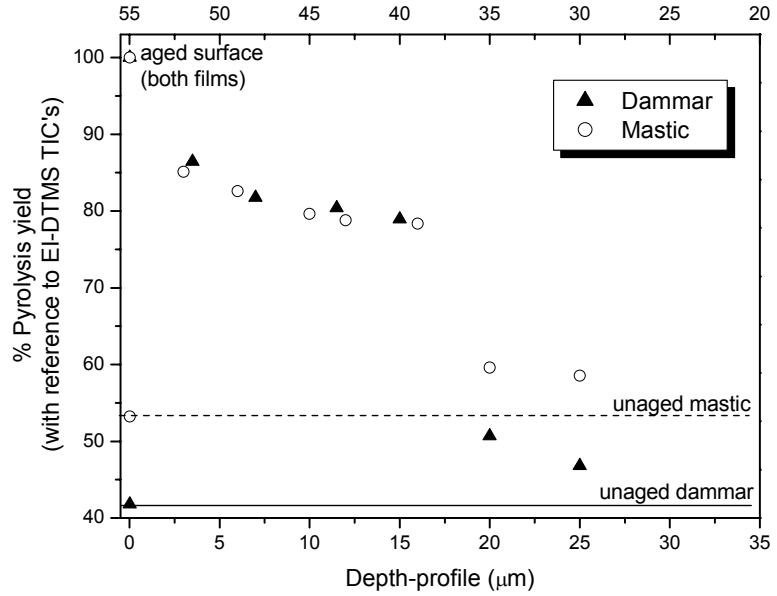

Figure 5.3.1.3 Gradient in pyrolysis yield relative intensity across depth.

(Figure 3.3.5.3), as well as with the minimisation of the carbon dimer emission as recorded with LIBS (Figure 3.3.4.2). From a photomechanical point of view, excimer laser ablation of organic materials is dependent on the degree of polymerisation and crosslinking (Srinivasan and Braren 1989, Zafiropulos 2002). Thus, all the results

presented in the present work demonstrate that below the 15 μm surface layers neither of the aged dammar and mastic films is heavily crosslinked.

Figures 5.3.1.4 and 5.3.1.5 present the ammonia chemical ionisation (NH_3/CI) DTMS summation mass spectra of the aged dammar and mastic films prior to laser ablation (i), after removal of ~12 and 25 μm from surface (ii, iii) and prior to ageing (iv). The electron ionisation (EI) DTMS summation mass spectra of the aged films prior to ablation, after removal of increasingly thicker surface layers ranging from 3 to 25 μm, and prior to ageing are presented in Figures 5.3.1.6 (dammar) and 5.3.1.7 (mastic). In NH_3/CI mode (250 eV) ammonia adduct molecular ions $[M+NH_4]^+$, $[M+H]^+$ and $[M+NH_4-H_2O]^+$ cations are obtained resulting in molecular weight information, while in EI mode (16 eV) minor fragmentation is obtained resulting in structural and more detailed information. Interpretation of the mass spectra was based on earlier DTMS studies (Van der Doelen, et al. 1998a, Van der Doelen 1999, Van der Doelen and Boon 2000, Scalarone, et al. 2003), as well as on GC/MS and HPLC-MS (Van der Doelen, et al. 1998a, Van der Doelen, et al. 1998b). The most characteristic molecular ions and ion fragments of the identified compounds are presented in Tables 5.3.1.1 and 5.3.1.2. Details of the incorporated compounds (Figure 2.2.1) and the ion fragments thereof are given in Section 2.3.

It is demonstrated that the thicker the layer removed from the highly deteriorated surfaces, the more the molecular configuration of the remaining films tends to resemble the composition of the resins prior to ageing. The depth-dependent shift towards a less oxidative state is evident even after removal of only 3.5 and 3 μm from the aged dammar and mastic films respectively, although the molecular changes are

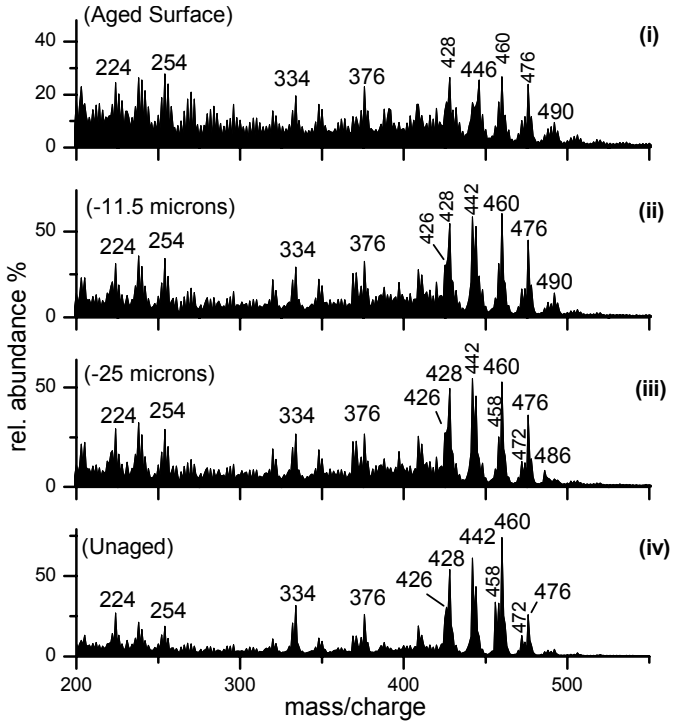

Figure 5.3.1.4 NH_3/CI DTMS summation mass spectra of the aged dammar film (total thickness: ~ 55 μm) prior to ablation (i), after removal of 11.5 μm (ii) and 25 μm (iii) from surface, and the NH_3/CI DTMS of the same film prior to ageing (iv)

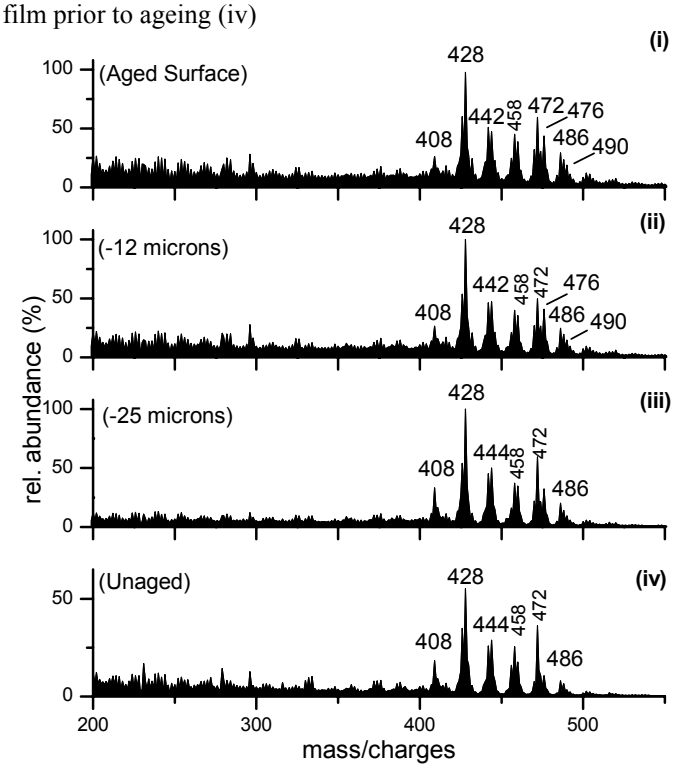

Figure 5.3.1.5 NH_3/CI DTMS summation mass spectra of the accelerated aged mastic (total thickness: ~ 55 μm) prior to ablation (i), after removal of 12 μm (ii) and 25 μm (iii) from surface, and the NH_3/CI DTMS of the same film prior to ageing (iv)

more obvious with increasing depth. The unreacted compounds observed are the dammarane type triterpenoids (**3**, **4**, **5**, **6** and **7**) with EI marker peaks at m/z 109, 143, 424 and NH_3/CI marker peaks at m/z 442, 446, 478 and the oleanane/ ursane triterpenoids (**1**, **2**, **8**, **9**, **10**, **11** and **12**) with EI marker peaks at m/z 189, 203, 204, 248, 409, 410 and NH_3/CI marker peaks at m/z 428, 456, 472. These marker peaks are evidently increasing with depth. Although both types of triterpenoids are contained in both dammar and mastic, molecules with the dammarane skeleton are more abundant than those with the oleanane / ursane skeleton in dammar resin, while the opposite occurs in mastic resin. The recovery of the ion fragments corresponding to these marker compounds is more impressive in dammar, because of the abrupt reduction of the triterpenoid compounds that is observed in dammar resin upon ageing (Section 2.3.1, Van der Doelen, et al. 1998a, Van der Doelen 1999, Scalarone, et al. 2003).

Oxidised compounds such as the oleanane / ursane type molecules with the A-ring opening at position C-2 (**17**/**18**, **19**/**20** for dammar and **18**/**22**, **20**/**23** for mastic) with EI marker peaks at m/z 428, 472 and NH_3/CI marker peaks at m/z 446, 490, which are in trace amounts in the aged films prior to ablation seem to disappear after removal of the uppermost 15 μm in both cases. Since these particular compounds are only formed upon UV irradiation during accelerated ageing (Van der Doelen, et al. 2000), it is indicated that the UV wavelengths of the incident radiation do not penetrate deeper than a 15 μm surface zone of the films. This finding is in a very good agreement with the optical absorption lengths, ℓ_α, determined for the aged dammar and mastic films tested (Figure 4.3.2.6), showing that both films absorb completely the incident

radiation with λ < 350 nm at depths shorter than 15 μm from surface. This observation is confirmed with MALDI-TOF-MS (Section 5.3.3).

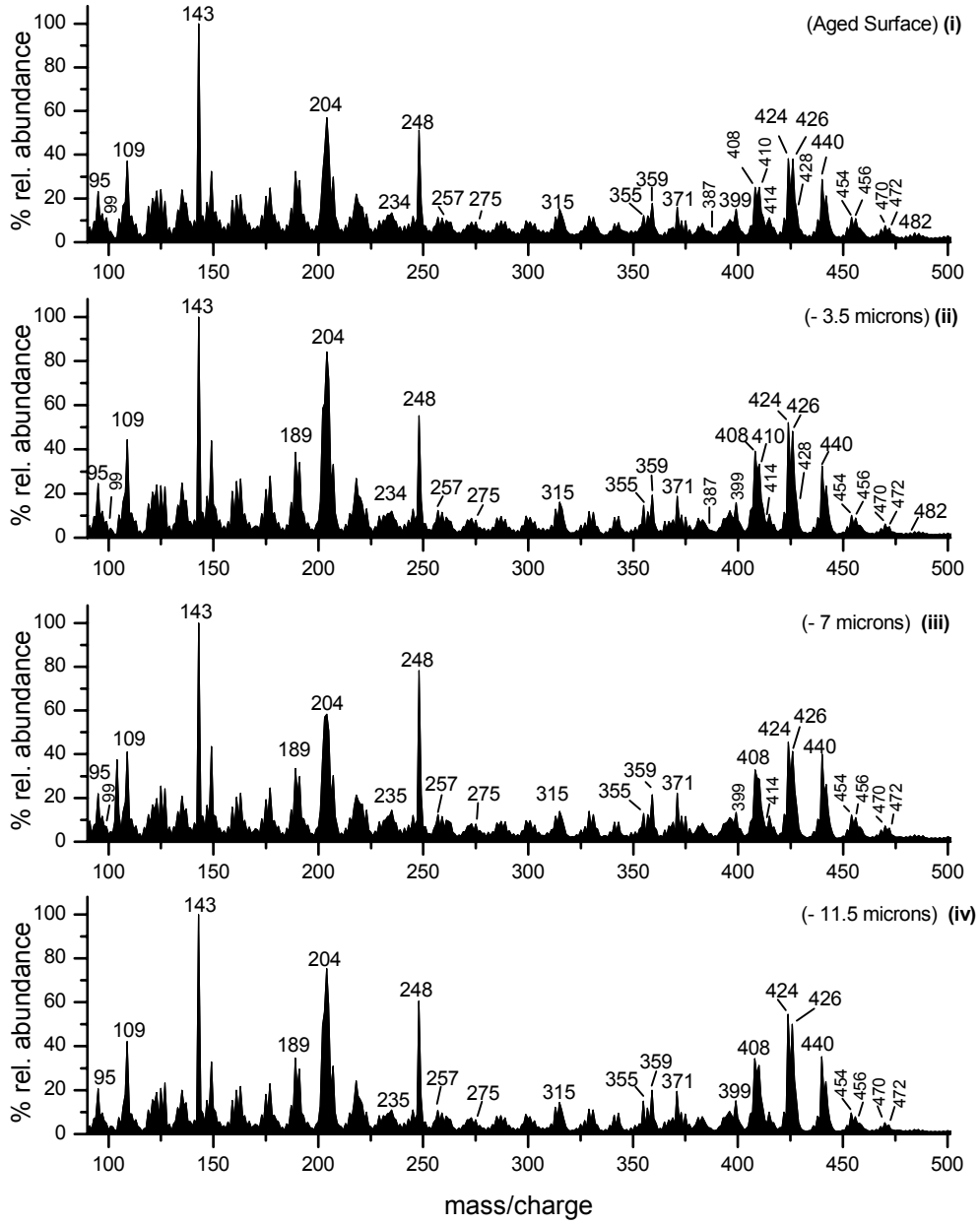

Figure 5.3.1.6 EI-DTMS summation mass spectra of the accelerated aged dammar film (total thickness: ~ 55 μm) prior to ablation (i), and after removal of 3.5 μm (ii), 7 μm (iii) and 11.5 μm (iv) from surface.

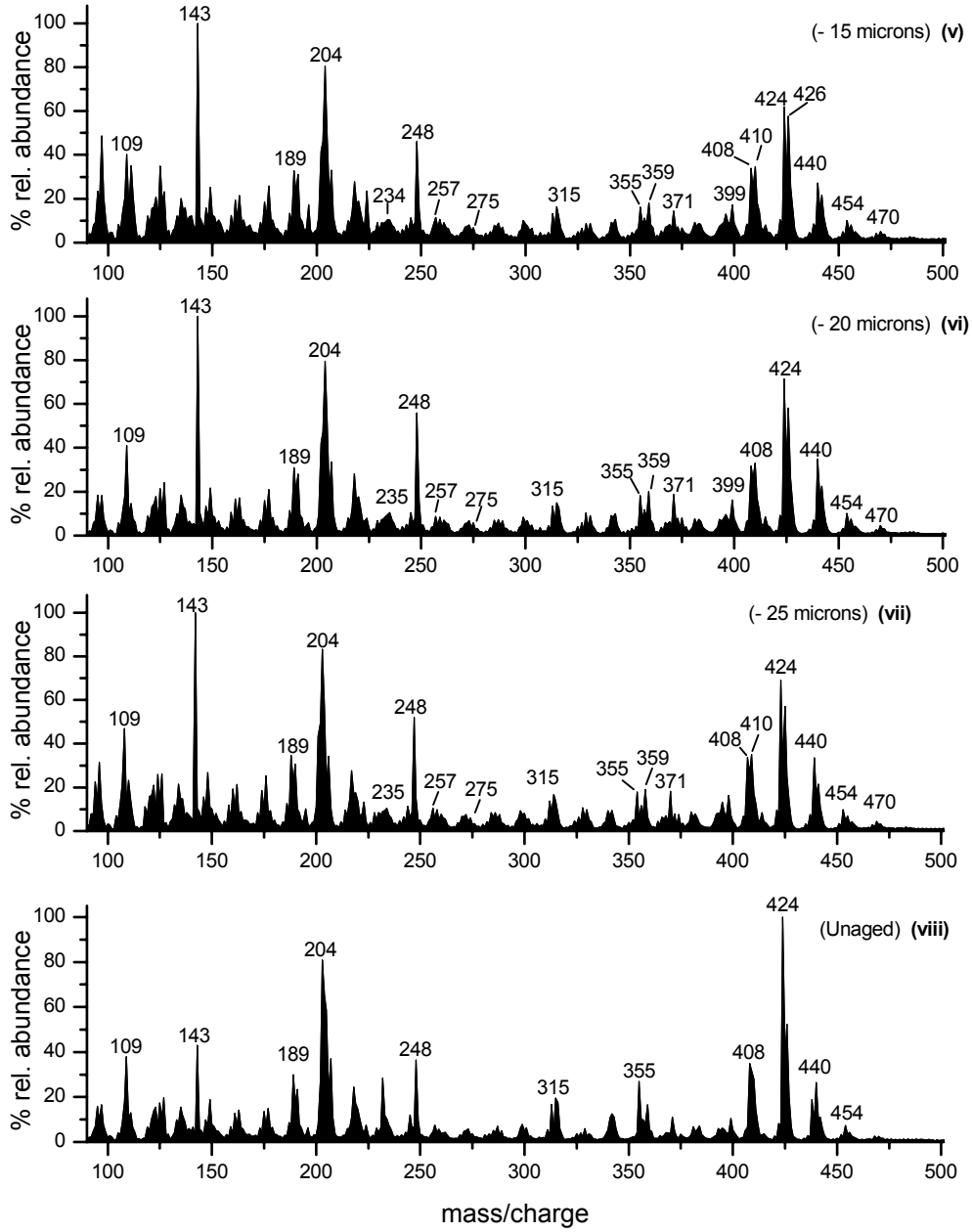

Figure 5.3.1.6 (continued) EI-DTMS summation mass spectra of the accelerated aged dammar film after removal of 15 μm (v), 20 μm (vi) and 25μm (vii) from surface and the corresponding EI-DTMS of the unaged film (viii) (total thickness: ~ 55 μm).

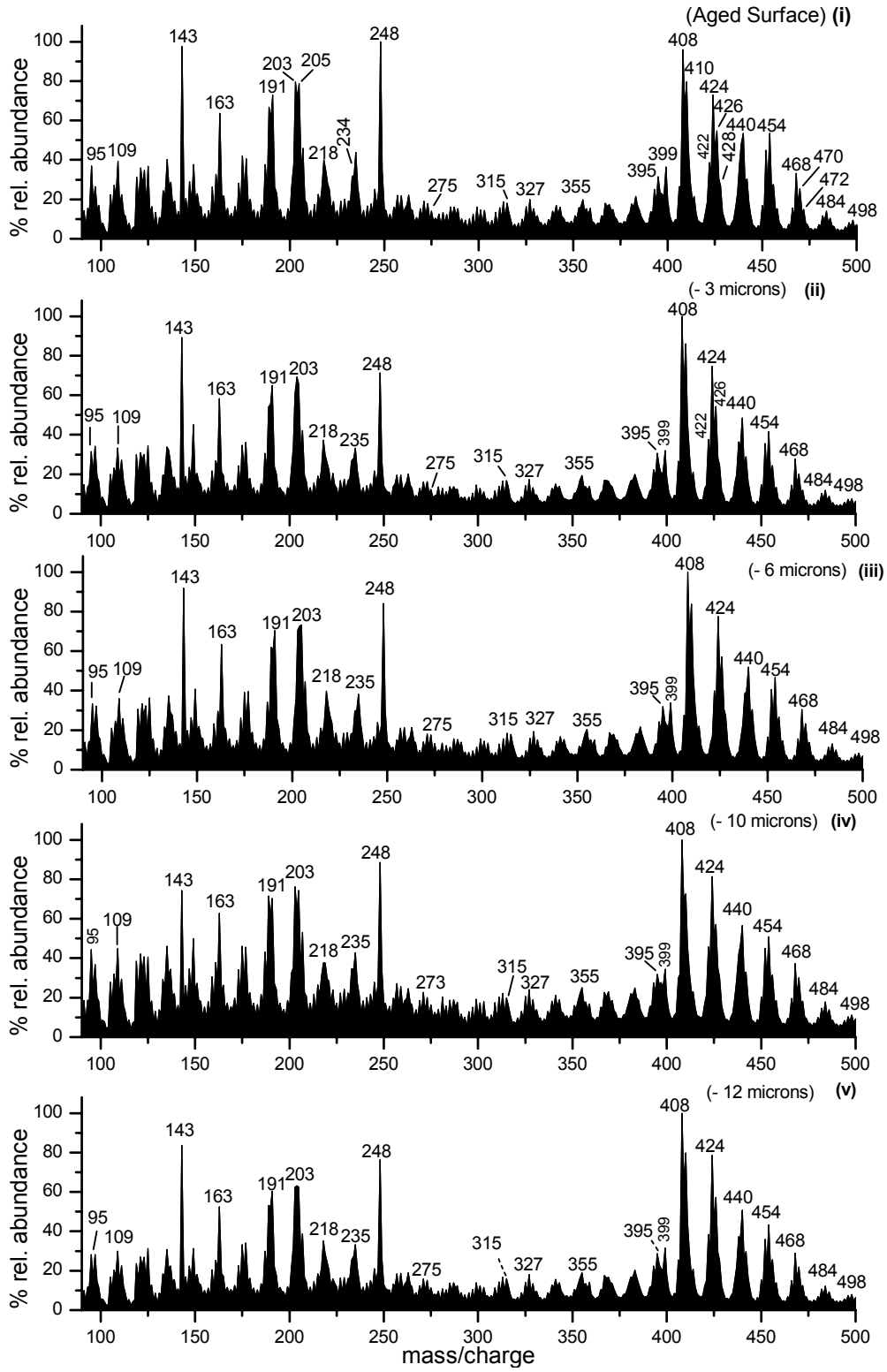

Figure 5.3.1.7 EI-DTMS summation mass spectra of the accelerated aged mastic film (total thickness: ~ 55 μm) prior to ablation (i), and after removal of 3 μm (ii), 6 μm (iii), 10 μm (iv) and 12 μm (v) from surface.

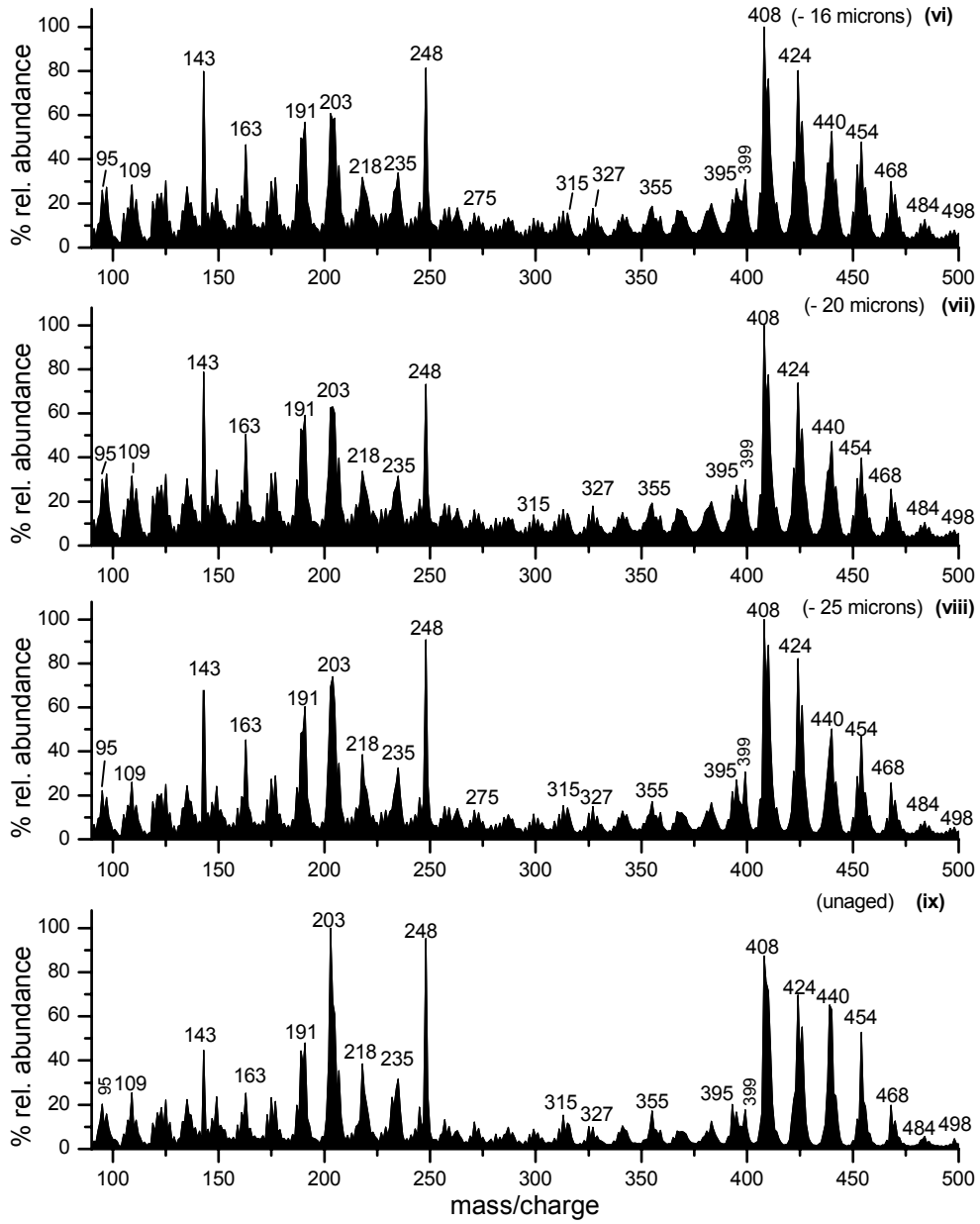

Figure 5.3.1.7 (continued) EI-DTMS summation mass spectra of the accelerated aged mastic film after removal of 16 μm (vi), 20 μm (vii), 25 μm (viii) from surface and the corresponding EI-DTMS of the unaged film (ix) (total thickness: ~ 55 μm).

The DTMS summation mass spectra also detect traces of some oleanane / ursane type molecules oxidised at positions C-11 and C-28, which are listed in Tables 5.3.1.1 and 5.3.1.2 as compounds **25-28** for dammar and **25** and **26** for mastic. The dammarane type compound **24**, which is present in both films, has the same type of side chain

oxidation (Figure 2.2.2b, Van der Doelen, et al. 1998a). Marker peaks of these particular oxidation products (**24**-**28**) are monitored at m/z 234, 317, 414, 482 in the EI mode and at m/z 432, 458, 486 in the NH_3/CI mode. These particular oxidation products have been detected by Van der Doelen and co-workers (1998a, 1999) in aged varnishes sampled from a large number of paintings kept in several galleries and museums. These products are reproducible in dammar and mastic resins upon light ageing excluding UV wavelengths or using an elaborate ageing process involving dissolution of the resins in a mixture of solvents with photosensitisers followed by irradiation in a fluorescent tube device (Van der Doelen and Boon 2000). Judged from the relative intensity of the corresponding m/z marker peaks, the abundance of these compounds is found to be equivalent to that of the UV-induced oxidation products with the oxidised A-rings in both the aged dammar and mastic 55 μm films prior to ablation (Tables 2.3.5 and 2.3.6). The marker peaks of the non-UV induced oxidation products **24**-**28** are in particular notable in the summation MS of the remaining films after removal of the 15 μm highly deteriorated surface layers. Some (minor) traces are also observed in the films even prior to ageing, indicating that the films prior to ageing were somewhat oxidised, as shown in Section 2.3.

According to the presented data, the molecular changes are apparent by monitoring the gradual recovery of the abundances of the ion fragments corresponding to the unreacted, non-oxidised dammarane (**3**, **4**, **5**, **6** and **7**) and oleanane / ursane type triterpenoids (**1**, **2**, **8**, **9**, **10**, **11** and **12**) with depth. The molecular changes are less pronounced in the uppermost 15 μm, which absorb highly the UV wavelengths of the incident radiation. Strong molecular changes between surface and deeper parts of the

films are observed after the removal of the highly deteriorated surface layers, especially in the case of dammar, where after removal of 20 μm from surface the characteristic ion fragments of the unreacted compounds produce relative intensities comparable to those of the same film prior to ageing. After removal of 25 μm from the surface of the aged mastic film the ion peak m/z 143, which is the characteristic ion fragment of the ocotillone type molecules, such as compound **7**, decreases, indicating that the dammarane type molecules and their oxidation products influence the composition of mastic less than that of dammar. This is a genuine characteristic of mastic resin since the oleanane / ursane molecules are more abundant than the dammarane ones (Van der Doelen, et al. 1998a, Van der Doelen 1999, Scalarone, et al. 2003). The demonstrated molecular changes across the depth-profiles of the aged films determine that with increasing depth the composition of the films is gradually shifted towards a less deteriorated state similar to that prior to ageing. These findings are in a very good agreement with the results of the excimer laser ablation (Chapter 3), the laser induced transmission, the UV/VIS and the ATR-FTIR measurements (Chapter 4).

5.3.2 Multivariant Factor Discriminant Analysis (DA) of the DTMS data across the depth-profiles of the aged dammar and mastic films.

The observation of the depth-dependent compositional gradients in the evidently complex DTMS summation mass spectra of the aged dammar and mastic films basically allows a qualitative demonstration of the molecular changes across depth. Multivariant factor discriminant analysis (DA) (Hoogerbrugge, et al. 1983, Windig, et al. 1983) was employed to quantify the modifications observed via the multivariate

mass data. Figure 5.3.2.1 shows the first discriminant function (DF1) mass spectrum for the EI-DTMS summation MS series of the remaining films after laser ablation at

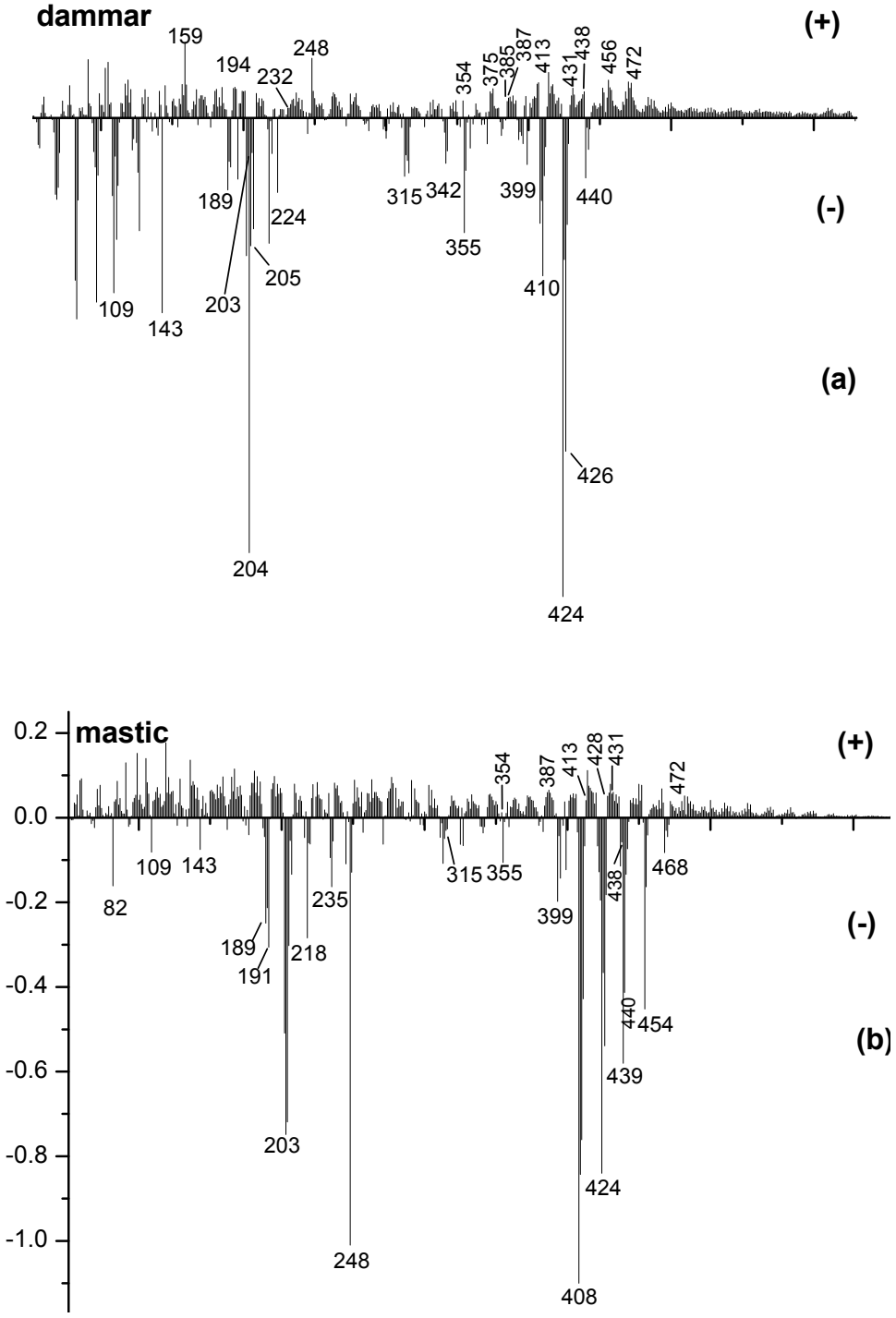

Figure 5.3.2.1 Projections of the EI-DTMS data classified with MFDA for the aged, laser ablated and unaged films of dammar (a) and mastic (b).

successive depth-steps of both dammar (a) and mastic (b). The DTMS mass spectra of the unaged films are also included, so that the two opposite compositional cases, i.e. aged-unaged, would mark the discrimination boundaries of the inserted analytical data.

In short, judging from the molecular ions of the identified compounds that are listed in Tables 5.3.1.1 and 5.3.1.2, DA analysis shows that across the thickness of dammar, oleanane / ursane molecules **1** and **2**, i.e. $[M]^{+\cdot} = 410$, and the dammarane molecules **3**, **4** and **6**, i.e. $[M]^{+\cdot} = 424, 426, 442$ respectively, peak intensely at the negative side of DF1. The characteristic and commonly most abundant ion fragments of the oleanane and ursane molecules **8**, **9**, **11** and **12**, such as m/z 189, 203 and 409, peak at the negative DF1 side. The molecular ions of the latter compounds, i.e. $[M]^{+\cdot} = 454$ for **8**, **9** and $[M]^{+\cdot} = 438$ for **11**, **12** and the characteristic ion fragment at m/z 248, peak at the positive side of DF1, possibly due to overlapping with ion fragments of oxidation products of these molecules. The molecular ions of the UV-induced oxygenated products with the characteristic A-ring openings, i.e., **17**/**18**, ($[M]^{+\cdot} = 428$), **19**/**20** ($[M]^{+\cdot} = 472$) and **21** ($[M]^{+\cdot} = 460$), peak weakly at the positive DF1 side. Similarly, m/z 234, 317, 414 and 482 representing the non-UV-induced oxidation products (**24**, **25**, **26**, **27** and **28**) peak in the negative side of DF1. The molecular ions of oxygenated compounds **5**, **7** ($[M]^{+\cdot} = 458$) and **15** ($[M]^{+\cdot} = 474$) with oxidised A-rings at C-2, which are also detected in the composition of unaged dammar (Mills and Werner 1955, Poehland, et al. 1987, De la Rie 1988a), peak weakly at the positive DF1 side. The ionic fragments of their dammarane skeletons, i.e. m/z 109 and 440 (**5**),

m/z 399 (**7**) and the ionic fragment m/z 143 derived from the ocotillone side chain (**7**, **15**) peak at the negative DF1 side.

The first discriminant function mass spectrum of the corresponding EI-DTMS mass spectra of mastic is somewhat different compared to the DA results of dammar. In agreement with the DA analysis of dammar, oleanane molecule **1**, i.e. $[M]^{+\cdot}$ = 410, and the dammarane type molecules **3** and **6**, i.e. $[M]^{+\cdot}$ = 424, 442 respectively, peak intensely at the negative side of DF1. In contrast to dammar, the molecular ions of the oleanane type molecules **8, 10** ($[M]^{+\cdot}$ = 454) and **11** ($[M]^{+\cdot}$ = 438), peak at the negative DF1 side, confirming that these molecules are abundant throughout the depth of mastic. The same molecular ion with that of **8** and **10** corresponds to (iso)masticadienonic acid (**13**), the abundant presence of which is monitored at the intense marker peak m/z 439 on the negative DF1 side. Compound **14**, which has an ionic fragment at m/z 438 that is also the molecular ion of **11**, does not seem to play any significant role in the final discriminant analysis, since its molecular ion at m/z 498 coincides with the DF1 axis. The same occurs with m/z 163 that is characteristic of compound **16**, although m/z 191, also corresponding to **16**, peaks clearly at the negative DF1 side. In addition, the molecular ion of compounds **5** and **7** ($[M]^{+\cdot}$ = 458) peaks at the positive DF1 side as in the case of dammar. The ionic fragments of these compounds, characteristic of their dammarane skeletons, i.e. m/z 109 and 440 for **5** and m/z 143, 399 for **7**, peak at the negative side, although their relative intensity is lower than that in dammar. Finally, the molecular ions of the UV-induced oxidised triterpenoids **18**/**22**, **20**/**23** (m/z 428, 472) and the marker peaks of the non-UV-induced oxidation

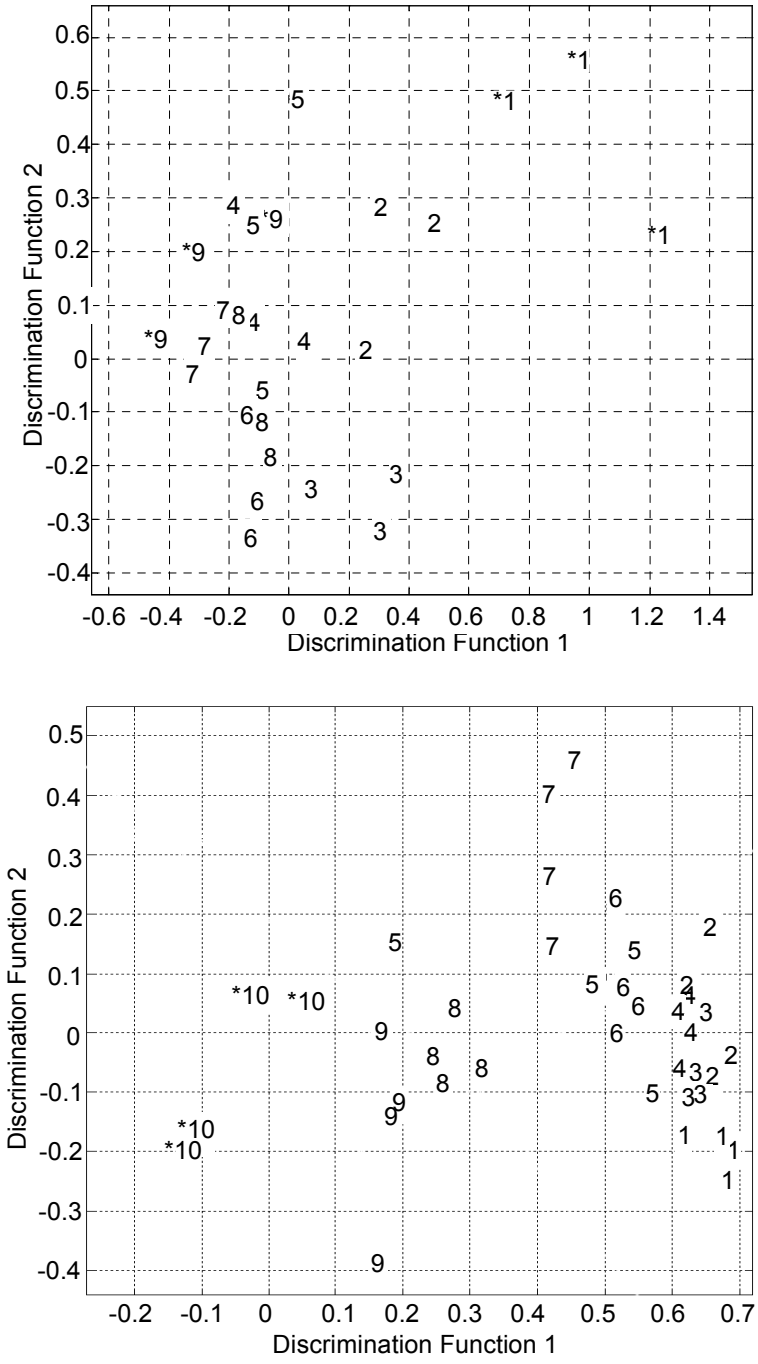

Figure 5.3.2.2 Score maps of DF2 versus DF1 of dammar (a) and mastic (b) depth steps. The ascending numbers represent the compositions of the successive laser ablated depth steps. Data points number (1) correspond to the aged surfaces, while numbers (9) for dammar and (10) for mastic to the unaged materials. The consecutive shifts across the DF1 from the very deteriorated surface layers towards the less deteriorated bulk, which resembles the composition prior to ageing, are evident.

products **24**, **25**, **26** (m/z 414, 234, 276 and 482) peak weakly at the positive DF1 side, since these compounds are found in traces across the depth of the aged mastic film.

Figure 5.3.2.2 presents the plots of the MS data points as coordinates in the score map of the first discriminant function (DF1) versus the second discriminant function (DF2). The geometric distance between the data points is an accepted measure of the demonstrated compositional differences (Hoogerbrugge, et al. 1983, Windig, et al. 1983). Therefore this distance is utilised here to illustrate the chemical changes across the depth-profiles of the tested films. The gradual shifts of the data points across DF1 represent the compositional gradient that is observed with the EI-DTMS mass spectra. The data points from the lower to the higher numbers correspond to the consecutive depth-steps from the surface towards the bulk, while the highest numbers represent the MS data of the resins prior to ageing.

Figure 5.3.2.3 demonstrates the data points along DF1 as a function of depth for the ~ 55 μm, aged dammar and mastic films. Both cases reveal a remarkable compositional gradient, which decreases from the surface. These results quantify the molecular modifications observed with DTMS and verify previous findings on the excimer laser ablation (Theodorakopoulos and Zafiropulos 2003, Theodorakopoulos, et al. 2005, Chapter 3) and the determined gradients in the optical properties characteristics of both films across depth (Zafiropulos, et al. 2000, Section 4.3.2). Although the delineated trends of the aged dammar and mastic films are not similar, there is a very significant common characteristic. As shown in Figure 5.3.2.2, DA analysis placed the origin of DF1 coordinate at a depth corresponding to 15 μm from the original aged surfaces. This is not irrelevant with the change of the ablative interaction upon 248

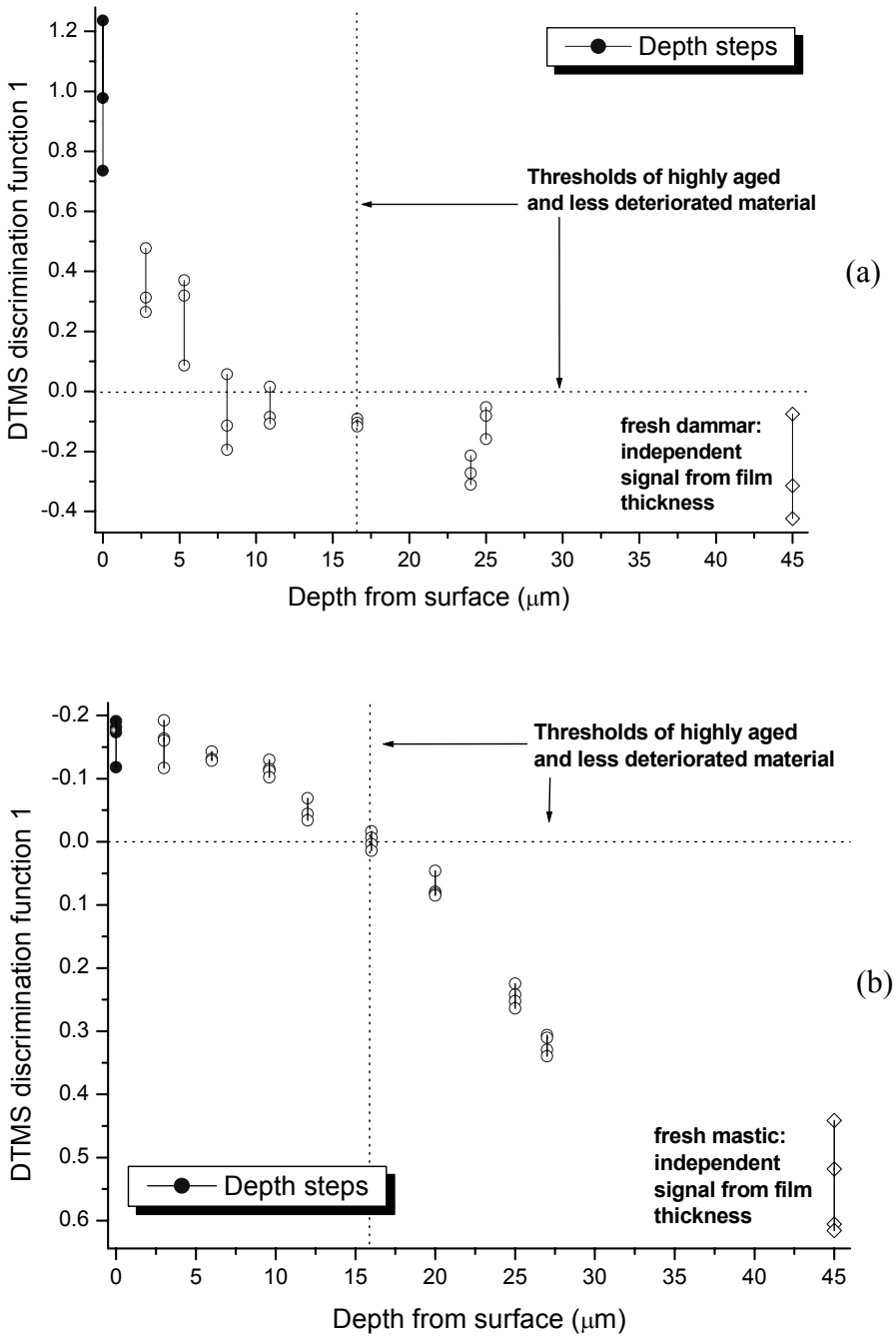

Figure 5.3.2.3 MS projections of DF 1 as a function of depth in the ~ 55 μm thick, aged dammar (a) and mastic (b) films.

nm pulses (Sections 3.3.2, 3.3.3, 3.3.5). At this particular depth the ablation step changes upon KrF excimer laser pulses in both films (Figure 3.3.5.3). Since photochemical ablation is basically affected by the degree of oxidation and

crosslinking of the laser irradiated material (Srinivasan 1994), these findings indicate that the 15 μm depth from surface of both the aged dammar and mastic films is the threshold between highly and poorly deteriorated material. This finding supports earlier findings by De la Rie (1988b), who determined that 10 μm dammar films deteriorate more than thicker films aged under the same conditions. It should be also noted that the data points corresponding to the deepest laser-ablated depth-steps (20-25 μm from surface) emerge near the data points of the unaged films. Given that the total film thicknesses were of the order of 55 μm, it should be expected that below a depth of 25 μm from the original surface the composition of the films would eventually become identical to that prior to ageing.

5.3.3 Matrix assisted laser desorption/ionisation (MALDI) time-of-flight (TOF) MS

Some quantification of the molecular changes – resulting in the compositional depth-dependent gradients – of the aged dammar and mastic films was obtained with MFDA based on the DTMS data. However, the changes monitored provided mean compositional information because the samples required for the DTMS analysis contained the remaining films. MALDI-TOF-MS, using 2,5-dihydroxybenzoic acid (DHB) as the matrix, was carried out to shed light on the composition of the ablated surfaces of the successive depth-steps across the thicknesses of the aged dammar and mastic films (Figure 5.3.3.1). Unfortunately, the low signal-to-noise ratio of the mass spectra obtained did not permit analysis of mastic and all of the depth steps of

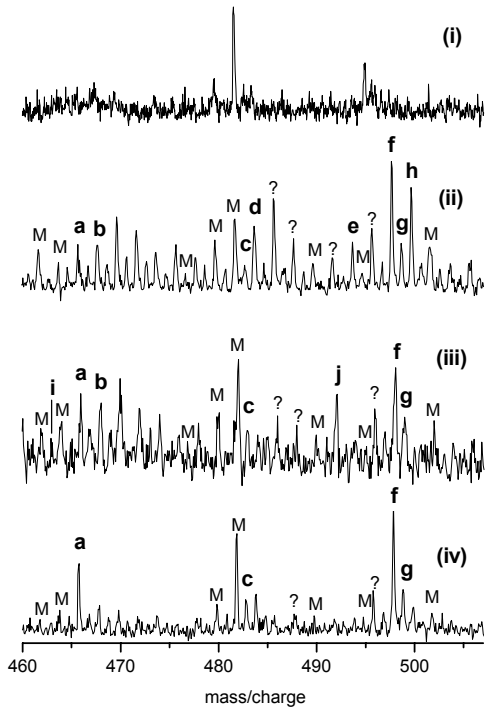

Figure 5.3.3.1 MALDI-TOF-MS of the DHB matrix (i), the aged dammar surface (ii), the surface of the film after laser ablation of the uppermost 15 μm (iii) and the surface of the dammar film before ageing (iv). Despite the relatively low peak-to-noise ratio some molecular changes between the aged surface and the ablated surface are discriminated. For the assignments refer to the text.

dammar. The problem of low signal-to-noise ratios of the MALDI/MS was also encountered in earlier studies of aged triterpenoid resin films and therefore similar measurements were carried out with graphite instead of the matrix (GALDI/MS), which results in spectra without chemical noise (from DHB) (Zumbühl, et al. 1998, Dietemann 2003). However, the novel TOF technique with the TLC plates (see Section 5.2.3), employed for the present analysis, is different from the established MALDI/MS method. It has been observed that with the present MALDI-TOF-MS technique the interference of DHB is minimal, while all the m/z peaks generated correspond to the material on the TLC plates. Hence, the low signal-to-noise ratio is most likely ascribed to the minimal subtraction of resin from the TLC plate. This phenomenon has been observed to be typical of the highly aged resin films (AMOLF, internal report).

In the present work crucial conclusions were drawn from the mass spectra at the surface of the aged dammar film prior to ablation, the surface of the remaining film after removal of 15 μm and the surface of the unaged dammar resin. The identification of the mass peaks is tentative and proposed by comparison with data from the

literature (Zumbühl, et al. 1998, Dietemann 2003). A representative mass / charge range observed in the MALDI-TOF mass spectra is within m/z 450 to 510, at which the sodiated ions $[M+Na]^+$ of unreacted and oxidised triterpenoids are discriminated from the corresponding ion peaks of DHB (Zumbühl, et al. 1998). However, even within this range there are several m/z peaks attributed to DHB (marked with M in Figure 5.3.3.1), which can potentially interfere with the sodiated molecular ions of characteristic triterpenoid compounds (Zumbühl, et al. 1998). A relatively intense peak of DHB is at m/z 451 (not shown), where the sodiated molecular ions of UV-induced oxidation products **17**/**18** (428 Da, Tables 5.3.1.1, 5.3.1.2) with oxidised A-rings are detected (Dietemann 2003). Other overlapping DHB mass / charges are at m/z 461 prohibiting detection of oleanonic and ursonic aldehydes **11**/**12** (438 Da), and m/z 477 that coincided with $[M+Na]^+$ of oleanonic and ursonic acids, **8**/**9** (454 Da) (Dietemann 2003). The highest DHB peak within the examined range was at m/z 480 near a marker peak of dammarenolic acid, **5** (458 Da) at m/z 481 due to the $[M+Na]^+$ (Dietemann 2003). In the unaged dammar film surface (Figure 5.3.3.1iv) peaks **a**, **c**, **f** and **g** at m/z 465, 481, 497 and 497.7 are discriminated respectively. Peak **a** at m/z 465 is assigned to the sodiated molecular ion of hydroxydammarenone (**6**) (442 + 23 = 465), **c** at m/z 481 to $[M+Na]^+$ of dammarenolic acid, **5** (458 Da), and **f** at m/z 497 to $[M+Na]^+$ of compound **15** (474 Da) (Dietemann 2003). Peak **g** at m/z 497.7 is attributed to the molecular ion of an oxidised dammarenolic acid **5**, $[M+Na+O]^+$, i.e 458+23+16 = 497 (Zumbühl, et al. 1998).

Some changes compared to the MALDI MS of the unaged dammar film are monitored in the mass spectrum of the aged film surface (Figure 5.3.3.1ii). It is shown that the

sodiated molecular ion peak of hydroxydammarenone, **6** (m/z 465, **a**) is less intense than in the unaged film. This is in good correspondence with the DTMS data showing that there is an abundance reduction of dammarane type triterpenoids upon ageing (Van der Doelen, et al. 1998a). Dammarenolic acid, **5**, is recognised by marker peaks, m/z 481, **c**, which is attributed to $[M+Na]^+$, and m/z 497.7, **g**, which is attributed to $[M+Na+O]^+$, with the latter peak being more intense compared to the unaged dammar film. The high intensity at m/z 497 (**f**) indicates that the dammarane type degradation compound **15**, which is generated during the biosynthesis of triterpenoid resins upon sunlight irradiation during exudation from the tree (Koller, et al. 1997, Dietemann 2003), is also abundant in the aged film. In the surface of the aged dammar film there are some peaks, such as m/z 467 (**b**), 483 (**d**), 495 (**e**) and 499 (**h**), which are not detected prior to ageing. These peaks correspond to the sodiated molecular ions of dammarenediol with a molecular weight of 444 Da (Mills and Werner 1955, Mills 1956, Poehland, et al. 1987, De la Rie 1988a), which was not reported in the present DTMS study, (**b**: 444 + 23 = 467), dihydro-dammarenolic acid **21**, (460 Da, **d**: 460 + 23 = 483), the UV-induced oleanane / ursane seco-products with oxidised A-rings **19**/**20**, (472 Da, **e**: 472 + 23 = 495) and 20,24-epoxy-25-hydroxy-3,4-seco-dammaran-3-oic acid that is a UV-induced dammarane type seco-product with a molecular weight of 476 Da (Van der Doelen, et al. 2000, Scalarone, et al. 2003). The sodiated molecular ion of this particular compound peaks at m/z 499 (476 + 23), **h**.

The MALDI MS of the film after the removal of the 15 μm surface layers is shown in Figure 5.3.3.1iii. It is observed that the marker peaks of the UV-induced seco-products, at m/z 483, 495, 499 (**d**, **e**, **h**) are not present at this particular depth. Instead,

peaks at m/z 463 and m/z 491 (**i** and **j** respectively) emerge, which are not detected in the mass spectrum of the aged or on the surface of the unaged dammar. These peaks represent the sodiated molecular ions of the oxidation compounds **25**/**27** (440 Da) and **26**/**28** (468 Da) respectively (Dietemann 2003). These are typical compounds formed upon oxidation of oleanane/ursane triterpenoids in the absence of UV wavelengths and have been reported in aged dammar varnishes on paintings (Van der Doelen, et al. 1998a, Van der Doelen 1999). This finding is in line with the decreasing number of carbonyl groups according to the ATR-FTIR measurements (Section 4.3.3), as well as with the decreasing optical densities determined with the UV/VIS measurements (Section 4.3.2). Given that the optical absorption lengths, ℓ_α, of both the aged dammar and mastic films at $\lambda > 350$ nm are longer than 15 μm from the surface (Figure 4.3.2.6), it is suggested herein that A-ring oxidation occurs under irradiation with $\lambda < 350$ nm. This suggestion agrees with findings by Van der Doelen and co-workers (1999, 2000), who determined the A-ring oxidation upon irradiation with $\lambda > 315$ nm and the non-UV-induced oxidation upon irradiation with $\lambda > 380$ nm. Regardless of the wavelengths employed, it is demonstrated here that the bulk of aged dammar and mastic films is protected from UV irradiation anyway.

5.3.4 A study on the molecular weight across depth of aged dammar and mastic films with High Performance - Size Exclusion Chromatography (HP-SEC)

Although a decreasing gradient in the condensed, high molecular weight fraction of the aged dammar and mastic films was indicated with the weakening of the EI-DTMS TIC's pyrolysis peak with depth (Figure 5.3.1.3), size exclusion chromatography was carried out to determine depth-wise molecular weight changes. Interpretation was

carried out using earlier SEC studies of triterpenoid varnishes (De la Rie 1988b, Van der Doelen 1999). De la Rie (1988b) used Gel Permeation Chromatography (GPC), which is a synonymous method to SEC, and determined an average increase in the molecular weight of accelerated aged dammar resins up to 1500 Da. Zumbühl and co-workers (1998) also reached the same conclusion measuring the mass/charges of light aged dammar films on the basis of GALDI/MS. Van der Doelen and co-workers (1999, 2000), used SEC with UV (240 nm) and VIS (400 nm) detectors to detect compatibility of naturally aged varnishes and accelerated aged resins. In the present work, SEC traces at 240 and 400 nm of the unaged, aged and laser ablated dammar and mastic films were studied to detect MW changes across depth. The same quantity of material was used from all the films tested and dissolved in THF (~10mg/μl), while about 20 μl of the prepared solutions were injected in the column. It was therefore expected that the final chromatograms would provide information about the molecular weight distribution across depth as a function of the absolute absorbance at 240 and 400 nm. However, this was not possible because of the depth-dependent gradients of the optical properties of the aged films (Figures 4.3.2.1b, 4.3.2.2b), which affected the intensities of the resulting SEC traces accordingly. Therefore, all the SEC traces were normalised at a % relative absorption.

Figure 5.3.4.1 presents the SEC traces at 240 and 400 nm of the dammar film prior to and after accelerated ageing. The molecular weight increase upon ageing is evident with both detectors. Absorption at both wavelengths is separated in a small fraction of sesquiterpenoids (~ 200 Da), the group of triterpenoid molecules (400/500 Da), which being the most abundant compounds absorb strongly, a small fraction of dimerised

and oxidised triterpenoid molecules (900/1000 Da) and traces of the condensed high MW fraction at 10 kDa, that are mainly formed upon the radical polymerisation of polycadinene (Van Aarssen, et al. 1990). The highest absorption at 240 nm of the aged dammar film is obtained at 900/1000 Da, while the triterpenoid molecules (400/500 Da) absorb slightly less than their dimers, forming a double peak within the range 400 to 1000 Da. This double peak broadens towards the higher MW regime, up to 15 kDa. Absorption of the ~ 200 Da group is critically reduced upon ageing indicating that both low MW components and triterpenoid molecules participate in the formation of longer molecular chains during degradation or that the low MW fraction escaped the film (Boon and van der Doelen 1999). The SEC trace at 400 nm of the aged film shows that the group of molecules absorbing intensely in the blue have a molecular weight in the order of 400 Da. This MW points to triterpenoid molecules, while the second intense peak at 800/900 Da shows that oxidised and dimerised triterpenoids absorb strongly in the blue region. SEC traces of aged varnishes from paintings at 400 nm detected a MW increase absorbing strongly at molecular weights greater than 1000 Da, while artificially aged dammar resins in solution absorbed intensely at ~ 2000 Da with shoulders at higher molecular weights (Van der Doelen 1999, Van der Doelen and Boon 2000). This mass increase was associated with yellowing. In the present work, the strongest absorption in the blue was obtained at 400 Da.

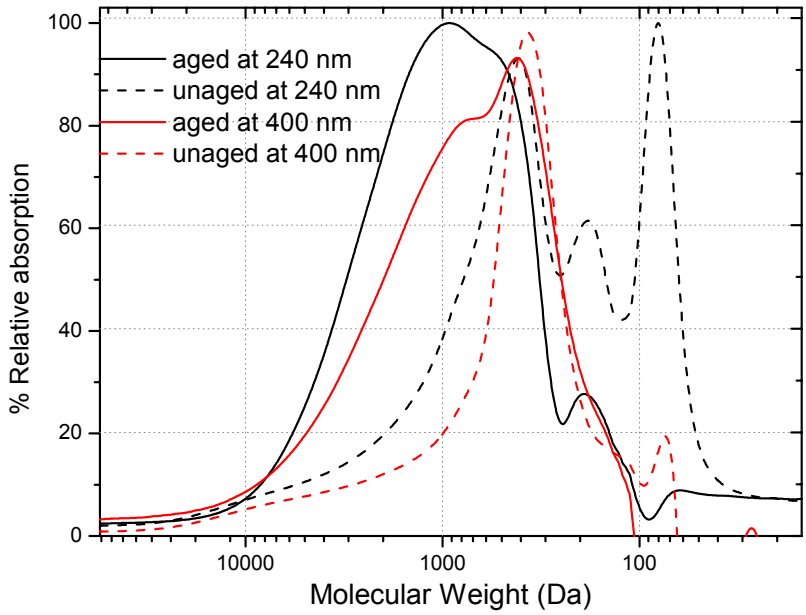

Figure 5.3.4.1 SEC traces of the aged and unaged dammar films at 240 nm and 400 nm.

Figure 5.3.4.2 demonstrates the SEC traces at 240 nm of consecutive depth-steps down to 15 μm from the surface of the aged dammar film and the SEC trace of the same dammar film prior to ageing. It is observed that the molecular weight across the highly deteriorated surface layers of the aged dammar film does not change significantly, which is in agreement with the intense carbon dimer emission upon 248 nm laser ablation (Figure 3.3.4.2) as well as with the constant ablation step in the 15 μm surface layers (Figure 3.3.5.3). The results agree also with the DTMS data of the 15 μm surface layers of the aged dammar film, showing that there is little change in the abundance of the mass/charges corresponding to the triterpenoid molecules, (400/500 Da). A small shoulder peak, increasing at about 200 Da on the SEC traces at 240 nm (Figure 5.3.4.2) of the ablated depth-steps, indicates the presence of some low MW products with depth, which eventually escape in the atmosphere (Boon and van der Doelen 1999). Figure 5.3.4.3 shows the SEC traces of the same depth-steps of the

aged dammar film at 400 nm and the SEC trace of the film prior to ageing. Two facts are apparent in this chromatogram. First, ageing results in a slight increase of the MW

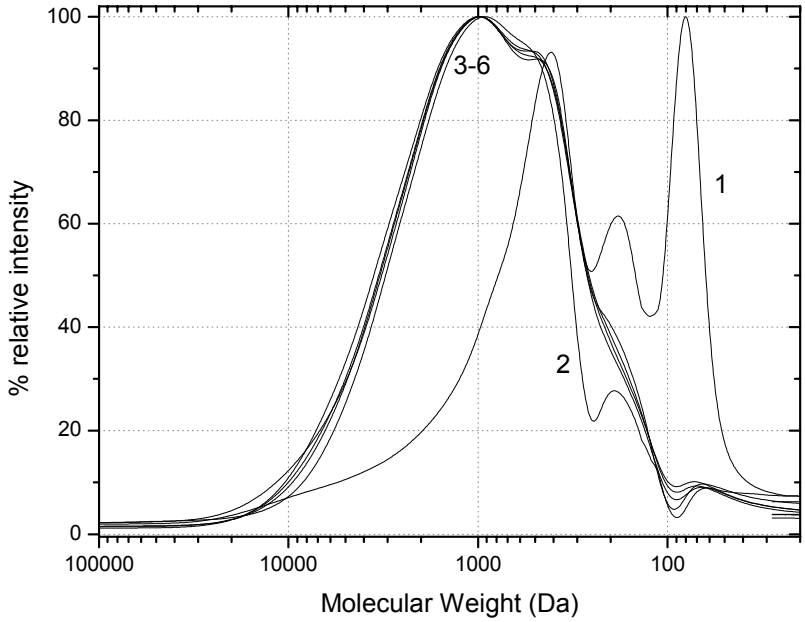

Figure 5.3.4.2 HP-SEC plots of dammar at 240 nm before ageing (1), after ageing (2) and those of the laser ablated depth steps between 3.5 and 15 μm (3-6).

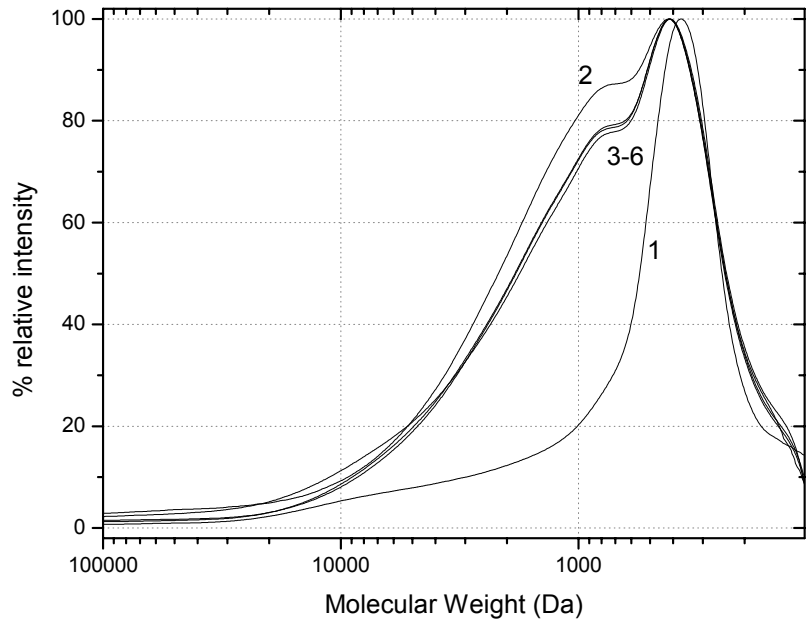

Figure 5.3.4.3 HP-SEC plots of dammar at 400 nm. For comparison the traces of the unaged (1), aged (2) and the ablated depths from 3.5 to 15 μm (3-6) are demonstrated.

of the triterpenoid compounds (400/500 Da), which is related to oxidation. Second, there is an abrupt decrease in the absorption from the crosslinked fraction of the dimerised triterpenoids (900 Da). These products participate in the formation of yellow compounds absorbing strongly in the blue and are responsible for the colouration effect in the aged dammar (Van der Doelen and Boon 2000). The decrease in the absorption at 400 nm between the aged surface and the layers below, especially at 900 Da, indicates a decreasing degree of yellowing with depth, which has been determined in laser ablated aged varnishes on paintings (Theodorakopoulos and Zafiropulos 2003, Section 1.4).

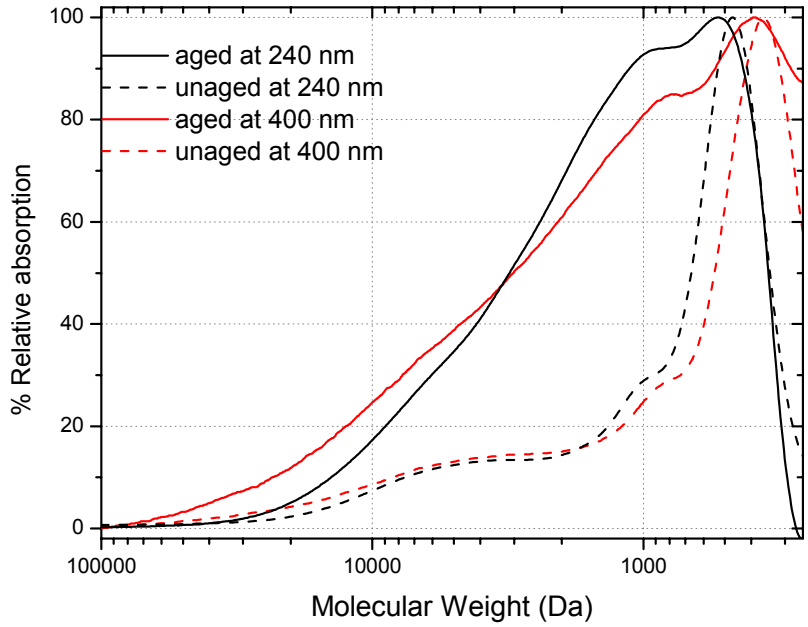

Figure 5.3.4.4 HP-SEC traces of the aged and unaged mastic film at 240 and 400 nm

Figure 5.3.4.4 presents the SEC traces of mastic prior to and after ageing at 240 nm and 400 nm. At 240 nm the unaged film absorbs strongly at 400 Da owing to the triterpenoid molecules. There is a shoulder peak at ~ 1000 Da caused by oxidised triterpenoid dimers and an apparent hump at ~ 10 kDa that represents a condensed fraction of mastic. At 400 nm the unaged film absorbs strongly at ~ 300 Da owing to

unsaturated triterpenoid ketones and quinones (Formo 1979) that are responsible for yellowing (Figure 2.2.4). The fraction of 1000 Da absorbs less intensely at 400 nm than at 240 nm, while there is also a small fraction at 10 kDa that absorbs the radiation equally at both wavelengths. Upon ageing absorption due to triterpenoids molecules (~400 Da) is strong in both wavelengths, but a shift towards higher MW indicates oxidation. The increased absorption at 1000 Da (240 nm) and ~ 900 Da (400 nm), indicates the increasing concentration in oxidised triterpenoid dimers (De la Rie 1988b). The broadening of the peaks suggests the existence of triterpenoid trimers, tetramers and longer crosslinked chains that appear as shoulders at 10 kDa. Absorption at 400 nm is relatively strong from about 3000 Da to almost 80 kDa compared to the SEC trace at 240 nm. According to Van der Doelen and Boon (2000) these long molecules absorb strongly in the blue and are responsible for the yellowing effect of the triterpenoid varnishes. Indeed, unlike the aged dammar film, the aged mastic film obtained a stronger yellow hue after several weeks in the dark following an extreme light ageing procedure, which initially bleached the yellow chromophores (Chapter 2). Therefore, the depth-dependent molecular weight decrease of the aged mastic film is better illustrated with the SEC chromatograms at 400 nm (Figure 5.3.4.5). The SEC traces of the unaged mastic film and the aged film prior to ablation are shown for reasons of comparison. It is observed that there is an evident gradient in the absorption from the high MW fraction across depth. In particular, the abundances of the 900/1000 Da components and the condensed fraction in the high MW regime up to 80 kDa are gradually decreasing with depth. As in the case of DTMS, sampling for SEC included the remaining varnish film (total thickness ~ 55 μm) resulting in average molecular weight determination of the remaining films. Therefore, the

absolute molecular weight as a function of depth will most likely display a sharper gradient than that demonstrated in Figure 5.3.4.5.

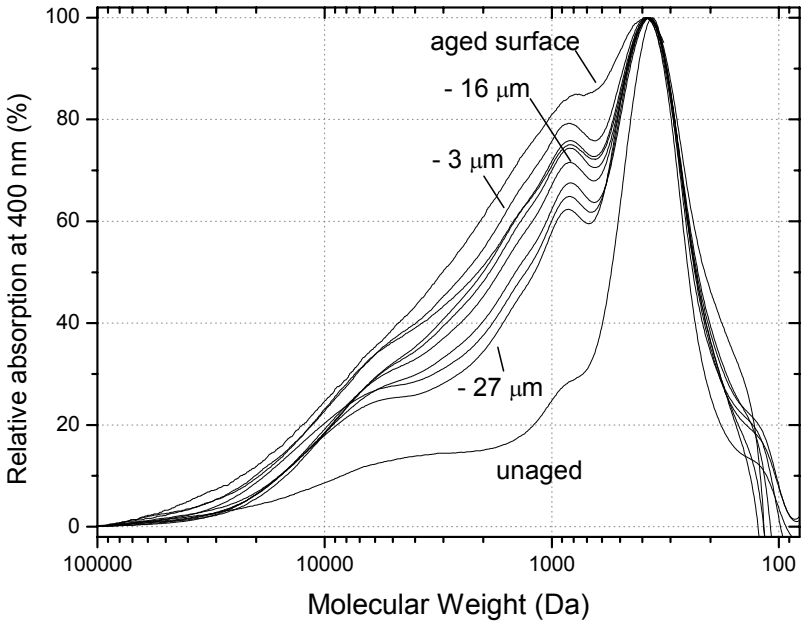

Figure 5.3.4.5 HP-SEC traces at 400 nm of the aged and unaged and laser ablated mastic film at successive etchings at 3, 6, 9, 12, 16, 20, 25 and 27 μm from the surface. The apparent MW reduction across the depth profile is evident.

5.4 Rationalisation of triterpenoid varnish ageing

Recently an ageing model of triterpenoid varnishes has been proposed (Boon and van der Doelen 1999). The model was based on experimental observations of molecular studies carried out with GCMS and LCMS analysis of fresh and aged triterpenoid varnishes and orientational studies on sterols, which have comparable carbon skeletal ring structures as the triterpenoid molecules. In view of the current mass spectrometric and chromatographic analytical data based on DTMS, MALDI-MS, HP-SEC, UV/VIS and ATR-FTIR (Chapter 4) on successive depths of the excimer laser ablated triterpenoid films, an updated schematic model on the degradation of these varnishes is proposed. The current findings are integrated into the previous model, aiming at a better understanding of the nature of aged triterpenoid varnishes. In line with the

previous model (Boon and van der Doelen 1999), we assume the existence of a considerable degree of orientation of the triterpenoid molecules forming flat sheet-like structures on a molecular level before the degradation process begins.

A first phase in triterpenoid varnish degradation corresponds to photoinitiation and the early oxidation stages. As soon as the varnish is exposed to light, the triterpenoid molecules lying on the surface varnish layers absorb the short wavelengths of the incident ambient radiation and hence the longer wavelengths ($\lambda > 350$ nm) are transmitted to the triterpenoids in the bulk. In line with Beer's Law, absorption of light from the resin compounds reduces logarithmically across the depth of the film. The depth-dependent qualitative and quantitative reduction of light leads to decreasing degrees of excitation. Thus, the free radicals formed across depth are quenching as the light propagates deeper into the bulk. Given the findings in the present work it is understood that the free radicals in the surface layers are more abundant than in the bulk because more intense bond-breakage occurs in the surface. Certainly, the presence of oxygen and the mobility of the radicals into the triterpenoid films play a significant role in the degradation process and the delineated quenching with depth. The excited molecules and the free radicals generate new covalent bonds between each other forming so new high molecular weight compounds. Because of the gradient in light propagation (Chapter 4), the extent of this condensation process decreases accordingly with depth.

At the same time, the oxygen diffusion from the air-surface interface into the bulk is also decreasing (Thomson 1965, 1979), thereby leading to high degrees of functionalisation on the surface layers and oxygen depletion in the bulk. Because of

the absorption of the short wavelengths ($\lambda < 350$ nm) from the surface layers only, different oxidation products are formed in the surface and the deeper layers, which is supported by the existence of A-ring oxidation at C-2 in the surface layers and oleanane / ursane type molecules oxidised at C-11 and C-12 in the bulk (Section 5.3.3). The degree of oxygen consumption across depth is important for the propagation reactions (Section 2.2), which originally are initiated in an decreasing rate across the depth profile of the film (top to bottom) (Schoolenberg and Vink 1991). Hence, depending on the degree and the type of oxidation, water molecules are attracted by the oxidised triterpenoids across the film thickness. This attraction leads to hydrogen bonding between the polar groups and the water molecules creating weak hydrogen bonded 'crosslinks' (Boon and van der Doelen 1999), the abundance of which decreases with depth. The sheet-like orientations of the triterpenoid compounds are disturbed, especially at the surface, as soon as these structural modifications take place from the first stages of degradation. Both types of crosslinking reduce the mobility of the triterpenoid compounds especially on the surface, thereby leading to surface stiffness, the degree of which is accordingly reducing with depth. At the same time an equivalent gradient in polarity across thickness is also formed.

At a second phase, the varnish proceeds to further degradation that is led by further oxygen consumption, bond breaking and polymerisation processes. The already modified triterpenoid molecules at the uppermost layers of the film are further degraded forming smaller molecular species, which no more have the characteristic triterpenoid carbon ring skeleton, as determined by analytical data based on GC and HPLC (Van der Doelen, et al. 1998b, Boon and van der Doelen 1999). The high

degree of functionalisation of the triterpenoids at the surface results in even stronger absorption of the short wavelengths by the outer layers, which prevents penetration of UV wavelengths into the bulk. The overall propagation of light into the film is shortened further and Beer's Law is no longer valid for all the film thickness because of the abrupt optical changes across depth. This is now well understood, because of the decreasing trends of the absorption coefficients progressing into the depths of aged mastic and dammar films (Section 4.3.2) (Zafiropulos, et al. 2000). According to the previous theoretical model on triterpenoid ageing, small degradation products, such as functionalised carbon compounds (aldehydes, ketones and acids) yielded from bond breaking and ring disintegration, escape to the atmosphere (Boon and van der Doelen 1999). At the same time bond-breakage, excitations and oxygen consumption is continued gradually in the underlying layers although all trends would be decreasing with time (Thomson 1965, 1979). Hence, further attraction of water molecules is consistent with the degree and the depth of oxygen consumption across the depth-profile. Crosslinked fractions have reduced molecular weight with depth. Crosslinks at the surface may well contain more polar that apolar groups, changing gradually the plasticity of the varnish at the exposed surface.

A final phase corresponds to further degradation of highly deteriorated triterpenoid varnish. Elimination reactions in the high molecular weight condensed fractions may lead to formation of aromatic centres, further influencing the light absorbing properties of the surface layers. On the surface, residual polar triterpenoid and polar parts of high molecular weight species are linked with water molecules. The high concentration of the three dimensional covalent-bonded polymer network may lead to

a certain degree of insolubility of the surface layers. Further exposure to radiation leads to depolymerisation of the surface by continuous bond-breakage resulting from excitation of the absorbing functional groups attached to the condensed surface layers. On the other hand, the bulk is preserved in a somewhat 'unaged' state, since all the deteriorative actions are carried out in the uppermost layers. Both the extent of polarity and crosslinking in the deep layers are comparable to that of the starting film, protecting the substrate from the deteriorative consequences of the ambient conditions.

5.5 Conclusions

In conclusion, deterioration of dammar and mastic varnish films formed upon ageing is critically dependent on their thicknesses. Based on the results shown above it is determined that thick dammar and mastic films protect photosensitive substrates from deteriorative UV light wavelengths and from exposure to oxygen, preserving them in the best possible condition for a considerable lifetime. The transition from the highly degraded surface to the less reacted or even unreacted bulk layers, is a matter of a depth-dependent gradient both in terms of oxidation, as shown herein with DTMS, and in terms of the photochemically induced high MW condensed material, detected by HP-SEC. The presented results support all the findings demonstrated above on the change of the interaction of the aged resin films with the UV laser photons (Figures 3.3.2.2, 3.3.2.4, 3.3.3.1), the decreasing carbon dimer emission upon consecutive laser pulses (Figures 3.3.4.2a, b), the reduction of the ablation step (Figure 3.3.5.3), the change of the laser-induced transmission rate (Figures 4.3.1.2.2a, b, 4.3.1.2.4), the decreasing optical densities (Figures 4.3.2.1b, 4.3.2.2b, 4.3.2.4b) and the decreasing

number of carbonyls (Figures 4.3.3.2i, ii, 4.3.3.3a, b, 4.3.3.4) as a function of depth, on the molecular level. Oxidation not only reduces gradually as a function of depth, but the transition from highly oxidative and polar states in the surface towards non-oxidative states in the bulk is, in addition, qualitative. Based on the MALDI-TOF-MS results, it is determined herein that UV-induced oxygenated triterpenoid compounds, such as oleanane / ursane type molecules with oxidised A-rings (Figure 2.2.2c), are formed only in the 15 μm surface layers despite the fact that both the 55 μm films tested were irradiated with light of $\lambda > 295$ nm for about 500 hours (Section 2.7.2.2). At less than 15 μm below surface only oleanane / ursane type molecules with side chain oxidation at positions C-11 and C-28 (Figure 2.2.2b); these are detected as typical compounds of oxidised varnishes found in paintings (Van der Doelen, et al 1998a). This finding is in line with the optical absorption lengths of light with $\lambda < 350$ nm that is completely absorbed in the 15 μm surface layers (Figure 4.3.2.6), which indicates that wavelengths shorter than 350 nm are responsible for the A-ring oxidation. Hence, wavelengths longer than 350 nm penetrate in the deeper layers of the film, as also shown in Figure 4.3.2.6. Similar results have been reported by (Feller 1994b), who noted that the penetration depth of 350 nm radiation is ten times that of 320 nm into aromatic polyester films. Although oxidation is considered as the main problem of natural resin varnishes (Section 2.2), the decreasing gradient in the high MW condensed fraction that is formed during photochemical degradation should not be underestimated. Provided that high MW crosslinks are insoluble (Stolow 1985, De la Rie 1988b), the suggestion that upon chemical treatments only the volatile compounds are removed and the condensed material remains on the treated surface (Boon and van der Doelen 1999) is fully supported here. As discussed in Section

2.2.2, this potential influences the appearance of the substrate, especially if this is paint, because of the overall rise of the MW and the high viscosity (De la Rie 1987, Berns and De la Rie 2002, 2003) formed in the new varnish, which eventually will be integrated with the high MW condensed fraction of the older varnish that remains on the surface. This possibility and the fact that no oxidative contribution of the 248 nm laser pulses to the remaining films was detected is a good argument for the excimer laser ablation of aged varnish films.

5.6 References

Berns, R. S. and De la Rie, E. R. 'The relative importance of surface roughness and refractive index in the effects of varnishes on the appearance of painitngs'. In *Preprints of the 13th triennial meeting of the ICOM Committee for Conservation*, Ed. V. R., Vol. I, James & James (Science Publishers) Ltd, Rio de Janeiro, (2002), 211-216.

Berns, R. S. and De la Rie, E. R., 'The effect of the refractive index of a varnish on the appearance of oil paintings', *Studies in Conservation* **48** (2003) 251-262.

Boon, J. J., 'Analytical pyrolysis mass spectrometry: new vistas opened by temperature-resolved in-source PYMS', *International Journal of Mass Spectrometry and Ion Processes* **118/119** (1992) 755-787.

Boon, J. J. and van der Doelen, G. A. 'Advances in the current understanding of aged dammar and mastic triterpenoid varnishes on the molecular level'. In *Firnis: Material - Aesthetik - Geschichte, International Kolloquium, Braunschweig, 15-17 Juni 1998*, Ed. A. Harmssen, Hertog-Anton-Ulrich-Museum, Braunschweig, (1999), 92-104.

Carlyle, L. A. *The artist's assistant: Oil painting Instruction manuals and handbooks in Britain 1800-1900: with reference to selected eighteenth century sources*, Archetype Publications, London, 2001.

Castillejo, M., Martin, M., Oujja, M., Silva, D., Torres, R., Manousaki, A., Zafiropulos, V., van den Brink, O. F., Heeren, R. M. A., Teule, R., Silva, A., and Gouveia, H., 'Analytical study of the chemcial and physical changes induced by KrF laser cleaning of tempera paints', *Analytical Chemistry* **74** (2002) 4662-4671.

Cunliffe, A. V. and Davis, A., 'Photo-oxidation of thick polymer samples. Part II: The influence of oxygen diffusion on the natural and artificial weathering of polyolefins', *Polymer Degradation and Stability* **Vol. 4** (1982) 17 - 37.

De la Rie, E. R., 'The influence of varnish on the appearance of paintings', *Studies in Conservation* **32** (1987) 1-13.

De la Rie, E. R., 'Stable Varnishes for Old Master Paintings', PhD Thesis University of Amsterdam, (1988a).

De la Rie, E. R., 'Photochemical and thermal degradation of films of dammar resin', *Studies in Conservation* **33** (1988b) 53-70.

Dietemann, P., 'Towards more stable natural resin varnihses for painintgs', PhD Thesis Swiss Federal Institute of Technology, Zurich, (2003).

Feller, R. L. 'Depth of Penetration of Light into Coatings; and Influence of Sample Thickness and Oxygen Diffusion'. In *Accelerated Aging: Photochemical and Thermal Aspects*, Ed. D. Berland, The Getty Conservation Institute, USA, (1994a), 56-61 and 135-137.

Feller, R. L. 'Depth of Penetration of Light into Coatings'. In *Accelerated Aging: Photochemical and Thermal Aspects*, Ed. D. Berland, The Getty Conservation Institute, USA, (1994b), 56 - 61.

Formo, M. W. 'Paints, varnishes and related products: Discolouration'. In *Baile's Industrial Oil and Fat Products*, Ed. D. Swern, Vol. 1, John Wiley & Sons, New York, (1979), 722-724.

Fukushima, T., 'Deterioration Processes of Polymeric Materials and their Dependence on Depth from Surfaces', *Durability of Building Materials* **Vol. 1** (1983) 327 - 343.

Hoogerbrugge, R., Willig, S. J., and Kistemaker, P. G., 'Discriminant analysis by double stage principal component analysis', *Analytical Chemistry* **55** (1983) 1710-1712.

Koller, J., Baumer, U., Grosser, D., and Schmid, E. 'Mastic'. In *Baroque and Rococo Lascquers*, Ed. J. Koller, Vol. 81, Arbeitshefte des Bayerischen Landesamtes fuer Denkmalpflege, Karl M. Lipp Verlag, Muenchen, (1997), 347-358.

Mantell, C. L., Kopf, C. W., Curtis, J. L., and Rogers, E. M. 'Oil Varnishes'. In *The technology of natural resins*, John Wiley & Sons, Inc., (1949), 265-319.

Mills, J. S. and Werner, A. E. A., 'The chemistry of dammar resin', *Journal of Chemical Society* (1955) 3132-3140.

Mills, J. S., 'The constitution of the natural, tetracyclic triterpenes of dammar resin', *Journal of Chemical Society* (1956) 2196-2202.

Mills, J. S. and White, R. *The Organic Chemistry of Museum Objects*, 2nd edition, Butterworth-Heinemann, Oxford, 1994.

Papageorgiou, V. P., Bakola-Christianopoulou, M. N., Apazidou, K. K., and Psarros, E. E., 'Gas chromatographic-mass spectrometric analysis of the acidic triterpenic fraction of mastic gum', *Journal of Chromatography A* **769** (1997) 263-273.

Poehland, B. L., Carte, B. K., Francis, T. A., Hyland, L. J., Allaudeen, H. S., and Troupe, N., 'In vitro antiviral activity of dammar resin triterpenoids', *Journal of Natural Products* **50** (1987) 706-713.

Scalarone, D., van der Horst, J., Boon, J. J., and Chiantore, O., 'Direct-temperature mass spectrometric detection of volatile terpenoids and natural terpenoid polymers in fresh and artifficially aged resins', *Journal of Mass Spectrometry* **38** (2003) 607-617.

Schoolenberg, G. E. and Vink, P., 'Ultra-violet degradation of polypropylene: 1. Degradation Profile and thickness of the embrittled surface layer', *POLYMER* **Vol. 32 No 3** (1991) 432 - 437.

Srinivasan, R. and Braren, B., 'Ultraviolet laser ablation of organic polymers', *Chemical Reviews* **89** (1989) 1303-1316.

Srinivasan, R. 'Interaction of laser radiation with organic polymers'. In *Laser Ablation: Principles and Applications*, Ed. J. C. Miller, Vol. 28, Springer Series of Material Science, Springer, Berlin, Heidelberg, (1994), 107.

Stolow, N. 'Part II: Solvent Action'. In *On picture varnishes and their solvents.*, Ed. E. H. Jones, Revised edition 1971. Cleveland, Ohio: Case Western Reserve University. Revised and enlarged edition 1985. Washington DC: National Gallery of Art., (1985).

Theodorakopoulos, C. and Zafiropulos, V., 'Uncovering of scalar oxidation within naturally aged varnish layers.' *Journal of Cultural Heritage (Suppl. 1)* **4** (2003) 216s-222s.

Theodorakopoulos, C., Zafiropulos, V., Fotakis, C., Boon, J. J., van der Horst, J., Dickmann, K., and Knapp, D., 'A study on the oxidative gradient of aged traditional triterpenoid resins using 'optimum' photoablation parameters', In *Lacona V Proceedings, Osnabrück, Germany, September 15-18, 2003*, Eds. K. Dickmann, C. Fotakis, and J. F. Asmus, Springer Proceedings in Physics, Vol. 100, Springer-Verlang, Berlin Heidelberg, (2005), 255-262.

Thomson, G. 'Topics in the conservation chemistry of surface.' In *Application of Science in Examination of Works of Art*, Museum of Fine Arts, Boston, (1965), 78 - 85.

Thomson, G., 'Oxygen Starvation in Paint and Other Films', *National Gallery Technical Bulletin* **Vol. 2** (1978) 66 -70.

Thomson, G., 'Penetration of Radiation into Paint Films', *National Gallery Technical Bulletin* **Vol. 3** (1979) 25 -33.

Van Aarssen, B. G. K., Cox, H. C., Hoogendoorn, P., and De Leeuw, J. W., 'A cadinene biopolymer present in fossil and extant dammar resins as a source for cadinanes and bicadinanes in crude oils from Southern Asia', *Geochimica et Cosmochimica Acta* **54** (1990) 3021-3031.

Van der Doelen, G. A., van der Berg, K. J., and Boon, J. J., 'Comparative chromatographic and mass spectrometric studies of triterpenoid varnishes: fresh material and aged samples from paintings', *Studies in Conservation* **43** (1998a) 249-264.

Van der Doelen, G. A., Van der Berg, K. J., Boon, J. J., Shibayama, N., De la Rie, E. R., and Genuit, W. J. L., 'Analysis of fresh triterpenoid resins and aged triterpenoid varnishes by high-performance liquid chromatography-atmospheric pressure chemical ionisation (tandem) mass spectrometry', *Journal of Chromatography A* **809** (1998b) 21-37.

Van der Doelen, G. A., 'Molecular studies of fresh and aged triterpenoid varnishes', PhD Thesis University of Amsterdam, (1999).

Van der Doelen, G. A., Van den Berg, K. J., and Boon, J. J., 'A comparison of weatherometer aged dammar varnish and aged varnishes from paintings'. In *Art Chimie: La Couleur: Actes du Congres*, Ed. J.-P. Mohen, CNRS Editions, Paris, (2000), 146-149.

Van der Doelen, G. A. and Boon, J. J., 'Artificial ageing of varnish triterpenoids in solution', *Journal of Photochemistry and Photobiology A: Chemistry* **134** (2000) 45-57.

Windig, W., Haverkamp, J., and Kistemaker, P. G., 'Interpretation of sets of pyrolysis mass spectra by discriminant analysis and graphical rotation', *Analytical Chemistry* **55** (1983) 81-88.

Zafiropulos, V., Manousaki, A., Kaminari, A., and Boyatzis, S., 'Laser Ablation of aged resin layers: A means of uncovering the scalar degree of aging', *ROMOPTO: Sixth Conference on Optics, Vlad V. I. (Ed.), SPIE Vol. 4430 (SPIE The International Society for Optical Engineering, Washington, (2001) 181-185.* (2000).

Zafiropulos, V. 'Laser ablation in cleaning of artworks'. In *Optical Physics, Applied Physics and Material Science: Laser Cleaning*, Ed. B. S. Luk'yanchuk, World Scientific, Singapure, New Jersey, London, Hong Kong, (2002), 343-392.

Zumbühl, S., Knochenmuss, R., Wülfert, S., Dubois, F., Dale, M. J., and Zenobi, R., 'A graphite-assisted laser desorption/ionisation study of light-induced ageing in triterpene dammar and mastic varnishes.' *Analytical Chemistry* **70** (1998) 707-715.

6. A direct temperature-resolved mass spectrometric study across the 248 nm laser-ablated depth-profile of an aged copal oil varnish

Abstract

Electron Ionisation (EI) – Direct Temperature-resolved Mass Spectrometry (EI-DTMS) was employed to characterise the molecular state across the depth profile of an aged (500h, xenon arc, $\lambda > 295$ nm), 15 μm thick, copal oil varnish, which was selectively ablated in five successive depth steps ranging from 2.5 to 12 μm with a KrF excimer laser (248 nm, 25 ns). Prior to ageing, the film contained short and long chain saturated, unsaturated, cyclic, oxygenated and saturated dicarboxylic fatty acid moieties, as well as oxidised dehydroabietic acid moieties. Upon ageing the concentration in unsaturated fatty acids reduced in favour of saturated diacids and other oxidation products, while the diterpenoid molecules reacted away leaving only trace amounts in the final film. According to the DTMS data, the composition of the aged film remains unchanged across the depth. All the compounds identified are part of a condensed, crosslinked, high MW polymer network, which upon ageing becomes more polar, thereby requiring higher thermal energy to induce desorption from the pyrolysis wire of the DTMS set-up. DTMS across the laser ablated depth profile of the film determined that both concentration and the extent of crosslinking remain constant at all depths.

6.1 Introduction

Oil varnishes, being manufactured by heat-bodying at strong temperatures in the range of 300 – 350 °C (Mantell, et al. 1949, Mills and White 1994, Carlyle 2001), are high molecular weight, polymerised, condensed, polar and oxidised mixtures, even prior to exposure to deteriorative environments (Section 2.4). The evidently advanced oxidation state of oil varnish films, compared to that of the component drying oil prior to the varnish-making process, is significant in the presence of air during manufacturing (open preparation vessels) resulting in a very viscous material, whose volatile fraction evaporates from the boiling mixture (Formo 1979). During boiling, the component drying oil degrades via three parallel actions: (a) hydrolysis in the glycerol ester bonds resulting in the formation of di- and monoacylglycerols, glycerol and free fatty acids (Frilette 1946, Crossley, et al. 1962, Paulose and Chang 1973, 1978, Frankel, et al. 1981, Perrin 1996), while the concentration in free fatty acids influences both the acid value and the oxidation rate of the oil (Privett 1959, Miyashita and Tagaki 1986, Frega, et al. 1999); (b) *cis*-*trans* isomerisation of double bonds in fatty acids with non-conjugated double bonds in a *cis*-configuration (Sonntag 1979, Martin, et al. 1998); and, (c) dimerisation by Diels-Alder type reactions (Figure 2.4.3a), which eventually leads to polymerisation following an essential first step at which conjugated dienes are formed (Boelhouwer, et al. 1967, Mills and White 1994). The latter action results in conjugation and leads also to intermolecular cyclisation generating cyclic fatty acids (Sebedio and Grandgirard 1989, Van den Berg 2002). Driers, such as lime, lead, zinc and manganese, which are occasionally employed during manufacturing to control the drying time of the oil varnish (Neil 1833, Scott

Taylor 1890), react with the volatile fraction of the mixture and enhance the viscosity of the final film (Keller 1973, Van den Berg 2002).

At the same time, the resin component, commonly being copal resin that was employed during the 18^{th} – 19^{th} centuries in Europe (Mills and White 1994, Carlyle 2001, Section 2.4), integrates in the three-dimensional polymerised fatty network. Py-TMAH-GC/MS data indicate that sturdy molecules, such as abietane type diterpenoids (Figure 2.4.5) remain in the varnish with little or no alterations, while the volatile resin components evaporate or break down during manufacturing (Figure 2.5.1). The use of turpentine oil to dissolve the resin prior to the heat bodying process, or to dilute the viscous oil varnish for the ease of the application of the final oil varnish film (Carlyle 2001), also results in a high concentration in abietane type diterpenoids and oxidation products thereof. However, even without the use of driers or the incorporation of turpentine oil, oil varnishes resemble stand oils with some resin molecules integrated in the high molecular weight, ester bonded polymer oil network. The absence or the moderate presence of a volatile fraction containing free fatty acids and possibly free resin molecules increases further the high viscosity of the final varnish film (Van den Berg 2002). Because of the absence of volatile material, oil varnishes become insoluble as soon as dried (Tingry 1804, Brommelle 1956, Gettens and Stout 1966, Stolow 1985, Carlyle 2001). Diterpenoid resins, such as copal, amber, sandarac and colophony, which were commonly used for the production of oil varnishes, polymerise so strongly (Scalarone, et al. 2002, 2003a, b) that they become insoluble even without being processed with drying oils (Gettens and Stout 1966). Upon ageing, oil varnish films result in a sharp reduction in the concentration

of the resin components, which react away with the polymerised lipids of the oil (Dunkerton, et al. 1990, Van den Berg, et al. 1999b, Section 2.5). Moreover, the degree of oxidation increases, as monitored (Section 2.5) by the increasing content of saturated fatty diacids in favour of unsaturated fatty acids (Sonntag 1979, Martin, et al. 1998). Ageing also leads to the production of oxygenated fatty acids from polyunsaturated fatty acids as well as the generation of cyclic C18 fatty acids formed via Diels-Alder cyclisation (Boelhouwer, et al. 1967, Martin, et al. 1998), indicating that the degree of polymerisation is increasing further with age. The intense condensed highly polar nature of such films forms a truly insoluble material.

Laser cleaning based on photochemical ablation (Luk'yanchuk, et al. 1994, Srinivasan 1994, Bäuerle 2000) is probably the only way to induce removal of such high molecular weight, condensed and polar material upon consecutive laser pulses with absolute control without affecting the substrate (Chapter 3). KrF (248 nm) excimer laser ablation of an aged copal oil varnish was obtained at a rate of ~ 2.5 μm per scan[1] using a ~ 0.9 J/cm^2 fluence, which remained constant as a function of depth (Chapter 3). The stability of the ablation step with depth of this particular coating contradicts the change of the ablation step across the thickness of aged dammar and mastic varnish films (Figure 3.3.5.3), whose optical densities as well as the degrees of oxidation and condensation follow a gradual depth-dependent reduction determined with a thorough study by means of LIBS, UV/VIS spectrophotometry, ATR-FTIR, DTMS, MALDI-TOF-MS and HP-SEC (Chapters 3, 4 and 5). Thus, the stability of the ablation step at all depths, using a KrF excimer laser, as well as the identical

[1] Resulted from the ablation rate that was ~ 0.5 μm per pulse and an 80% pulse-to-pulse overlap across the Gaussian profile of the laser front (Chapter 3).

interaction of the 248 nm laser pulses at a wide range of fluences, spanning from 0.1 to 1 J/cm^2, with surface and bulk layers of aged 15 and 30 μm thick copal oil varnish films are due to the unchanged optical density (Figures 4.3.2.3b, 4.3.2.5) and the stability of the degree of polymerisation and crosslinking with depth. The constant degree of crosslinking with depth was indicated by the constant carbon dimer emission monitored online with 248 nm laser ablation using LIBS (Figure 3.3.4.2c), and the unchanged ratios of methylene to methyl groups monitored with their bending vibrations using ATR-FTIR (Figure 4.3.2.10b). In other words, such films are optically saturated as reflected by the corresponding optical absorption lengths, ℓ_α, at various wavelengths of the incident light radiation (Figure 4.3.2.6). In particular, light with $\lambda < 320$ nm penetrates as deep as 20 μm from the surface and light with $\lambda > 350$ nm is transmitted across the entire 30 μm film thickness, which indicates that ageing with UV wavelengths occurs almost identically at all depths, although the light intensity is expected to reduce with depth. At the same time, it is realised that such films are very weak absorbers, pointing out that oil varnishes provide poor protection to the underlying layers compared to natural resin films, which completely block light with $\lambda < 350$ nm from penetrating deeper than 15 μm from surface (Figure 4.3.2.6). Despite these findings, the composition across the depth profile of an aged copal oil varnish remains unresolved. It may be suggested that the stability of the ablation step and the constant signals of optical properties, carbon dimer emission and CH_2-to-CH_3 ratios with depth are due to (coincidental) depth-wise changes in the proportions of the incorporated lipid and resin components both having carboxylic acid groups.

Consequently, this chapter aims to shed more light in the molecular state across the depth profile of oil varnishes. To enlighten this aspect direct temperature-resolved mass spectrometric (DTMS) analysis was carried out across the laser ablated depth profile of the film. DTMS has been very effective in the degradation studies of dammar, mastic (Van der Doelen, et al. 1998) Manila copal, sandarac (Scalarone, et al. 2003b) and colophony (Scalarone, et al. 2003a) and has been a valuable tool for uncovering a depth-depended compositional gradient of laser ablated, aged dammar and mastic films (Sections 5.3.1, 5.3.2). DTMS of polymerised linseed oil films provides a sufficient fingerprint molecular study, based on the classification of the molecular and fragment ions in volatile and crosslinked fractions corresponding to the successive temperature windows they desorb, as well as on the selection of specific m/z marker peaks thereof (Van den Berg 2002). Interpretation of the results was facilitated with DTMS data on aged linseed oil (Van den Berg 2002), diterpenoid resins (Scalarone, et al. 2003b, Scalarone, et al. 2003a) and mixtures thereof (Van den Berg, et al. 1999b). The results are correlated with a Pyrolysis-TMAH-GC/MS study on the same film prior to and after ageing (Section 2.5). While Py-TMAH-GC/MS, being a sensitive online derivatisation technique, enables the monitoring of a larger variety of compounds as determined in a wide range of relative studies on the characterisation of paint (Van den Berg, et al. 1999a), oil (Van den Berg, et al. 2002), oxidised diterpenoids (Anderson and Winans 1991, Pastorova, et al. 1997), copaiba balsam (Van der Werf, et al. 2000) or complex mixtures thereof (Van den Berg, et al. 1996), DTMS allows the separate monitoring of the compositions of volatile and high MW condensed fractions (Boon 1992). Since the two influential factors of excimer laser ablation are absorption, owing to oxidation, and crosslinking, owing to

condensation, (Srinivasan and Braren 1989, Zafiropulos 2002), DTMS was chosen as a suitable technique to monitor the depth-wise changes of an aged copal oil varnish film. Py-TMAH-GC/MS and DTMS, have been also coupled in earlier investigations of oil varnishes (Van den Berg, et al. 1999), since they provide complementary information about the molecular state of such complex, oxidised and crosslinked mixtures.

6.2 Experimental

6.2.1 Direct temperature-resolved mass spectrometry (DTMS)

DTMS was applied for a fast fingerprint analysis of the remaining laser-ablated, 15 μm copal oil varnish films with etchings at 2.5, 6, 8.5, 10 and 12 μm below the original surface and applied also to the films prior to and after ageing. From each sample a minute quantity in the range of 20 to 60 μg was removed, then homogenised and brought in suspension with a few drops of ethanol. A volume of 2-3 μl of the mixture was applied to a Pt/Rh (9:1) filament (100μm diameter) of a direct insertion probe, and dried *in vacuo*. After insertion in the ionisation chamber a gradual temperature increase of the filament was set at a rate of 0.5 A/min to a final temperature of approximately 800ºC, while the MS was monitoring the evolved compounds in the electron ionisation (EI) mode. The compounds were ionised at 16 eV energy to induce minimal fragmentation. Analysis was finally obtained in a JEOL SX-102A double focusing mass spectrometer (B/E/B/E) over a mass range of 20-1000 Da at a cycle time of 1s. The EI-DTMS total ion currents and summation mass spectra are examined based on available DTMS mass spectra of aged linseed oil (Van den Berg 2002), diterpenoid resins (Scalarone, et al. 2003b, Scalarone, et al. 2003a) and

mixtures thereof (Van den Berg, et al. 1999b). The results are correlated with a Py-TMAH-GC/MS study on the same film prior to and after ageing (Section 2.5).

6.3 Results and Discussion

6.3.1 EI-DTMS study of copal oil varnish prior to and after ageing

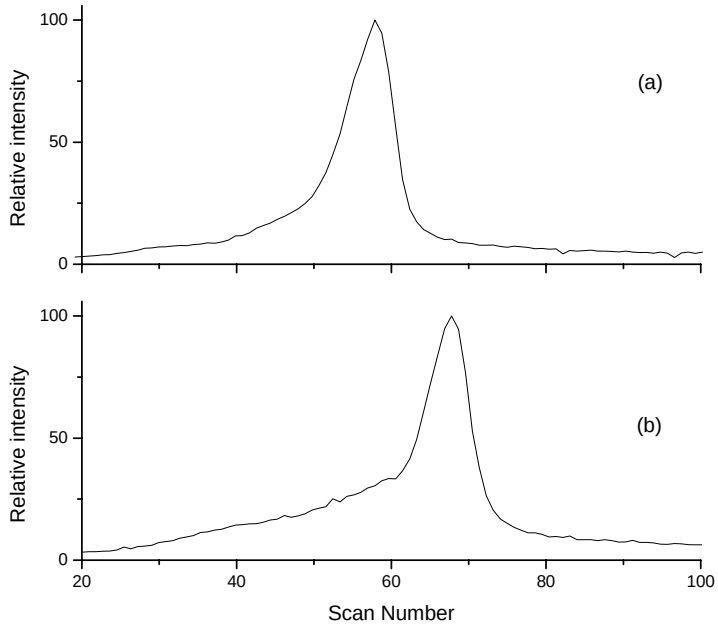

Figure 6.3.1.1 EI-DTMS total ion currents of copal oil varnish prior to (a) and after 500 h under xenon arc radiation ($\lambda > 295$ nm).

The EI-DTMS total ion currents of the copal oil varnish film prior to and after ageing are presented in Figure 6.3.1.1. The single peak detected in the EI-DTMS-TIC's indicates that all the components of the tested films prior to and after ageing desorbed in the ionisation chamber via pyrolysis. However, despite the lack of a clear vaporisation peak at low scan numbers (i.e. low temperature), a few volatile molecules escape into the ionisation chamber, such as remaining ethanol (m/z 46, 45, 31) and/or other low mass contaminants. The absence of a considerable volatile fraction particularly in the unaged oil varnish film contradicts DTMS data of a 'fresh' stand oil film analysed by Van den Berg (2002). The latter, had a volatile fraction

desorbed via evaporation at a relatively low temperature containing some free saturated and unsaturated fatty acid moieties. On the contrary, the EI-DTMS TIC of the unaged heat-bodied oil varnish examined herein produced a pyrolysis peak only, indicating that the film is highly crosslinked. Consequently, the component fatty acids, diacids and diterpenoid molecules that were detected by Py-TMAH-GC/MS (Table 2.5.1) and monitored by the summation mass spectra of EI-DTMS showing in Figure 6.3.1.2 are part of a high molecular weight crosslinked polymer network.

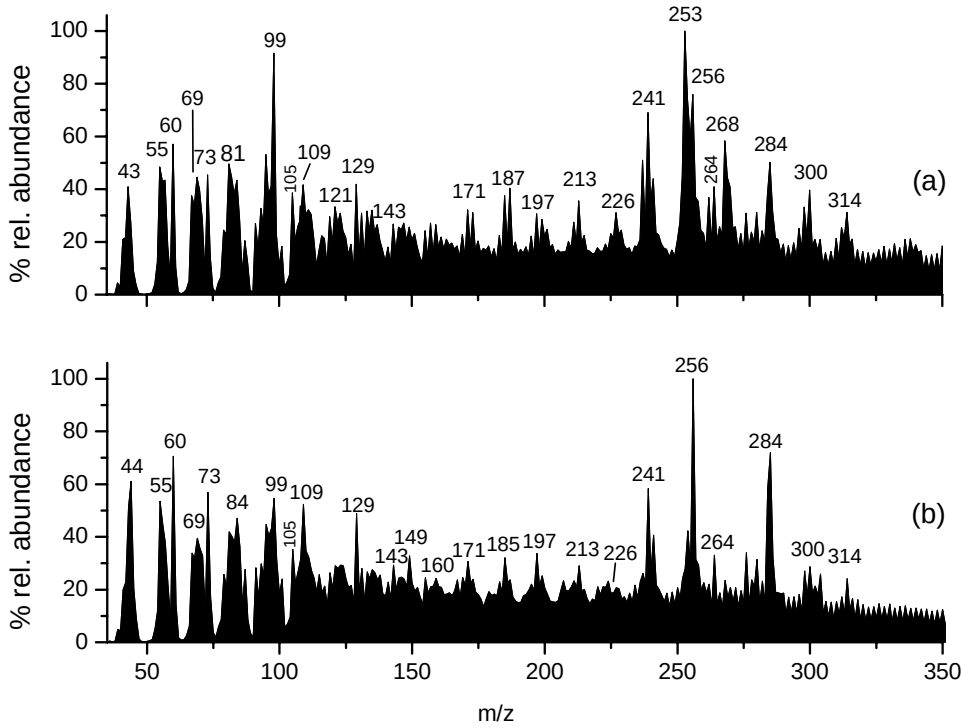

Figure 6.3.1.2 The EI-DTMS summation mass spectra of the copal oil varnish film prior to (a) and after (b) 500 h under xenon arc (λ > 295 nm) exposure.

Pyrolysis of the unaged oil varnish was obtained between scan numbers 45 and 65 (peak at scan no 58) corresponding to a temperature window spanning from 360°C to 520°C (peak at ~ 465°C). The EI-DTMS TIC of the aged oil varnish shows no virtual change, except that higher thermal energy was required to induce sufficient bond breaking. In this case pyrolysis occurs at temperatures in the range of 440°C to 600°C

corresponding to scan numbers 55 to 75, and peak at scan number 68 that is approximately 545°C. The shift of the TIC trace of the film after ageing towards a higher temperature, is in line with the Py-TMAH-GC/MS data showing that the film develops a high degree of saturation and increased polarity after ageing.

The EI-DTMS summation mass spectra of the copal oil varnish film prior to and after light ageing are demonstrated in Figure 6.3.1.2. The main molecular information is obtained in a mass range between 40 and 350 Daltons. High MW crosslinks are not detected and it may be suggested that these desorb from the pyrolysis wire as condensed species of short chain alkanes and alkenes resulting in a variety of peaks in the low mass / charge region (Hartgers, et al. 1991). Similar observations have been reported by Van den Berg (2002). The detected ion fragments have been verified with mass spectra databases at 16 eV and 70 eV (Ryhage and Stenhagen 1959, 1960b, Christie 1998, Van den Berg, et al. 1999b, Scalarone, et al. 2002, Van den Berg 2002, Van den Berg, et al. 2002). The list of compounds with the most characteristic ion fragments identified by EI-DTMS is shown in Table 6.3.1.1. Several ion fragments, the mass / charges of which are underlined in Table 6.3.1.1, correspond to more than one species. These m/z values were not taken into account in the interpretation of the mass spectra. Despite this complexity DTMS results were in a good agreement with the Py-TMAH-GC/MS study (Section 2.5).

For efficient discrimination of the desorbed compounds, some ion peaks that correspond to the condensed fraction obtained during pyrolysis were first detected. These peaks are identified in all the mass spectra presented herein and their presence is in line with earlier findings of mass spectrometry both at 70 eV in the analysis of

Table 6.3.1.1 EI-DTMS ion fragments corresponding to the identified compounds of the copal oil varnish film

Label	Compound		Ion Peaks					
	Saturated Fatty Acids (Short Chain)	Mw	M - CH_2CH_3 (M - 29)	M - $(CH_2)_2CH_3$ (M - 43)	M - CH_2–COOH (M - 59)	$C_6H_{12}O$+ $(CH_2)_n$ (84+n·14)	HOOC–$(CH_2)_n$ (59+n·14)	C_2H_5–$(CH_2)_n$ (29+n·14)
1	octanoic acid	144	115*	101	85	n =1-6		
3	nonanoic acid	158	129	115	99	n =1-7		
5	decanoic acid	172	143	129	113	n =1-8		
11	dodecanoic acid	200	171	157	141	n =1-10		
Long Chain Saturated Fatty Acids								
15	tridecanoic acid	214	185	171	155	n =1-11		
18	tetradecanoic acid	228	199	185	169	n =1-12		
20**	pentadecanoic acid	242	213	199	183	n =1-13		
22	hexadecanoic acid	256	227	213	197	n =1-14		
23**	heptadecanoic acid	270	241	227	211	n =1-15		
25	octadecanoic acid	284	255	241	225	n =1-16		

Label	Compound		Ion Peaks		
	Unsaturated Fatty Acids	Mw	M-H_2O (M-18)	M - C_4H_8 (M - 56)	C_2H_3– $(CH_2)_n$ (27+n·14)
27	octadecenoic acid	282	264	226	n =1-16
~	octadecadienoic acid	280	262	224	

* Underlined m/z values indicate overlapping of peaks

Table 6.3.1.1 (continue)

Label	Compound		Ion Peaks						
	Saturated Fatty Diacids	Mw	M - OH (M - 17)	M - H_2O+H (M - 35)	M – $2H_2O$ (M - 36)	M - CH_2–COOH+H_2O (M - 77)	M - CH_2–COOH+H_2O+H (M - 78)	$C_6H_{12}O$+$(CH_2)_n$ 84+n·14
2	pentanedioic acid	132	115	125	96	55	54	n =1-3
4	hexanedioic acid	146	129	139	110	69	68	n =1-4
6	heptanedioic acid	160	143	153	124	83	82	n =1-5
7	octanedioic acid	174	157	167	138	97	96	n =1-6
12	nonanedioic acid	188	171	181	152	111	110	n =1-7
16	decanedioic acid	202	185	195	166	125	124	n =1-8
19	undecanedioic acid	216	199	209	180	139	138	n =1-9
	Diterpenoids	Mw	M - H (M - 1)	M - H_2O (M - 18)	M - H_2O–CH_3 (M - 33)	M - COOH (M - 45)	M - H_2O–HCOOH (M - 64)	M - H_2O -CH_2–COOH (M - 77)
35a	15-hydroxy-7-oxo-DHA	330	329	312	297	285	266	253
35b	15-hydroxy-DHA	316	315	298	283	271	252	239
36	7-oxo-DHA	314	313	296	281	269	250	237
37	7,15-hydroxy-DHA	332	331	314	299	287	268	255

long chain saturated fatty acids (Ryhage and Stenhagen 1960a) and at 16 eV in the DTMS analysis of paint oil films (Van den Berg 2002). These are: (a) fragment ions $[C_nH_{2n}COOH]^+$ identified at m/z 73, 129, 143, 157, 171 and 185 that are generated via a complicated breakdown mechanism of the fatty acid carbon skeletons, involving distonic ions (Spiteller, et al. 1966); (b) ion fragments of saturated chains ($[C_nH_{2n+1}]$) identified at m/z 43, 57, 71, 85, 99, etc. and ion fragments of unsaturated chains ($[C_nH_{2n-1}]$) with characteristic m/z 41, 55, 69, 83, 97, etc., and (c) a peak at m/z 60 which is present in all mass spectra and attributed to a McLafferty γ(H) rearrangement (Ryhage and Stenhagen 1960a). The saturated fatty acids produce some peaks of low to medium masses due to ion fragments: (a) $[–(CH_2)_n–COOH]^+$ resulting in a mass range of (14·n + 59); (b) $[–(CH_2)_n–C_2H_5]^+$ resulting in an m/z series of (14·n + 29); and, (c) $[C_6H_{12} + (CH_2)_n]^+$ generating a mass range of (84 + 14·n). Moreover, $[C_6H_{12}+(CH_2)_n]^+$ fragments are characteristic of saturated diacids, while the unsaturated fatty acids generate ion fragments $[–(CH_2)_n–C_2H_3]^+$ corresponding to a mass range of (14·n + 27) (Van den Berg 2002). In addition to these mass / charge series, there are some marker m/z peaks that are described below.

A comparison of the relative intensity of the characteristic ion fragments and molecular ions of the saturated, long chain fatty acids, such as tridecanoic (**15**[2]), tetradecanoic (**18**), pentadecanoic (**20**), palmitic (C16, **22**), margaric (C17, **23**) and stearic (C18, **25**) acids, indicates that their abundance remains reasonably unchanged when comparing the copal oil varnish film prior to and after ageing. The two most characteristic saturated long chain fatty acids of linseed oil, palmitic (**22**) and stearic

[2] The labels correspond to compounds listed in Tables 2.5.1 and 6.3.1.1

(**25**) acids, are identified by their molecular ions at m/z 256 and 284 respectively (Ryhage and Stenhagen 1960a). The typical P/S ratios determined by the intensity of their molecular ion peaks (peak height measured) are 1.5 for the unaged and 1.4 for the light aged film. Both these ratios are in the range of linseed oil (Mills and White 1994). The unsaturated fatty acids desorbed from the crosslinked ester bonded triacylglycerols of the film are less abundant than the saturated fatty acids, since these compounds have been very reactive during the heat induced oil varnish preparation (Section 2.5). In particular, polyunsaturated fatty acids, such as linolenic acid (18:3), when heated, undergo Diels-Alder cyclisation reactions resulting in cyclic fatty acids (Boelhouwer, et al. 1967, Martin, et al. 1998). Compound (**26**), (9-(-o-propylphenyl)-nonanoic acid, monitored at m/z 105, is a characteristic product of such reactions (Van den Berg 2002). Marker peaks of the dual unsaturated linoleic acid are its molecular ion at m/z 280, an ion fragment at m/z 224 due to elimination of C_4H_8, which typically occurs in the alkyl chain of unsaturated fatty acids, and at m/z 262 due to $[M\text{-}H_2O]^{+\cdot}$ (Van den Berg 2002). The monounsaturated oleic acid (**27**) is detected at its molecular ion at m/z 282 and at m/z 226 due to $[M\text{-}C_4H_8]^+$. However, the most characteristic marker peak of oleic acid is at m/z 264 due to the corresponding acyl ions of C18:1 fraction of the crosslinked triacylglycerols (Van den Berg 2002). According to Van den Berg (2002), the relatively high intensity of this particular peak implies that upon formation of the oligomeric material, polyunsaturated fatty acyl moieties have a higher reactivity and react away leading to a relative enrichment of the monounsaturated species. A comparison of the marker peaks indicates that less oleic than linoleic acid is consumed upon autoxidation during ageing, owing to the higher unsaturation of the latter (Ucciani and Debal 1996).

Indeed, processing the heights of the m/z marker peaks a reduction of 16% of the oleic-to-stearic and 38.5% of linoleic-to-stearic ratios upon ageing is in line with this theory and the results of the Py-TMAH-GC/MS described in Section 2.5.

Furthermore, the presence of fatty diacids, which are formed via isomerisation and subsequent consumption of the unsaturated fatty acids (Sonntag 1979, Martin, et al. 1998), is highlighted with several ion peaks shown in Table 6.3.1.1. The most representative saturated fatty diacid formed upon autoxidation of linseed oil is azelaic acid (**12**), which along with pimelic (**6**) and suberic (**7**) are the most abundant diacids according to the Py-TMAH-GC/MS data. The molecular ion of azelaic acid (m/z 188) is remarkably low as has been also observed in earlier investigations (Van den Berg 2002), but the ion fragment $[M\text{-}2H_2O]^{+\cdot}$ at m/z 152 indicates its presence (Ryhage and Stenhagen 1959). The typical azelaic-to-stearic ratio based on marker peaks m/z 152 and 284 respectively showed a 67% increase of the former upon ageing.

Finally, the diterpenoid compounds of the copal resin are relatively more abundant in the film prior to ageing. Upon pyrolysis, fragmentation of the DHA acids is obtained generating fragments by loss of carboxylic acid groups, hydrogen atoms and a methyl group resulting in a fragment at m/z 239 (Scalarone, et al. 2003a). A marker peak at m/z 253 corresponds to 15-hydroxy-7-oxo DHA acid (**35a**), due to $[M\text{-}(H_2O\text{–}CH_2\text{–}COOH)]^+$, and 15-hydroxy-DHA acid (**35b**) due to $[M\text{-}(H_2O\text{–}COOH)]^+$ (Van den Berg, et al. 2000, Scalarone, et al. 2003a). Dehydroabietic (DHA) acid is detected at m/z 300 owing to its molecular ion and a fragment ion at m/z 285, while peak at m/z 314 represents an oxidation product of dehydro-DHA (m/z 298) having reacted with an additional oxygen atom (Scalarone, et al. 2003a). However, the same peak at m/z

314 overlaps with the molecular ion of 7-oxo-DHA acid (**36**), as well as the dehydrated molecular ion of 7,15-hydroxy-DHA (**37**), whose presence is signified at m/z 268 owing to $[M\text{-}H_2O - HCOOH]^+$ (Van den Berg, et al. 2000). The results of the light aged oil varnish film show an evident decrease of peaks at m/z 239, 253, 268, 300 and 314, indicating a reduction in the concentration of the diterpenoid compounds. The abrupt decrease in the intensity of m/z 253 and m/z 268 peaks in the EI-DTMS summation mass spectrum of the aged film delineates the change in composition after the light ageing procedure Figure 6.3.1.2. This particular finding is in a very good agreement with earlier mass spectrometric investigations of oil varnishes (Dunkerton, et al. 1990, Van den Berg, et al. 1999b) and is consistent with the Py-TMAH-GC/MS results (Section 2.5)

6.3.2 EI-DTMS study across the laser ablated depths of the aged copal oil varnish

EI-DTMS was subsequently employed for a fingerprint molecular study across the depth profile of the aged oil varnish film that was uncovered across successive depth etchings at 2.5, 6, 8.5, 10 and 12 μm below the original film surface, using a KrF excimer laser (248 nm, 25 ns) with optimal fluences (Chapter 3). Basically, no molecular changes were monitored at the successive depths, which supports the findings above showing that the distribution of carbonyls as well as the methylene-to-methyl ratios remains constant at all depths (Chapter 4). Since this particular film is optically saturated at all depths (Section 4.3.2), there are indeed a few, if any at all, changes expected to be detected on the molecular basis. An example of the EI-DTMS total ion currents for the ablated film at depths 2.5, 6 and 12 μm is shown in Figure 6.3.2.1, while the EI-DTMS TIC of the aged film prior to ablation is also

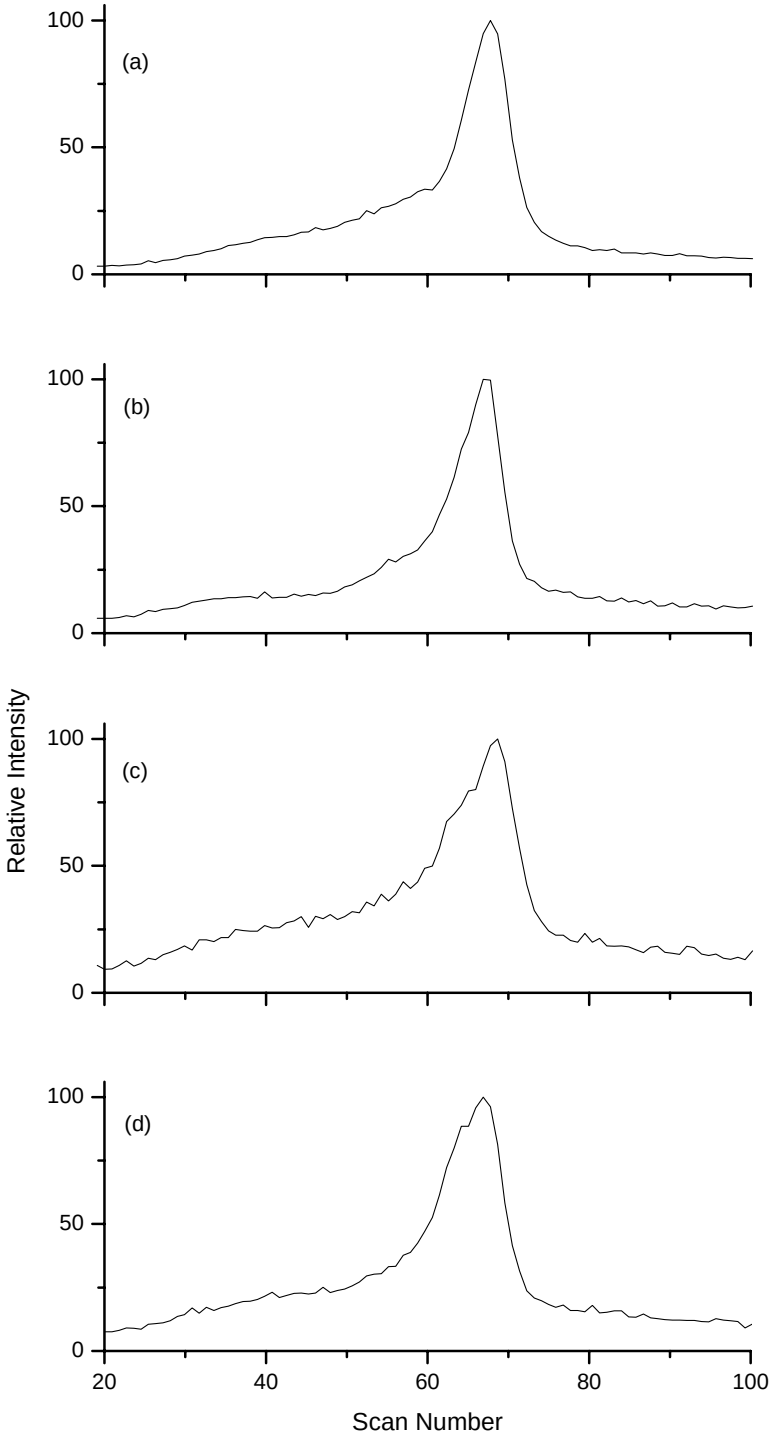

Figure 6.3.2.1 The EI-DTMS TIC's of the aged copal oil varnish film prior to laser ablation (a) and the KrF excimer laser ablated depth-steps at 2.5 μm (b) 6 μm (c) and at 12 μm (d).

demonstrated for comparison reasons. The EI-DTMS-TIC traces show that none of the remaining films after removal of the uppermost layers has a volatile fraction and therefore the fragments desorbed in the ion source were released predominately upon

pyrolysis. In addition, the pyrolysis peaks in all cases are obtained at the same temperature (scan no 68, 545°C). It is verified then that there is no gradient in the polarity and polymerisation profile across the depth of the film, in contrast to the case of aged triterpenoid varnishes, which obtain a sharp depth-dependent gradient in oxidation and crosslinking (Chapter 5).

EI-DTMS summation mass spectra provide further information about the molecular state across the depth-profile of the film. An example is shown in Figure 6.3.2.2 demonstrating the EI-DTMS summation mass spectra of two ablated depth steps at 6 and 12 μm below surface and the aged film prior to ablation. The relative abundances of the m/z peaks of the corresponding ion fragments of all the samples tested, including the aged film prior to ablation, remain virtually unchanged, so providing no significant evidence for any molecular change across the depth of the film.

Therefore, a suitable description of the EI-DTMS study of the ablated depth steps is similar to that of the aged film prior to ablation. In abstract, the concentration across the depth of the film is rich in diacids that are formed upon the oxidative degradation of unsaturated fatty acids, such as oleic and linoleic acids, and poor in the latter compounds. Marker peaks of the heat-bodied, aged and laser-ablated linseed oil components are observed at m/z 152 for azelaic acid (**12**), m/z 256 for palmitic acid (**22**), m/z 284 for stearic acid (**25**), m/z 264 for oleic acid (**25**) and m/z 280 for linoleic acid (Van den Berg 2002). Moreover, the EI-DTMS summation mass spectra indicate that the abietane-type diterpenoid molecules of the ablated copal resin, with marker peaks at m/z 239, 253, 268, 300 and 314, remain only in trace amounts at all depths,

indicating that the resin components have virtually reacted away during ageing across the whole depth profile of the film.

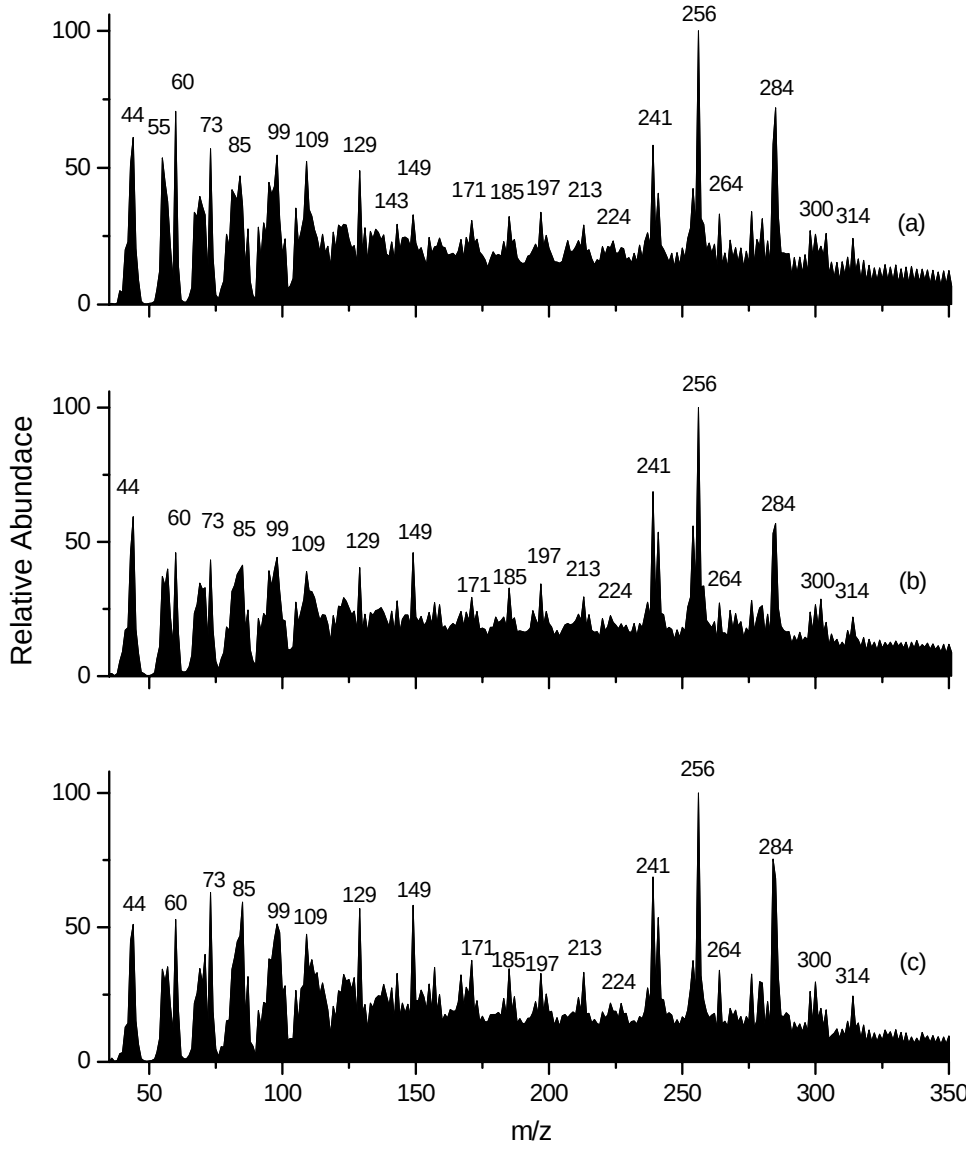

Figure 6.3.2.2 The EI-DTMS summation mass spectra of the aged copal oil varnish film prior to laser ablation (a) and the laser ablated depth-steps at 6 μm (b) and 12 μm (c) below the surface, using a KrF excimer laser.

These findings indicate that such a highly saturated, polar and crosslinked oil varnish film resembles the composition of aged stand oils and that the difference with the latter is the minute concentration in the resin components. The delineated high degree of polymerisation and the lack of volatile compounds not only at the surface but also

across the depth profile, explain the insolubility problems of aged oil varnishes (Tingry 1804, Brommelle 1956, Gettens and Stout 1966, Stolow 1985, Carlyle 2001). An indication of the unchanged concentration across the depth of the oil varnish film

Ablated material from original film (μm)	Azelaic : Stearic [m/z 152] : [m/z 284]	Oleic : Stearic [m/z 264] : [m/z 284]	Linoleic : Stearic [m/z 280] : [m/z 284]
0	0.611	0.506	0.447
2.5	0.586	0.495	0.434
6	0.588	0.485	0.422
8.5	0.581	0.485	0.428
10	0.570	0.492	0.424
12	0.574	0.482	0.437

Table 6.3.2.1 Azelaic-to-Stearic, Oleic-to-Stearic and Linoleic-to-Stearic ratios based on marker peaks identified in the EI-DTMS mass spectra of a 500h light aged (λ>295 nm), laser ablated copal oil varnish film at successive depth steps, using a KrF excimer laser

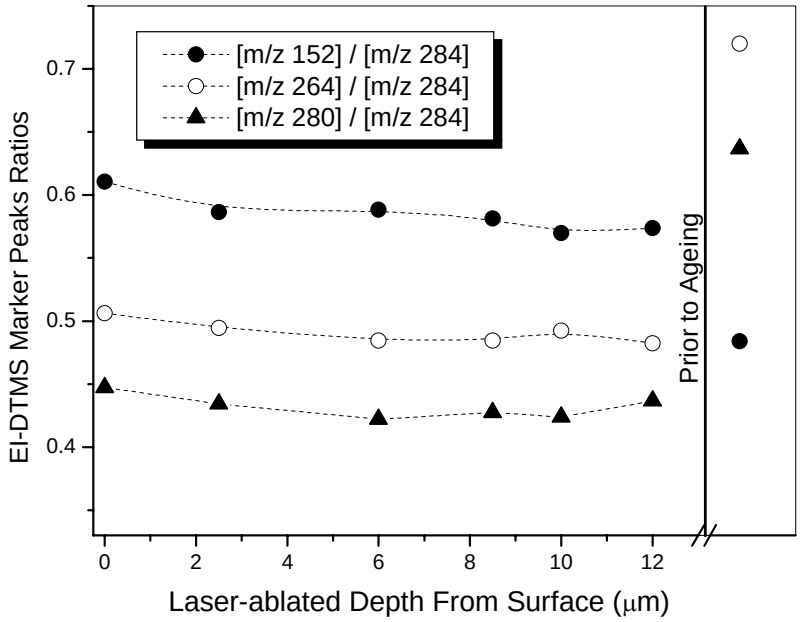

Figure 6.3.2.3 (a) Uncorrected ratios of EI-DTMS marker peaks of azelaic (m/z 152), oleic (m/z 264), and linoleic (m/z 280) acids to stearic acid (m/z 284) as a function of the laser ablated depth profile of a 500 h light aged (λ > 295 nm), copal oil varnish using a KrF excimer laser. (b) At the right hand side the same ratios are shown for the copal oil varnish film prior to ageing.

is provided by comparison of the azelaic-to-stearic, oleic-to-stearic and linoleic-to-stearic ratios (Mills and White 1994), as a function of depth. The abundance of these compounds was obtained by measuring the intensity of the corresponding marker

peaks. Table 6.3.2.1 and Figure 6.3.2.3 show that these ratios remain virtually constant along the depth profile.

6.3.3 A note about the contribution of KrF excimer laser ablation in the concentration across the depth profile of the aged copal oil varnish

KrF excimer laser ablation leads to an initial absorption of the 248 nm photons from the carboxylic acid groups of the various acids and diacids of the film (Srinivasan and Braren 1989), which break down to various photofragments including gaseous products, such as CO and CO_2, that finally drive the ablation plume away from the surface (Dyer and Srinivasan 1989). It could therefore be suggested that the most reactive component molecules have reacted with the UV laser photons (248 nm) during ablation, and degraded via radical chain reactions leading to further autoxidation and crosslinking (Al-Malaika 1993). It may, therefore, be implied that the lack of gradient characteristics across the depth of the tested laser ablated film is just a coincidence. This suggestion, however, is untrue for the simple reason that no laser-induced oxidation has been found upon ablation of volatile films, such as aged triterpenoid varnishes examined with UV/VIS spectrophotometry, ATR-FTIR (Chapter 4), DTMS, MALDI-TOF-MS and HP-SEC (Chapter 5), nor in other aged organic films, including proteinaceous (egg) binding media, neat or mixed with organic pigments, examined with LIF, LIBS, FT-Raman, FTIR, DTMS, LDI-MS and MALDI-TOF-MS analysis (Castillejo, et al. 2002). These findings provided further evidence that the mechanisms that apply upon excimer laser ablation are of mainly photochemical nature (Luk'yanchuk, et al. 1994, Srinivasan 1994) and that thermal effects on the surface, which would have caused thermally assisted molecular

modifications, have negligible contribution. Hence, the present study represents the molecular state of the depth profile of the copal oil varnish film, despite the use of the KrF excimer laser.

6.4 Conclusions

The composition of a 15 μm aged copal oil varnish film, aged under xenon arc radiation (500h, $\lambda > 295$ nm), was studied with DTMS at successive depth steps (2.5, 6, 8, 10, 12 μm) etched by means of KrF excimer laser ablation (248 nm, 25 ns). A pilot, detailed characterisation was first obtained with Py-TMAH-GC/MS of the film prior to and after ageing (Section 2.5). Oxidation of the heat bodied oil-resin mixture was monitored by the abundance increase of saturated fatty diacids, including azelaic acid, in favour of unsaturated fatty acids, such as oleic and linoleic acids (Sonntag 1979, Martin, et al. 1998), which were eliminated. Upon the heat-induced manufacturing of the copal oil varnish several oxygenated fatty acids were generated from polyunsaturated fatty acids, such as linolenic acid, including traces of a cyclic octadecanoic fatty acid formed via Diels-Alder cyclisation (Boelhouwer, et al. 1967, Martin, et al. 1998) and/or intermolecular cyclisation of heat-induced conjugation (Sebedio and Grandgirard 1989). Finally as a result of light ageing, the concentration in oxidised dehydroabietic acids of the resin is strongly reduced in line with earlier findings in oil varnishes (Dunkerton, et al. 1990, Van den Berg, et al. 1999b).

EI-DTMS provided a fingerprint analysis based on pyrolytic bond-breakage. It confirmed the presence and the polar modifications of the aforementioned compounds by monitoring specific m/z marker peaks. All the identified species are part of a polar,

crosslinked polymer network, since virtually no volatile fraction was evaporated at low and intermediate temperatures. In conclusion, the EI-DTMS study across successive depth-steps showed that crosslinking, polarity and composition maintain virtually unchanged as a function of depth. The constant degree of crosslinking and composition across depth reflect the unchanged ablation step upon successive 248 nm laser pulses (Figure 3.3.5.3), the constant optical properties of the ablated species, determined with LIBS (Section 3.3.4) and the optical properties of the remaining film, tested by UV/VIS and ATR-FTIR spectroscopy (Section 4.3.2). These findings explain the insolubility of aged oil varnishes (Tingry 1804, Brommelle 1956, Gettens and Stout 1966, Feller, et al. 1985, Stolow 1985, Carlyle 2001) and establish excimer laser ablation as a valuable tool for their removal, given that a certain methodology should be followed (Chapter 3) for enhanced selectivity, control and safety of the underlying layers. Finally, the KrF excimer laser pulses are suggested not to influence the composition of the film at the successive depth steps, since the interaction of the 248 nm with the surface is basically photochemical (Luk'yanchuk, et al. 1994).

6.5 References

Al-Malaika, S. 'Autoxidation'. In *Atmospheric oxidation and antioxidants*, Ed. G. Scott, Vol. I, Elsevier Science Publishers B.V., Amsterdam, (1993), 45 - 82.

Anderson, K. B. and Winans, R. E., 'The Nature and Fate of Natural Resins in the Geosphere I. Evaluation of Pyrolysis-Gaschromatography-Mass Spectrometry for the Analysis of Plant Resins and Resinites', *Analytical Chemistry* **63** (1991) 2901-2908.

Bäuerle, D. *Laser Processing and Chemistry, Third, revised and enlarged edition*, Springer-Verlag, Berlin, Heidelberg, New York, 2000.

Boelhouwer, C., Knegtel, J. T., and Tels, M., 'On the mechanism of the thermal polymerization of linseed oil', *Fette, Seifen, Anstrichmittel* **69** (1967) 432-436.

Boon, J. J., 'Analytical pyrolysis mass spectrometry: new vistas opened by temperature-resolved in-source PYMS', *International Journal of Mass Spectrometry and Ion Processes* **118/119** (1992) 755-787.

Brommelle, N., 'Material for a history of conservation', *Studies in Conservation* **2** (1956) 176-186.

Carlyle, L. A. *The artist's assistant: Oil painting Instruction manuals and handbooks in Britain 1800-1900: with reference to selected eighteenth century sources*, Archetype Publications, London, 2001.

Castillejo, M., Martin, M., Oujja, M., Silva, D., Torres, R., Manousaki, A., Zafiropulos, V., van den Brink, O. F., Heeren, R. M. A., Teule, R., Silva, A., and Gouveia, H., 'Analytical study of the chemcial and physical changes induced by KrF laser cleaning of tempera paints', *Analytical Chemistry* **74** (2002) 4662-4671.

Christie, W. W., 'Gas chromatography-mass spectrometry methods from structural analysis of fatty acids', *Lipids* **33** (1998) 343-353.

Crossley, A., Heyes, T. D., and Hudson, B. J. F., 'The effect of heat on pure triglycerides', *Journal of American Oil Chemists' Society* **39** (1962) 9-14.

Dunkerton, J., Kirby, J., and White, R. 'Varnish and early Italian tempera paintings'. In *Cleaning, Retouching and Coatings. Preprints of the Brussels Congress, 3-7 September*, IIC, London, (1990), 63-67.

Dyer, P. E. and Srinivasan, R., 'Pyroelectric detection of ultraviolet laser ablation products from polymers', *Journal of Applied Physics* **66** (1989) 2608-2612.

Feller, R. L., Stolow, N., and Jones, E. H. 'On picture varnishes and their solvents.' Revised and enlarged edition 1985. Washington DC: National Gallery of Art., (1985).

Formo, M. W. 'Paints, varnishes, and related products'. In *Baile's Industrial Oil and Fat Products*, Ed. D. Swern, Vol. 1, John Wiley & Sons, New York, (1979), 687-817.

Frankel, E. N., Neff, W. E., and Selke, E., 'Analysis of autoxidized fats by gas chromatography - mass spectrometry: VII. Volatile thermal decomposition products of pure hydroperoxides from autoxidized and photosensitized oxidized mehtyl oleate, linoleate and linolenate', *Lipids* **16** (1981) 279-292.

Frega, N., Mozzon, M., and Lercker, G., 'Effects of free fatty acids on oxidative stability of vegetable oil', *Journal of American Oil Chemists' Society* **76** (1999) 325-329.

Frilette, V. J., 'Drying oil and oleoresinous varnish films', *Industrial and Enginering Chemistry Research* **38** (1946) 493.

Gettens, R. and Stout, G. *Painting materials: a short encyclopaedia*, Dover Publications, New York, 1966.

Hartgers, W. A., Sinninghe Damste, J. S., and De Leeuw, J. W., 'Flash pyrolysis of silicon-bound hydrocarbons', *Journal of Analytical Applied Pyrolysis* **20** (1991) 141-150.

Keller, R., 'Leinol als malmittel', *Maltechnik* **2.** (1973) 74-105.

Luk'yanchuk, B., Bityurin, N., Anisimov, S., and Bäuerle, D. 'Photophysical Ablation of Organic Polymers'. In *Excimer Lasers*, Ed. L. D. Laude, Kluwer Academic Publishers, The Netherlands, (1994), 59-77.

Mantell, C. L., Kopf, C. W., Curtis, J. L., and Rogers, E. M. 'Oil Varnishes'. In *The technology of natural resins*, John Wiley & Sons, Inc., (1949), 265-319.

Martin, J. C., Nour, M., Lavillonniere, F., and Sebedio, J. L., 'Effects of fatty acid positional distribution and triacylglycerol composition on lipid by-products formation during heat treatment: II *Trans* isomers', *Journal of American Oil Chemists' Society* **75** (1998) 1073-1078.

Mills, J. S. and White, R. *The Organic Chemistry of Museum Objects*, 2nd edition, Butterworth-Heinemann, Oxford, 1994.

Miyashita, K. and Tagaki, T., 'Study on the oxidative rate and proxidant activity of free fatty acids', *Journal of American Oil Chemists' Society* **63** (1986) 1380-1384.

Neil, J. W. 'The art of making copal and spirit varnishes, Transactions of the Society Instituted at London for the Encouragement of Arts, Manufacturers and Commerce' Vol. XLIX, Part II, Society's House, Housekeeper, London, (1833), 33-87 (cited by L. Carlyle 2001 p. 317).

Pastorova, I., van der Berg, K. J., Boon, J. J., and Verhoeven, J. W., 'Analysis of oxidised diterpenoid acids using thermally assisted methylation with TMAH', *Journal of Analytical and Applied Pyrolysis* **43** (1997) 41-57.

Paulose, M. M. and Chang, S. S., 'Chemical reactions involved in deep fat frying of foods: VI. Characterization of nonvolatile decomposition products of trilinolein', *Journal of American Oil Chemists' Society* **50** (1973) 147-154.

Paulose, M. M. and Chang, S. S., 'Chemical reactions involved in deep fat frying of foods: VIII. Characterization of nonvolatile decomposition products of triolein', *Journal of American Oil Chemists' Society* **55** (1978) 375-380.

Perrin, J. L. 'Chemical and physical changes in edible fats'. In *Oils & fats manual*, Eds. A. Karleskind and J.-P. Wollf, Vol. 2, Intercept Ltd., Andover, (1996), 1025-1042.

Privett, O. S., 'Autoxidation and autoxidative polymerisation', *Journal of American Oil Chemists' Society* **36** (1959) 505-512.

Ryhage, R. and Stenhagen, E., 'Mass spectrometric studies III. Esters of saturated dibasic acids', *Ark. Kemi* **14** (1959) 497-509.

Ryhage, R. and Stenhagen, E., 'Mass spectrometry in lipid research', *Journal of Lipid Research* **1** (1960a) 361-391.

Ryhage, R. and Stenhagen, E., 'Mass spectrometric studies. VI. Methyl esters of normal chain oxo-, hydroxy-, methoxy- and epoxy-acids', *Ark. Kemi* **15** (1960b) 545-574.

Scalarone, D., Lazzari, M., and Chiantore, O., 'Ageing behaviour and pyrolytic characterisation of diterpenic resins used as art materials: colophony and Venice turpentine', *Journal of Analytical Applied Pyrolysis* **64** (2002) 345-361.

Scalarone, D., van der Horst, J., Boon, J. J., and Chiantore, O., 'Direct-temperature mass spectrometric detection of volatile terpenoids and natural terpenoid polymers in fresh and artifficially aged resins', *Journal of Mass Spectrometry* **38** (2003a) 607-617.

Scalarone, D., Lazzari, M., and Chiantore, O., 'Ageing behaviour and analytical pyrolysis characterisation of diterpenic resins used as art materials: Manila copal and sandarac', *Journal of Analytical Applied Pyrolysis* **68-69** (2003b) 115-136.

Scott Taylor, J. 'Oil Painting'. In *Modes of Painting Described and Classified*, Winsor and Newton, Ltd, London, (1890), 38-39 (cited by L.Carlyle 2001 p. 321).

Sebedio, J. L. and Grandgirard, A., 'Cyclic fatty acids: natural sources, formation during heat treatment, synthesis and biological properties', *Progress in Lipid Research* **28** (1989) 303-336.

Sonntag, N. O. V. 'Reactions of fats and fatty acids'. In *Bailey's industrial oil and fat products*, Ed. D. Swern, Vol. 1, John Wiley & Sons, New York, (1979), 158-164.

Spiteller, G., Spiteller-Friedmann, M., and Houriet, M., 'Klärung massenspektrometrischer Zerfallsmechanismen durch Verwendung kalter Ionenquellen und von Elektronen niedriger Energie, 1. Mitt.: Aliphatischer Ester', *Mh. Chem.* **97** (1966) 121.

Srinivasan, R. and Braren, B., 'Ultraviolet laser ablation of organic polymers', *Chemical Reviews* **89** (1989) 1303-1316.

Srinivasan, R. 'Interaction of laser radiation with organic polymers'. In *Laser Ablation: Principles and Applications*, Ed. J. C. Miller, Vol. 28, Springer Series of Material Science, Springer, Berlin, Heidelberg, (1994), 107.

Stolow, N. 'Part II: Solvent Action'. In *On picture varnishes and their solvents.*, Eds. R. L. Feller, N. Stolow, and E. H. Jones, Revised edition 1971. Cleveland, Ohio: Case Western Reserve University. Revised and enlarged edition 1985. Washington DC: National Gallery of Art., (1985).

Tingry, P. F. 'The Painter and Varnisher's Guide', J. Taylor, Black-Horse-Court, London, (1804), 138 (cited by L. Carlyle 2001 p.327).

Ucciani, E. and Debal, A. 'Chemical properties of fats'. In *Oils & Fats Manual*, Eds. A. Karleskind and J.-P. Wolff, Vol. 1, Intercept Ltd., Andover, (1996), 325-443.

Van den Berg, J. D. J., Van den Berg, K. J., and Boon, J. J., 'Chemical changes in curing and ageing oil paints', *in 12th triennial ICOM-CC meeting, Lyon, France* (1999a) 248-253.

Van den Berg, J. D. J., 'Analytical chemical studies on traditional linseed oil paints', PhD Thesis University of Amsterdam, (2002).

Van den Berg, J. D. J., Van den Berg, K. J., and Boon, J. J., 'Identification of non-cross-liked compounds in methanolic extraxts of cured and aged linseed oil-based paint films using gass chromatography - mass spectrometry', *Jounral of Chromatography A* **950** (2002) 195-211.

Van den Berg, K. J., Pastorova, I., Spetter, L., and Boon, J. J., 'State of oxidation of diterpenoid *Pinaccae* resins in varnish, wax lining material, 18th century resin oil paint, and a recent copper resinate glaze'. In *Preprints ICOM Committee for Conservation 11th Triennial Meeting, Endinburgh, Scotland, 1- 6 September 1996*, Ed. J. Bridgland, Vol. 2, James & James, (1996).

Van den Berg, K. J., Van der Horst, J., and Boon, J. J., 'Recognition of copals in aged resin paints and varnishes'. In *Preprints ICOM Committee for Conservation 12th Triennial Meeting, Lyon, France, 29 Aug. - 3 September 1999*, Vol. II, James & James, London, (1999b), 855-861.

Van den Berg, K. J., Boon, J. J., Pastorova, I., and Spetter, L. F. M., 'Mass spectrometric methodology for the analysis of highly oxidized diterpenoid acids of Old Master paintings', *Journal of mass Spectrometry* **35** (2000) 512-533.

Van der Doelen, G. A., van der Berg, K. J., and Boon, J. J., 'Comparative chromatographic and mass spectrometric studies of triterpenoid varnishes: fresh material and aged samples from paintings', *Studies in Conservation* **43** (1998) 249-264.

Van der Werf, I. D., Van den Berg, K. J., Schmitt, S., and Boon, J. J., 'Molecular characterization of copaiba balsam as used in painting techniques and restoration procedures', *Studies in Conservation* **45** (2000) 1-18.

Zafiropulos, V. 'Laser ablation in cleaning of artworks'. In *Optical Physics, Applied Physics and Material Science: Laser Cleaning*, Ed. B. S. Luk'yanchuk, World Scientific, Singapure, New Jersey, London, Hong Kong, (2002), 343-392.

7. Conclusions and Future Outlook

7.1 Conclusions

This thesis provides a study on the laser cleaning of three painting coatings (dammar, mastic and copal oil varnishes) with KrF excimer laser (248 nm) nanosecond pulses. Unlike previous studies on the photochemical laser ablation of polymers, most of the attention herein is paid to the contribution of the chemistry to the process across the depth profiles of the aged varnishes. Such an approach was essential because consecutive laser pulses interact with subsequent depths across the thickness of the same ablated film. Moreover, in laser cleaning applications for conservation the remaining material is more important than the material ablated. The coatings tested were clearly separated into two groups: (i) natural resin 'spirit' varnishes, which are initially dissolved in a solvent for the formation of the final film and (ii) pre-polymerised resin-oil varnishes, which undergo a strong heating manufacture towards the formation of viscous and insoluble films. Findings of the first group are expected to correspond to the majority of aged organic coatings with low or moderate molecular weights, which are the most frequently used varnishes on painted works of art. The second group is an exceptional case, which highlights the efficiency of UV short-pulsed laser induced removal of coatings that chemical methods fail to remove.

Taking advantage of the etching resolution in the sub-micron scale obtained by 248 nm laser pulses, this work is the first systematic study on the depth-dependant oxidation and crosslinking profiles of aged natural resin varnishes. It is established herein that after ageing, natural resin varnishes undergo depth-dependant, decreasing gradients in the degrees of oxidation and condensation (crosslinking and polymerisation). In addition, it is determined that their oxidation profiles change qualitatively with depth. Direct Temperature-resolved Mass Spectroscopic (DTMS) studies showed that prolonged UV-including accelerated light ageing of these coatings resulted in inhomogeneous mixtures, which contained (i) UV-induced A-ring oxidised dammarane type triterpenoids, (ii) non-UV-induced oxidised oleanane and dammarane type compounds and (iii) unaffected triterpenoid molecules. A first indication of the existence of the gradients across the films was the change of the ablation rate against fluence with depth. Using constantly 'optimal' fluences, which maximised the ablation yield per incident laser photon, as determined on the surface of the films, it was observed that the ablation step was minimised particularly after the removal of the 15 μm surface layers in both films. Analysis of the ablation plume across depth with Laser-induced Breakdown Spectroscopy (LIBS) showed that the carbon dimer emission, the intensity of which has been previously associated with the degree of polymerisation, decreases abruptly after the removal of the 15 μm surface layers. Moreover, the intensity and the rate of the laser light transmission as a function of the reducing thickness, measured behind the ablated films, were different upon ablation of surface and bulk layers. Under these conditions, a range of subsequent depth-steps was etched in the films to study the chemical profiles across depth. Analysis was separated into two groups to determine the chemical properties of the

varnishes as a function of depth: (i) directly on the ablated surfaces with Attenuated Total Reflection - Fourier Transformed Infrared Spectroscopy (ATR-FTIR) and Matrix-Assisted Laser Desorption/Ionisation - Time-Of-Flight - MS (MALDI-TOF-MS) and (ii) on the remaining films with UV/VIS spectrophotometry, DTMS Total Ion Currents (TIC's), the corresponding summation MS and the Multivariant Factor Discriminant Analysis (DA) thereof, as well as High Performance - Size Exclusion Chromatography (HP-SEC).

The results showed that there is a decreasing gradient in the abundance of the oxidised, polar and high MW fractions across the depth profiles of dammar and mastic films, which explains initial observations such as increasing solubility, decreasing yellowing and the decreasing ablation steps with depth. The decreasing oxidation with depth highlights that there is no laser-induced deterioration of the ablated varnishes. The formation of the gradients is attributed to the decreasing intensity and the longer wavelengths of the ambient light transmitted from the surface towards the bulk, showed by UV/VIS data. MALDI-TOF-MS indicated that UV-induced oxidation, resulting in A-ring openings of oleanane / ursane type molecules, is limited at the 15 μm surface layers, which completely absorbed radiation with $\lambda < 350$ nm according to the results of UV/VIS spectrophotometry. Below this depth other oxidation products were formed which were previously ascribed to non-UV radiation. The abrupt change of the ablation step below 15 μm is also attributed to the change of the MW as shown with the DTMS-TIC's and the HP-SEC data. Both films were almost unaffected from ageing at depths longer than ~ 25 μm from surface. In other words, the compositions of the films at depths equal to and longer than 25 μm from

surface was similar to their composition prior to ageing. Thus, the depth-wise reduced yellowing was not a matter of laser induced bleaching of known chromophores formed during autoxidation, such as conjugated diketones and unsaturated quinones. Instead, it is proven herein that these chromophores are not even produced at long depths from surface in such coatings.

In a sharp contrast, the depth profile of the aged copal oil varnish was virtually homogenous. Evaluation of the ageing of the film was carried out with Pyrolysis-Gas Chromatography / MS with online derivatisation with tetramethylammomium hydroxide (TMAH) (Py-TMAH-GC/MS). The results supported earlier studies on the reduction of the concentration of the resin component upon ageing. Oxidation was monitored by the increased concentration of saturated fatty diacids over unsaturated fatty acids of the oil component. Several oxygenated fatty acids were generated from polyunsaturated fatty acids, such as cyclic octadecanoic fatty acids formed via Diels-Alder cyclisation and/or intermolecular cyclisation of heat-induced conjugation. In contrast to the aged natural resin films, the aged oil varnish had a stable interaction with the KrF excimer laser at all depths, determined by (i) the identical laser ablation rate versus fluence, (ii) the constant ablation step, (iii) the steady laser induced transmission through surface and bulk layers and (iv) the constant intensity of carbon dimer emission across depth monitored by LIBS. ATR-FTIR showed that both absorption due to carbonyl groups and corresponding ratios of methyl to methylene remain constant at all depths, while UV/VIS data showed that the film was a low absorber and optically saturated, since the absorption coefficients of the film in the near UV remained unchanged at all depths. A fingerprint DTMS study on successive

depth steps showed that the aged film was a homogeneous, polar and crosslinked polymer in which there was a negligible volatile fraction. This fraction is unable to change the fate of the high MW substance and eventually escapes the film. The main conclusion with respect to these varnishes is that these are very low absorbers in the ambient UV light and that such films do not have gradient characteristics, because they have been almost completely degraded during their manufacturing and not during their curing on the painted surface. This partly explains why such films are completely insoluble in common cleaning solvents used in paintings and why they are readily photodissociated with excimer lasers (Chapters 3, 4 and 6). Unfortunately, such films being low absorbers do not protect the underlying surface as much as natural resin films do.

7.2 Future Outlook

7.2.1 Future aspects for painting conservation

In the first chapter (page 2) the objectives of this work, which are associated with the practical conservation of paintings, were highlighted. The main questions to be addressed, which in the future would improve the preservation of painted works of art after their cleaning and as a consequence would benefit the performance of the conservator's work, were:

i. Is there a simple way to employ laser cleaning to remove an aged varnish from a painted surface without running the risks for laser-induced damage to the paint?
ii. Does the high-powered laser action on varnish damage the remaining varnish?
iii. Are the theories of the degradation gradients valid?

iv. Using the deterioration properties of aged varnishes and the selectivity of excimer lasers, can we obtain a methodical and simple strategy for an acceptable cleaning of paintings (both in terms of aesthetics and of cleaning-induced damage elimination)?

Based on the findings of the present work, a certain methodology derives for the safe laser cleaning of painted works of art coated with aged varnishes requiring removal. It must be understood that these findings were based on the action of a KrF excimer laser on aged varnishes under controlled parameters (chapter 3) rather than tests on paintings. Nevertheless, these points are efficiently addressed given the understanding of the chemistry of the varnishes across their depth-profiles. A competitent conservator must recognise that cleaning of an object (regardless of the technique employed) is case-specific. Therefore the points mentioned above are answered separately for the two different types of coatings studied.

7.2.1.1 Laser cleaning of oil-resin varnishes.

In the case of highly polymerised and insoluble oil varnishes, which do not have gradient characteristics, laser cleaning is the only known method that can readily induce removal and at the same time can improve the appearance of a painting without affecting the painted layers.

i. For such cases the conservator may employ an excimer laser to remove as much varnish as possible down to a depth, where the optical absorption length of the varnish to the laser wavelength, determined at the surface of the varnish, is at least equal to or slightly shorter than the remaining varnish thickness. This way unwanted transmission of the laser beam into the underlying and preservable paint layers is prevented. Under these lines, no damage to the paint is possible because

there will be no contact of the laser photons with the valuable layers of the painting.

ii. As determined in chapters 4 and 6, the laser action does not cause any further damage to the remaining aged oil varnish during the ablation process, as long as the fluence used is optimised using the procedure described in chapter 3. This knowledge is crucial to the conservator, because it gives the essential confidence to remove oil varnishes with absolute control of the process.

iii. No gradient characteristics were found in oil varnishes. This explains why such films, once they become insoluble, remain insoluble at all depths. Therefore, cleaning of paintings with such coatings using conventional cleaning techniques and especially solvents is an impossible task and unlikely to improve the preservation of these works of art. All the findings of the present work show that laser cleaning in these cases should be seriously considered as the solution to this problem.

iv. A possible reason why laser cleaning may succeed in the cleaning of paintings is that, despite the advanced physics and physicochemistry behind the laser ablation phenomenon, the process needed for the selection of the appropriate fluence for a certain varnish is simple. In practice, one should test a series of fluences at a discreet corner of the work of art, as conservators always do, e.g. testing of solvents or other cleaning agents on a discreet corner of the working surface of an artwork. The exact methodology for choosing the optimum fluence is described step by step in Section 3.2. Once the "optimum" fluence for an oil varnish has been determined, cleaning may be terminated as soon as a few microns of the same material have been removed. The analytical results of the present work

showed that there should be an improvement of the appearance of the painting, without being necessary to remove the whole varnish from the surface. To the convenience of the conservator there is no need to change any parameters of the laser during the ablation of polymerised oil varnishes.

7.2.1.2 Laser cleaning of natural resin varnishes.

It was shown herein that natural resin varnishes superiorly protect underlying layers from photodegradation, because they block both oxygen and the damaging UV wavelengths of the ambient light from penetrating deeper than a few microns from the surface. This probably explains why painted surfaces that are coated with such films are usually preserved in a better condition compared to surfaces coated with any other type of varnish. The aims with respect to practical conservation as set at the beginning of this thesis (page 2) are addressed as follows:

i. For the removal of aged natural resin varnishes the conservator can employ an excimer laser to remove only the most degraded 10-15 microns from the surface of the varnish. This way there is no risk of damaging the underlying paint because the laser-varnish interaction is limited to the highly degraded surface layers of the aged varnishes, while the remaining varnish is preserved in a less deteriorated condition than the original surface. At the same time the remaining varnish prevents the laser photons from penetrating on the paint. It should be highlighted that below the deteriorated surface layers the transmission of the laser photons increases more than the optical absorption lengths at the surface of the varnishes indicate. By limiting ablation on the surface layers no damage to the paint is possible because there will be no contact of the laser photons with the valuable layers of the painting. A very important finding was that even after having

removed the UV-affected layers from the surfaces of the particular dammar and mastic films studied, measurable transmission was initiated after removal of a considerable amount of varnish (Section 4.3.1.2). This finding highlights that laser cleaning can be applied to natural resin varnishes aged in the protected UV-free environment of museums and galleries (no A-ring oxidation) with no risks of damaging the underlying paint, if the protocol of superficial ablation is maintained.

ii. The removal of surface layers of a maximum thickness of 10-15 μm improves the appearance of the underlying paint, because no significant yellowing has been identified in the varnishes at these depths. The fact that decreasing gradients in degrees of condensation, oxidation and polarity were experimentally proven is the strongest argument that the action of the laser does not induce further degradation of the remaining film during laser cleaning.

iii. Indeed following the conclusions on the natural resin films (Section 7.1) there are gradients formed as a function of depth for these varnishes. This finding must have a strong impact in conservation and especially in the cleaning of works of art coated with aged natural varnishes. In conservation, one should consider that cleaning requires the removal of only the most degraded material from the film and not all of the film just because it is considered “aged”. Besides, compared to their state prior to ageing, such films retain all their visual advantages at depths where degradation has been prevented.

iv. In terms of conservation the steps preceding the application remain as described in detail in Section 3.2. Once the “optimum” fluence on the surface of the aged varnish has been determined, the process is simple and, most significantly, the

user has absolute control of the cleaning. There is no need to remove more material than the most degraded surface layers. Following the gradual, visually assessed appearance of the painted surface (reducing yellowing and micro-cracking of varnish film with depth), cleaning can terminate when the conservator decides that the object has been aesthetically improved. If such a visual assessment is difficult, there are two additional clues that may help the practitioner to understand when to stop the process. These are: (a) a significant change of the ablation yield after removal of the degraded layers (unfortunately this can only be determined by mechanical surface measurements of the depth profiles obtained by each pulse, see chapter 3) and (b) the beginning of melting of the surface of the remaining varnish at some stage of the process. Both these signs provide evidence that the cleaning has reached a less deteriorated material and that the remaining varnish could be then preserved. In practice, the remaining varnish can be then removed with less polar solvents than those required to remove the surface layers of the aged varnish. However, this may not be necessary because of the better appearance of the painting (significantly reduced yellowing and cracking) after only 10-15 μm have been laser ablated.

7.2.2 A possible impact to technology

There is no doubt that laser applications are gradually taking over in the industry for accomplishing previously laborious tasks, such as micro-etching, carving and removal of inorganic and organic thin films. The great advantages of excimer lasers, such as (i) their highly multimode output containing about 10^5 transverse modes, (ii) the high photon energies provided by the short UV laser wavelengths, (iii) the high energy per pulse of some excimer laser beams with a minimal effort, (iv) the short pulse

durations, which are typically in the nano- and femtosecond scales and (v) the high relative homogeneity in the beam profile: top-hat and Gaussian profiles in direct directions, make it possible to succeed in multidisciplinary areas such as manufacture, analytical technology and medical micro-operations. It is unusual for technology to benefit from applications on works of art. However, the present work opens up an aspect that technologists may be interested in. This is basically derived from the easy manipulation of photosensitive films with gradient characteristics that were studied in the present thesis. It would have been impossible to discover these findings without the appropriate use of laser cleaning. It has been determined here that natural resins not only provide a superior visual performance when applied on painted works of art, but also provide the best possible protection of the substrate. Their only disadvantage is that they degrade significantly with age, although this occurs only at the surface. This is exactly the point where technology may take into account. It may be a future challenge to fabricate synthetic organic films, with similar characteristics in order to protect photosensitive substrates. It would be a great achievement to produce coatings that could degrade less at the surface (e.g. use of photosensitisers) and at the same time remain almost unaffected by ageing in the bulk. Such coatings could be then used in conservation and other disciplines where both protection and visual perception is significant, e.g. coating of architectural surfaces. Given that removal of only the degraded layers is no longer a problem by the appropriate use of laser cleaning, such a development would certainly provide a longer lifetime of the coating as well as a superior preservation of the substrate.